Electromagnetic Interference and Radio Frequency Interference Shielding of Carbon-Filled Conductive Resins

By

Quinton J. Krueger

Bachelor of Science, Michigan Technological University, 2001

A Thesis

Submitted to the Graduate Faculty

of

Michigan Technological University

In partial fulfillment of the requirements

For the degree of

Master of Science

In

Chemical Engineering

Houghton, Michigan

May 2002

This thesis, **"Electromagnetic Interference and Radio Frequency Interference Shielding of Carbon-Filled Conductive Resins,"** is hereby approved in partial fulfillment of the requirements for the degree of MASTER OF SCIENCE in the field of Chemical Engineering.

DEPARTMENT **– Chemical Engineering**

Signatures:

Dissertation Advisor: _____

Dr. Julia A. King

Department Chair: _____

Dr. Michael Mullins

Date: _____

ACKNOWLEDGEMENTS

I must acknowledge the National Science Foundation and Conoco, Inc. for financial and materials support respectively. I have several people to thank. I owe a lot of my career at Michigan Tech to Dr. Julia King. You have helped me through my undergraduate experience and took me on as one of your graduate students. I appreciate having you always being there for me. Your continued support has made me what I am today. I consider you a teacher and a dear friend. Thank you.

I need to thank the members of my committee for their aid in this project. Dr. Jason Keith, Dr. Tony Rogers, Dr. Ibrahim Miskioglu and Dr. David Chesney. Without all of your input this never could have been completed. I would like to thank my office partner Jeremiah Konell. Thanks for all of your help and going out of your way to help me with my experiments when you didn't have to. Thanks to all the undergraduates that helped me on this project especially, Travis Swalve and Jessica Heiser. We spent many hours in close quarters and found away to laugh it off at the end of the day. To you I say thanks.

Also I would like to thank all of my friends who helped me through the toughest year of my life to date. Without you guys I don't know if I ever could have got this done. Thank you; Kirk Opella, Anna Siemeniko, Andy Wellbaum, Beth Krenek, Ryan Betker, Mark Rivord, Wolf Pack Hockey Club, Geoff Roelant, Jason Thibodeaux, Anthony Morretti, Paul Munsterman and Josh Tolk. A big thanks to Jason Flemming. Thanks for hanging with me for all these years. I will leave knowing I had the support of many.

I need to thank my family especially my Mom and Dad. Thanks guys, I appreciate all of the support you gave me and everything you did to make me who I am. I am proud to be your son. Thanks Jackie and Trent for your support too.

Abstract

"Electromagnetic Interference and Radio Frequency Interference Shielding of Carbon-Filled Conductive Resins"

Engineering thermoplastics have made tremendous inroads into the market for housings used in the electronics, computer, and business equipment industries. The trend has also highlighted one of the deficiencies of plastics. Plastics are inherently non-conductive and cannot shield electronics from Electromagnetic Interference or Radio Frequency Interference (EMI/RFI). They must comply with the Federal Communication Committee's regulations governing shielding. In addition, plastics cannot protect components from the destructive effects of Electrostatic Discharge (ESD).

The electrical conductivity of polymers can be increased by the addition of carbon fillers, such as carbon fibers, carbon black and graphite. The resulting composites can be used in applications where metals have typically been the materials of choice. The electrical conductivity for pure polymers typically ranges between 10^{-14} and 10^{-17} Siemens/cm (S/cm). Typical electrical conductivity values for other materials are 10^{2} for electrically conductive carbon black, 10^{3} for polyacrylonitrile (PAN)-based, 10^{4} for pitch-based carbon fibers, 10^{5} for high purity synthetic graphite, and 10^{6} for metals such as aluminum and copper. All conductivity values are given in S/cm.

The objective of this thesis is to study the effects of single and multiple carbon based filler systems in conductive resins and their effect on shielding attenuation. In this research, compounding runs followed by injection molding and shielding effectiveness testing of carbon filled resins was performed. Two different polymers were used: nylon 6,6 and polycarbonate. The three carbon fillers included an electrically conductive carbon black, synthetic graphite particles and a milled pitch based carbon fiber. For each polymer fourteen formulations were produced and tested that contained varying amounts of these single carbon fillers. In addition, combinations of fillers were investigated by conducting a full 2^{3} factorial design and complete replicate in each polymer. Shielding effectiveness results from a flanged coaxial holder were measured and compared to theoretical shielding values based on experimental electrical conductivity.

Factorial design results concluded that single and multiple carbon fillers have a significant effect on increasing the shielding effectiveness of conductive resins. Two filler interactions proved to be statistically significant. Carbon black had the highest effect on shielding effectiveness out of all the fillers tested. Composites that had an electrical resistivity less than 100 ohm-cm fit the theoretical model for a homogenous metal well. Suggestions for developing a new model for heterogeneous composites are also discussed.

TABLE OF CONTENTS

LIST OF FIGURES

LIST OF TABLES

TABLE OF NOMENCLATURE

A ..... Main Effect
A_{db} ..... Adsorption Loss
B ..... Main Effect
B_{db} ..... Internal Reflection Loss
C ..... Main Effect
AB ..... Two-Factor Interaction
AC ..... Two-Factor Interaction
ABC ..... Three-Factor Interaction
AR ..... Aspect Ratio
a ..... Replicate Number
ab ..... Replicate Number
abc ..... Replicate Number
ac ..... Replicate Number
b ..... Replicate Number
BC ..... Two Factor Interaction
bc ..... Replicate Number
C ..... Celsius
c ..... Replicate Number
CB ..... Carbon Black
CF ..... Carbon Fiber
cm ..... Centimeter
D ..... Diameter
DAM ..... Dry as Molded
dB ..... Decibel
dc ..... Diameter of Circle of Contact Between Fibers
DR ..... Dynamic Range
ε ..... Random Error
E ..... Electric field
E_1 ..... Impinging Field Intensity
E_2 ..... Exiting Field Intensity
EC ..... Electrical Conductivity
EM ..... Electromagnetic
EMI ..... Electromagnetic Interference
ER ..... Electrical Resistivity
ESD ..... Electrostatic Dissipation
f ..... Frequency in Hertz
f_{MHz} ..... Frequency in Mega Hertz
G ..... Conductivity Relative to Copper
GHz ..... Giga Hertz
H ..... Magnetic Field
Hz ..... Hertz
MHz ..... Mega Hertz
J ..... Joule

K ..... Kelvin
L ..... Length of Fiber
λ ..... Wave Length
l ..... Length
LED ..... Light Emitting Diode
lbs ..... Pounds
MPa ..... Mega Pascal
m ..... Meter
μm ..... Microns
N ..... Unit Volume
n ..... Number of Samples
nm ..... Nanometer
P ..... Statistical Significance
PAN ..... Polyacrylonitrile
ϕ ..... Volume Fraction
ϕ_c ..... Percolation Threshold
ϕ_f ..... Volume Fraction of Filler Material
ϕ_m ..... Volume Fraction of Matrix Material
ϕ_p ..... Percentage of Fibers Participating in Strings
ϕ_t ..... Threshold Value at Which All Fibers Participate in Strings
r ..... Distance from Source
R_{db} ..... Reflection Loss
RFI ..... Radio Frequency Interference
rpm ..... Revolutions per Minute
P_1 ..... Power Level
P_2 ..... Power Level
p ..... Probability
ρ ..... Density of Liquid
ρ_c ..... Composite Density
ρ_i ..... Density of Composite Constituent
PT ..... Percolation Threshold
PVC ..... Polyvinyl Chloride
S ..... Siemens
s ..... Seconds
SE ..... Shielding Effectiveness
S_{eff} ..... Shielding Effectiveness
σ_r ..... Electrical Conductivity relative to Copper
TC ..... Synthetic Graphite
SS ..... Sum of Squares
σ_c ..... Conductivity at Percolation Threshold
t ..... Thickness
T ..... T-Distribution Statistic
TEM ..... Transmission Electromagnetic Mode
θ ..... Contact Angle
θ_a ..... Angle of Orientation
μ_r ..... Magnetic Permeability Relative to Copper

μ_r ..... Magnetic Permeability Relative to Copper
μ ..... Average Mean
UHF ..... Ultra-High Frequency
W ..... Filler
w_i ..... Weight Fraction of Composite Constituent
X ..... Polymer
Y ..... Weight % Conductive Filler
Z ..... Test Method
Z_b ..... Surface Impedance
Z_w ..... Wave Impedance

Notes:

1. If the variable has subscript of 'c' it stands for a composite and 'p' is for the polymer.
2. If the variable has a subscript of 1 it stands for the polymer and numbers 2 and greater stand for the filler.

CHAPTER 1: INTRODUCTION

1.1 Introduction

The electrical conductivity of polymers can be increased by the addition of carbon fillers, such as carbon fibers, carbon black and graphite (1, 2, 3). The resulting composites can be used in applications where metals have typically been the materials of choice (4, 5, 6, 7). Engineering thermoplastics have made tremendous inroads into the market for housings used in the electronics, computer and business equipment industries. The trend has also highlighted one of the deficiencies of plastics. Plastics are inherently non-conductive and cannot shield electronics from electromagnetic interference or radio frequency interference (EMI/RMI). They must comply with the Federal Communication Committee's (FCC) regulations governing shielding, because energy emitting sources can be harmful to living things. In addition, plastics cannot protect components from the destructive effects of electrostatic discharge (ESD).

Several conductive fibers such as carbon fibers, nickel-coated graphite fibers, copper fibers, brass fibers, stainless steel fibers, etc. have been used to overcome these deficiencies. The degree of conductivity of the composite depends on the type of conductive filler, filler content and end-use applications or requirements (8). The advantages of using plastic materials include lighter weight, resistance to corrosion and the ability to be readily adapted to the needs of a specific application. By adding conductive fillers to polymers, materials can be designed with specific properties tailored to each application. In order for composites materials to be used for conductive applications, the materials should have an electrical conductivity in the

range of 10^{-12} and 10^{-8} S/cm for ESD applications, 10^{-8} and 10^{-2} S/cm for moderately conductive applications and 10^{-2} S/cm and higher for shielding applications (4, 5, 9). One possible application for electrically conductive resins includes electromagnetic and radio frequency interference (EMI/RFI) shielding for electronic devices, moderately conductive composites for parts such as fuel gauges, and electrostatic dissipation (ESD) (4, 5, 9).

Significant advances have been made in past years in an effort to make EMI-shielded electronic enclosures, with the focus on injection-molded conductive resins. FIBRIL ™ nanotubes are one particular example. Nanotubes are used in automotive painting applications and in fuel systems (43). The primary focus of this research will involve carbon fibers and particles in multiple filler systems. Shielding attenuation will be measured in order to find a successful combination of carbon fillers (8).

Researchers at Michigan Technological University have performed compounding runs followed by injection molding and electrical conductivity testing of carbon-filled resins. Two different polymer matrices were used: nylon 6,6 and polycarbonate. The three carbon fillers investigated included an electrically conductive carbon black (Akzo Nobel's Ketjenblack EC-600 JD), synthetic graphite particles (Conoco's Thermocarb ™ Specialty Graphite), and a milled pitch based carbon fiber (Amoco's ThermalGraph DKD X). Conductive resins containing varying amounts of a single filler were produced. Table 1.1-1 displays the loading levels used in this experiment.

Table 1.1-1: Single Filler Loading Levels for Nylon 6,6 and Polycarbonate

Filler	Loading Levels, wt%
Ketjenblack EC-600 JD	2.5, 4.0, 5.0, 6.0, 7.5, 10.0
Thermocarb™ Specialty Graphite	10.0, 15.0, 20.0, 30.0, 40.0
ThermalGraph DKD X	5.0, 10.0, 15.0, 20.0, 30.0, 40.0

In addition, combinations of fillers were investigated by conducting a full 2^3 factorial design and a complete replicate in each polymer. For all fillers, the low loading level was zero wt%. The high loading level was varied for each filler. The high levels were 5 wt % for Ketjenblack EC-600 JD (CB), 30 wt % for Thermocarb ™ TC-300 Specialty Graphite (TC), and 20 wt % for ThermalGraph DKD X (CF). Table 1.1-2 shows the factorial design filler loadings. Factoral design is discussed in Chapter 8 of this paper.

Table 1.1-2: Factorial Design Formulations for Nylon 6,6 and Polycarbonate

	Ketjenblack EC-600 JD, wt%	**Thermocarb™ Specialty Graphite, wt%**	**ThermalGraph DKD X, wt%**
No filler	0	0	0
CB	5	0	0
TC	0	30	0
CB*TC	5	30	0
CF	0	0	20
CB*CF	5	0	20
TC*CF	0	30	20
CB*TC*CF	5	30	20

The objective of this research is to measure the shielding attenuation of all the carbon-filled resins and then relate the EMI/RFI shielding results to various properties. These include electrical conductivity, filler size, shape, concentration, and orientation.

1.2 Conductivity of Various Materials

The electrical conductivity for pure polymers typically ranges between 10^{-14} and 10^{-17} Siemens/cm (S/cm). Typical electrical conductivity values for other materials are 10^{2} for electrically conductive carbon black, 10^{3} for polyacrylonitrile (PAN)-based, 10^{4} for pitch-based carbon fibers, 10^{5} for high purity synthetic graphite, and 10^{6} for metals such as aluminum and copper. All conductivity values are given in S/cm.

By adding conductive fillers to polymers, materials can be designed with specific properties tailored to each application. In order for composites materials to be used for conductive applications, the materials should have an electrical conductivity in the range of 10^{-12} and 10^{-8} S/cm for ESD applications, 10^{-8} and 10^{-2} S/cm for semi-conductive applications, and 10^{-2} S/cm and higher for EMI/RFI shielding applications (4, 5, 9).

There are numerous examples where conductive fillers have been added to plastics to produce conductive composites. Metal fibers/particles, including aluminum, steel, iron, and copper, and nickel-coated glass fibers have been used (4, 5). Carbon black and carbon fiber have also been used to improve the conductivity of polymers (10). Carbon black fillers have been successfully used to improve electrical conductivity. GE Plastics have introduced a resin based on conductive carbon Fibrils ™ technology (43). These resins can be used for electrostatic painting in automotive parts and it can be used for static dissipation in business machines.

Demand for conductive resins in the U.S. in 1995 was 221 million pounds. Conductive polymer demand in the U.S. is projected to grow 6.1 % annually to 565

million pounds (including both resins and additives) in 2004. Value will reach $1.5 billion, consisting of the cost of resins and additives, as well as labor and other overhead costs incurred during the production of the conductive compound (11). The growth in conductive resin demand is due to stringent regulations on electronic noise and increased sensitivity of electronic parts and components. For example, increased demands for high-speed electronic devices, combined with miniaturization trends, stimulates the demand for EMI/RFI shielding and ESD protection. Smaller, more densely packed electronic components produce more electronic noise, and therefore require more EMI/RFI shielding and are more susceptible to static discharges. Additional conductive resin demand is driven by high levels of static electricity generated by moving parts, such as rollers in copiers and printers, which must be controlled for proper operation.

1.3 Synergistic Effects of Combinations of Fillers

A significant amount of work has been conducted varying the amount of single conductive fillers in a composite material (3, 12, 13, 14, 15, 16). In contrast, very limited work has been conducted concerning the effect of combinations of various types of conductive fillers, such as carbon black, carbon fiber or synthetic graphite on the electrical conductivity of conductive resins and their effect on shielding effectiveness. The electrical resistivity (1/electrical conductivity) results given in Table 1.3-1 have been obtained for conductive nylon 6,6-based resins (17, 18, 19, 20) from previous work completed at MTU. Three different carbon-based fillers were used in this project. One material called Thermocarb™ Specialty Graphite was used.

This material is high-quality milled synthetic graphite that is available from Conoco, Inc. An electrically conductive carbon black was also used since it efficiently imparts its electrical conductivity with a minimum loading. The highly branched, high surface area carbon black structure allows it to contact a large amount of polymer, which results in improved electrical conductivity. The third filler was a PAN-based carbon fiber chopped to 3.2 mm long. This was used to improve the thermal and electrical conductivity, and the tensile strength of the composite.

Table 1.3-1: Prior Results for Nylon 6,6 (17, 18, 19, 20)

Material Number	Description	Actual Wt%		Vol. Elec. Resistivity ohm-cm
19	Nylon 6,6	75	Avg	**13.02**
	Thermocarb	**10**	Standard Deviation (s)	2.85
	Carbon Black	**5**	Samples (n)	12
	3.2 mm long PAN-Based Carbon	**10**		
	Total	100		
Z2	Nylon 6,6	95	Avg	**10^3**
	Carbon Black	**5**	Standard Deviation (s)	-
	Total	100	Samples (n)	5
Z4	Nylon 6,6	90	Avg	**10^{14}**
	Thermocarb	**10**	Standard Deviation (s)	-
	Total	100	Samples (n)	5
Z9	Nylon 6,6	90	Avg	**10^{14}**
	3.2 mm long PAN-Based Carbon	**10**	Standard Deviation (s)	-
	Total	100	Samples (n)	5

The data in Table 1.3-1 show that there is a positive synergistic effect produced by the combination of carbon black, Thermocarb™ Specialty Graphite, and PAN-based carbon fiber, which caused the electrical resistivity to be reduced from 1000 to 13 ohm-cm. The values obtained in Table 1.3-1 are consistent with that available in the open literature for similar amounts of carbon black and PAN-based carbon fiber used

alone in polyethylene, nylon and polyvinyl chloride matrix materials (1, 15, 19). Other researchers have shown that graphite filler at 30-vol% (approximately 40-wt %) used alone with polyethylene and polyvinyl chloride resin produce a material with electrical resistivity of 10^5 ohm-cm (1). Hence, the data in Table 1.3-1 shows it is likely that addition of the electrically conductive carbon black allows for pathways to form with the Thermocarb™ Specialty Graphite and PAN-based carbon fiber which results in enhanced electrical conductivity. A similar synergistic effect between graphite and carbon black in polyacetal and polyimide matrix has been noticed in the past (18, 20). It would appear that the data in Table 1.3-1 contains the first data available in the open literature that shows the effect of three different carbon-based conductive fillers in a conductive resin.

1.4 Electromagnetic Shielding

Plastics are an integral part of the electronics/electrical industry. They are used in packaging, handling, and interconnections. Their increased growth in this industry is proof of their acceptance as a material of preference for design engineers. The inherent property of electrical insulation is a great asset. However, EMI/RFI protection and electrostatic discharge (ESD) protection are also important uses. Therefore, this creates a need for electrically conductive composites. The most widely accepted solution which allows plastics to meet the necessary requirements for EMI/RFI shielding and ESD is to apply a conductive metal coating through a secondary post-molding operation. Conductive metal coatings have proven well in shielding tests, but they have flaws that only plastics can solve.

Zinc spray, nickel paint and electroless nickel painting all provide excellent protection for shielding. The disadvantages of conductive coatings are centered on secondary handling and long-term adhesion. The latter is often cause for concern in terms of reliability. In small intricate parts, the application costs can be extremely high. If the part is very complex, application can be very difficult. Any additional handling caused by secondary molding or handling adds in extra costs (21). By having to coat a surface with many layers of shielded conductive resins becomes very expensive and adds more operations to the manufacturing process.

One advantage of highly conductive plastics as an EMI shield is the elimination of expensive and time consuming secondary coatings, which were necessary at one time (22). A new way of thinking is to incorporate conductive constituents or fillers into the plastic matrix through means of compounding (i.e., extrusion and molding). Conductive composites are easily injection molded into parts and conductive coatings are not needed. Only normal assembly is required. The smaller and more complex the part is, the more favorable the economics for conductive resins. Parts weighing as little as a gram have been EMI-shielded with conductive composites. Conductive composites have a few disadvantages. In some applications, a concern with conductive resins can be the raw material cost and appearance. This can prevent their use in large electronic plastic enclosures such as cathode ray tube housing (21). A goal of this project is to manufacture a cost-effective conductive resin.

1.5 Electrostatic Discharge

ESD is a very complex problem for the electronics industry. ESD protection is needed within the manufacturing process and in packaging to ensure safe deliveries of acceptable electronic devices to the customer. As electronic components become increasingly smaller and have a higher packaging density, the sensitivity to ESD increases. Most malfunctions or non-functioning equipment failures are caused by ESD (23). Today, ESD protection is applied both during production and in transport and handling of most electrical/electronic goods. The problem with ESD damage is that it strikes randomly, sometimes with a sudden mass emergence of faults, and at other times, with sporadic faults. This is all dependent upon the sensitivity of the electronic components.

1.6 Motivation

The rapid growth of electronic devices has resulted in increasing the amount of equipment that emits radiation in the same region of the electromagnetic spectrum as communication broadcasting stations. In order to maintain clear broadcasting signals, the FCC regulates and controls the emissions from electronic devices (FCC 981). The FCC limits emission between 30 MHz and 1 GHz (24). Within this frequency bandwidth are radios, cellular phones and television signals. This range has the most traffic and congestion of signals which leads to interference and signal loss.

Two major advantages of current electronic devices are that they are small and lightweight, which both save space and increase the mobility of the units. Citing a drive by electronics manufacturers to miniaturize products, consolidate parts, and

build in higher levels of electrical conductivity, plastics have introduced the semi-conductive resins (25). Conductive plastics are being integrated into many common electronics devices and the need for semi-conducting and shielding composites is on the rise.

Since the demand for conductive resins is still growing, further research is needed to keep pace and to meet the needs of new, high-tech applications. By combining electrically conductive carbon with lightweight plastics, composites can be formed that provide the electrical properties necessary for various electronic components. Continual research into conductive resins could lead to the production of materials that are increasingly more cost effective than those previously used. By studying the behavior of multiple fillers in a resin, one can determine if a synergistic effect exists that might increase the shielding of a plastic component using a combination of loadings from various materials.

1.7 Project Objectives

The objective of this research project is to study the effects of single and multiple carbon-based filler systems in conductive resins for use in EMI/RFI shielding applications. There is research that documents the shielding attenuation of a single filler type in a conductive resin, but there is very little information on synergistic systems that involve multiple fillers with an application in EMI/RFI shielding. The goal is to make a less expensive, more efficient composite that can meet current market demand for applications in EMI/RFI shielding.

CHAPTER 2: ELECTRICAL CONDUCTIVITY

2.1 Introduction

It has been previously discussed that the demand for conductive resins for use in high-tech applications is growing. To fully understand the usefulness of these materials, it is necessary to develop fundamental knowledge of the factors that control composite conductivity. This would include studying the basic principles of composite conductivity, in addition to understanding how different constituent material properties could change the conductivity values and hence, affect the EMI/RFI shielding. This information must then be applied to the development of new composites for use in shielding applications.

One way to understand conductive resins is to use electrical conductivity models. Using accurate models can be an advantage for several reasons. Models can allow for more efficient materials design through the targeting of a specific conductivity range, which could also reduce costly material use and time. Therefore, understanding the mechanisms that control conductivity will help us understand how the conductivity affects the composite's shielding effectiveness.

2.2 Percolation Theory and Electrical Conductivity

The electrical conductivity of a composite is generally characterized by its dependence on filler volume fraction. As the filler amount in the composite is increased, the filler particles begin to contact each other and a continuous path is

formed through the volume of the sample for electrons to travel. The formation of this conductive network is based on the principles of percolation theory.

The beginnings of percolation theory are attributed to Hammersley and Broadbent in 1957 (26). It was introduced to show how the random properties of a "medium" influence the spread of "fluid" through it. Fluid and medium can take on several definitions here, including a solute diffusing through a solvent, molecules penetrating a porous solid, a fire spreading through a forest, and the flow of electrons through an atomic lattice. This theory was proposed as an alternative to random mechanisms that were typically associated with a flow process within a diffusion process.

One example laid out by Hammersley and Broadbent was that of a system of channels (Figure 2.1-1). Each channel divides into two new channels, and each has the probability q of being dammed. This random set of dams will thus determine how a fluid will spread through the network of channels. This is a percolation process. This is also known as bond percolation. This process can be described as a fluid flowing through interconnected pipes, which are the bonds. The fluid (Figure 2.2-1) has a continuous path of bonds to travel through the channel network.

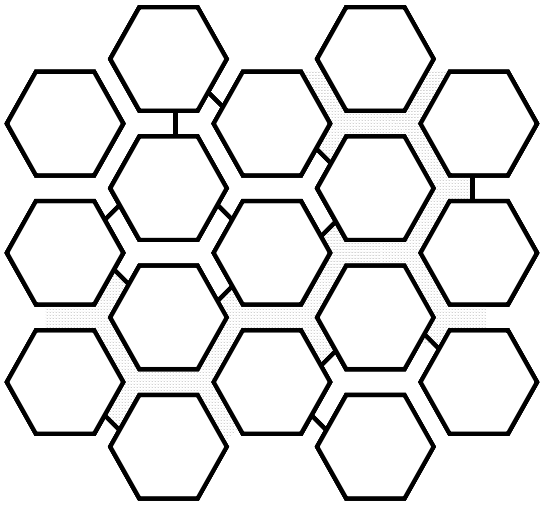

Figure 2.2-1: Percolation of a Porous Medium That is Modeled as a Network of Interconnected Channels (52)

Another way to view percolation theory is to visualize a large array of squares, as described by Stauffer (27). This is shown in Figure 2.2-2 (A). Panel (B) shows a portion of the squares occupied by dots, with clusters of these dots outlined in panel (C). Percolation theory is used to describe the number and properties of these clusters, and is defined here as site percolation. The dots are randomly distributed within the lattice, and there is a probability, p, that a site will be occupied by a dot. At a certain probability, there will be a cluster than extends from, in the case of a square lattice, top to bottom and left to right. This cluster is said to be percolating through the system. There is a specific concentration at which this cluster is formed, and it is called the percolation threshold, denoted by ϕ_c.

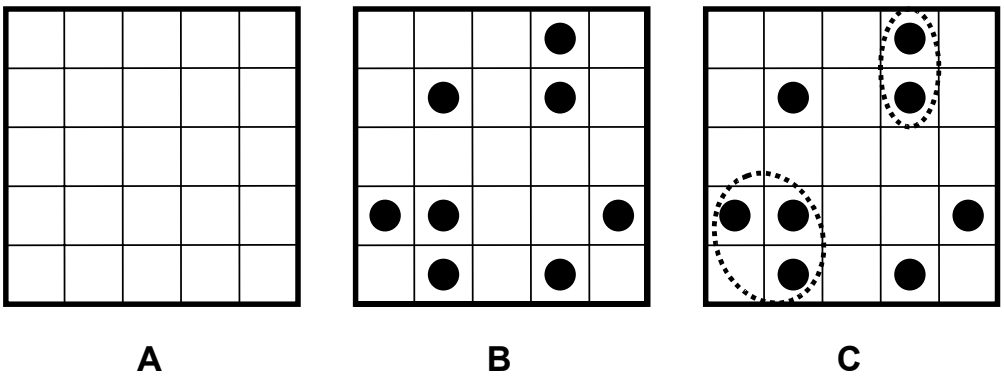

Figure 2.2-2: Square Lattice With Some Squares Occupied by Dots With Clusters Circled (52)

Stauffer applied this to forest fires as a simple way to explain the idea of a percolation threshold. The question posed in this example was, "How long does a forest fire take to either penetrate the forest or to be extinguished?" Since it would take a significant number of fires to answer this question with minimal statistical error, the problem was carried out on a computer. A large square lattice similar to that in Figure 2.2-2 (A) will represent the forest. The probability that an individual square would be occupied by a dot, or tree, is p. The probability is $(1-p)$ that a site would be empty. If $p = 1$, each site would be occupied by a tree.

The trees in the first column on the left of the matrix are allowed to burn, whereas the remaining trees are not. It must then be determined if the fire on this one side can move through the entire forest to the last column on the right. In order for the fire to spread, there must be a neighboring tree present. If there is no tree for the fire to spread to, the forest fire is terminated. The lifetime of the forest fire is defined as how many sweeps it takes on each successive column to reach termination. It is at the percolation threshold when this termination occurs at the last column, and the fire has penetrated through the entire forest (27).

An analysis similar to that of the water in the channels can be applied to conductive resins in describing electrical conductivity. The conductive fillers, such as carbon fibers, act as channels for the electrons to flow through. The electrons are free to flow through the carbon fibers. However, once they reach the end of the fiber, they encounter the polymer matrix, which acts as dam, blocking the flow of the electrons. Once enough filler has been added, the carbon fibers begin to come in contact with each other, forming a complete path for the electrons to travel throughout the full volume of the composite.

In general, there are three main regions that control the conductivity of filled-polymer composites. The dependence of conductivity on volume fraction is illustrated in Figure 2.2-3. At low filler loadings, shown in Region A in Figure 2.2-3, the conductivity of the composite is still very close to that of the pure polymer matrix. At critical loading the percolation threshold is reached. This means that enough filler has been added to form a continuous conductive network through the composite. Following the percolation threshold is a region that produces a significant increase in conductivity with very little increase in filler amount, as displayed by Region B. After this region of drastic increase, the conductivity again levels off, and approaches that of the filler material. This occurs because the conductive network through the sample is complete, and the electrons are following the path created by the connected filler particles. This is depicted in Region C of Figure 2.2-3.

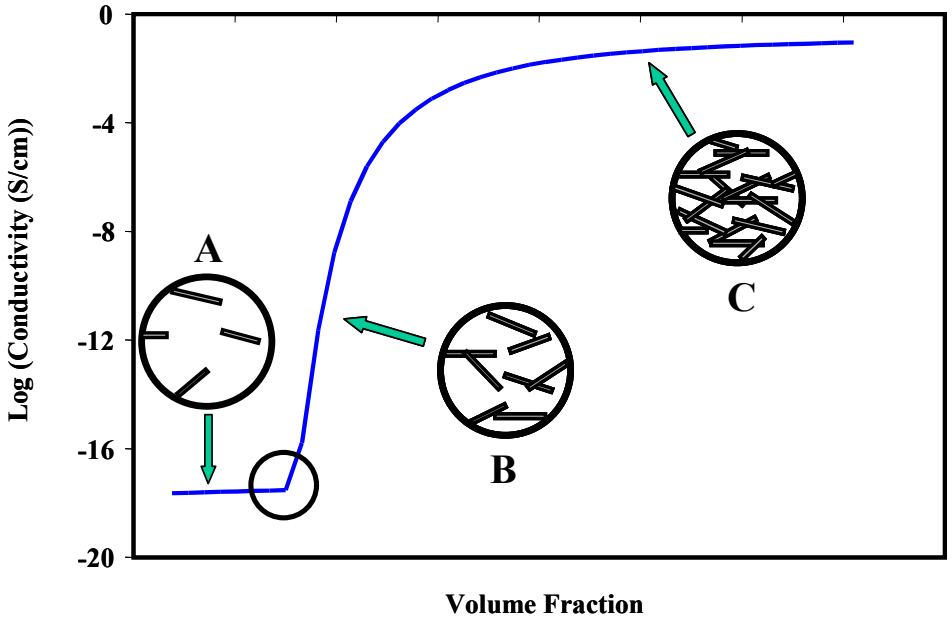

Figure 2.2-3: Dependence of Electrical Conductivity on Filler Volume Fraction (52)

There are several factors that can have a significant effect on where the percolation threshold lies and the plateau conductivity level. In addition, various models have been proposed in an effort to predict the electrical conductivity behavior of composites based on numerous factors. While the majority of the models base the calculations on filler volume fraction, other factors can affect the conductivity of the composite. These same factors can also affect the volume fraction at which the percolation threshold occurs. These properties will vary in carbon black and other carbon-based fibers.

It has been observed that a trend in conductivity with the addition of conductive carbon black to the polymer is a non-linear relationship and it was observed that for up to 5 wt % carbon black the composite is not sensitive to loading, but it is still insulating as a polymer. This is confirmed by examining our model in Figure 2.2-3 (28).

It has been suggested that to transfer electrons through the conductive resin, there must be less than 10 nm between the particles. As the carbon black concentration increases interconnection between the particles occur and the conductivity starts to rise sharply. The ability in which electrons can hop across a physical gap increases exponentially with decreasing distance between particles. An average of two contacts per particle is needed to produce an electrically conductive network (29). Once a continuous conductive network is formed, percolation occurs near 10.0 wt % carbon black (28). It can be rationalized that the conductivity will increase as more carbon black filler is added. Hence, stabilizing of the network is occurring. When such a network is formed, the composite changes from an insulator to a conductor over a narrow range of increasing filler concentrations as shown in Figure 2.2-3. The volume resistivity of the composite changes by as many as 12 orders of magnitude during this transition period.

Carbon polymer composites have been shown to be good model materials for studying the isotropic percolative conduction when spherical carbon particles are used. Research that determined the influence of particle shape on percolation by using short carbon fibers as particles, the length of which being varied as desired in the millimeter range and oriented at random, has been done by Carmona et al. (30).

They determined that the onset of electrical conduction, percolation threshold, is related to the existence of an infinite chain of connected particles. In the case of carbon black spheres, there is a limited number of possible contacts per particle. There are only so many spheres that can be touching at any one given time. ThermalGraph DKD X consists of long, rod-shaped fibers. When considering long

disordered rods, the number of rods can be very high depending on the L/D Ratio. Where (D) is the diameter of the rod and L is the length of the fiber. Assuming that a given number of particles per unit volume N, the possibility of forming an infinite chain depends directly on the lengths of the fibers (30).

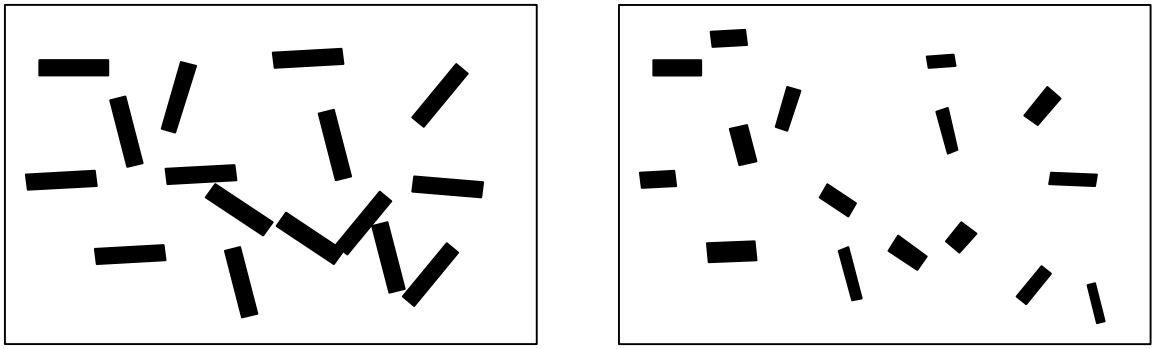

(A) **(B)**

Figure 2.2-4: Conductivity Diagram of Carbon Rods

In Figure 2.2-4 (A), the rods have a large L/D ratio and have a better chance of touching and therefore, conduction between rods will occur. In Figure 2.2-4 (B), the same number of rods are present, but they have smaller L/D ratios. The chance of a conductive network being formed decreases as this ratio gets smaller and the number of particles or rods remain the same.

2.3 Factors Affecting Electrical Conductivity

The properties of the filler play a significant role in determining the conductivity of the composite. Carbon, when used as filler, comes in many different forms, from small carbon particles to graphite fibers, and the conductivity of each is different. Typical electrical conductivity values for other materials are 10^2 for electrically

conductive carbon black, 10^3 for polyacrylonitrile (PAN) based carbon fibers, 10^4 for pitch-based carbon fibers, and 10^5 for high purity synthetic graphite. All conductivity values are given in S/cm. The value for filler conductivity will be the upper limit for the electrical conductivity of the composite.

Other filler properties, such as particle size, can also have an effect on the electrical conductivity. It has been shown that for spherical particles, smaller particle size will lower the percolation threshold (31). It has also been shown that an aspect ratio (ratio of length to diameter, L/D) greater than one, as well as a broader range of aspect ratios, will lower the percolation threshold (32, 33, 34). In this case, other properties of the filler should be taken into consideration when choosing the right filler for the application.

Another important item for consideration is the method by which the composites are made and subsequently molded into parts. There are several studies that show the effects that filler orientation has on the electrical conductivity of composites and how this effect can be quantified (35, 36, 37, 38, 39, 40). Extrusion and injection molding of a composite can align fillers that have an aspect ratio (AR=L/D) greater than one in a certain direction due to the flow through the nozzle of the different machines and the mold. This alignment will produce anisotropic conductivity within the sample, meaning that conductivity will be greater in one direction over another.

The surface properties of the filler and polymer also have a significant effect on the conductivity and the percolation threshold of the composite. The surface free energies of the filler and matrix will influence the interaction between two materials. How well the polymer wets the surface of the filler can be quantified by the

difference between the surface energies of the two materials. Mamunya showed that smaller differences between the two surface energies lead to better wetting of the filler by the polymer (41). Therefore, better wetting of the filler can improve its dispersion within the matrix material. While this can increase the percolation threshold of the composite, it can also improve the overall conductivity of the composite. In general, a smaller difference between the surface energy of the filler and polymer is desirable to obtain high composite electrical conductivity.

CHAPTER 3: SHIELDING THEORY

3.1 Introduction

Conventional plastics are electrically insulating and transparent to electromagnetic radiation. The primary requirement a material must have to be a shield against electromagnetic radiation interference, commonly called EMI, is that it be electrically conductive. As a result there has been considerable interest in developing moldable, electrically conductive plastic compounds. As a result of developments in this area, a number of electrically conductive fillers are available which will produce plastic parts having sufficient conductivity to act as EMI shields. These fillers include carbon black, carbon fibers and metal fibers.

There is a considerable difference in the composition of conductive molding compounds and coatings. While it is desirable to minimize the concentration of filler used as a conductive coating, it is essential to do so in a molding compound. Since high levels of filler will increase the cost of a molded compound, this increases the weight of the molded part and significantly increases molding problems (24).

Conductive fillers currently being used in molding compounds produce conductive resins at low filler loadings by virtue of the geometrical characteristics of the filler particles. The filler particles all have a measurable aspect ratio. By having a large aspect ratio, a conductive network within the matrix will form. In order to minimize filler concentration in a conductive compound, it is important to maintain the aspect ratio of the filler. Aspect ratio is equal to the length of filler divided by the filler diameter (24).

3.2 What is Electromagnetic Interference (EMI)?

EMI is a kind of environmental pollution. With the national emphasis today on the elimination or reduction of environmental pollution, most people readily recognize and understand water, air, noise and other forms of pollution. Most people probably have not heard or know much about spectrum pollution. It cannot be directly seen, tasted, smelled, or felt. Therefore, how can it be a problem?

It is readily known that certain types of electronic devices will jam household radios. The resulting buzzing or crackling noise results in the inability to listen to the radio while the device is in use. Conducted or radiated electrical noise jams radios picking up broadcast signals or cellular phones trying to make calls. Another example is an unsuppressed automobile idling outside of a house causing interference to the television picture in the house by blotching, developing intermittent dash lines or even total loss of the picture. Electrical noises from radiated automobile ignition systems cause these problems.

More serious examples of spectrum pollution are evident if a person with a pacemaker is near certain electronic devices that emit radiation. Microwaves and many appliances are devices that give off these energy waves. These are characterized as radio frequency (RF) energy emitting sources, which can cause medical devices, such as a pacemaker, to operate improperly with results that can be deadly. High electrical interference or noise background can interfere or cause crossing of communication lines. In the business community these problems could cause adverse effects on electronic transactions. EMI/RFI can be a serious threat in our modern day and age of information technology

The spectrum pollution problem can affect human life and the global economy (49). Thus, EMI/RFI is giving rise to spectrum pollution and it is indeed of national concern even though many do not readily perceive it as a problem. Fortunately, the government and certain industries have specifications and regulations on electrical, electrochemical, electro-mechanical, and electronic equipment. However, enforcing these regulations is difficult. Many commercial goods may have to meet a regulation when they are purchased, but many consumers modify these devices to their own needs or desires.

3.2.1 Basics of Frequency Spectrum Use

Unlike water and air pollution problems, there is only one frequency spectrum for all of us to use. There exists no other natural resource to substitute or replacement for the spectrum. Thus, in many respects the problem is severe. The rate of intentional and unintentional electrical and electronic noise is doubling every 10 years (49). A few scientists are predicting by the year 2010 that our society would collapse due to EMI/RFI problems. This may sound far-fetched, but it is a realistic concern.

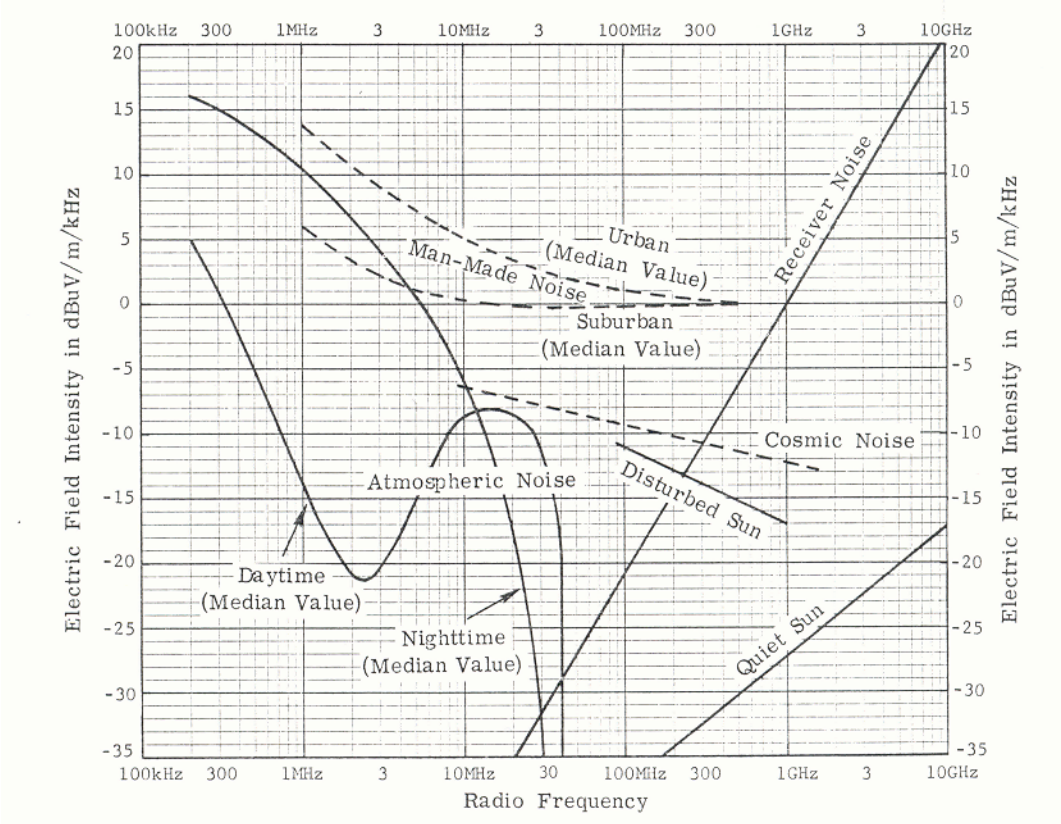

Figure 3.2-1: Summary of Electromagnetic Noise Sources and Levels (24)

Figure 3.2-1 summarizes many of the above sources of electromagnetic noise over five decades or 16 octaves of the frequency spectrum from 100 kHz to 10 GHz. All the communications (electronics, scientific, industrial, medical and man-made noise) are grouped together under the categories of urban and suburban. Non-man-made noise consists primarily of atmospheric origin below approximately 10 MHz. This noise originates primarily from lightning or electrical source storms in the lower latitudes, which propagate around the Earth by wave-guide action between the ionosphere and the ground. Cosmic noise comes from the galaxy (excluding the sun) and the solar radiation is shown for both the quiet sun and disturbed sun. This occurs

from sunspots and solar flares. The sun goes though cycles and this year, 2002, is a peak year for solar flares.

Figure 3.2-2 illustrates the three basic elements required to produce EMI. They consist of electrical noise emitters, propagation media and receptors as the necessary but not sufficient conditions required to produce either degradation or malfunction in receptors. The method of coupling between emitters and receptors of electrical noise are divided between radiation (space separation with no-hard line connection) and conduction such as through wires or cables.

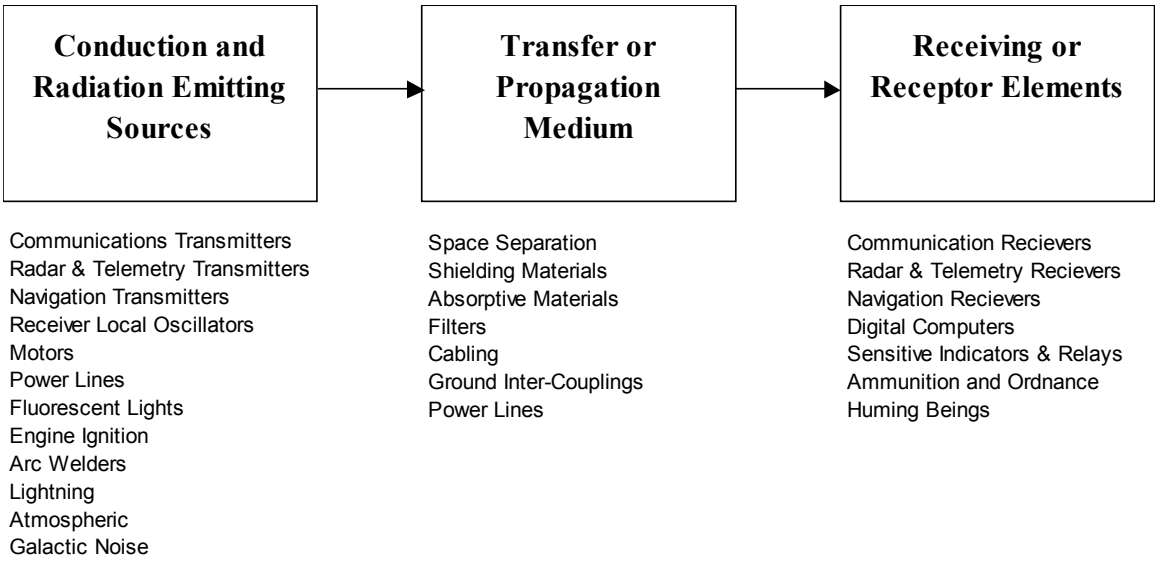

Figure 3.2-2: Basic Elements of Electromagnetic Interference (49)

In order to obtain a mental picture of the frequency spectrum, Figure 3.2-3 illustrates the nominal frequency assignment to those communications electronics devices, which intentionally radiate. The spectrum portrait covers from below power line frequencies at 60 Hz to some scientific devices and radars operating at 40 GHz.

When this is overlaid with the large amounts of unintentional radiations, it is readily seen that the spectrum crowding and pollution problem is reaching threatening proportions (49).

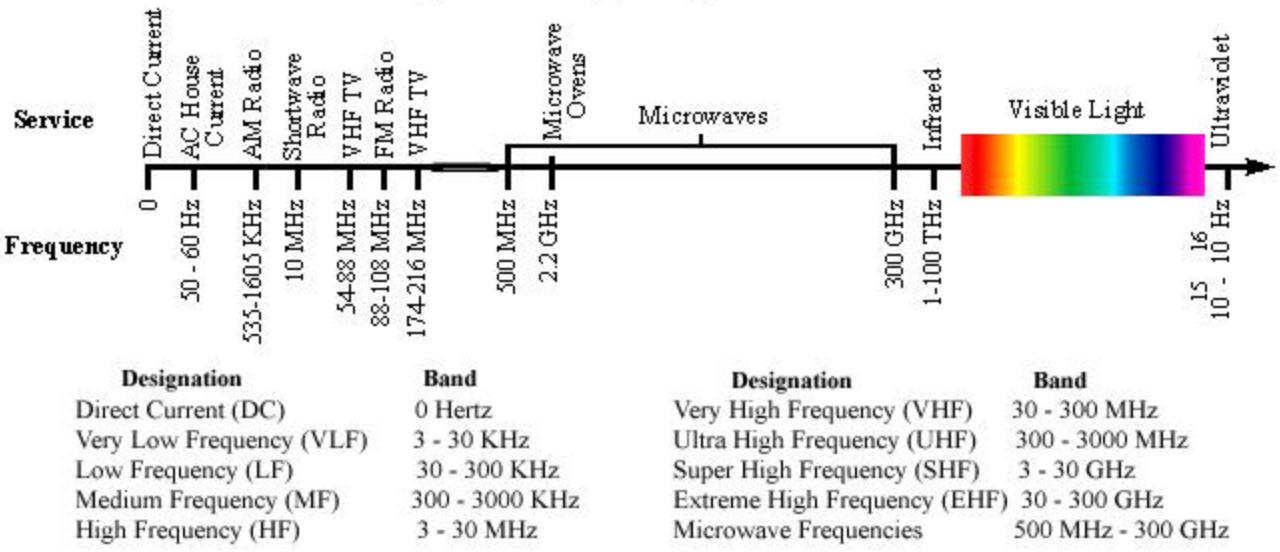

Designation	Band	Designation	Band
Direct Current (DC)	0 Hertz	Very High Frequency (VHF)	30 - 300 MHz
Very Low Frequency (VLF)	3 - 30 KHz	Ultra High Frequency (UHF)	300 - 3000 MHz
Low Frequency (LF)	30 - 300 KHz	Super High Frequency (SHF)	3 - 30 GHz
Medium Frequency (MF)	300 - 3000 KHz	Extreme High Frequency (EHF)	30 - 300 GHz
High Frequency (HF)	3 - 30 MHz	Microwave Frequencies	500 MHz - 300 GHz

Figure 3.2-3: The Frequency Spectrum

A unique characteristic of pollution of the radio frequency spectrum, which is not a characteristic of air, water and land pollution, is that upon removal of the sources of pollution, the spectrum is instantly available to serve again at its maximum efficiency. However, the large number of problem sources involved in spectrum pollution makes this difficult to realistically implement or capitalize upon.

3.3 Requirements for Shielding

A material is shielded if the surface of the material is electrically conductive enough to shield against influence from outer fields. Normally this only applies to electric fields, while magnetic fields require completely different precautions, such as thicker material, a sealed package, etc. as shown below.

a) Shielding against electrostatic fields
b) Protection against direct charge
c) Static discharge through contact with grounded conductors: a minimum build-up of electrostatic discharging through friction.

Electrical conductivity is necessary but not a sufficient condition to provide signal attenuation. Bigg states that a material must have a volume resistivity of 2 ohm-cm or less to provide a minimum of 30 dB attenuation (29). 30 dB of attenuation stops 99.9 % of an impinging signal. 20 dB to 30 dB of attenuation is considered acceptable for most industrial and consumer applications. Table 3.3-1 shows how much attenuation is blocked at given shielding effectiveness. According to Bigg (29), the higher level of conductivity beyond the transition from insulator to conductor implies that the particles in the network be either closer together or have more contacts per particle or both. As the concentration of the filler increases in a composite both situations occur. With the larger size filler particles, actual physical contact is believed to exist between adjacent particles, while very small particles do not necessarily touch. Since the mechanism for inducing conductivity in a polymer is not a bulk effect but depends on the existence of a continuous network, any external influence, which serves to separate or increase the distance between neighboring particles, will negatively affect the bulk conductivity of the material (29).

Table 3.3-1: Shielding Effectiveness and % Attenuation

SE (dB)	Attenuation %
20	99
30	99.9
40	99.99
50	99.999
60	99.9999
70	99.99999

3.4 Compounding Considerations for Shielding

Engineering thermoplastics, which electrically conduct through the use of carbon fillers, were considered in this paper. The fillers are usually particles or fibers. Factors that influence electrical properties are the following:

a) Aspect ratio of the filler
b) Processing
c) Conductivity of the filler
d) Amount of filler
e) Resin matrix

For grounding or preventing charges on a plastic surface, a composite that exhibits 10^3 to 10^{10} ohms/sq surface resistivity is considered excellent (See FTS 101 C, Method 4046 – static decay rates) (21). For finding a level of acceptable performance for conductivity which can be used in EMI/RFI shielding applications, one must pay close attention to the guidelines.

Correlation between the volume resistivity of a conductive composite and its shielding effectiveness has shown that a volume resistivity of approximately 1.0 ohm-cm to 2.0 ohm-cm should produce a composite with 20 to 30 db of shielding attenuation (29). The exact performance will vary depending on the type of

conductive filler present. The type and viscosity of the polymer will also affect conductivity (21).

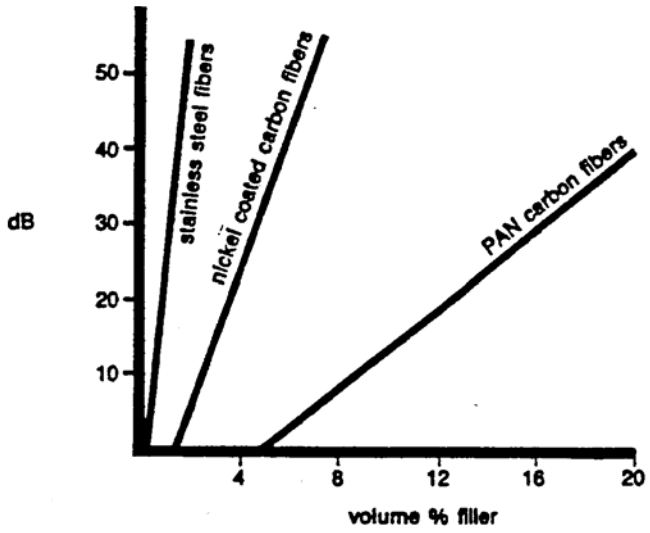

Figure 3.4-1: Shielding Effectiveness (dB) vs. Volume % of Filler (21)

Figure 3.4-1 demonstrates the general relationship between fiber loading and average dB of shielding (21). The more fiber present causes more conductivity and therefore, a greater shielding effectiveness. The question is how much fiber is required to provide consistent performance for shielding. Notice how metal fiber composites outperform carbon-based fiber composites at low loading levels. The shielding test used in this thesis can only be used as a relative comparison tool versus other samples in a laboratory setting.

It has been shown that PAN fibers offer the greatest strength in a composite matrix (21). Metal fibers have less mold shrinkage than carbon-based fibers and have high shielding in nylon, but low shielding in polycarbonate. The high viscosity of polycarbonate versus nylon 6,6 causes metal fiber breakage and increased shear (21).

Stainless steel fibers have good shielding properties and are traditionally used. There are two main reasons. First, the long fiber process for compounding these materials and secondly, having proper molding conditions to maintain fiber length (21). Carbon fibers experience considerable damage during processing so it is important to minimize this. By controlling process conditions, you can control the fiber lengths.

Carbon fibers offer the best mechanical reinforcement while having a moderate conductivity. Nickel-coated graphite fibers offer the most conductivity and potential for shielding but lack easy processing (21). Stainless steel fibers are efficient in producing adequate conductivity. Loading levels of stainless steel from 5% wt to 7% wt are currently being used in industry (21).

Stainless steel offers minimal mold shrinkage, but difficult processing. Carbon fibers were chosen for this project because of easy processing. Using metal-filled surface coatings is still prevalent in large volume shielding applications. Cathode ray tubes (CRT), keyboards, computer housings, and cellular phone casings are industries that were once dominated by metal enclosures. Thermoplastics are overtaking metals in these applications and also creating new markets.

Conductive composites, when used for small complex parts, have been found to be effective in cost and performance. Their use in injection-molded composites is on the rise. Conductive composites have the potential for a significant market share if the processing cost proves to be lower than that of current standards (21). Currently, plastic-molded parts are volume dependent for case-by-case scenarios. By compounding plastics with carbon fibers and being able to match current market

applications for metal-based composites, only then will injection-molded plastics have more widespread use.

3.5 Direct Method

ASTM Standard D4935-89 was used to measure shielding effectiveness in this thesis. Please refer to the experimental method outlined in Chapter 6.6 for a full explanation of the method. The direct method allows for a real time reading of the shielding effectiveness for any material inserted in the test apparatus. By taking the difference of a known reference sample and a load sample, the relative shielding effectiveness of a carbon-filled composite can be calculated. All calculations for shielding effectiveness were based on the direct method. The theoretical method was examined for modeling purposes only in Chapter 9.6.

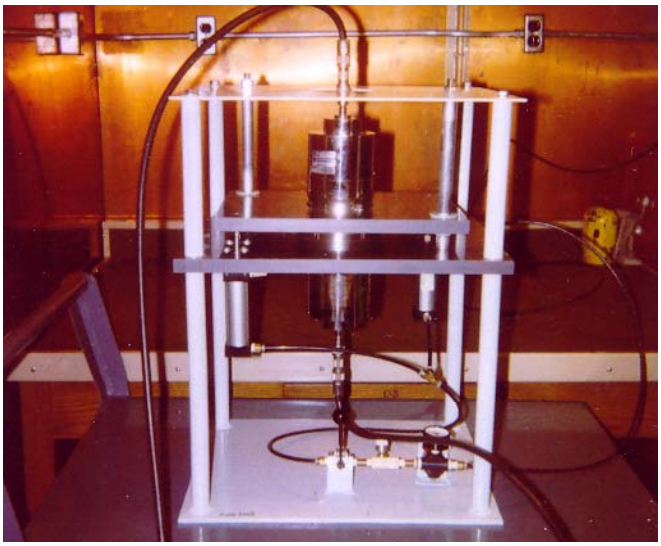

Figure 3.5-1: Direct Method Shielding Set-Up

3.6 Theoretical Method

The relationship between shielding effectiveness and the resistivity of a conductive compound can be obtained by considering what happens when a plane wave impinges on a planar material. Shielding provided by a metallic or composite barrier can be analyzed from either one of two viewpoints, wave theory or circuit theory (49). In the circuit-theory approach, currents from the interference source induce currents in the shield such that the associated external fields due to both currents are out of phase and tend to cancel. The wave theory approach will be used in this thesis since it is more widely accepted in open literature. In this thesis samples of heterogeneous material that consisted of carbon fillers in a composite resin were used. In the wave theory it is assumed that the material is electrically conductive at all points and the material is modeled as a solid planar metal. This way one can understand the way energy and waves are being absorbed and reflected by the solid metal barrier.

Figure 3.6-1 depicts the phenomena of both reflection and transmission that are utilized in removing energy from an incident wave (plane wave example shown). If an incident plane wave is intercepted by a barrier to its passage at the Region A of the interference, both reflection and transmission error occur. The amplitudes of these two portions of the original wave depend on the surface impedance of the barrier material with respect to the impendence of the wave. Since the reflected wave is not proceeding in a direction that contributes to the surviving wave on the far side of the barrier, this is considered a loss mechanism (49).

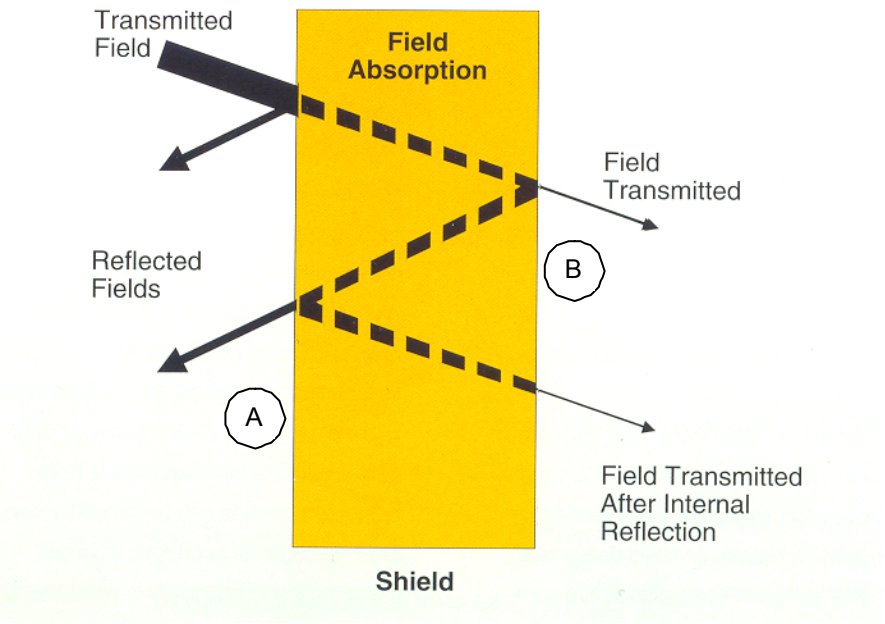

Figure 3.6-1: Representation of Shielding Phenomena for Plane Waves through a Homogeneous Metal Barrier (49)

The transmitted portion of the incident wave, continuing on in approximately the same direction after penetrating the interface, experiences absorption while traversing the finite thickness of the material barrier. At the second material barrier interface B of Figure 3.6-1, reflection and transmission phenomena again occur. The transmitted portion is the amount of energy that traversed the first interface less the energy absorbed in traversing the barrier and the reflected at B. The second reflection contributes an insignificant amount in the removal of energy and is usually neglected (49).

At plane-view (far-field) frequencies, the shielding effectiveness of a barrier in reducing the energy of an electromagnetic field can be readily computed. Each of the contributing factors discussed above is computed separately and their total

contribution is summarized. This is accomplished in the following manner for expressing shielding effectiveness in dB (S_{dB}) (49).

$$S_{dB} = R_{dB} + A_{dB} + B_{dB} \qquad \text{Equation 3.6-1}$$

R_{dB} = Reflection loss in dB
A_{dB} = Transmission or absorption loss in dB
B_{dB} = Internal reflection loss at exiting interface in dB (usually neglected)
S_{dB} = Shielding Effectiveness in dB

The shielding effectiveness to electric or electromagnetic fields may also be measured in terms of the fraction of the impinging field, which exists at the other side of the barrier (49).

$$S_{dB} = 20 * Log_{10}(\frac{E_1}{E_2}) \qquad \text{Equation 3.6-2}$$

E_1 = Impinging field intensity in V/m
E_2 = Exiting field intensity in V/m
S_{dB} = Shielding Effectiveness in dB

The absorption loss, (A_{dB}) is independent of the type of wave impinging on the shield and is expressed as follows (49).

$$A_{dB} = 3.34 * 10^{-3} * t\sqrt{f * G\mu} \qquad \text{Equation 3.6-3}$$

$$A_{dB} = 3.34 * t\sqrt{f(MHz) * G\mu}$$

A = Attenuation in dB
t = Thickness of barrier in mils (unit of 0.001")
f = Frequency in Hz
f_{MHz} = Frequency in MHz
G = Conductivity, relative to copper (G for Cu =1)
μ = Magnetic permeability of material relative to vacuum or copper ($\mu = 1$)

Absorption loss is the dependent variable and frequency is the independent variable with the thickness in mills as a second parameter.

The internal reflection loss B in equation 3.6-1 is negligible when A_{dB} is greater than about 4 dB. When A_{dB} is not greater than 4 dB, B_{dB} is negative since it is a coherent term which would have made E_2 in equation 3.6-2 is larger. Reflection loss, (R_{dB}) is represented by forming the ratio of the wave impedance (Z_W) to the surface impedance of the barrier material (Z_b) (49). Wave impedance is the total passive opposition offered to the flow of electric current. It is determined by the particular combination of resistance, inductive reactance, and capacitive reactance in a given circuit system and is a function of frequency.

$$R_{dB} = 20 * Log_{10} \frac{(K+1)^2}{4K} \qquad \text{Equation 3.6-4}$$

$$R_{dB} \approx 20 Log_{10} (\frac{Z_W}{4Z_b}) \quad \text{For } K \geq 10$$

Equation 3.6-4 indicates that if either the wave impedance is high (electric field) and/or the barrier surface impendence is low (copper), the loss will be substantial. Conversely, if the wave impedance is low (magnetic field) and/or the barrier impedance is relatively high (iron), the reflection loss will be significantly less. The reflection loss of a plane wave R_{dB} may also be calculated from the equation below.

$$R_{dB} = 108 + 10 * Log_{10} (\frac{G}{\mu * f_{MHz}}) \qquad \text{Equation 3.6-5 (49)}$$

Compared with absorption loss, the reflection loss of plane waves at low frequencies is the major attenuation mechanism. High conductivity, low permeability material is more effective in establishing reflection loss, since the barrier surface impedance is lower with regard to that of a plane wave. At ultra-high frequency (UHF), the reflection loss becomes less effective since the barrier skin depth decreases (surface resistvity increases) and the barrier impedance increases resulting in a smaller ratio of the plane wave to the barrier impedance.

When there is a substantial difference in the impedance of the incident wave and the shielding barrier, reflection at the boundary is significant and good shielding is obtained. The high impendence wave in the near field is known as an electric-field wave, and its reflection loss is shown in Equation 3.6-6 (49).

$$R_{dB} = 354 + 10Log_{10}\left(\frac{G}{f^3 * \mu * r^2}\right) \qquad \text{Equation 3.6-6}$$

$r =$ Distance from source to barrier in inches

The frequency is the independent variable and reflection loss (R_{dB}) is the dependent variable. For low impedance or magnetic field waves, the reflection loss is Equation 3.6-7 (49).

$$R_{dB} = 20 * Log_{10}\left[\left(\frac{0.462}{r}\right)\sqrt{\frac{\mu}{f * G}} + 0.136 * r\sqrt{\frac{G * f}{\mu}} + 0.354\right] \qquad \text{Equation 3.6-7}$$

The reflection loss of a magnetic field increases with frequency until the source to barrier separation distance is about ($\frac{\lambda}{2\pi}$) (49). Bushko determined that the conductivity of a material can be used to roughly estimate far field shielding values of planar materials according to the widely accepted industry formula. The formula in Equation 3.6-8 is a simplified form of the White derivation for planar materials (73).

$$S_{eff} = 3.34t\sqrt{f\mu_r\sigma_r} + 168 - 10 * Log_{10}\left(\frac{f\mu_r}{\sigma_r}\right) \qquad \text{Equation 3.6-8}$$

$t =$ Thickness of material in inches
$f =$ Frequency in Hz
$\sigma_r =$ Electrical conductivity relative to copper; [For copper, ($5.87*10^{-5}$ S/cm)]
$\mu_r =$ Permeability relative to copper
$S_{eff} =$ Shielding Effectiveness in dB

The above equation is a variation of the equation derived by White in 1979 for homogeneous materials (49). It also explained by Bigg (24). Bushko (73) tried to prove its irrelevance to shielding at low and moderate electrical conductivity levels for heterogeneous composites. Composites containing fillers are difficult to model due to the complexity of the material and the particles contained in them. Trying to repeatedly process material exactly each time under the same conditions and model the system is difficult. Equation 3.6-8 has been only proven for homogenous materials, mostly metals (73). The purpose of its use here is to see how good of an estimator it actually is compared to experimental results. Values obtained using the direct method (ASTM D 4935-89) will be compared to theoretical values calculated

from experimentally measured electrical conductivities. Refer to Chapter 9.6 for a full discussion of shielding effectiveness results and their comparison to theory.

3.7 Shielding Apparatus Selection

Measurement of shielding effectiveness (SE) of plastic materials is difficult due to the insulating nature of many plastics. A method of making these measurements using a flanged coaxial holder overcomes these limitations. Equation 3.7-1 is used to determine shielding effectiveness according to ASTM D4935-89. There are a number of methods for evaluating shielding either in use or in development. There are problems both in making measurements and interpreting results. It is important to compare materials tested using the shielding effectiveness test under the same conditions. The FCC requires extensive testing on incidental radiation regulations on whole products and systems.

$$S_{dB} = 10 * Log_{10}\left(\frac{P_2}{P_1}\right) \qquad \text{Equation 3.7-1}$$

P_2 = Power levels with and without a sample material present in dB
P_1 = Power levels with and without a sample material present in dB
S_{dB} = Shielding Effectiveness in dB

Conditions such as angle of incidence and polarization of waves are often omitted or are not known but are essential factors in influencing P_2 and P_1. There are five commonly used methods to determine SE, shown below:

1. MIL-STD 285
2. Dual Transverse Electromagnetic (TEM) Cell
3. Flanged coaxial holder (ASTM D4395-89)
4. A time domain measurement system in free space.
5. A time domain measurement system through an aperture or a shielded room.

3.7.1 The MIL-STD 285

This method measures continuous waves (CW) through an aperture of a shielded room (Modified MIL-STD 285). The multitude of resonance within the room and resonance of the aperture cause such a wide range of values over short frequency intervals that, only after taking millions of measurements and averaging data, can any useful information be resulted. This is very time consuming and costly.

3.7.2 Dual Transverse Electromagnetic (TEM) Cell

The dual cell (TEM) is useful for measurements with the electric field (E) normal to the surface of the material and for frequencies up to occurrence of modes of higher orders than the TEM modes. The upper frequency is a function of the size of the TEM cell (50). A major limitation and problem is the variation in measured data due to contact resistance. Many materials, especially those made from plastic, give large variations in contact resistance. This is also a problem for some other measurement systems.

3.7.3 Flanged Coaxial Holder (ASTM D4935-89)

There are several variations of a flanged coaxial holder. Some designs require electrical contact with both inner and outer conductors, since the measurement relies on conduction current. Other methods that allow insertion of a sample between

flanges of a transmission line can depend on displacement current. This method is the most effective way for measurement of insulating samples. Additional steps must be taken to prevent leakage and to account for the transmission line perturbation caused by insertion of a sample. Plastic bushings around the apparatus must be used to direct the flow of electrons away from the test fixture. Normally, nylon or Teflon™ insulators are used.

This method seems to give the best results between 10 MHz to 1000 MHz. At frequencies below 10 MHz, compensation for transmission perturbation becomes larger and difficult to deal with. At frequencies above 1 GHz, higher order modes cause problems with measurements (50). Coaxial holder has the greatest potential for giving repeatable measured values as done in ASTM D4935-89. The results for homogeneous materials compare favorably with theoretical values (49).

3.7.4 A Time Domain Measurement System (Closed and Free Space)

For time domain techniques sub-nanosecond pulses are obtained to provide SE information from 100 MHz to 4 GHz. The pulses are received and filtered to eliminate unwanted diffracted and reflected signals. A Fourier transform on the received pulse shapes is performed with the sample present, and then again without the sample present. A comparison can be made on the spectrum that is being evaluated to determine shielding effectiveness.

The first time-domain technique requires samples larger than 1 meter square so a direct signal path can be established and separated from the diffracted signal coming around the material. The direct difference in spectra response gives SE value (50).

The second method involves a small 10 cm sample over an aperture consisting of a fully shielded room, or a large planar metal sheet. SE values are measured but are subject to error from aperture loading, contact impendence, and aperture resonance at higher frequencies (50).

For this thesis, a flanged coaxial holder was chosen. It was purchased according to the ASTM Standard Test Method. A delivery system to enclose the device was used that consisted of nylon bushings and polycarbonate plastic. To ensure no leakage, all tests were performed in a Faraday cage. This measurement system should give good measured shielding effectiveness values regardless of the type of material being evaluated.

3.8 Error in Direct Measurements

There are several sources of error that have been identified that can lead to error in measurement of shielding values. The most common sources of error are operator induced, specimen faults and measurement system-based error (51).

Having different operators doing the same job during the same experiment causes operator error. For this thesis, there were three operators. One person operated the shielding device, another recorded the data and the third person took readings directly from the Hewlett Packard Network Analyzer 8752C. Two separate trials were run using the same operator at each position to ensure that the results were repeatable and determine what the acceptable error would be. After several trials, it was ensured that the results on different known shielding effectiveness specimens were repeatable before actually testing an unknown shielding effectiveness material.

Specimen-caused errors occur from fabrication or secondary handling. Isotropic, homogenous specimens with smooth surfaces will give the most repeatable results. Each load and reference sample must be precisely the same thickness in order to ensure proper repeatability. Secondary handling also causes problems. Human sweat and natural oils on the body can contaminate the sample and cause a spike in conductivity that would be read by the analyzer. Non-homogeneities in specimens cause effects based on size, distribution and geometric distribution. These errors are results of inconsistent processing. A summary of measurement system errors is shown below (51):

A) Impendence mismatches
B) Generator instability
C) Leakage paths
D) Limited dynamic range
E) Limited frequency range
F) Receiver errors

The standard error under normal operation is assumed to be ± 0.5 dB according to the manufacture's manual (74). Once all possible sources of error are considered, it can be shown that $\pm$ 1.0 dB is a more just assumption for a random system as shown below from the ASTM test procedure (51):

Source	**Systematic**	**Random**
Mismatch	0.5 dBm	0.5 dBm
Power instability	0.4 dBm	0.4 dBm
Receiver calibration	0.3 dBm	0.1 dBm
Total Error	**1.2 dBm**	**1.0 dBm**

Systematic errors in the receiver are irreverent since the SE values are based on the difference of measurements in the direct method. The main concern is random errors that could happen in the system. Random error that relates to drift over a few minute time periods is very relevant to this test.

The actual change in impedance is greatly reduced by the attenuator (filter) between the signal generator and the specimen holder. The actual change of impendence level seen by the signal generator may also load the signal generator and cause the output power to vary from one condition to another. In the experiment performed the attenuators were eliminated in order to have enough power to elevate our data off of the noise floor.

These changes can be monitored, but it is not necessary. By using a bi-directional coupler, corrections can be made to compensate for them (51). This coupler is not shown as part of the set-up in Figure 3.5-1 as shown in the ASTM D4935-89 and was not used in this paper. However, it is important to note the existence of this error. Error given for generator instability is based on no compensation. The sizes of these corrections measured with a coupler are the basis to determine the magnitude of this effect if no compensation is used. Experimental methods are discussed in Chapter 6.

CHAPTER 4: ELECTROSTATIC DISCHARGE (ESD)

4.1 ESD Information

According to Becker (43) it was estimated that products valued at about 22 billion dollars (about 5 % of a 450 billion dollar annual revenue) of electronic equipment in the USA were affected by ESD. According to Beck (44) American estimates show an annual savings potential of about 5 billion dollars by eliminating ESD damage (23). Consider an arithmetic case examination of the problem. If you treat electrostatic discharge as a cost-dependent problem you can see the amount of impact each problem causes. Assume each step down the ladder is a ten-fold increase in cost. Each step down the ladder in Table 4.1-1 is more harmful than the previous.

Table 4.1-1: Relative Effect Cost of Repair and Service

Event	Cost Factor
Cost of repair	1
Cost of a printed circuit board	10
Cost of installation	100
Cost of Field Service	1000

It means more liability and cost to a company. It was shown that for 60% of phone calls regarding service, which resulted in “no faults found”, ESD was the cause in a urban/city environment (45). A no fault is an unexplained interruption of signal interference or loss that causes electronic equipment to malfunction. ESD also prescribes to the “yo-yo effect”. A technician comes to solve your problem and he introduces another problem. Then the same thing happens over and over again (23).

Factors that contribute to the ESD phenomena come from electrostatic discharges. Electrostatic discharges from static electricity, which can be explained as electric charge at rest. The electric charge is caused by polarization (i.e., the concentration of electrons in the same object, or through conductive charging from one object to another.) Permanent electrostatic charges arise on the surface of one material when separated from another. Normally electrostatic charges are built up by rubbing or friction, known as triboelectricity. See Figure 4.1-1 for the triboelectric series. In this regard, the rubbing of two surfaces against each other can be considered as repeated separations.

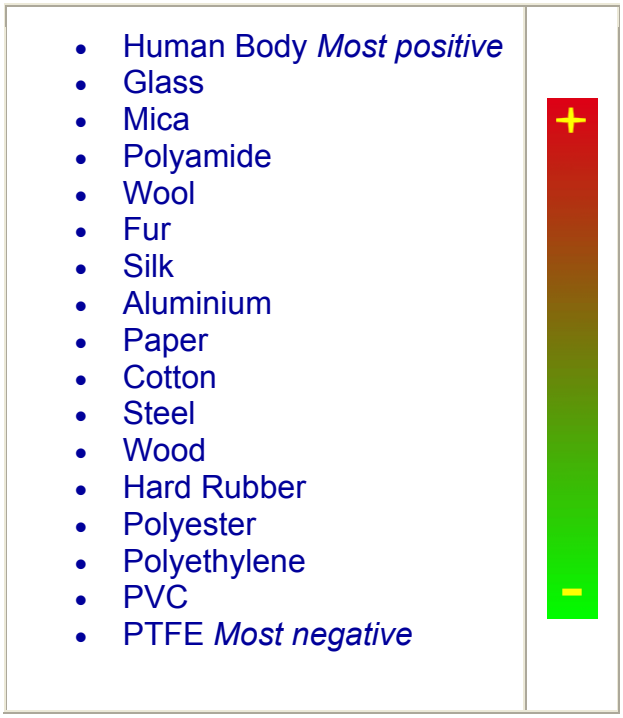

Figure 4.1-1: Triboelectric Series

Several studies have been done on triboelectricity on surface resistivity and chargeability. Fowler has demonstrated there isn't any natural correlation between the triboelectric properties, i.e. chargeability and the surface resistivity (47). Electrically conductive composites consist of an electrically insulating polymer matrix filled with an electrically conductive filler, which is often either a metal particle or carbon black. These types of composites have the disadvantage of not having controllable conductivity in the electrically static dissipative range, which usually is between 10^{-7} S/cm to 10^{-3} S/cm (46).

The ESD range is typically hard to achieve for many polymer-filler systems. The percolation graph, see Figure 2.2-3 in Chapter 2, describes why producing a composite with the conductivity in the ESD range is difficult. The graph represents the conductivity as a function of filler volume fraction and often termed a percolation diagram. The y-axis scale is a logarithmic scale and the conductivity difference between the lower and higher plateaus is many orders of magnitude. For common inexpensive conductive fillers, the ESD range is contained within the step increase and the plateau conductivity is above the ESD range. Making a product with the exact volume fraction required for the ESD range is difficult because the increase is so steep. Further, this plot is sensitive to processing (i.e. mixing speeds can shift this curve right or left leaving the manufacturer with a material not having the desired conductivity) (46).

4.2 ESD Electrostatic Discharge Protection

The triboelectric effect, associated with relative movement of contacting objects of different materials, can cause electrostatic charge on insulated materials. Steel fibers can be used to bleed the charge away continuously to the ground. A sufficient surface or volume conductivity is required.

4.3 Protection of Electronics against Discharges

Electronics can be damaged or disturbed through sudden discharges on their housing or on another conductor outside but nearby the housing. In both cases, these discharges create EM waves far into the MHz range. A test according to IEC801/2 (now called IEC61000-4-2) is used to investigate the ESD behavior of plastic model enclosures made out of different materials. In this paper, the researchers shot charges with an ESD Gun of 15kV on the plastic and metal enclosures and on a metal and plastic plate outside but near the enclosure (46). The discharge current creates a magnetic field, which induces a voltage in the coils that caused LED's to light up and give results to the researchers. If all lights illuminate then there isn't any discharge capability.

Table 4.3-1: Tests Near Enclosure EMI Problems

a) Discharges near the enclosure on a metal plate are EMI/RFI problems with material
b) Steel fibers are good even at low loadings
c) Non-conductive plastics do not work
d) Carbon black offers little protection against discharge. Carbon fiber is limited as well.
e) Metal housing performed well.

Table 4.3-2: Discharges on Enclosures

a) Steel fibers perform well on discharges if enclosure is grounded
b) Carbon fibers are weak in both grounded or isolated enclosures and offer no protection. The enclosure with carbon black performs well, even when the enclosure is not earthed.
c) Metal housings perform well if there isn't a direct discharge on the conductive layer. It interrupts the electronics right away if a discharge is direct.

Table 4.3-3: EMI Test Conclusions

a) Carbon blacks with different resistivities show comparable performance
b) Steel fibers with different volume conductivities shoe comparable performance to carbon blacks
c) Carbon fiber performs less than carbon black, but surface conductivity for the carbon fiber housings is higher.

The researchers found that there is no relation between surface resistivity and the discharge shielding performance. Therefore, due to the discharge-shielding performance, the surface resistance is not the correct parameter to characterize the behavior of the fiber filled plastic, although it is generally believed (47). In the case of steel fiber systems an electric discharge looks for the steel fibers, which act as little "lightning arrestors".

4.4 Carbon Loaded Polymers

Carbon loaded polymers are often used as electrostatic dissipative materials. Certain types of carbon black are very conductive, which means that the dispersion of polymers and carbon black at significantly high concentration can result in conductivity within the desired range. However, it has been shown that the conductivity mechanism is characterized by a threshold value for the passage of

current. This means that there are no conduction paths for electricity through material at concentrations below this threshold value. For concentrations above this threshold value, the conduction paths are present and the resistivity (1/conduction) level then drops significantly. See Figure 2.2-3 for description of percolation threshold in Chapter 2.2.

One problem with carbon-loaded materials could be due to the tendency of carbon particles to be released after processing, thereby contaminating the surroundings. If parts are manufactured very small then the edges can have carbon black particles that can be rubbed off on contact. These particles fall on nearby microelectronic components and can induce a charge, which could lead to a malfunction in the equipment. Printed circuit boards and backed-up battery printed circuit board manufacturing operations have this problem. They are unsuitable for clean room environments or printed circuit boards with battery backing-up due to leakage currents. Currents can escape through faults in the carbon-loaded materials. The charge leakage can also cause shortages in the electronic equipment.

Investigation by Huntsman and Yenni demonstrated that conductive (carbon-treated) plastics did not produce corrosion in microcircuits if the carbon-loaded resin was clean and uncontaminated when put into place (48). However, if the carbon contacts were handled manually and thus became contaminated, severe corrosion was found after the test periods, which in both cases was in a climate of 65 C and 80 % relative humidity (RH) for 14 days. Handling issues are present with carbon black that can induce a static charge to take place.

4.5 Environmental Post Application

EMI shielding has received the most attention, because devices that require EMI shielding include small computers, video games, video recorders, business machines, process control equipment, and electronic automotive devices. Very few researchers consider the effect of conductive fillers on the mechanical properties of the resulting molded parts.

Each of these applications is subjected to various environmental stresses, which may influence the electrical behavior of the polymer compound. Business machine housings are often cleaned with alcohol and detergent solutions. Under-hood units in automobiles and trucks are subjected to wide temperatures extremes, and possible oil and ethylene glycol spills. Process control units are exposed to a variety of gaseous and condensation products, as well as thermal stresses. It is important that the polymer composition maintain it's electrical conductivity throughout the life of the product (29). By designing materials that can shield one can use them for ESD applications over a specific range. The research in this project was geared towards EMI/RFI shielding ranges.

CHAPTER 5: PROJECT MATERIALS

5.1 Introduction

Materials were chosen for this project based on their commercial availability, cost effectiveness and their widespread use. The two polymers used, nylon 6,6 and polycarbonate, are commonly used in a number of applications, including conductive resins. The different carbon fillers used in this project were also chosen based on their ability to impart high conductivity to the composites, while still maintaining a relatively low cost and high availability. The synthetic graphite is expected to produce the highest composite thermal conductivity of any of the other fillers. Carbon black, due to its high surface area, can effectively impart high electrical conductivity at relatively low concentrations. The pitch-based carbon fibers can also produce good conductivity while generating improved mechanical properties that the other two fillers cannot provide.

Therefore, this chapter has been written to provide information regarding the formation and properties of the various materials used in this project. General descriptions of the formation processes of the fillers have been given, in addition to various physical properties for each material.

5.2 Polymer Matrices

In order to determine the effect of the matrix material on the conductive resin, all of the composites will be made using two different matrix materials, one thermoplastic and one semicrystalline polymer. The first matrix material to be used in this study is DuPont's Zytel 101 NC010. This nylon 6,6 is a semicrystalline

thermoplastic and was chosen for this project since it is a commonly used engineering polymer. These are the two main types of thermoplastic matrices available today and it is important to see how chosen fillers would interact in these matrices. This material has a high use temperature and therefore, it is commonly used in automotive under-the-hood applications. Nylon 6,6 is a polymer that is commonly used by other researchers (16, 17, 19, 20, 54). Therefore, a significant amount of data is available in the open literature with which to compare the results of this proposed study. The properties of Zytel NC010 are shown in Table 5.2-1 (55). The chemical structure for nylon 6,6 is shown in Figure 5.2-1 (B).

Table 5.2-1: Properties of Zytel 101 NC010 (55)

Melting Point	262°C
Tg (Glass Transition Temp, DAM)	65°C
Melt Flow Rate	12.35 g/10 min
Shear Viscosity at 1000 sec^{-1} shear rate and 280°C	137 Pa-sec
Tensile Strength at 23°C (DAM)	82.7 MPa
Flexural Modulus at 23°C (DAM)	2,827 MPa
Tensile Elongation at Break at 23°C (DAM)	60%
Notched Izod Impact, 23°C	53 J/m
Density at 23°C	1.14 g/cm^3
Electrical Resistivity at 23°C	10^{15} ohm-cm
Thermal Conductivity at 23°C	0.25 W/mK

The amorphous thermoplastic polycarbonate, Lexan HF1110-111N, is manufactured by GE Plastics. This material has an electrical conductivity of 10^{-17} S/cm. Polycarbonate is widely used for conductive resins due to its high heat resistance up to 125°C, high impact strength, good dimensional stability, and good processing. Conductive polycarbonate is currently used for electrostatic dissipative chip carrier trays and electronic equipment housings. Also, other researchers have studied this resin system for use as conductive resins so there is open literature data available with

which to compare results (16, 56, 57). The properties of Lexan HF1110-111N are shown in Table 5.2-2 (52). The chemical structure for polycarbonate is shown in Figure 5.2-1 (A).

Table 5.2-2: Properties of Lexan HF1110-111N (52)

Melt Index	25 g/10 min
Average Molecular Wt	Approx. 16,000 g/gmole
Tensile Strength at 23°C	65.5 MPa
Flexural Modulus at 23°C	2310 MPa
Tensile Elongation at Break at 23°C	120%
Density at 23°C	1.20 g/cm^3
Notched Izod Impact, 23°C	640 J/m
Volumetric Electrical Resistivity at 23°C	10^{17}ohm-cm
Thermal Conductivity at 23°C	0.19 W/mK

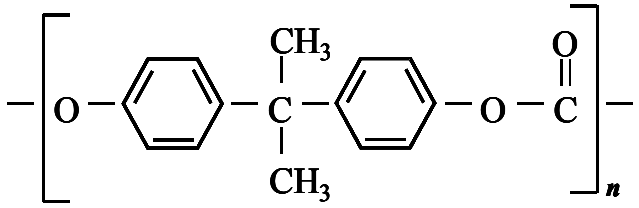

(A)

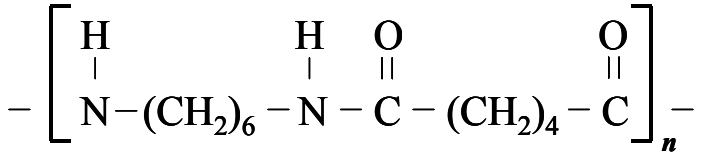

(B)

Figure 5.2-1: Chemical Structures for (A) Polycarbonate and (B) Nylon 6,6 (52)

5.3 Carbon Black

Carbon black is a material that has widespread use in a number of applications. It consists mainly of elemental carbon, and it is in the form of spherical particles that have been fused together to form primary aggregates that are typically around 30-100 nm in size. Traditionally, carbon black had been used a pigment in black ink, as well as for toners in copy machines and printers, where it is still used. Carbon black has also been added to rubber to enhance the tear strength and improves the wear characteristics. Plastics have been filled with carbon black in order to improve their electrical conductivity for use in conductive resins.

Carbon black comes in several different forms, depending on the feedstocks and the process used to produce the material (58). The most common process for the production of carbon black is the thermal-oxidative process. Approximately 98 % of the carbon black consumed annually is produced from this method. In this process, natural gas is combusted in air and then mixed with the feedstocks, which are typically coal tar or crude oils. The products from the reaction are then sent through filters that separate the carbon black from the tail gas. Large particles are then reduced in size by hammer mills and the carbon black is sent to a pelletizer, where they are mixed with water. The wet pellets are then dried, screened for a size distribution, passed through magnets to remove any iron or rust contamination and sent for storage in silos (58).

Carbon black can also be formed from another process that creates a material that is better suited for electrical applications. This highly electrical conductive type of carbon black, known as acetylene black, is a product of the thermal decomposition of

acetylene in the absence of oxygen. Acetylene is a thermally unstable material, and in a highly exothermic reaction will split into hydrogen and carbon. To carry out this reaction, the reactor vessel is initially heated by burning acetylene in air. To produce carbon black, the air input is stopped while the reaction is allowed to continue. The continuation of the reaction produces the carbon black. The reaction will proceed until the flow of the acetylene feed is stopped. This process will produce a carbon black that is very pure and has a higher degree of crystallinity than other blacks. Carbon black particles will also aggregate in this process, producing a high surface area agglomerate with very low density. The high surface area and inherent conductive properties are reasons why this particular type of carbon black is used in conductive applications (58).

The type of carbon black used in this project is Ketjenblack EC-600 JD. This is an electrically conductive carbon black available from Akzo Nobel, Inc. This filler was chosen since it efficiently imparts its electrical conductivity at relatively low loadings. The highly branched, high surface area carbon black structure allows it to contact a large amount of polymer. This results in improved electrical conductivity at low carbon black amounts. This particular black also out-performs carbon blacks from several other sources when used in electrically conductive applications. Narkis (59) tested the electrical conductivity of several different carbon black-filled composites. By comparing carbon blacks available from different companies while using the same matrix material, he found that Akzo's Ketjenblack EC-600 JD provided performance that was superior for both the critical concentration and the lowest volumetric resistivity when compared to other carbon blacks. The physical

properties of Ketjenblack EC-600 JD are given in Table 5.3-1, with Figure 5.3-1 showing the physical structure of this material. The carbon black is in the form of pellets that are 100 microns to 2 mm in size and, upon mixing into a polymer, easily separate into primary agglomerates 30-100 nm long (60). Ketjenblack is composed of very porous carbon particles which produce a conductive network by occupying a large excluded volume at low concentrations (24). Because of its small primary particle size, Ketjenblack does form agglomerates and has structure.

Table 5.3-1: Properties of Ketjenblack EC-600 JD (52)

Electrical Resistivity	0.01-0.1 ohm-cm
Primary Aggregate Size	30-100 nm
Specific Gravity	1.8 g/cm^3
Apparent bulk density	100-120 kg/m^3
Ash content, max %	0.1
Moisture, max. %	0.5
BET Surface Area	1250 m^2/g
Pore volume	480-510 cm^3/100g
pH	8-10

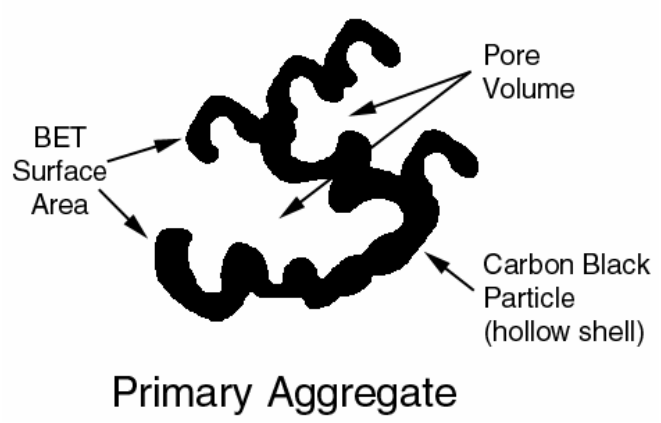

Figure 5.3-1: Physical Structure of Carbon Black (52)

5.4 Synthetic Graphite

From the previous sections, it can be seen that a wide array of materials can be formed into various carbon particles and fibers. These materials can also be used to form a synthetic material with a structure and properties similar to graphite. The multi-step process used to make synthetic graphite is complicated and slow, but the product it yields is useful for many conductive applications.

The main raw material used in the production of synthetic graphite is petroleum coke, which is a by-product of the processing of crude oil. Since it is the collection of the residues from the many distillation processes in a refinery, the supply is abundant and inexpensive. However, petroleum coke is not very useful as is. Other types of cokes can be used, including coke derived from coal processing, shale oil, asphalts, and pitch (61).

In order for this raw material to be used, there are several steps that must be taken to prepare the coke before processing (61). This often involves calcining, grinding and the application of a binder material. Coke from a refinery has usually been heated to approximately 450-500°C and contains up to 15 % volatile materials. If this is heated any further, the remaining volatiles can be removed and graphitic crystallites can form in the coke. This can cause volume shrinkage of up to 30 %. The coke is calcined in nitrogen to a temperature of 1200-1300°C before any further processing. After this, the coke is crushed to reduce porosity, ground to a powder, and then sieved to determine the particle size.

In some cases, a binder such as coal tar pitch is added so that the processed coke can be formed into blocks or other shapes that will remain intact through the rest of

the graphite formation. In these processes, the mixing and forming stages, the coke and binder materials are added to a mixer that is heated to approximately 120°C. Enough binder, often coal tar pitch, is added so that it can seep into the pores that remain in the coke particles and so no air can mix between the particles. The resulting mixture can then be molded into the desired shapes. In this process, the blocks are placed in an autoclave with the air removed. Pitch is then added and forced into the pores of the blocks under pressure. The carbonization steps that follow will convert the pitch into useful carbon.

All of the preceding steps produce a solid block with physical and chemical properties similar to that of the raw material. To convert this block into synthetic graphite, the materials are subjected to high temperatures of approximately 2400-3000°C in the absence of air. The product is then either used as solid blocks, for applications such as electrodes, or it is ground down to the desired particle size. The particulate form is often used as filler in various materials, such as the applications studied in this project (61).

One form of synthetic graphite was used in this project. Thermocarb™ TC-300 Specialty Graphite, available from Conoco, Inc., is a high purity synthetic graphite. This material has been milled to an average particle size of approximately 70μm and an aspect ratio of about 1.7, as determined by optical microscopy at MTU. Properties of the Thermocarb™ Specialty Graphite can be found in Table 5.4-1 (62).

Table 5.4-1: Physical Properties of Thermocarb™ TC-300 Specialty Graphite

Ash	<0.1 wt%
Sulfur	0.02 wt%
Vibrated Bulk Density	0.66 g/cm^3
Density	2.24 g/cm^3
Thermal Conductivity at 23 ºC	600 W/mK on a 6 mm particle
Electrical Resistivity	10^{-5} ohm-cm
Particle Aspect Ratio	2
Particle Shape	Irregular
Particle Sizing, vol% (by Sieve Method)	
+48 Tyler Mesh* (+297 μm)	4
-48/+80 Tyler Mesh (-297/+177 μm)	22
-80/+200 Tyler Mesh (-177/+74 μm)	48
-200/+325 Tyler Mesh (-74/+44 μm)	16
-325 Tyler Mesh (-44 μm)	10

5.5 Pitch-Based Carbon Fibers

Pitch is an abundant and inexpensive material that is used to produce carbon fibers. It is a by-product of petroleum refining but can also be found as a residue of refined coal and the processing of chemicals such as naphthalene and anthracene. In general, pitch is a mixture of molecules of different sizes and shapes, usually aromatic compounds with a complex structure and molecular weights between 300 and 400 g/gmole (63).

Since there are several sources from which pitch can be obtained, and the fact that it can contain many impurities, the preparation stage is very important. There are two main types of pitch: isotropic and mesophase. Isotropic pitches is prepared from the high-boiling fractions of petroleum feed stocks, and have heavy slurry oils that are the products of catalytic cracking of crude oil. Mesophase pitch is formed from a pitch-like liquid that has been pyrolyzed at 425 °C, where it forms a liquid-crystal, or mesophase, structure capable of orientation through flow and shear (64).

In order for isotropic pitch to be converted into carbon fibers, it must first be prepared to increase the softening point and to prevent the formation of mesophase pitch. A mixture of the two types of pitch is undesirable, as it will not perform well in the spinning portion of the processing. This involves heating the pitch at reduced pressures to promote dehydrogenation, cross-linking, condensation, and the release of H_2, H_2O, H_2S, and other low-molecular weight compounds. This increases the molecular weight and the softening point of the pitch.

The goal of the preparation of mesophase pitch is similar. Mesophase pitch can be converted to high-performance carbon fibers if there is 100% mesophase content, a softening point of 230-280°C, a low viscosity for spinning, high oxidation activity and high carbon yield. One successful way to prepare the mesophase pitch is through catalytic modification. This method uses aromatic hydrocarbons as raw materials combined with a Lewis acid such as $AlCl_3$. Catalytic polymerization would then take place at low temperatures that would produce a soluble mesophase with 100 % anisotropic content (64).

After the preparation of the pitch, it is then spun into fibers. This is the first step of the process shown in Figure 5.5-1 (64). In this step, pitch is fed through an extruder to be evenly mixed. The pitch is fed into a spinnerette and then forced out under pressure. The resulting continuous fibers can then be drawn, solidified and wound. The spun fibers are wound up quickly to obtain a fiber diameter of approximately 8-14μm. In this form, the pitch fibers are easy to break, so the wind-up plays an important role in producing a quality pitch fiber. The fibers undergo high-speed drawing with air blowing and wound with a speed of 10-1000 m/min.

Another method is to collect the fibers on a conveyer belt, and then send them directly through the stabilization furnace.

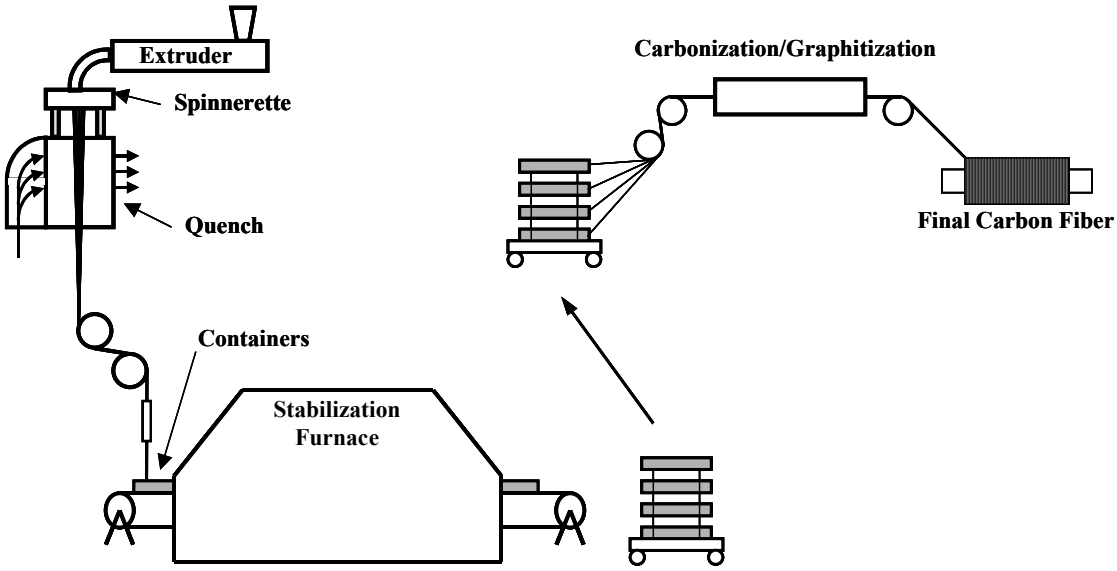

Figure 5.5-1: Typical Process for the Production of Pitch-Based Carbon Fibers (64)

Stabilization is important in the production of pitch carbon fibers because without this step, pitch cannot be carbonized. It is necessary for the pitch fibers to undergo an oxidation reaction so that the fibers develop the characteristics of a thermoset and will not soften when exposed to high temperatures. The important parameters in the stabilization portion of the process include temperature, time, oxidant concentration, and the stress on the fibers. For isotropic pitch, the best conditions under which the reaction is carried out are a temperature of 325-340°C and an oxygen content of approximately 20 %. The best operating conditions for anisotropic pitch are a temperature of 300-310°C and an oxygen concentration of 8-10 % (64). The time for each can vary between one to three hours depending on the other two parameters. The application of stress on the fibers can improve the properties of the final carbon

fibers. Stress can help avoid some of the damage to the fiber that can occur from shrinkage during the oxidation.

Once the fibers have been stabilized, they are then subjected to carbonization, which is the heat treatment of the fibers below temperatures of 2000 °C. This is done to remove all atomic species other than carbon so that the carbon content becomes greater than 96 % and to improve the mechanical, electrical and thermal properties of the final carbon fiber. To overcome the weak mechanical properties of the pitch fibers, they are normally collected in containers, as shown in Figure 5.5-1. The fibers are heated to 400°C in air to become infused fibers followed by heating to 700 °C in nitrogen. This produces fibers with good tensile strength and flexibility. These fibers are then sent through the carbonization furnace at temperatures between 1000 °C and 1600°C. The fibers give off H_2O, CO_2, CO, and H_2 during this stage, leading to the formation of a graphitic structure.

The graphitization step that follows further changes the properties of the pitch carbon fibers due to heat treatment at temperatures as high as 3000°C. The tensile strength and modulus of mesophase-pitch will increase with higher temperatures, whereas the opposite trend will occur with isotropic pitch-based fibers.

In this project, Amoco's ThermalGraph DKD X petroleum pitch-based carbon fibers was used. This material is a mesophase fiber that is highly anisotropic and highly graphitized. This particular fiber was used since it improves the thermal and electrical conductivity and tensile strength of the conductive resin. The properties of ThermalGraph DKD X are shown in Table 5.5-1 (65).

Table 5.5-1: Properties of Amoco ThermalGraph DKD X (65)

Tensile Strength	>1.39 GPa
Tensile Modulus	687-927 GPa
Electrical Resistivity	<3 μohm-m
Thermal Conductivity	400-700 W/mK
Fiber Density	2.15 to 2.25 g/cm^3
Bulk Density	0.25 to 0.55 g/cm^3
Fiber Diameter	10 microns
Filament Shape	Round
Average Filament Length	200 microns
Filament Length Distribution	<20 % less than 100 microns <20% greater than 300 microns
Carbon Assay	99+ wt%
Surface Area	0.4 m^2/g

CHAPTER 6: EXPERIMENTAL METHODS

6.1 Introduction

To completely characterize the polymer composites, several different experimental techniques were used. These included a variety of tests for electrical conductivity, density and surface characterization. Composites were first prepared using pilot-scale extrusion and injection molding equipment. Several ASTM standards were used to analyze the composite materials. In some cases, ASTM standards were unavailable, and therefore techniques common throughout the literature were utilized for the remaining tests. This chapter will discuss in detail the various experimental methods used to create and analyze the carbon-polymer composites.

6.2 SAMPLE PREPARATION

6.2.1 Drying

For this project, nylon 6,6 and polycarbonate were first dried in a dehumidifying drier in order to eliminate the presence of water that could influence the experimental results. The nylon 6,6 and the polycarbonate were dried at 79°C and 121°C, respectively, in a Bry-Air Systems dehumidifying dryer for four hours for every 80 pounds of polymer. The dryer can be seen in Figure 6.2-1. This dryer used indirect heating with recirculating air at a dew point of -40 °F. After drying, the polymer was stored in moisture barrier bags. All of the carbon fillers were used as received and were not dried prior to composite preparation.

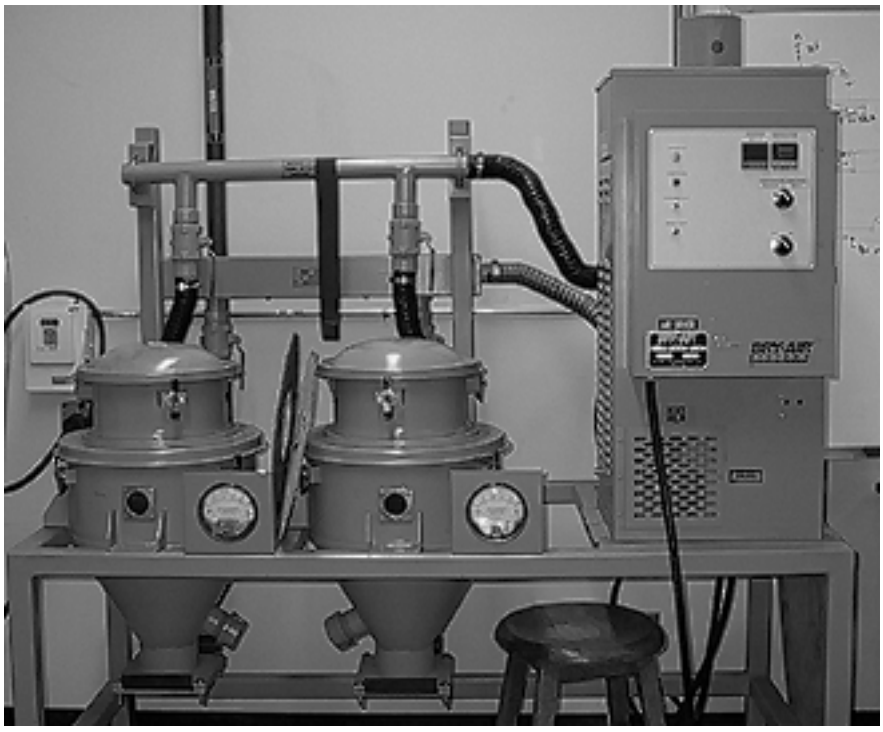

Figure 6.2-1: Bry-Air Dryer

6.2.2 Extrusion

The extruder used was an American Leistritz Extruder Corporation Model ZSE 27. This extruder has a 27 mm co-rotating intermeshing twin screw with 10 zones and a length/diameter ratio of 40. This extruder is shown in Figure 6.2-2. The screw design, (Appendix A), was chosen to obtain the maximum possible conductivity. Hence, a minimum amount of filler degradation was desired while still dispersing the fillers well in the polymers. The same screw design was used for this entire project. The polymer pellets (Zytel or Lexan) were introduced in Zone 1. The first side stuffer, utilized to introduce carbon black and Thermocarb ™ TC-300 Specialty Graphite into polymer melt, was located in Zone 5. The second side stuffer was located at Zone 7 and was used to introduce the carbon fibers into the polymer melt.

Four Schenck AccuRate gravimetric feeders were used to accurately control the amount of each material added to the extruder. Table 6.2-1 lists the typical extrusion conditions for the nylon 6,6 based resins. Table 6.2-2 lists the typical extrusion conditions for the polycarbonate based resins. A complete list of all formulations extruded is given in Appendix B. The exact extrusion conditions for each formulation are described in detail by Weber (53) and Clingerman (52).

Table 6.2-1: Extrusion Conditions for Conductive Nylon 6, 6 (52)

Zone 1 Temperature (by feed hopper)	210°C
Zone 2 Temperature	250°C
Zone 3 to Zone 5 Temperature	270°C
Zone 6 to Zone 7 Temperature	275°C
Zone 8 to Zone 10 Temperature	280°C
Total Throughput	19.0 kg/hr
Screw rpm	300 rpm

Table 6.2-2: Extrusion Conditions for Conductive Polycarbonate (52)

Zone 1 Temperature (by feed hopper)	210°C
Zone 2 Temperature	277°C
Zone 3 to Zone 7 Temperature	288°C
Zone 8 to Zone 10 Temperature	299°C
Total Throughput	19.0 kg/hr
Screw rpm	300 rpm

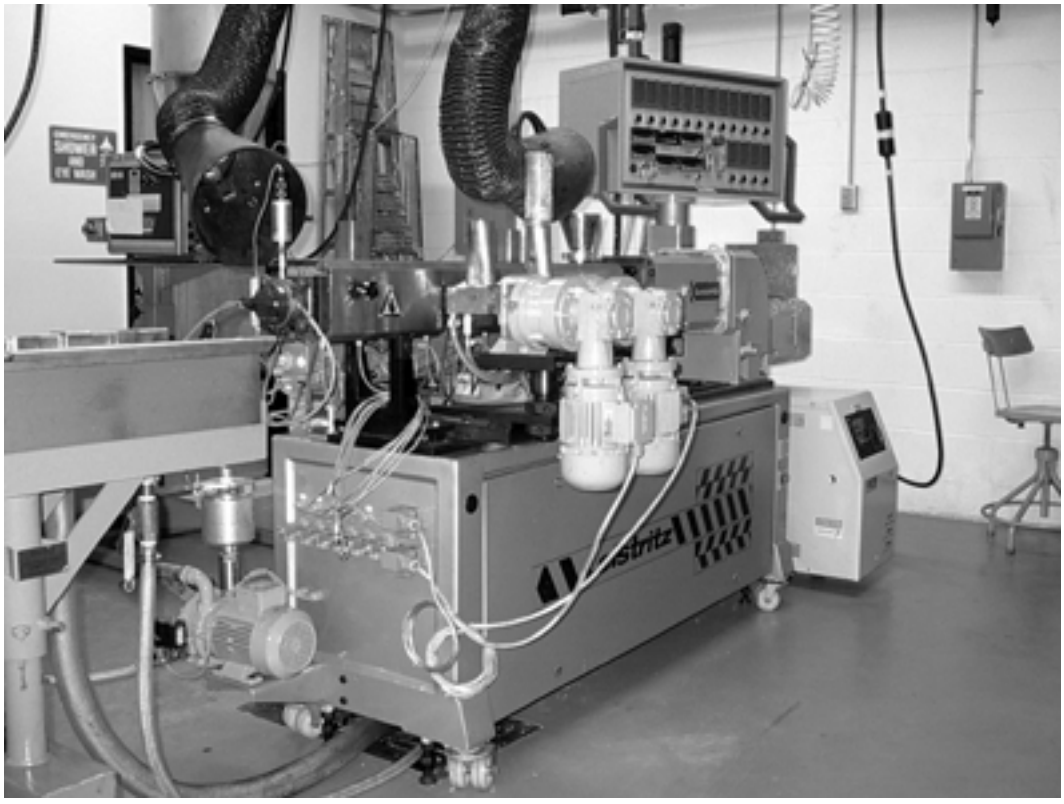

Figure 6.2-2: Extruder Used for Compounding of Composites

After passing through the extruder, the polymer strands (3 mm in diameter) entered a water bath and then a pelletizer that produced 3 mm long pellets. Figure 6.2-3 shows the pelletizer and water bath used. Typically 10 kg of each formulation were compounded. After compounding, the pelletized composite resin was dried again in a vacuum oven at 660 mm Hg and 80^{o}C for 20 to 24 hours and stored in moisture barrier bags prior to injection molding.

Figure 6.2-3: Pelletizer and Waterbath

6.2.3 Injection Molding

A Niigata injection molding machine, model NE85U A_4, was used to produce test specimens (Figure 6.2-4 (A)). This machine has a 40 mm diameter single screw with a length/diameter ratio of 18. The lengths of the feed, compression and metering sections of the single screw are 396 mm, 180 mm and 144 mm, respectively.

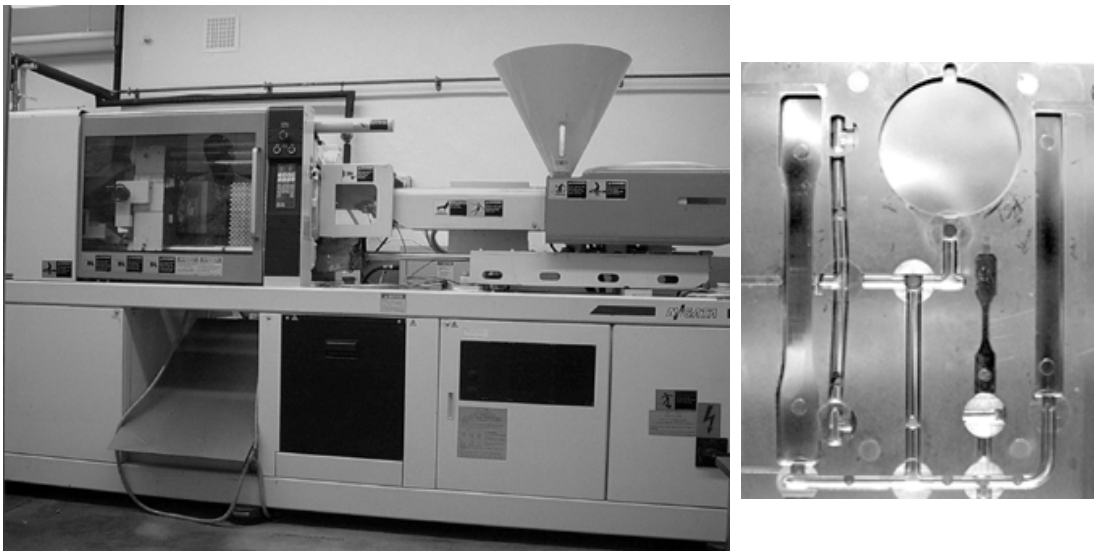

(A) **(B)**

Figure 6.2-4 Injection Molder (A) and Four-Cavity Mold (B)

Two different molds were used for this project. A four cavity mold shown in Figure 6.2-4 (B) was used to produce a 3.2 mm thick ASTM Type I tensile bars (end gated) and 6.4 cm diameter disks. The mold is shown in Figure 6.2-1 (B). These disks were used for thermal and electrical conductivity tests. Table 6.2-3 shows the typical injection molding conditions used for the nylon 6,6 and polycarbonate based resins using the four-cavity mold. The exact molding conditions for each formulation using the four-cavity mold are shown in Clingerman and Weber (52, 53). The second mold used produced a single 130 mm diameter and 3.2 mm thick disk. Figure 6.2-5 shows this mold. These large disks were used to determine shielding effectiveness (SE) of all of the formulations.

Figure 6.2-5: Shielding Disk Mold

Table 6.2-3: Injection Molding Conditions for Conductive Nylon and Polycarbonate

Zone 1 Temperature (by feed hopper)	285^{o}C
Zone 2 Temperature	290^{o}C
Zone 3 Temperature	299^{o} C
Zone 4 Temperature (die nozzle heater)	31 ^{o}C
Mold Temperature	88^{o}C
Screw rpm	54 rpm
Injection Pressure	154 MPa
Hold Pressure	109 MPa
Back Pressure	3 MPa
Injection Time	15 seconds
Cooling Time	15 seconds
Interval Time	2 seconds

Test specimens composed of pure Zytel 101 or Lexan were molded first as standards in order to verify the test methods and for comparison to literature data. After the pure polymer was molded, approximately four pounds of each composite formulation was then molded into test specimens. Ten specimens of each formulation were molded. When switching materials, approximately six to eight samples were discarded after the new material was inserted into an empty hopper. This was done to

ensure that all of the first material had been removed from the barrel. Injection molding conditions for this experiment can be found in Appendix C.

6.2.4 Test Design and Sample Distribution

As stated previously, ten molded (SE) disks were made for each material formulation. The disks were labeled from 1-10 with each number representing the order of production. Samples 2, 4 and 6 were used for density determination. Sample 5 was used as the reference sample. Samples 3, 7 and 8 were designated for use in the shielding test. Samples 1, 9 and 10 are extra samples that were used if a disk was warped and could not be tested. Warping is when the sample disk would not lay flat. For shielding tests some of the number 5 samples were warped and could not be used as the reference sample. In these cases, sample 3 was used as the reference sample.

All nylon 6,6 based samples were immediately sealed into moisture barrier bags. Hence, all the samples were dry as molded (DAM). All polycarbonate-based composites were stored in plastic Ziploc®-style bags.

6.2.5 Formulation Naming

Test specimens were labeled according to the material, weight percent filler, and the order that the specimen came out of the injection molder. All samples had the following form:

N – W – X – Y – Z - ##

N = National Science Foundation Project
W = Filler used
X = Polymer used
Y = Weight percent of conductive filler
Z = Test method

All formulations were designated with an "N" as the first letter to denote that it was the NSF project. Following was a multi-letter combination to denote the filler ("W") and the polymer ("X") used. "A" was used for carbon black, "B" was used for the synthetic graphite, and "C" denoted the carbon fibers. Combinations of these letters were also used in the factorial design formulations. Polymers, X in the nomenclature above, were designated with a "N" for nylon 6,6 and a "P" for the polycarbonate. The "Y" in the above formula was the weight percent of the conductive filler. The "Z" term was either labeled "D" for a density tested or "S" for a shielding effectiveness disk. For example, the sample labeled NCP20-S-5 indicates that this particular sample was the fifth shielding effectiveness disk from the molder that consisted of 20 weight percent carbon fiber in polycarbonate.

6.2.6 Water Jet Fabrication

A water jet was used to cut the reference samples that were used in the EMI/RFI shielding test. For our method the 0.28-inch holes as indicated in Figure 6.2-6 were not drilled. An apparatus was designed to eliminate the machining of the holes in every reference and load sample. Samples were cut to have the dimensions as shown in Figure 6.2-6 (74).

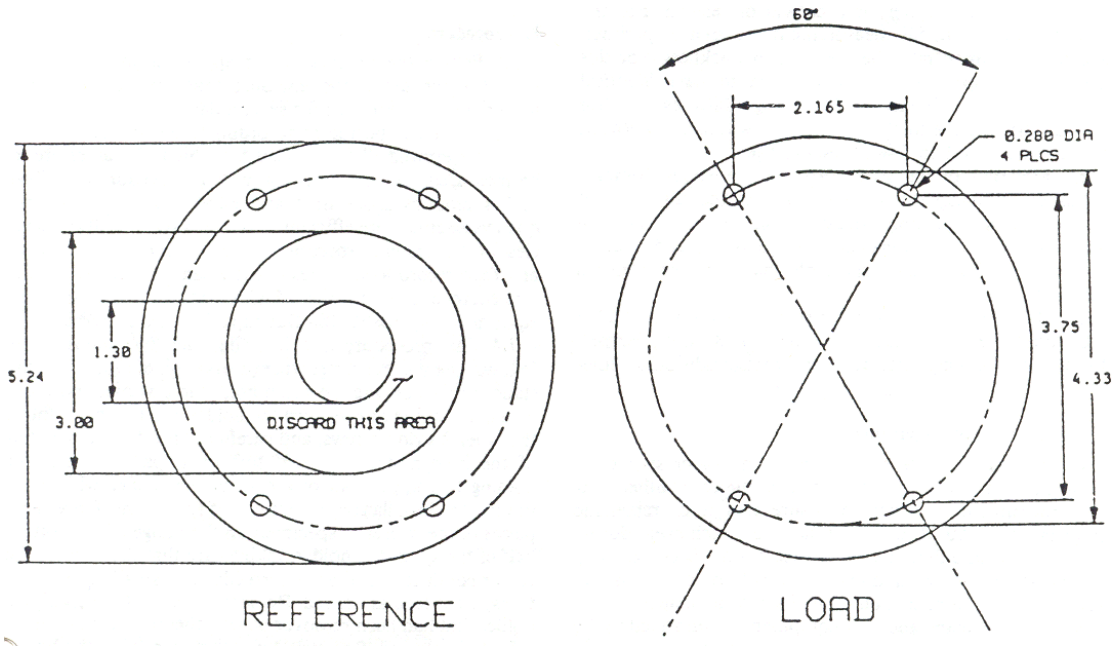

Figure 6.2-6: Dimensions for Reference and Load Disks (74)

Figure 6.2-8 shows the three sample pieces that were fabricated. The reference sample consists of a large ring and a small inner disk as shown in Figure 6.2-8 (A). The scrap piece that was left over from the water jet cutting was used in determining fiber lengths via solvent digestion and image analysis. The shielding load samples were not cut and are shown in Figure 6.2-8 (B). The (SE) of a formulation is determined by taking the difference between the reference sample and the average of 3 load samples as shown in Equation 6.2-1 (51).

S_{eff} = (Average of 3 Load Samples) – Reference Sample Equation 6.2-1

S_{eff} = Shielding Effectiveness in dB

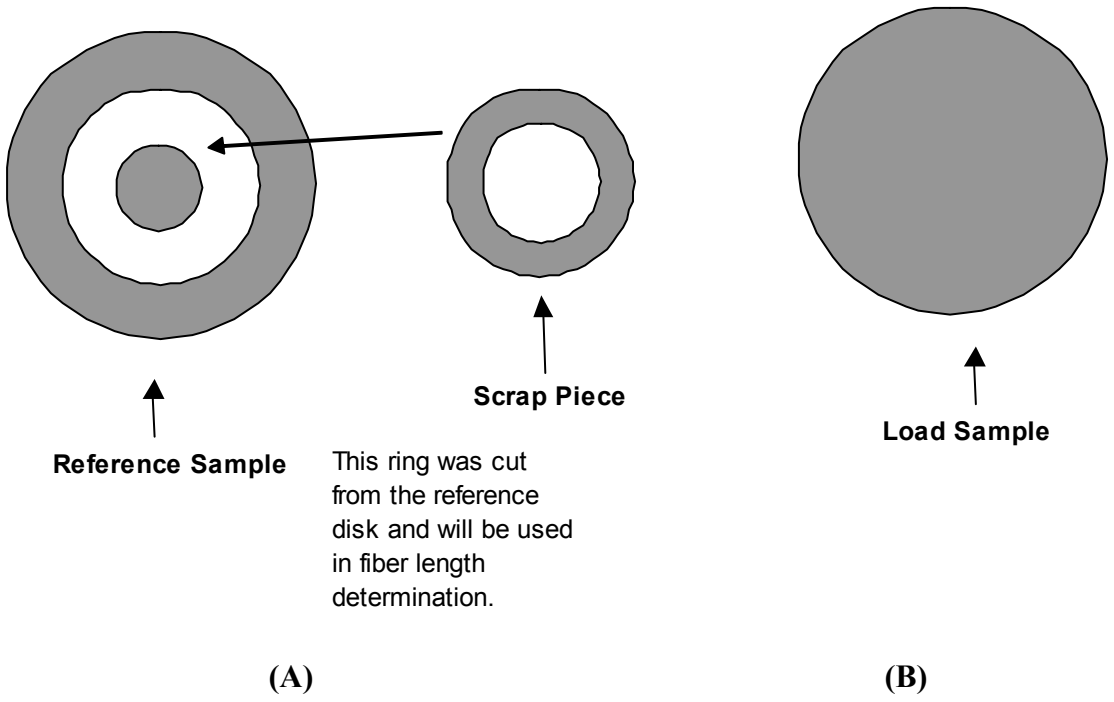

Figure 6.2-7: Fabricated Sample Explanation

6.2.7 Drying Water Jet Fabricated Reference Samples

The nylon 6,6 and the polycarbonate were dried at 79°C and 12°C, respectively in a Bry-Air Systems dehumidifying dryer for a period of 24 hours. Two dryers were used. Each set of ten disks were laid on the dryer bed and separated by a thin layer of paper towels. This had to be done for the reference samples only, because of the small inner circle part. This was done to avoid confusion and mixing up of center circles. All of the nylon formulations were equally divided between two dryers. The load sample shielding disks were done the same as the reference samples; expect a boundary layer between different formulations was not necessary. This dryer used indirect heating with re-circulating air at a dew point of -40°F.

6.3 Composite Density

The actual composite density was measured using ASTM D792, a standard test that measures the density of plastics by water displacement (66). For this test, the mass of a dry 130 mm diameter and 3.2 mm thick disk was measured using a four-place balance. This same disk was then clipped and suspended from the bottom of the balance and completely submerged into a beaker of water at room temperature. The mass of the disk is then measured, and the density of the composite (ρ_c) can then be calculated according to Equation 6.3-1.

$$\rho_c = \left(\frac{dry\ weight}{dry\ weight - wet\ weight} \right) \cdot H_2O\ density \qquad \text{Equation 6.3-1}$$

These measured values were then compared to the theoretical formulation density calculated according to Equation 6.3-2, which uses the density values of the individual constituents (ρ_i) and the weight percent of each constituent (w_i).

$$\rho_c = \frac{1}{\sum_{i=1}^{n} \frac{w_i}{\rho_i}} \qquad \text{Equation 6.3-2}$$

In this equation, ρ_c is the density of the composite; w_i and ρ_i are the weight fraction and density of the constituent materials, respectively. Three density measurements were taken for each formulation. Disks 2, 4 and 6 were used for this calculation. The average density was calculated and compared to the theoretical density. Density results are located in Appendix D

6.4 Thickness Measurements

For the EMI shielding test it is important that all of our samples are the same thickness. Parts that are warped were not tested, but replaced by a different numbered sample. For the reference and load samples five thickness measurements were made using calipers around the edges of the large rings of the reference sample or solid rings of the load sample, respectively. Figure 6.4-1 shows where measurements were taken in the disks. The calipers used for measurement were accurate to ± 0.03 mm according to the manufacturers manual. Three measurements were made at the center area of the small solid reference disk or center portion of a load disk as well. For the load sample, the same eight measurements were made on three disks from the sample. Samples 3, 7 and 8 were measured for thickness and then compared to the reference samples thickness. This was done to make sure that the reference sample was roughly the same thickness as the load samples. Overall averages of each material thickness were also compared to the reference sample. All of the samples used in thickness measurements were used in EMI/RFI shielding determination. Overall, the reference and load sample had the same thickness within 0.1 mm of each other. Therefore, shielding testing could be performed. If the samples had a different thickness then the measurement error would have been very large in the actual EMI/RFI shielding tests. Thickness results can be found in Appendix E.

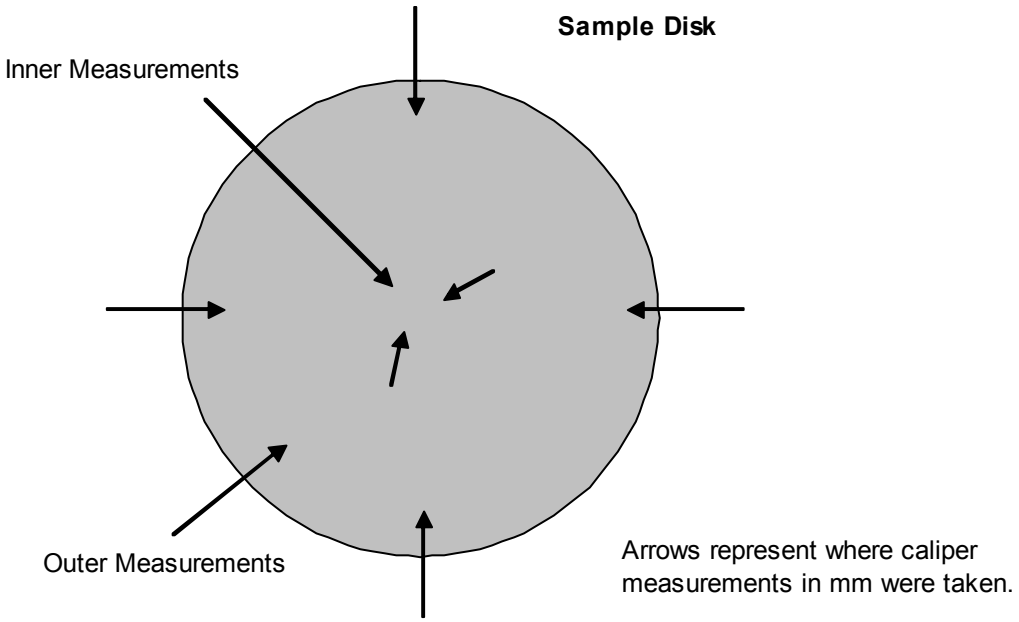

Figure 6.4-1: Thickness Determination Method

6.5 Shielding Test Information

ASTM D4935-89 provides a procedure for measuring the electromagnetic (EMI) shielding effectiveness (SE) of a planar material due to a plane wave, far-field electromagnetic wave. Electric (E) field SE values may be calculated from far-field data. The method is valid over a frequency range of 30 MHz to 1.5 GHz. These limits are not exact, but are based in decreasing displacement current due to decreased capacitive coupling at lower frequencies and on overmoding (excitation of modes other than the Transverse Electromagnetic Mode (TEM)) at higher frequencies for the size of the specimen holder (51). In this experiment an anisotropic material was tested at ten different frequencies ranging from 30 MHz to 1 GHz.

There are some terms that need to be discussed in order to understand the experiment. First, the dynamic range (DR) is the difference between the maximum and minimum signals measurable by the system. Measurement of materials with good SE requires extra care in order to avoid contamination of extremely low power or voltage values by unwanted signals from leakage paths. The far field region is where the electric field (E) and the magnetic field (H) are orthogonal to each other and to the direction of propagation of energy. A Faraday cage is a shielded enclosure made from copper that block incoming EMI/RFI waves and prevents any leakage from escaping into the environment.

Figure 6.5-1 shows the placement of the reference sample on the transmission fixture. The small disk must be aligned perfectly for accurate readings. The large outer ring must also be aligned for good results. The load sample must be aligned as well to ensure proper measurement.

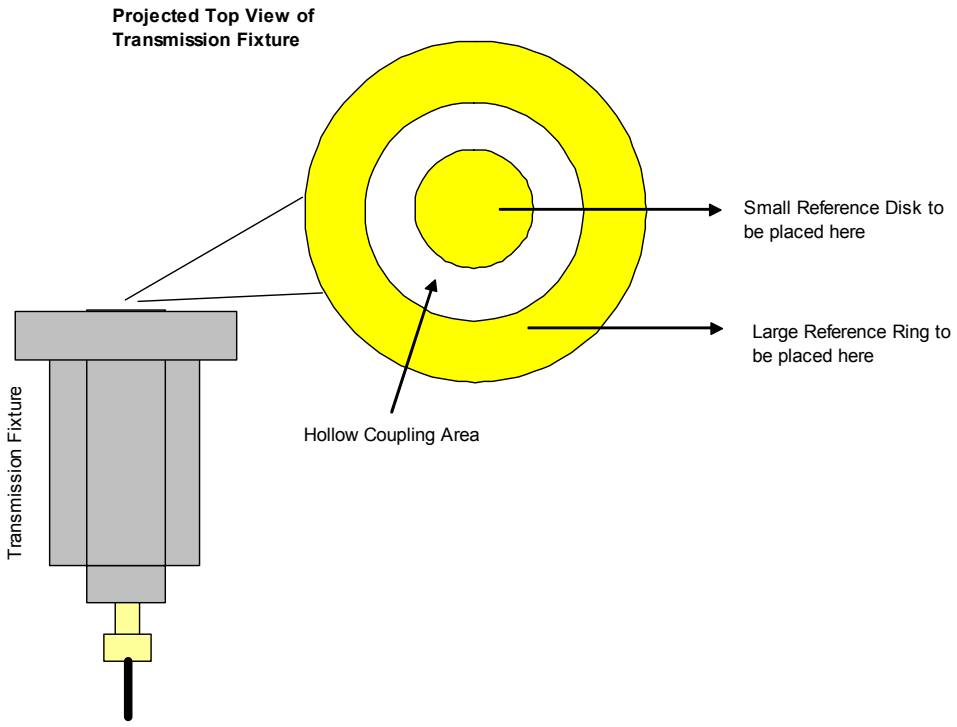

Figure 6.5-1: Transmission Holder Sample Placement

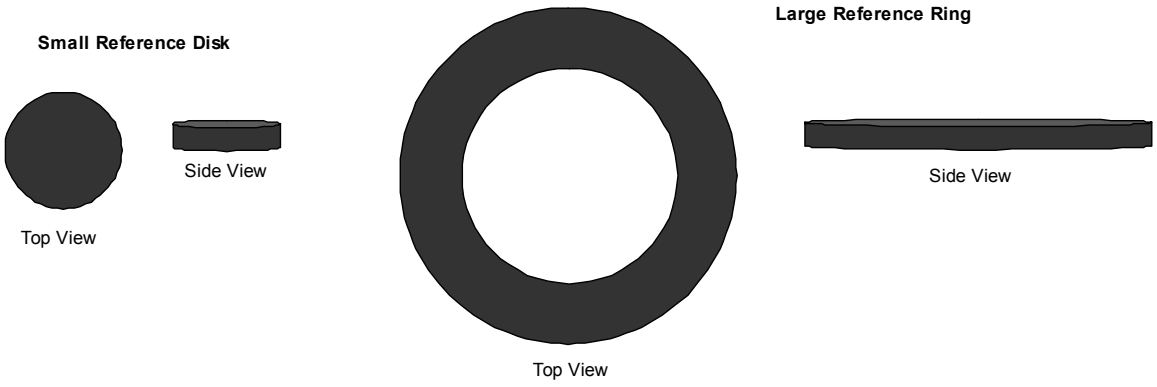

Figure 6.5-2: Reference Sample Diagrams

6.6 Shielding Effectiveness Determination

Equation 6.6-1 is used to calculate the shielding effectiveness of a planar material according to ASTM D4935-89 (51). In our system measurements were made directly for the shielding effectiveness. Shielding effectiveness was calculated by subtracting the average of the three load samples from the reference sample for each formulation and replicate. Results for shielding effectiveness (SE) can be found in Appendix F.

$$S_{dB} = 10 * Log_{10}\left(\frac{P_2}{P_1}\right) \qquad \text{Equation 6.6-1}$$

S_{dB} = Shielding effectiveness in dB
P_2 = Power levels with and without a sample material present in dB
P_1 = Power levels with and without a sample material present in dB

SE will have negative value if less power is received with the material present than when it is absent. Practical use of this test method is valid for measurement of planar materials under normal incidence, far field, plane-wave conditions (E) and (H) are tangential to the surface of the material (49).

The uncertainty in measurement is a function of material, losses throughout transmission line path, dynamic range of the measurement system, and the accuracy of the equipment. Uncertainty analysis is discussed in Chapter 3 to illustrate uncertainness that may be achieved in a systematic or closed system. Deviation from the test method will also cause problems.

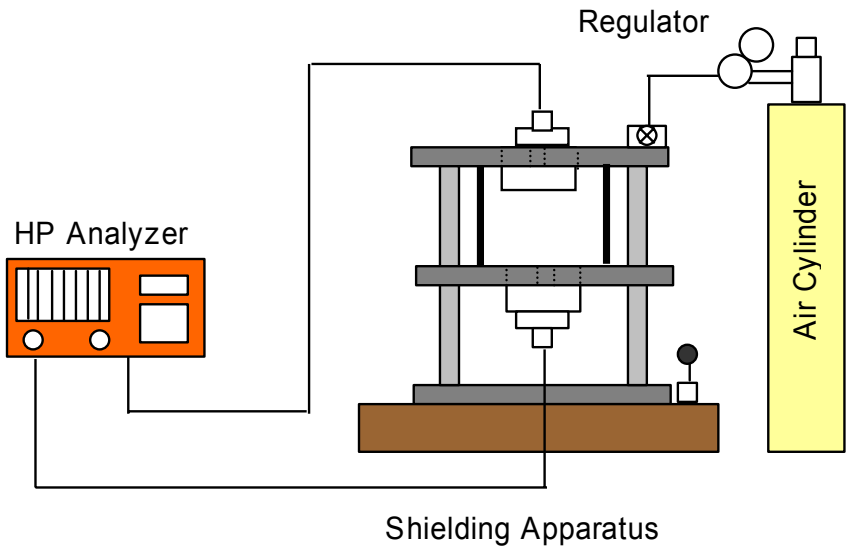

Figure 6.6-1: Shielding Effectiveness Test Set-Up

The general test set-up is shown in Figure 6.6-1. A custom in-house designed support was used to hold the transmission fixture. Jerry Norkol and Quinton Krueger developed the design at Michigan Technological Univeristy in the Chemical Engineering Machine Shop. The support plates are made of solid polyvinyl chloride (PVC), which does not induce charges or allow leakage of current. Steel beams act as guides for the movable plate that depresses the samples. Figure 6.6-2 shows a photo of the actual set-up. The transmission fixture was mounted into the (PVC) plate using nylon screws. Nylon was chosen because it also does not allow for current leakage. Teflon bushings were used on the steel guide rods to deflect any possible charges.

A compressed air system was implemented to lift the table of the support fixture. This allowed the operator to put in a sample. Compressed air was regulated at 40 psi to lift the table with the transmission fixture. A lever was made that slowly let the pressure out to ensure that slamming of the fixture would not occur. For safety

purposes, two regulators were used to ensure that the system could not be over pressurized. The apparatus was mounted to a movable cart that allows for easy mobility for testing. Samples can be stored on the area beneath the cart as well. The experiment we used the following equipment as shown in Table 6.6-1. This test measures the net or total SE caused by reflection and absorption. Separate measurement of reflected and absorbed power may be accomplished by the addition of a calibrated bi-directional coupler to the input of the holder.

Table 6.6-1: Experiment Equipment

1. HP 8752 Network Analyzer
2. ASTM D4395-89 Test Fixture
3. Shielded cables
4. Faraday Cage
5. Test Fixture Support

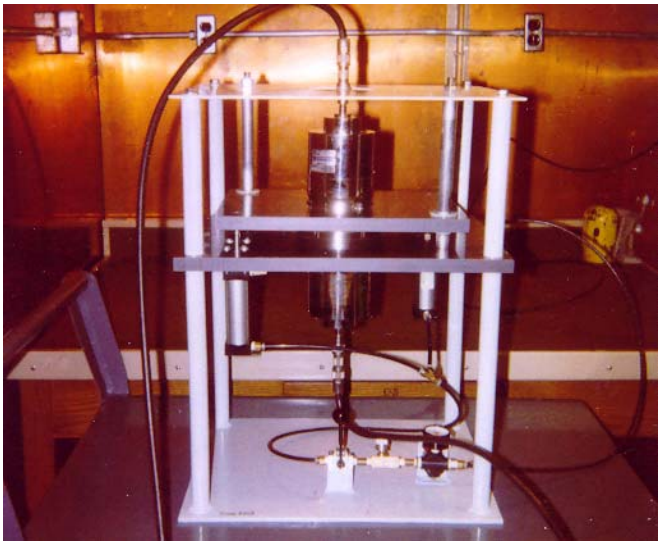

Figure 6.6-2: Actual Test Set-Up in Faraday Cage

6.7 Coaxially Transmission Apparatus

The specimen/sample holder is an enlarged coaxial transmission line with special tapered sections and notched matching grooves to maintain a characteristic impendence of 50-ohm throughout the entire length of the holder. The three important aspects to this design are shown below (74).

a) A pair of flanges in the middle of the structure holds the sample. This allows for capacitive coupling of energy into insulating materials through displacement current.

b) A reference specimen of the same thickness and electrical properties as the load specimen causes the same discontinuity in the transmission line as is caused by the load specimen.

c) Non-conductive support structure. This ensures that minimum leakage will occur from the testing equipment. A Faraday cage was also used to prevent excess leakage to and from the samples.

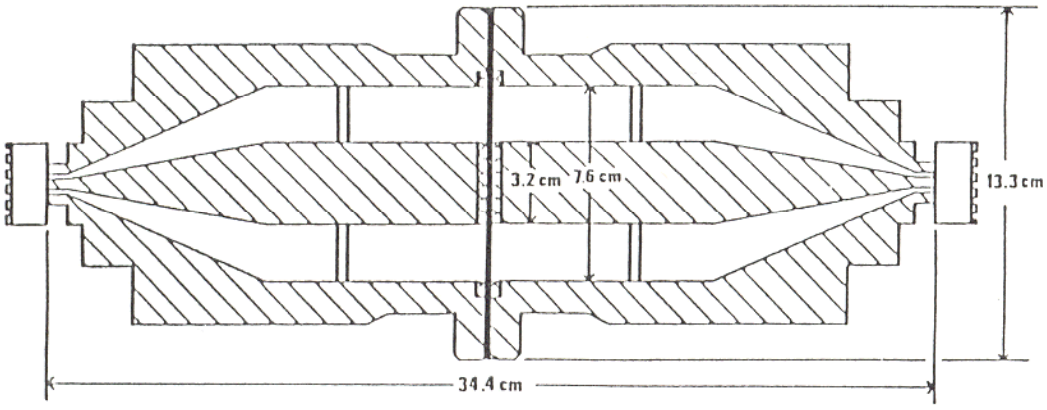

Figure 6.7-1. Cross Sectional View of Transmission Test Apparatus (74)

A diagram with dimensions is displayed in Figure 6.7-1. In our case, we are using an air pressure system that raises one flange to remove one sample and insert the next. The natural weight of the other flange with gravity is used to close and hold the

sample in place while testing is occurring. Figure 6.7-2. Shows the transmission fixture outside of the support apparatus.

Figure 6.7-2 Transmission Holder Without Sample

6.8 Signal Generator and Receiver HP 8752C Network Analyzer

This source is capable of generating a sinusoidal signal over the desired portion of the frequency range of 30 MHz to 1.1 GHz. A 50-ohm output impedance is needed to minimize reflections due to mismatches. Attenuators, devices that reduce power, can be used, but in our case we wanted the power to be as high as we could go in order to lower the noise floor, but as low a possible for safety reasons. Figure 6.8-1 shows the HP 8752C Network Analyzer.

The HP Network Analyzer also has a 50-ohm input impedance capability of measuring over the desired frequency range. A wide dynamic range is desirable in order to achieve a wide dynamic range of measured SE values. The dynamic range for our system was found to be 70 dB (74).

Figure 6.8-1 HP 8752C Network Analyzer

6.9 Coaxial Cables and Connectors

Cables and connectors are devices for connecting power between specific components without causing interference with other components. The cables used had a 50-ohm characteristic impedance. Impedance is the degree to which an electronic component impedes the flow of current. In general it is a frequency-dependent quantity. Impedance is commonly called resistance. Also double-shielded cables were used, because they provide lower leakage than single shielded cables. No connectors were used, because the distance between the test apparatus and analyzer was small.

6.10 Attenuators

These are devices used to isolate the specimen holder from the signal generator and the receiver. Their main purpose in this system is for impedance matching. A 10 dB, 50-ohm attenuator is often used on each end of the specimen holder. The

material under test usually causes a large reflection of energy back into the signal generator. This may cause vibrations of the incident power by changing the generator impedance loading. Attenuators greater than 10 dB will excessively decrease the dynamic range of the measurement system. Attenuators were removed for our experiment to lower the noise floor and allow for better repeatability. In order to maintain a low noise floor we had to increase the power and was advised to do so by several electrical engineering professors at Michigan Technological University. Dr. Warren Perger of Electrical Engineering and Dr. David Chesney of Chemistry at Michigan Technological University offered suggestions for proper sampling and collecting of data.

6.11 Test Specimens

The reference and load specimens must be the same material and thickness. The load sample can be larger than the outer dimension of the holder, but the reference cannot be. Both were measured to ensure relative thickness and electrical properties to each other were assumed to be true. The thickness is the most critical dimension in shielding determination. For the most accurate and repeatable SE measurements, reference specimens and load specimen must be identical in thickness. For this method, two identical specimens were used. Measured SE values of anisotropic materials (i.e. carbon composites) are dependent on geometry and orientation. The results are less repeatable than for a homogenous mixture. Through repeated testing we could achieve relative repeatability within ±1.0 dB in each trial during an experimental run. In order to test the specimens they had to be conditioned before testing. The specimens were conditioned for 48 hours at 23 ± 2^{0}C and 50 ± 2 %

relative humidity for polycarbonate. The shielding test was then performed immediately once removed from the conditioning environment. The nylon 6,6 samples were stored in moisture proof bags and tested was removed. Nylon 6,6 samples were tested dry as molded (DAM).

6.12 Preparation of Apparatus

A time-domain reflectometer was used in order to ensure a characteristic impedance of 50 ohm $\pm$ 0.5 ohm has been achieved during construction and that this impedance has not been degraded. A time-domain system can give location of mismatch in addition to magnitude of a problem. The dynamic range can be checked by comparing the maximum signal level obtained with a reference specimen to the minimum signal level obtained when using a metallic load specimen. This was done by using the aluminum reference sample and gold plated sample that came with the shielding TEM flange.

Leakage due to connectors or cables may reduce the direct resistance (DR) of the system by providing a parallel signal path that does not pass through the specimen. If a step attenuator placed in a series with the specimen holder causes a change in the minimum signal detected that corresponds to a change in attenuator setting, and if the step attenuator itself does not cause a leakage path, leakage is negligible and the DR measured above is correct. If the levels do not correspond, the attenuation should be increased until a one to one correspondence is achieved.

Since leakage from a coaxial connectors determined not only by the quality of the connector, but also by the amount of torque used in tightening the connector,

connections should be rechecked. By having a calibrated reference sample you can ensure proper working operation each and every time.

6.13 Justification of ASTM Method

The design of the sample holder and the measurement procedure given in the ASTM standard were developed at the National Institute of Standards and Technology (NIST) formerly the National Bureau of Standards (NBS) (67). Shielding Effectiveness was determined to be independent of frequency, but was dependent on the material and loading levels (68). They determined that the limiting conditions of ASTM D4935-89 were the following:

a) Uniformly thick sample (Reference and Load)
b) The electrical parameters of the material do not vary over the frequency range of interest.
c) Relatively small separation distance between the transmitting and receiving dipoles

6.14 ASTM Test Procedure D4935-89

The ASTM procedure was rechecked and confirmed by a national standards committee (67). ASTM D4935-89 was used to obtain shielding effectiveness for all formulations (51). All of these tests were done in a Faraday cage because of its RF insulating qualities. Figure 6.14-1 shows a picture of the Faraday cage in Electrical Engineering Resource Center (EERC) in room 818. This way we can achieve repeatable results in the lab. This was done to eliminate outside interference sources, especially RF sources and EMI/RFI sources as well.

Figure 6.14-1: Faraday Cage located in the 818 Room of the EERC at MTU

6.15 Solvent Digestion

Solvent Digestion (ASTM D5226), filler length and aspect ratio were measured on scrap reference shielding effectiveness samples as shown in Figure 6.17-1 (69). Solvent digestion was used to dissolve the matrix or polycarbonate or nylon surrounding the different carbon fiber. Then the fiber was measured using microscope techniques and analyzed and compared to unprocessed fiber. The following is a discussion of the methods implemented to achieve this. Results can be found in Appendix G.

A 0.2 grams sample was obtained from the ring of the shielding reference sample that was cut during the water jet fabrication. This resulted in one solvent digestion sample from each shielding disk tested per formulation. Tests were run on four

different formulations than compared to previous results from MTU and checked with statistical methods to verify accuracy.

The 0.2 grams composite sample was placed in a 2.0 oz. glass vial with a polytetrafluoroethylene lid. The vials were filled approximately half full with the appropriate solvent. The exact amount of solvent is not critical since the solvent was pulled through the filler and disposed of. The only constraint on the amount of solvent used is it has to completely dissolve the 0.2g samples.

The nylon-based samples were dissolved with Fisher Scientific formic acid that contains 89.6 % by assay formic acid with the balance comprised of water and trace contaminates. Formic acid was selected since it readily dissolves nylon at room temperature. Methylene chloride was chosen as the other solvent because it dissolves the polycarbonate-based composites quickly at room temperature. The methylene chloride used was from Fisher Scientific and was ACS certified. The methylene chloride was 99.9 % pure. The samples were allowed to soak in the solvent until the entire polymer matrix, nylon or polycarbonate was completely dissolved.
Nylon samples usually took over night to dissolve, although the polycarbonate samples were typically done in two hours.

While the samples were dissolving, filter papers and petri dishes were weighed separately using a four-place Denver Instruments A-250 scale and the weights of each were recorded. The filters used were 0.45 μm pore size modified polyvinylidene fluoride filters produced by Millipore. All samples used only one filter, except for nylon samples with filler loadings of 40 wt % or greater where two or three were needed in order to collect all the fillers on the filter paper.

Once the matrix was completely dissolved, the polymer/filler/solvent solution was filtered. This was carried out using the apparatus seen in Figure 6.15-1. The apparatus contained a Fisher Brand 47 mm microanalysis filter assembly, vacuum flask, and vacuum pump. The pre-weighed filter paper was placed in the filtration assembly, and the shaken solution was poured on the filter. The vacuum pulled the solvent and dissolved matrix through the filter leaving the filler on the filter paper.

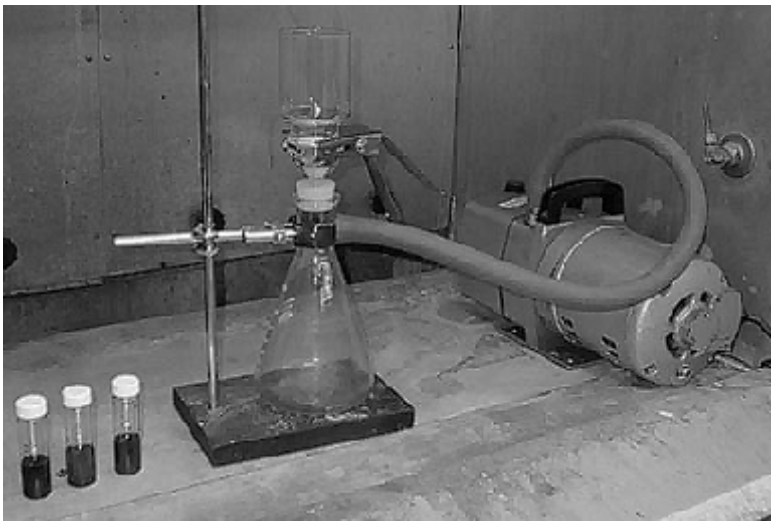

Figure 6.15-1: Solvent Digestion Filtration Apparatus

The vacuum was kept on until the filter and filler were completely dry for polycarbonate samples and until all standing liquid was removed from the nylon samples. The filter paper and filler were placed in the pre-weighted and labeled petri dishes. The petri dishes were left open and placed in a hood overnight to allow the remaining solvent to evaporate. It was quickly found in this process that carbon black would immediately plug the filter; therefore, only composites filled with milled pitch-based carbon fiber and synthetic graphite particles could be run. Once the samples

were completely dried, the petri dish containing the filter paper and filler were weighed. The weight percent filler was calculated using Equation 6.15-1. The results for each sample for this test can be found in Appendix G.

$$wt\% = \frac{Wt_{Final} - W_{Filter(s)} - W_{PetriDish}}{W_{Composite}} * 100 \qquad \text{Equation 6.15-1}$$

Solvent digestion produced four samples of fibers per formulation, but for this test, only two were used. The as-received fillers were also measured to see how the material changed due to extrusion and injection molding. The two samples that were used were chosen at random from the four that were digested.

Microscopic analysis was then used to determine the length of the fibers and graphite particles. The filler particles remaining from the solvent digestion experiments were removed from the filter paper and approximately 0.02 to 0.05 g were placed into a small crucible. The crucible was mounted inside a vacuum flask that had the bottom removed. A rubber stopper with one hole was used cap the flask, and a microscope slide was then placed at the bottom of the flask. The nozzle of a compressed air duster containing 1,1,1,2-tetrafluoroethane was then placed through the hole. A small shot of air was then released to disperse the fillers on to the microscope slide. This set up is shown in Figure 6.15-2.

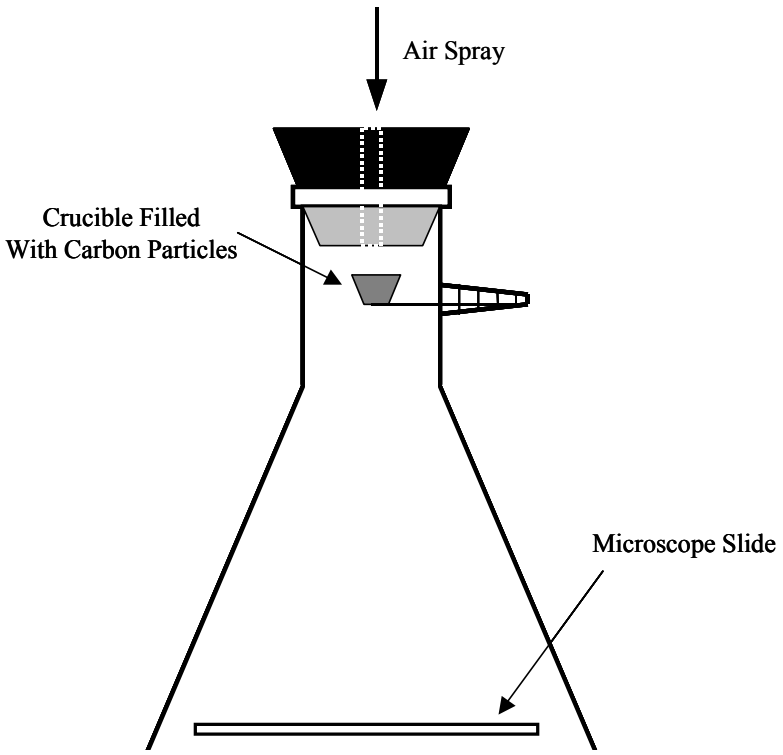

Figure 6.15-2: Set-Up Used to Disperse Carbon Particles On to A Microscope Slide For Image Analysis

6.16 Image Acquisition and Length Measurements

The glass slide with the dispersed filler was placed on a Prior automatic stage for the microscope setup. An image of this setup can be seen in Figure 6.16-1. The microscope used for the imaging was an Olympus SZH10 optical microscope with an Optronics Engineering LX-750 video camera for digital imaging. The images were collected using an automated series of steps (macro) in Scion Image version 1.62. The macro that was used was originally written by Dr. Larry Sutter and it was modified by Dr. Erik Weber for this project (53). All images were collected at 60X magnification.

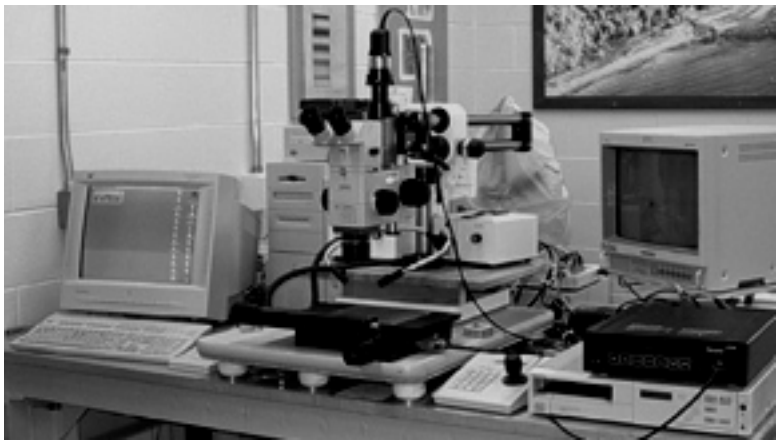

Figure 6.16-1: Image of Microscope Setup used for Filler Length and Aspect Ratio

The resulting images were processed and measured using the academic version of Adobe Photoshop[1] 5.0 and a package of filters called The Image Processing Tool Kit[2] (version 3.0). An action was created so the batch operation could be used for the processing of the images, since between 20 and 85 images were collected for each sample examined. The action contained the following steps:

1. Convert image from RGB to grayscale
2. Fit and remove the background to remove the uneven lighting of the image
3. Automatic leveling of the image, which standardizes the contrast of the image
4. Threshold, this converts the image to a binary image in which all the fillers are in black
5. Feature cutoff and threshold, this removed all the features that came in contact with the edge of image
6. Calibrate, this loaded a predetermined calibration based on the magnification and resolution of the image
7. Measure all, this measured 26 different items of each feature in the image and stored them in a text file that was appended to for each new image

[1] Current versions of Photoshop® are produced by Adobe Systems Inc.
[2] Current versions of The Image Processing Tool Kit are produced by Reindeer Games, Inc.

This process was used for all single filler samples. Between 1000 and 6000 particles were measured for each sample. The aspect ratio was also calculated automatically during this process. Below in Figure 6.16-2 is a sample picture of carbon fibers.

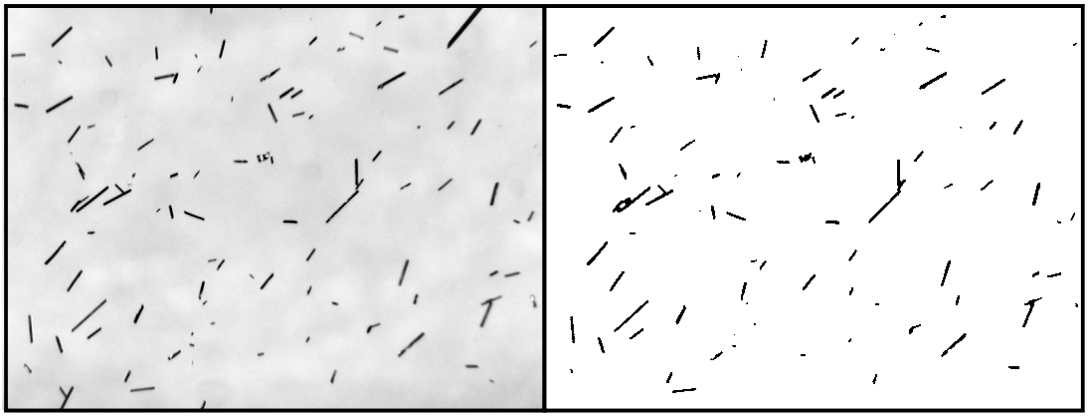

(A) **(B)**

Figure 6.16-2: Image Collected of Carbon Fibers (A) and Binary Image (B) Used to Measure Lengths of Carbon Particles

To check the accuracy of the automated measurements, the lengths of the particles from several formulations were determined by hand using the "Measure Tool" in Adobe Photoshop. The hand measurements confirmed that the automated results were accurate. Aspect ratio was also measured automatically for the graphite particles. For the fibers, the length as calculated by the computer was divided by the diameter of 10 μm provided in the product literature. Results of the fiber length determination for this experiment can be found in Appendix H.

6.17 Orientation

One 12.7 mm by 12.7 mm square was cut out of the scrap piece of each of the shielding reference samples. An illustration of this can be seen in Figure 6.17-1. The square was placed in the same orientation as in the shielding sample so that the through plane of the sample could be viewed. The specimen that showed the sample thickness was stood vertically with a plastic sample clip acquired from Mager Scientific.

The square was placed in a 31.75 mm diameter sample cup in the orientation as describe above. An epoxy mixture was used to set the sample in place. The epoxy was mixed by weight in a ratio of five parts resin to one part hardener ratio. The epoxy plugs were allowed to cure overnight at room temperature and atmospheric pressure, and were subsequently removed from the sample holders the following day.

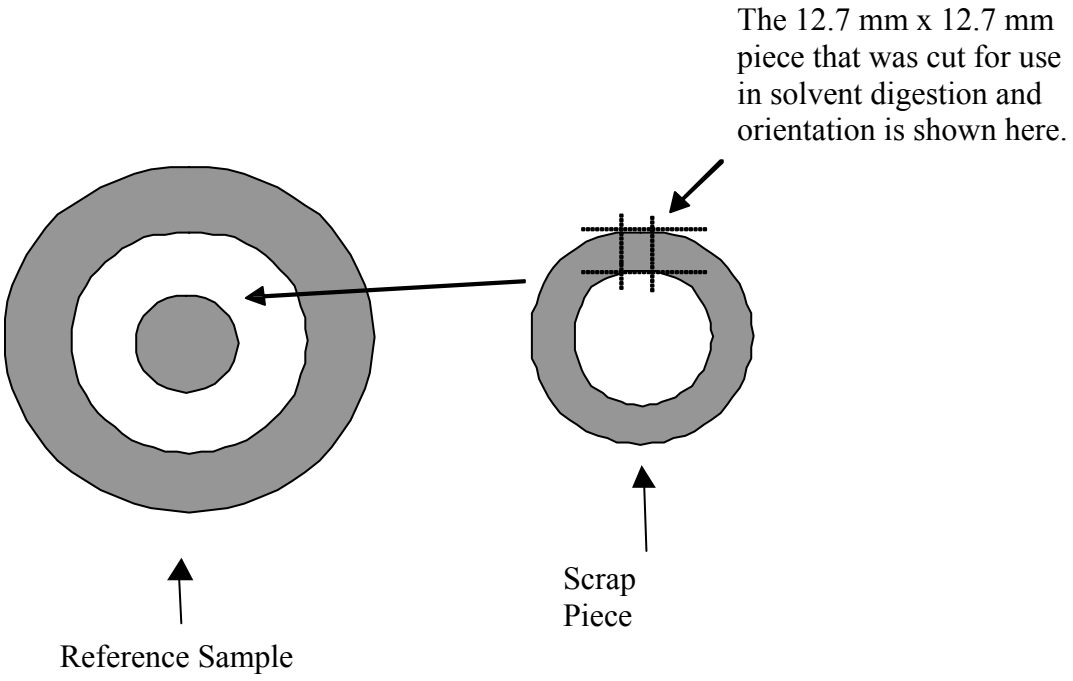

Figure 6.17-1: Diagram of Location of Image Analysis Specimens

Figure 6.17-2: Epoxy Plug Sample Holder

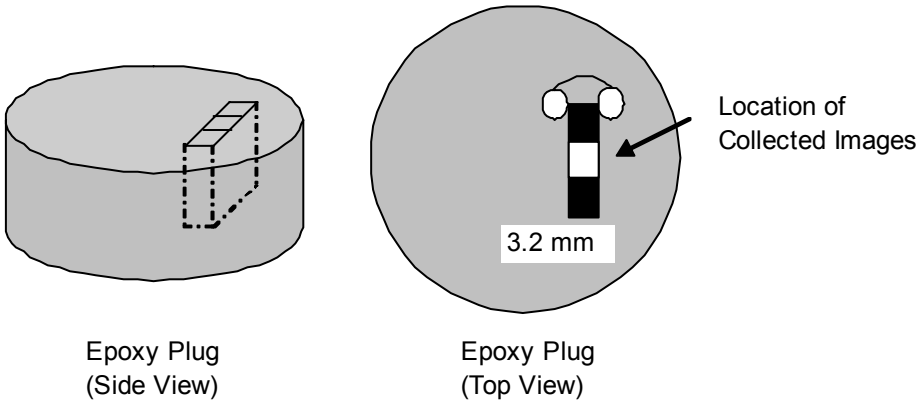

Figure 6.17-3: Orientation of Image Analysis Specimens

6.18 Polishing

After curing, the epoxy plugs were polished using a 4-step process. The polishing was done using a Buehler Ecomet 4 Grinder/Polisher with an Automet 2 Power Head. A ten-sample holder was used to hold the samples. An image of this apparatus can be seen in Figure 6.18-1. The procedure that was used for polishing is shown in Table 6.18-1.

Figure 6.18-1: Polishing Apparatus

Table 6.18-1: Polishing Procedure

	Polishing Media	Time	RPM	Polishing Cloth	Direction	Force Per Sample	Lubricant
1	320 Grit SiC	30 sec	250	None	Contra	4 lbs.	Water
2	9 μm Mono Crystalline Diamond	4 min	150	Ultra-Pol™*	Contra	5 lbs.	None
3	3 μm Mono Crystalline Diamond	4 min	120	Texmet® 1000*	Co-Current	6 lbs.	None
4	0.05μm Deagglomerated Alumna Suspension	3 min	120	Mastertex®*	Contra	3 lbs.	None

*** Buehler Products**

6.19 Optical Imaging Methods

The polished samples were imaged using an Olympus BX60 microscope at 20x magnification. An image of the microscope can be seen in Figure 6.19-1. The images were collected using Scion Image Version 1.62. The images were taken

across the thickness of the sample, which was the direction of conduction. This is illustrated by the white strip on the right sample in Figure 6.19-3. These images in the white strip on the sample on the right reveal a cut plane of the sample, showing cross-section of the fillers. This view gives a representation of fillers orientation. Eight images were needed to view the entire sample. This resulted in an image that covered of about 560 by 3200μm. These images were pieced together to get a large composite image for each epoxy plug. Results for orientation can be found in Appendix I.

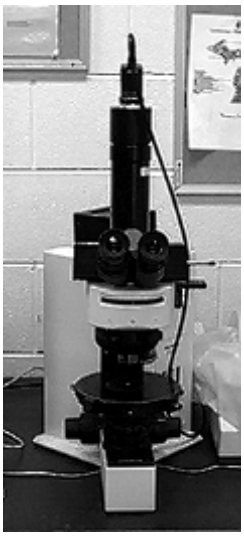

Figure 6.19-1 Olympus BX60 Microscope

6.20 Image Processing

The image processing was carried out using the Image Processing Tool Kit and Adobe Photoshop®. The first step in the image processing was to take each of the sixteen images and remove the color and then fit and remove the background variation. This step turned each image into an 8 bit gray scale image and leveled the uneven lighting. The next step was to paste each of the sixteen images into one

composite image making sure all the image edges matched. The image was then thresholded to produce a binary image with the fillers being black. Next, an Euclidean distance map (EDM) open operation was done to remove small artifacts in the image and better separate the fillers from the matrix. The EDM open operation shrunk each feature by a set number of pixels then dilated them the same number of pixels. The EDM version of "open" command kept the shape of the particle better then the standard morphological open. A "cutoff" operation was then completed to remove all features touching the edge and remove features smaller than 50 pixels.

6.21 Image Analysis and Measurement

The moment angle was measured for each filler particle as a measure of the orientation. This measurement gives some insight into the orientation of the fillers in the composites. It was calculated using the following equations (Equations 6.21a-i) (70). The summations of the location of each pixel in each particle are calculated in Equations 6.21-e. The moment around the x and y-axes are calculated in Equations 6.21 f-g. The angle of minimum momentum or moment angle is calculated in Equation 6.21i. This method uses each pixel in a particle as a separate data point. The moment angles from each feature were measured using PhotoShop® and the Image Processing Tool Kit®.

Equations for Photoshop

$$S_x = \sum x_i \quad \textbf{(6.21a)}$$

$$S_y = \sum y_i \quad \textbf{(6.21b)}$$

$$S_{xx} = \sum x_i^2 \quad \textbf{(6.21c)}$$

$$S_{yy} = \sum y_i^2 \quad \textbf{(6.21d)}$$

$$S_{xy} = \sum x_i \cdot y_i \quad \textbf{(6.21e)}$$

$$M_{xx} = S_{xx} - \frac{S_x^2}{Area} \quad \textbf{(6.21f)}$$

$$M_{yy} = S_{yy} - \frac{S_y^2}{Area} \quad \textbf{(6.21g)}$$

$$M_{xy} = S_{xy} - \frac{S_x \cdot S_y}{Area} \quad \textbf{(6.21h)}$$

$$\theta = \tan^{-1}\left\{\frac{M_{xx} - M_{yy} + \sqrt{\left(M_{xx} - M_{yy}\right)^2 + 4 \cdot M_{xy}^2}}{2 \cdot M_{xy}}\right\} \quad \textbf{(6.21i)}$$

6.22 Limitations of Imaging Methods

While this method may simplify the image processing analysis, there are still several limitations in using digital image analysis. The quality of the image, and consequently the quality of the information, can be significantly affected by several factors, including microscope illumination, magnification settings, and sample placement. All three of these could affect the transformation to a binary image by such things as causing multiple particles to appear as a single feature. Poor resolution due to an image being out-of-focus could produce similar results. In addition, smaller particles could completely disappear from the image due to microscope or software settings. However, if careful consideration is given to these possible limitations, then

the affect can be significantly decreased and the results will be more accurate than if features were measured without the aid of digital processing techniques.

CHAPTER 7: MISCELLANEOUS RESULTS

7.1 Density Results

The density of each of the formulation was determined and compared to theoretical values. Table 7.1-1 below shows a sample with measured density and theoretical density. The density method is explained in Chapter 6. Average density was calculated and compared to the theoretical density. Standard deviation was also calculated. The theoretical density provided an excellent estimate of the sample density and compared and compared to values available in the open literature. Refer to Appendix D for density results.

Table 7.1-1: Density Results for NCP40

#	Tested	Sample Number	Theoretical Density (g/mL)	Measured Density (g/mL)
1	11/27/2001	NCP40-S-2	1.4576	1.4537
2	11/27/2001	NCP40-S-3	1.4576	1.4578
3	11/27/2001	NCP40-S-6	1.4576	1.4557
			Average	1.4558
			Standard Deviation	0.0028
			Number of Samples	3

7.2 Thickness Results

The thickness of each formulation, reference and load samples, was calculated and compared versus each other to ensure the consistent thickness. The thickness testing method is explained in Chapter 6.4. The thickness of the samples was found to be approximately 3.2 mm thick and the thickness differed by no more than ± 0.1 mm.

The thickness was uniform in the reference and load sample. Refer to Appendix E for full results.

7.3 Solvent Digestion Results

The weight percent (wt %) of fillers in each matrix was determined to ensure that each formulation was processed correctly. The solvent digestion procedure is explained in Chapter 6.15. Samples taken from the factorial design were used to calculate the actual amount of filler in each sample and compared to the theoretical value. Using these samples, we determined that the formulations made were on target when compared to theoretical values. The carbon black samples could not be analyzed, because the carbon black is so small that it clogs the filter used in the test. Refer to Appendix G for full results.

7.4 Filler Length Results

The filler lengths of the several factorial design formulations were measured according to the procedure in Chapter 6.16. Again we could not test carbon black due to its small size. It was determined, by using a two-sided t-test at the 95% confidence level, that our fiber lengths were comparable to those obtained by Clingerman in 2001 (52). In Table 7.4-1 Clingerman's results for the factorial design formulations are shown (52). This complete set of filler lengths will be used as needed for any modeling. In Figure 7.4-1 (A) you can see carbon fibers before image processing. In Figure 7.4-1 (B) is the same image after processing. This binary image is what was

used to measure filler length. Refer to Appendix H for t-test information and formulations tested.

Table 7.4-1: Mean Length and Aspect Ratio Results for Factorial Design Formulations (52)

Formulation	Nylon 6,6		Polycarbonate	
	Length(μm)	Aspect Ratio	Length(μm)	Aspect Ratio
As Received Carbon Fibers (CF)	167.5	16.75	167.5	16.75
As Received Synthetic Graphite	68.3	1.80	68.3	1.80
TC Only Composites	74.8	1.68	42.6	1.66
TC Only Replicate Composites	56.0	1.61	49.7	1.70
CF Only Composites	95.7	9.57	85.7	8.57
CF Only Replicate Composites	94.1	9.41	78.3	7.83
CF (TC*CF Composites)	71.7	7.17	71.4	7.14
TC (TC*CF Composites)	59.7	1.84	33.6	1.67
CF (TC*CF Replicate Composites)	82.3	8.23	70.8	7.08
SG (TC*CF Replicate Composites)	41.9	1.72	33.0	1.67

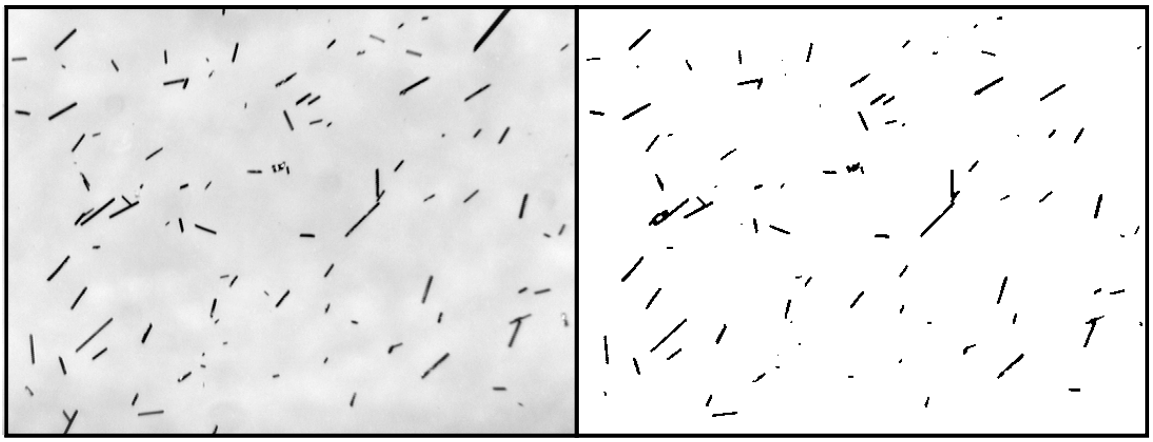

(A) **(B)**

Figure 7.3-1: 30 wt% Carbon Fiber in Polycarbonate Length Determination at 60X

7.5 Orientation Results

The filler orientation was determined according to the procedure in Chapter 6.17 It was determined, by using a two-sided t-test at the 95% confidence level, that the fiber orientation was comparable to those obtained by Weber in 2001 (53). Appendix

J has the filler lengths and two-sided t-test results. It was found that the fillers were generally transverse to the normal plane. If the fiber orientation was 90° it was transverse. If the filler was orientated at 0° then the fibers would be flowing I the same direction as the measurement. Again, carbon black could not be tested due to its small size. Filler orientation is shown in Table 7.5-1. Therefore, Weber's complete set of filler orientation will be used as needed for any modeling. Figure 7.5-1 shows Thermocarb™ Synthetic Graphite on the left in (A) and carbon fiber on the right in (B). The thin arrows on top of Figure 7.5-1 represent the direction of flow. The large thick arrow represents the angle of measurement. Refer to Appendix J for t-test information and formulations tested.

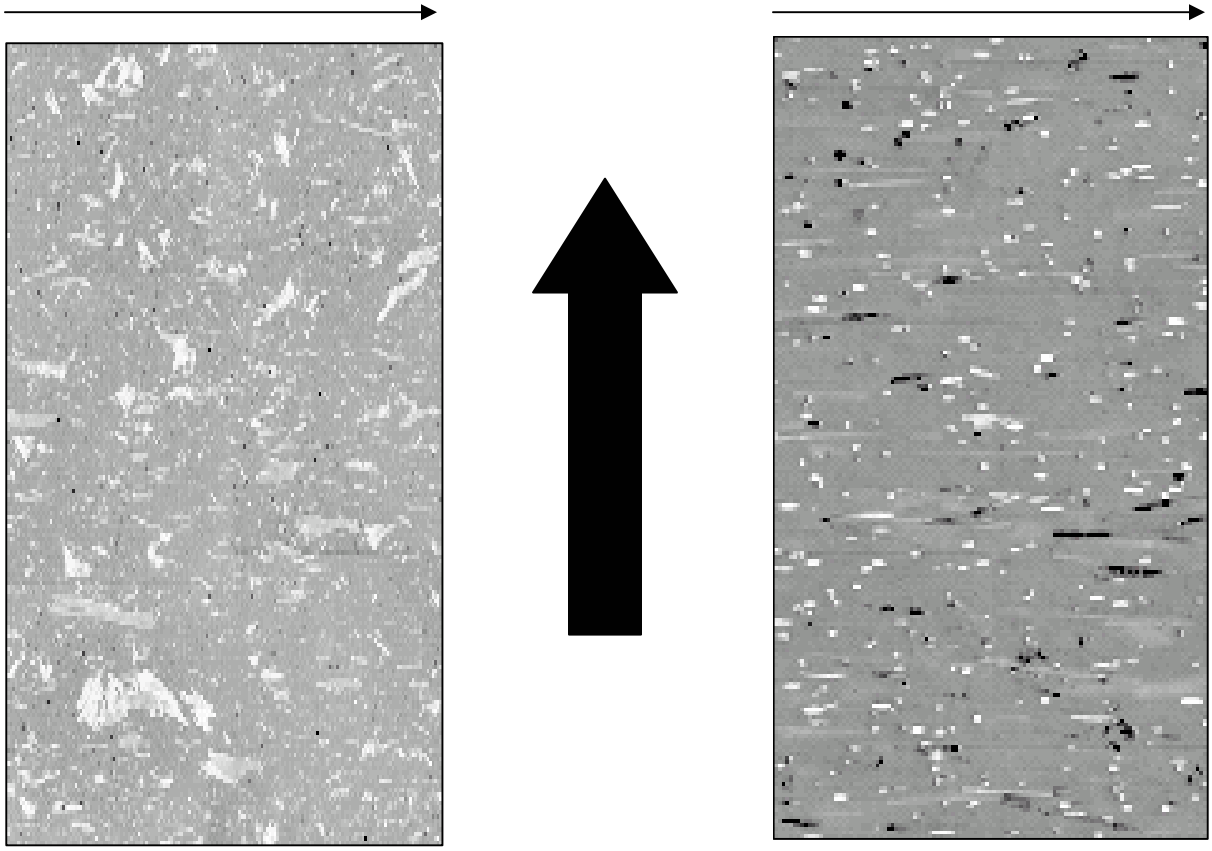

(A) 30 wt% Thermocarb™ Synthetic Graphite in Nylon

(B) 20 wt% Carbon Fiber in Polycarbonate

Figure 7.5-1: Orientation Images at 20X

Table 7.5-1 Orientation Results (53)

	Nylon 6,6	Polycarbonate
Formulation	**Orientation (Degrees)**	**Orientation (Degrees)**
Synthetic Graphite		
10 wt%	58.716 ± 23.918 n= 733	66.468 ± 21.480 n= 2690
15 wt%	60.235 ± 23.483 n=2118	67.924 ± 20.793 n= 3173
20 wt%	61.546 ± 24.632 n=3755	66.352 ± 22.345 n= 5271
30 wt%	57.457 ± 25.024 n=3784	67.199 ± 22.698 n= 4945
40 wt%	58.250 ± 25.721 n=3235	66.993 ± 22.124 n= 1180
Carbon Fiber		
5 wt%	72.477 ± 21.299 n= 831	77.351 ± 17.918 n= 1636
10 wt%	71.609 ± 21.830 n=2058	69.470 ± 22.137 n= 1819
15 wt%	66.455 ± 24.737 n=2595	66.536 ± 23.717 n= 6321
20 wt%	68.558 ± 22.449 n=4183	64.465 ± 24.388 n= 4599
30 wt%	63.374 ± 23.811 n=4405	61.114 ± 25.017 n= 4014
40 wt%	65.113 ± 22.542 n=4142	62.256 ± 24.658 n= 4516

CHAPTER 8: FACTORIAL DESIGN METHODS AND RESULTS

8.1 Factorial Design Information for Shielding Effectiveness

This analysis was performed using the Minitab Version 13 Statistical Software package. Calculations were also performed using Microsoft Excel 2000 to verify and understand the results obtained with the Minitab calculations. Excel calculations can be seen in Appendix L. For this analysis, the effects, coefficients, and T and P values for the shielding effectiveness were calculated. For all statistical calculations, the 95% confidence level was used.

Factorial designs were used in the project since they are the most efficient type of experiment to determine the effect of each filler and any possible interactions between fillers. Factorial design experiments are more efficient than performing one-factor-at-a-time experiments. Examining multiple factors at one time can significantly reduce the total number of experiments that must be run to determine the effects of the factors. By using factorial design, one can determine the effect that each factor (filler) has on the system by calculating a single value to quantify the increase in conductivity as the weight percent of a filler is increased. These calculated effects can then be ranked to determine which fillers and combinations of fillers produced a larger change in the thermal conductivity values. In addition, the use of factorial designs can prevent the misinterpretation of data that can occur when interaction effects are present in an experiment.

A 2^k factorial design was used with $k = 3$. It has eight factor level combinations. Geometrically, the design is a cube as shown in Figure 8.1-1 (75).

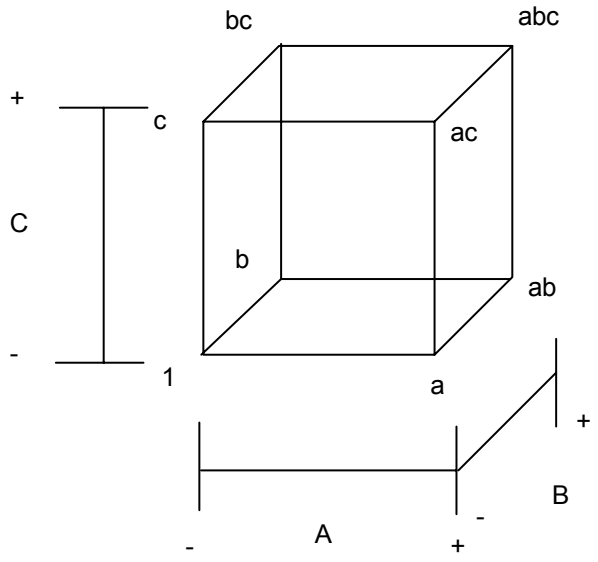

Figure 8.1-1: The 2^3 Factorial Design (75)

The eight runs form the corners of the cube. The (-) sign represents the low level used and the (+) sign represents the high level used. The number 1 represents all factors at lowest level (-). That is all of the polymers in this case. This design allows three main effects to be estimated (A, B, and C) along with three two factor interactions (AB, AC, and BC) and a three-factor interaction (ABC). Therefore, the full factorial model could simplify as shown in Equation 8.1-1.

$$y = \mu + A + B + C + AB + AC + BC + ABC + \varepsilon \qquad \text{Equation 8.1-1}$$

$\mu =$ Overall mean

$\varepsilon =$ Random error term

Main Effects = A, B, C

Two factor interaction = AB, BC, AC

Three factor interaction =ABC

The main effects can be estimated easily. Lowercase letters of the effects (a, b, c, ab, ac, bc, abc) represent the total number of (n) replicates at each of the eight runs in the design (75). By looking at Figure 8.1-2 we can estimate the main effect of A by averaging the four runs on the right side of the cube where A is at the highest level (+) and subtracting from that quantity the average of the four runs on the left side of the cube where A is the lowest (-). A similar method is used to get the (B) and (C) effects. So for effect (A), (B), and (C) can be determined using the following equations:

$$A = \overline{y_{A^+}} - \overline{y_{A^-}} = \frac{1}{4n}\left(a + ab + ac + abc - b - c - bc - (1)\right) \qquad \text{Equation 8.1-2}$$

$$B = \overline{y_{B^+}} - \overline{y_{B^-}} = \frac{1}{4n}\left(b + ab + bc + abc - a - c - ac - (1)\right) \qquad \text{Equation 8.1-3}$$

$$C = \overline{y_{C^+}} - \overline{y_{C^-}} = \frac{1}{4n}\left(c + ac + bc + abc - a - b - ab - (1)\right)$$ Equation 8.1-4

To calculate the two-factor interaction, a similar procedure is described in Figure 8.1-1 and by using the equations below.

$$AB(C_{low}) = \frac{1}{2n}\left[ab - b\right] - \frac{1}{2n}\left[a - (1)\right]$$ Equation 8.1-5

$$AB(C_{high}) = \frac{1}{2n}\left[abc - bc\right] - \frac{1}{2n}\left[ac - c\right]$$ Equation 8.1-6

By averaging the above components you can obtain the expression for (AB).

$$AB = \frac{1}{4n}\left[ab + (1) + abc + c - b - a - bc - ac\right]$$ Equation 8.1-7

The AB interaction is just the difference in the averages on two diagonal planes in the cube as shown in Figure 8.1-3. By using the same principal we derive the following combined interaction.

$$AC = \frac{1}{4n}\left[ac + (1) + abc + b - a - c - ab - bc\right]$$ Equation 8.1-8

$$BC = \frac{1}{4n}\left[bc + (1) + abc + a - b - c - ab - ac\right]$$ Equation 8.1-9

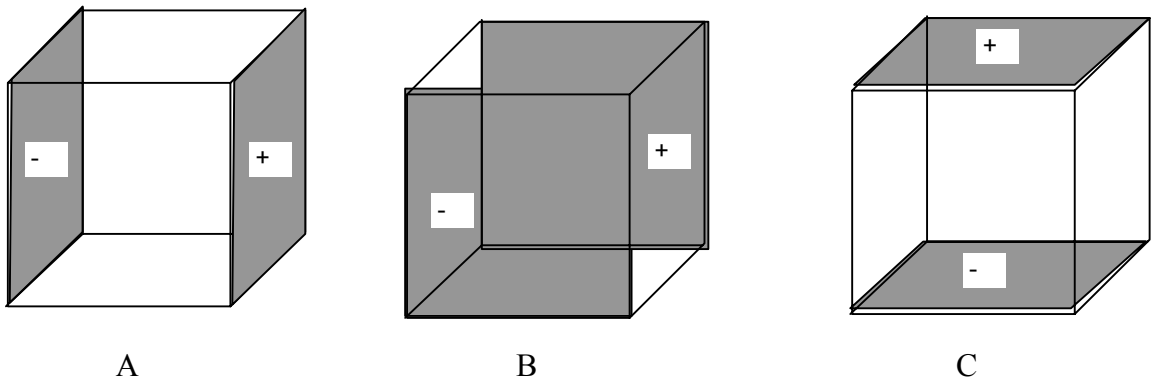

A B C

Figure 8.1-2: Factorial Main Effects (75)

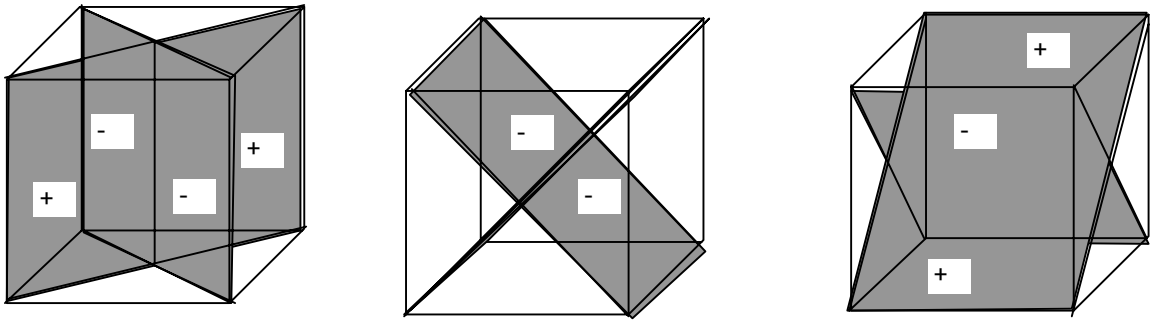

AB AC BC

Figure 8.1-3: Factorial Two-Factor Interaction (75)

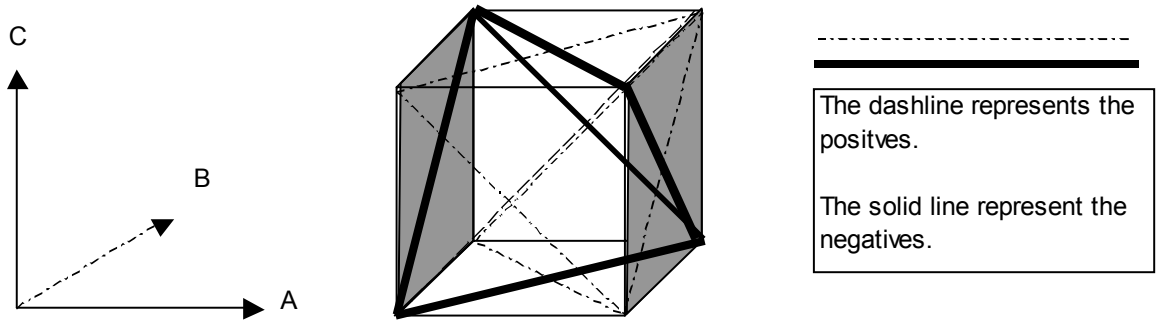

ABC

Figure 8.1-4: Factorial Three Factor Interaction (75)

In order to calculate the ABC interaction, we use the average difference between the AB interactions at the two levels of c. Therefore, the equation for three interactions:

$$ABC = \frac{1}{4n}\left[abc - bc - ac + c - ab + b + a - (1)\right] \qquad \text{Equation 8.1-10}$$

See the bottom row of the Figure 8.1-4 for a visual representation of the effect for a three-factor combination.

The quantities in brackets are contrasts in the eight factor-level combinations. These contrasts can be obtained from a table of plus (high level) and minus (low level) signs for the 2^3 factorial design as shown in Table 8.1-1.

Table 8.1-1: Factorial Effect Design Table (75)

Treatment Combination	Factorial Design Effects							
	I	A	B	AB	C	AC	BC	ABC
1	+	-	-	+	-	+	+	-
a	+	+	-	-	-	-	+	+
b	+	-	+	-	-	+	-	+
ab	+	+	+	+	-	-	-	-
c	+	-	-	+	+	-	-	+
ac	+	+	-	-	+	+	-	-
bc	+	-	+	-	+	-	+	-
abc	+	+	+	+	+	+	+	+

Signs for the main effects are obtained by associating a plus with the high level and a minus with the low level. Once the signs for the main effects have been established, the signs for the remaining columns are found by multiplying the appropriate preceding columns, row by row. It can be observed from Table 8.1-1:

1. Except for the identity column (I), each column has an equal number of plus and minus signs.
2. The sum of products of signs in any two columns is zero: that is, the columns in the table are orthogonal.
3. Multiplying any column by column (I) leaves the column unchanged: that is, (I) is an identity element.
4. The product of any two columns yields a column in the table.

The estimate of the main effect or interaction is determined by multiplying the factor-level combinations in the first column of the table by the signs in the corresponding

main effect or interaction column, adding the result to produce a contrast, and then dividing the contrast by one-half the total number of runs in the experiment.

$$Effect = \frac{Contrast}{n * 2^k} \qquad \text{Equation 8.1-11}$$

The sum of squares for any given effect is given below.

$$SS = \frac{(Contrast)^2}{n * 2^k} \qquad \text{Equation 8.1-12}$$

Now that a background of a statistical approach has been made we can pursue with the results of the problem.

8.2 Factorial Design Results for Shielding Effectiveness

The project studied here is a 2^3 factorial design, defined as three factors at two different levels. Therefore, a total of eight different combinations have been created. The formulations that make up this experimental design are shown in Table 8.2-1. For all fillers, the low level is zero weight percent. The high level varied for each filler. The levels are 5 wt % for Ketjenblack EC-600JD (CB), 30 wt % for Thermocarb™ Specialty Graphite (TC), and 20 wt % for ThermalGraph DKD X (CF). Since this project is focusing on producing highly conductive composites, the levels for all fillers were chosen so that filler amounts would be above the percolation threshold. This would ensure an increase in the electrical conductivity over that of

the pure polymer. These formulations were extruded and injection molded according to the previously described conditions. Additionally, complete sets of replicate formulations, designated with an "R" in formulation names, were also produced. Therefore, two complete sets of the formulations in the factorial design were fabricated and available for testing. By running the design twice, this allowed for further verification of experimental results and for a sufficient number of degrees of freedom when performing the statistical analysis.

Table 8.2-1: Weight Percent Filler in Factorial Design Formulations

Terms	Ketjenblack EC-600JD	Thermocarb™ Specialty Graphite	ThermalGraph DKD X
1	0	0	0
A	5	0	0
B	0	30	0
AB	5	30	0
C	0	0	20
AC	5	0	20
BC	0	30	20
ABC	5	30	20

The total number of experiments that must be run to determine the effects of the factors can be significantly reduced by examining multiple factors at one time. By using factorials, one can determine the effect that each factor (filler) has on the system by calculating a single value to quantify the increase in conductivity as the weight percent of filler is increased. These calculated effects can then be ranked to determine which fillers and combinations of fillers produced a larger change in the SE values. In addition, the use of factorial designs can prevent the misinterpretation of data that can occur when interaction effects are present in an experiment. Table

8.2-2 and Table 8.2-3 displays the shielding effectiveness values that were reported for the factoral design formulations in nylon 6,6 and polycarbonate.

Table 8.2-2: Shielding Effectiveness Results at 300MHz and 800 MHz for Factoral Design Formulations in Nylon 6,6

Formulation	Shielding Effectiveness, dB		Shielding Effectiveness, dB Mean
	Original	Replicate	
300 MHz			
No filler	-0.03 ± 0.05	-0.07 ± 0.19	-0.05
CB	7.35 ± 0.23	7.42 ± 0.03	7.39
TC	1.30 ± 0.06	1.74 ± 0.08	1.52
CB*TC	23.11 ± 0.40	22.90 ± 0.26	23.01
CF	2.32 ± 0.16	2.34 ± 0.17	2.33
CB*CF	21.00 ± 0.45	20.19 ± 0.36	20.60
TC*CF	10.08 ± 0.06	12.81 ± 0.23	11.45
CB*TC*CF	42.63 ± 0.32	40.88 ± 0.40	41.76
800 MHz			
No filler	0.10 ± 0.04	0.07 ± 0.05	0.09
CB	7.17 ± 0.20	7.18 ± 0.01	7.18
TC	2.22 ± 0.04	3.04 ± 0.17	2.63
CB*TC	23.11 ± 0.10	23.09 ± 0.23	23.10
CF	4.24 ± 0.28	4.25 ± 0.13	4.25
CB*CF	20.88 ± 0.40	19.89 ± 0.15	20.39
TC*CF	13.08 ± 0.17	15.34 ± 0.17	14.21
CB*TC*CF	42.44 ± 0.83	42.01 ± 0.32	42.23

Table 8.2-3: Shielding Effectiveness Results at 300MHz and 800 MHz for Factoral Design Formulations in Polycarbonate

Formulation	Shielding Effectiveness, dB		Shielding Effectiveness, dB
	Original	Replicate	Mean
300 MHz			
No filler	-0.10 ± 0.00	-0.07 ± 0.06	-0.09
CB	10.19 ± 0.25	10.43 ± 0.15	10.31
TC	3.03 ± 0.21	3.23 ± 0.31	3.13
CB*TC	27.87 ± 0.26	28.37 ± 0.89	28.12
CF	3.10 ± 0.10	3.43 ± 0.06	3.27
CB*CF	27.07 ± 0.06	26.77 ± 0.32	26.92
TC*CF	16.95 ± 0.15	17.83 ± 0.35	17.39
800 MHz			
No filler	0.00 ± 0.00	0.03 ± 0.06	0.02
CB	10.73 ± 0.21	10.83 ± 0.25	10.78
TC	5.27 ± 0.32	5.60 ± 0.44	5.44
CB*TC	27.60 ± 0.10	27.70 ± 0.30	27.65
CF	5.43 ± 0.12	5.87 ± 0.06	5.65
CB*CF	26.10 ± 0.10	26.33 ± 0.06	26.22
TC*CF	18.70 ± 0.10	19.40 ± 0.30	19.05

The effects, coefficients and T and P-values for the nylon 6,6 and polycarbonate-based composites are given in Table 8.2-4 and Table 8.2-5 respectively. To determine if these statistics are significant, the T-distribution and the P values were examined. For an effect to be significant, the value for the T-distribution must be greater than 1.753. Likewise, the P value must be smaller than 0.05 for an effect to be significant at the 95% confidence level. It can be seen from Table 8.2-4 that all of the factoral design formulations have a significant effect, having satisfied both conditions previously described with the exception of using three filler combinations. All results were significant at the level of 99.9 %.

Table 8.2-4: Factorial Design Analysis for Nylon 6,6 Based Conductive Resins at 300 and 800 MHz

Term	Effect	Coefficient	T	P
300 MHz				
Constant		13.50	63.9	0.000
CB	**19.37**	**9.69**	**45.9**	**0.000**
TC	**11.87**	**5.93**	**28.1**	**0.000**
CF	**11.07**	**5.53**	**26.2**	**0.000**
TC*SG	**6.52**	**3.26**	**15.5**	**0.000**
CB*CF	**4.91**	**2.46**	**11.6**	**0.000**
TC*CF	**3.27**	**1.64**	**7.8**	**0.000**
CB*TC*CF	**0.50**	**0.25**	**1.2**	**0.269**
800 MHz				
Constant		14.26	86.6	0.000
CB	**17.93**	**8.96**	**54.4**	**0.000**
TC	**12.57**	**6.28**	**38.2**	**0.000**
CF	**12.02**	**6.01**	**36.5**	**0.000**
CB*TC	**6.31**	**3.16**	**19.2**	**0.000**
CB*CF	**4.15**	**2.07**	**12.6**	**0.000**
TC*CF	**3.33**	**1.67**	**10.1**	**0.000**
CB*TC*CF	**0.38**	**0.19**	**1.1**	**0.286**

Investigation of Table 8.2-4 yields some important information regarding the effects that fillers have on SE at 300 MHz and 800 MHz. First, all the effect terms are positive, which indicates that the addition of any filler increases the SE of the composite. Second, the effects, coefficients, and T and P-values are similar for 300 MHz and 800 MHz. Third, the effect term is the largest for carbon black, which indicates that carbon black causes the largest increase in composite SE. Fourth, the effect terms for Thermocarb™ Specialty Graphite and carbon fiber are similar, and they cause the second largest effect on SE. After, Thermocarb™ Specialty Graphite and carbon fiber combination, the effect of the fillers follows the following order: the

combination of carbon black and Thermocarb™ Specialty Graphite, the combination of carbon black and carbon fiber, and last the combination of Thermocarb™ Specialty Graphite and carbon fiber. The six formulations mentioned are all statistically significant at the 95% confidence level ($P<0.05$). One formulation, the carbon black, Thermocarb™ Specialty Graphite and carbon fiber combination, is not statistically significant ($P>0.05$).

Table 8.2-5: Factorial Design Analysis for Polycarbonate Based Conductive Resins at 300 and 800 MHz

Term	Effect	Coefficient	T	P
300 MHz				
Constant		18.09	166.5	0.000
CB	**24.32**	**12.16**	**111.9**	**0.000**
TC	**15.97**	**7.98**	**73.5**	**0.000**
CF	**15.44**	**7.72**	**71.0**	**0.000**
CB*TC	**7.30**	**3.65**	**33.6**	**0.000**
CB*CF	**6.63**	**3.32**	**30.5**	**0.000**
TC*CF	**5.46**	**2.73**	**25.1**	**0.000**
800 MHz				
Constant		18.23	207.3	0.000
CB	**21.39**	**10.70**	**121.6**	**0.000**
TC	**15.14**	**7.57**	**86.1**	**0.000**
CF	**14.53**	**7.26**	**82.6**	**0.000**
CB*TC	**5.73**	**2.86**	**32.6**	**0.000**
CB*CF	**4.90**	**2.45**	**27.9**	**0.000**
TC*CF	**3.99**	**2.00**	**22.7**	**0.000**

Table 8.2-5 shows the results of the factorial design analysis for the polycarbonate-based composites at 300 MHz and 800 MHz. Once again, the effects, coefficients, and T and P-values are similar for 300 MHz and 800 MHz. In addition, as was the case for nylon 6,6, carbon black causes the largest increase in composite SE, followed by synthetic graphite and carbon fiber, which once again have similar

effect values. The rest of the statistically significant effects in order of their ability to increase SE of the composite are the combination of carbon black and synthetic graphite, the combination of carbon black and carbon fiber, and last the combination of Thermocarb™ Specialty Graphite and carbon fiber. All of these fillers and combinations of fillers are statistically significant at the 95% confidence level ($P<0.05$). These results agree with what was obtained for the nylon-based composites.

One important result from this study is that the combinations that contained two different carbon fillers; namely, carbon black and Thermocarb™ Specialty Graphite, carbon black and carbon fiber, and Thermocarb™ Specialty Graphite and carbon fiber were statistically significant. The fact that all the two-way interaction terms were significant indicates that the composite SE is higher than what would be expected from the additive effect of each single filler. To the authors' knowledge, this is the first time in the literature that a synergistic effect of combining different carbon fillers on the composite SE has been observed. It is likely that conductive pathways are forming links in the high surface area carbon black, Thermocarb™ Specialty Graphite, and carbon fiber.

One additional way to examine how the different fillers affect the composite electrical conductivity is to look at a cube plot. This type of graph displays the conductivity results on a three-dimensional figure. The two levels of weight percents are plotted on the x, y and z-axes. Figure 8.2-1 and Figure 8.2-2 show the cube plots for nylon 6,6 and polycarbonate respectively. Each corner of the cube represents a different factorial design formulation and gives the average shielding effectiveness result for that formulation based on the weight percent level.

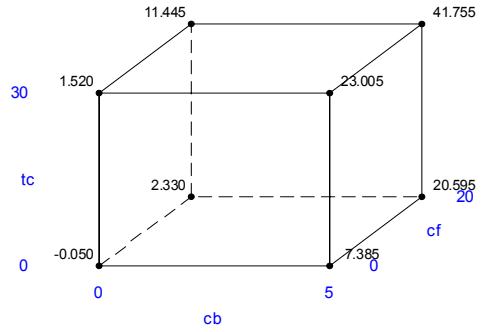

Figure 8.2-1: Cube Plot for Nylon 6, 6 at 300 MHz

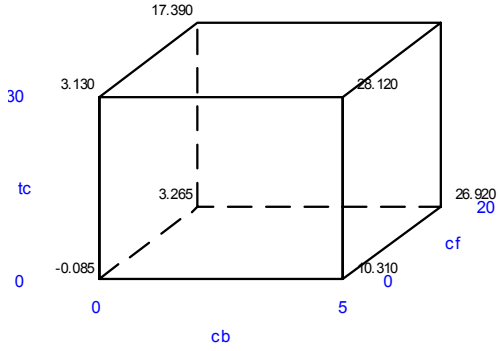

Figure 8.2-2: Cube Plot for Polycarbonate at 300 MHz

It can be seen that the main effects, or single filler effects, rank in order from carbon black (CB) to Thermocarb™ Specialty Graphite (TC) to carbon fibers (CF). Also, all three main effects are statistically significant at the 95 % confidence level ($P<0.05$). Figures 8.2-3 and 8.2-4 show the main effects plot for shielding effectiveness results in nylon 6,6 and polycarbonate at 300 MHz, respectively. This figure is a graphical representation of the effects that single fillers have on the shielding effectiveness. A steeper slope signifies a higher effect number. The slope also shows that as the filler amount is increased, the conductivity increases. A higher effect number for carbon black means that the filler produced the largest change in shielding effectiveness when compared to all of the other fillers. Thus, adding carbon black significantly increased the shielding effectiveness of the composite. These results are not unexpected, as this particular material was chosen specifically because of its ability to impart shielding to a matrix material. Therefore, this material should out-perform the other two fillers as the results indicate.

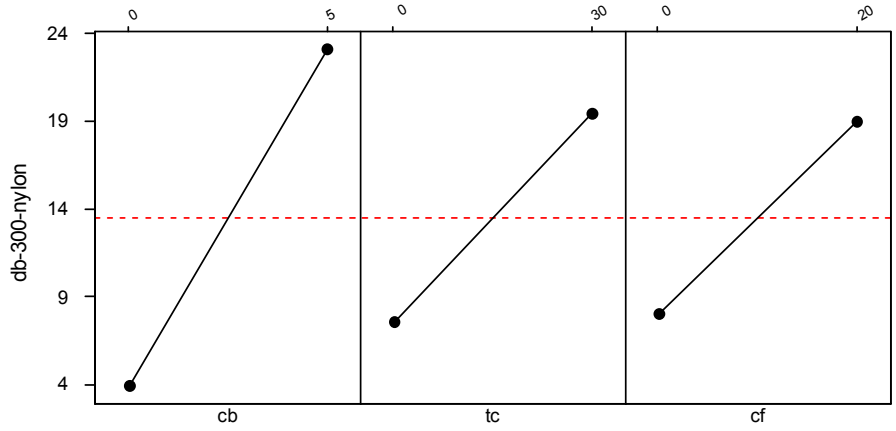

Figure 8.2-3: Main Effects Plot for Nylon 6,6 at 300 MHz

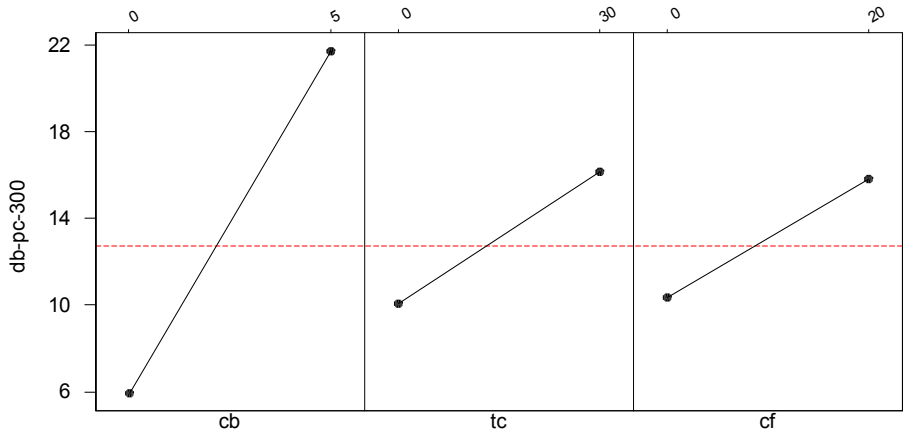

Figure 8.2-4: Main Effects Plot for Polycarbonate at 300 MHz

Additionally, the results for the two-way interactions show that there is an effect on the shielding effectiveness when fillers are combined. All two-way interactions are statistically significant at the 95 % confidence level. The most significant combination was that of the carbon black and Thermocarb™ Specialty Graphite combination, followed by the carbon black and carbon fiber combination and the Thermocarb™ Specialty Graphite and carbon fiber combination. This means that, for example, when carbon black and the Thermocarb™ Specialty Graphite were combined and added to the polymer, the shielding effectiveness of the composite increased significantly. This could be said for all of the interaction terms. However, the effects of the interactions were not as high as the main effects. In general the two-way interaction terms are approximately half the value of the main effects. These results show that the two-way interactions do have some influence on the conductivity of the composites; however, it is much smaller than that of the main effects.

These results are further supported by the interaction plot for nylon 6,6 at 300 MHz shown in Figure 8.2-5 and the results for polycarbonate are shown in Figure 8.2-6. These figures show how the shielding effectiveness changes with increases in the concentrations of the various fillers. The slope of the lines indicates how a particular filler effects the shielding effectiveness in the combinations. If the two lines are parallel, then there is no significant interaction. Non-parallel lines indicate that there is an interaction present in the combination of fillers. The dashed line represents the high level of filler and the solid line represents the low level of filler

added. A full analysis of cube plots, main effect plots and interaction plots for nylon 6,6 and polycarbonate at varying frequencies can be found in Appendix J.

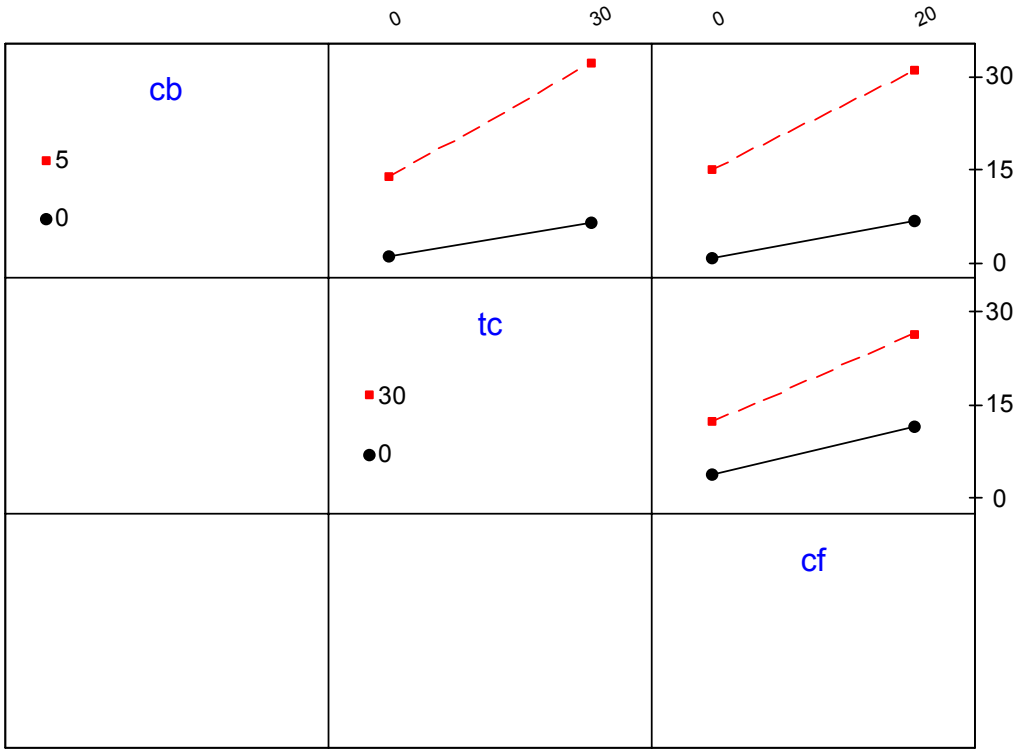

Figure 8.2-5: Interaction Plot for Nylon 6,6 at 300 MHz

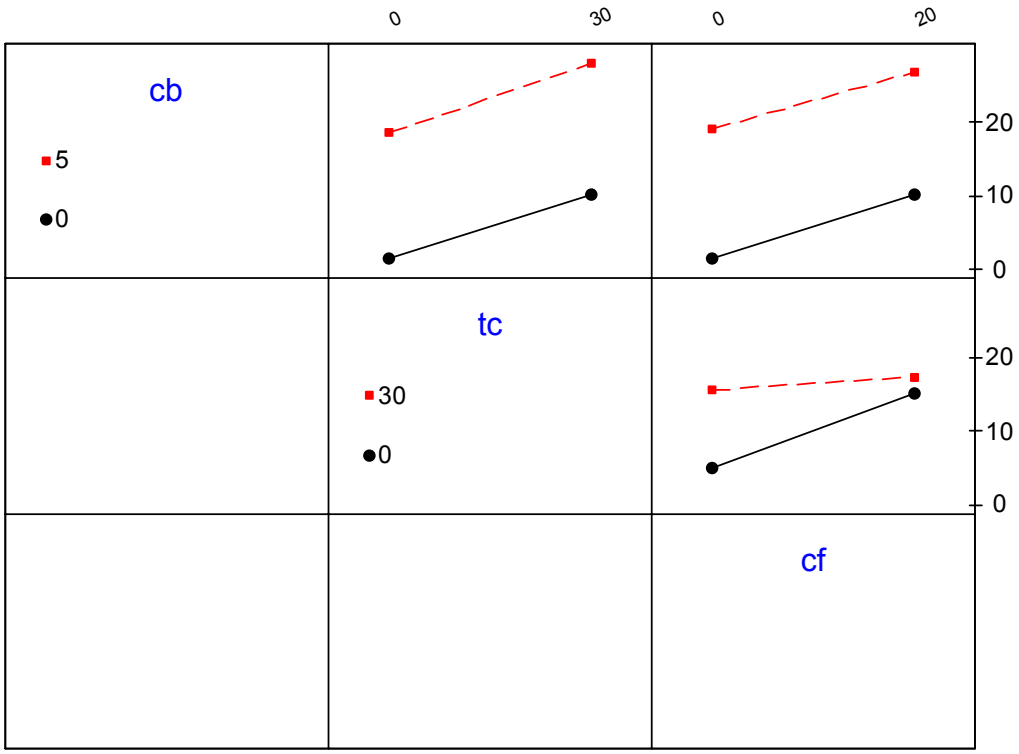

Figure 8.2-6: Interaction Plot for Polycarbonate at 300 MHz

CHAPTER 9: SHIELDING RESULTS

9.1 Pure Matrix

For pure nylon 6,6 and polycarbonate it can be shown that shielding effectiveness remains constant at all frequencies. Nylon 6,6 and polycarbonate have a very low electrical conductivity because they are insulators and are expected to give the lowest shielding effectiveness as shown in Figure 9.1-1 and Figure 9.1-2 below. This can also be confirmed by factorial design analysis as performed in Chapter 8. The shielding effectiveness should be 0 dB, because pure matrix material is an insulator. All shielding results for each formulation can be found in Appendix E. Replicates of each test formulation are indicated to show consistent manufacturing ability. The replicates lie on top of each other, because the values are close.

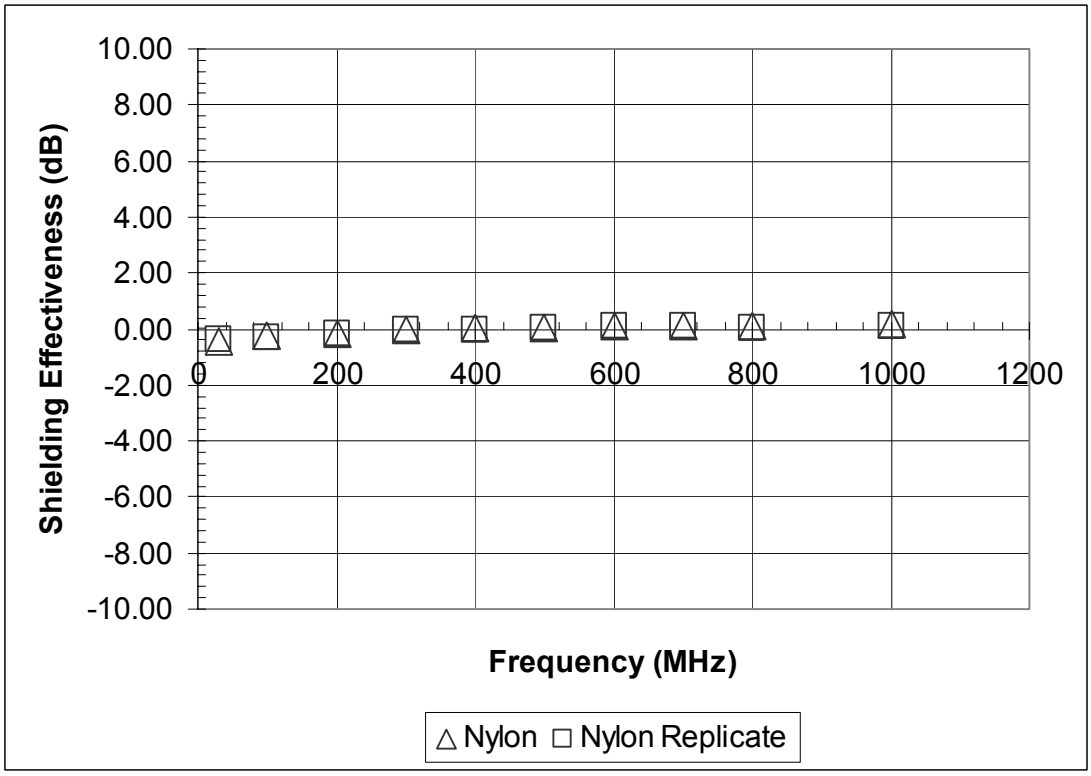

Figure 9.1-1: Shielding Effectiveness of Pure Nylon 6,6

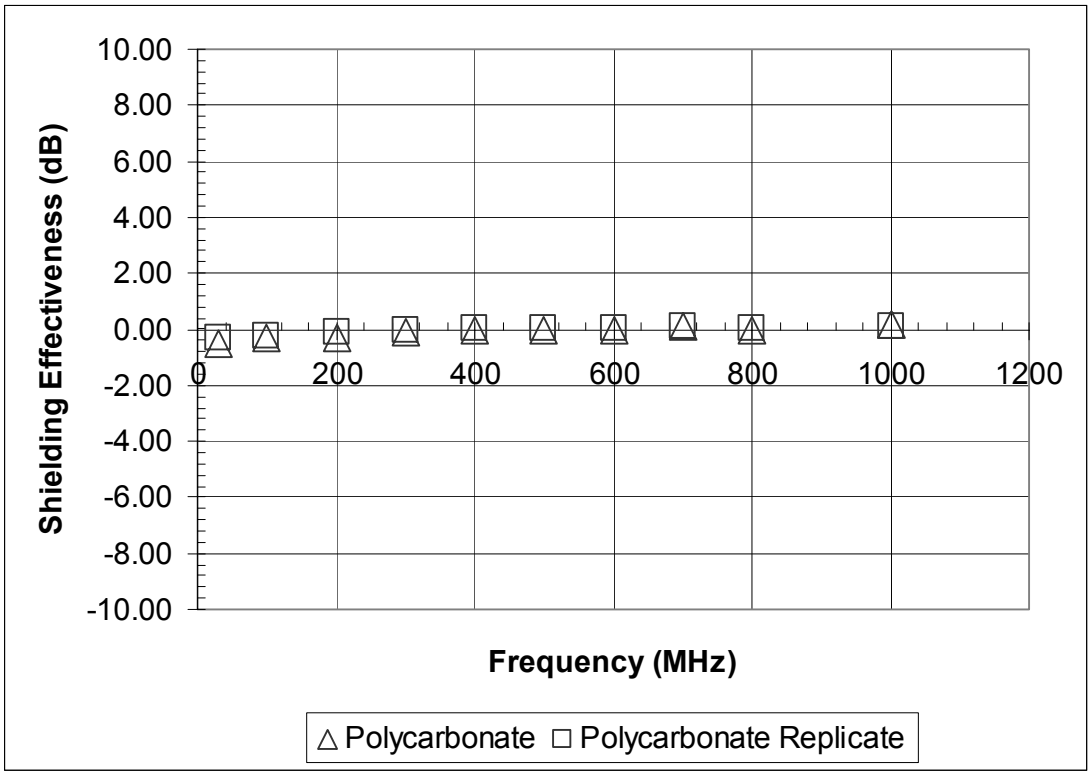

Figure 9.1-2: Shielding Effectiveness of Pure Polycarbonate

9.2 Single Filler Results

For carbon black it can be shown that shielding effectiveness increases with volume percent. All formulation compositions can be found in Appendix B. Carbon black has a high electrical conductivity and is expected to give the highest shielding effectiveness as shown in Figure 9.2-1 below. This can also be confirmed by factoral design analysis as performed in Chapter 8. Notice that frequency did not impact how effective carbon black is in either the nylon 6,6 or polycarbonate matrix.

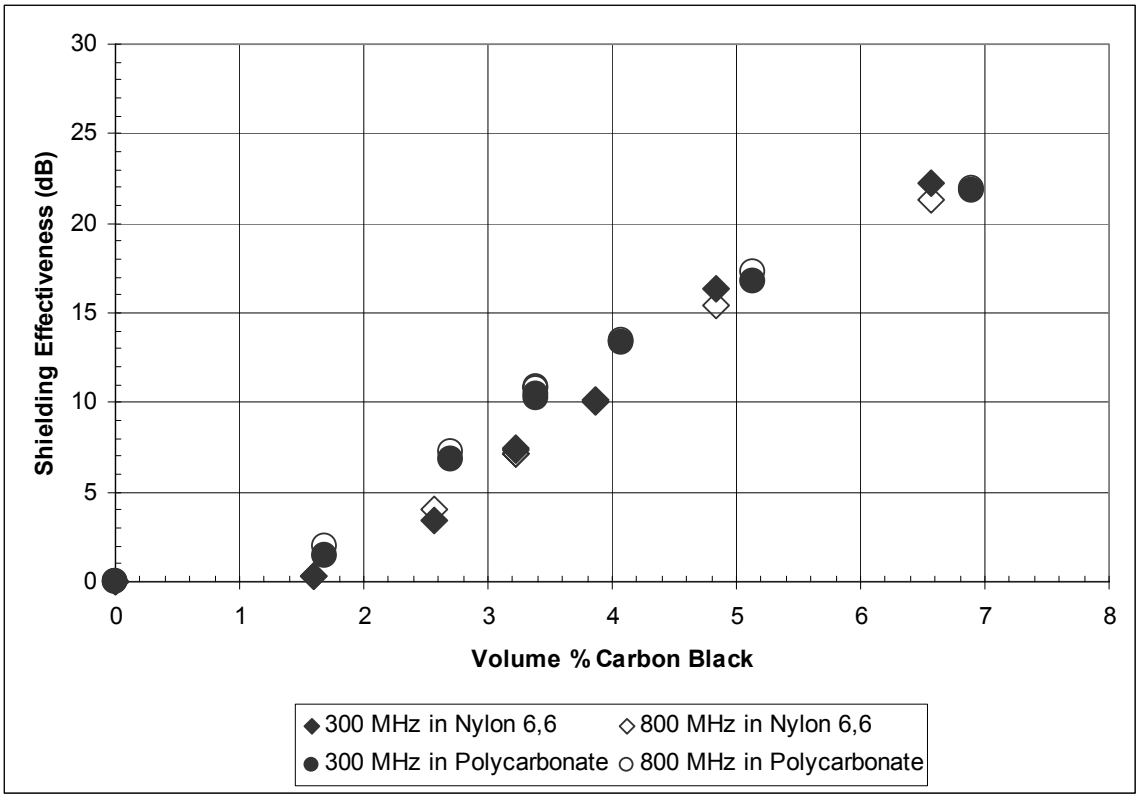

Figure 9.2-1: Shielding Effectiveness of Carbon Black

For Thermocarb™ Specialty Graphite it can be shown that shielding effectiveness increases with volume percent. Thermocarb™ Specialty Graphite has a moderate electrical conductivity and is expected to give us a moderate shielding effectiveness as shown in Figure 9.2-2 below. This can also be confirmed by factoral design analysis as performed in Chapter 8. Typically, the shielding effectiveness in polycarbonate was higher than in nylon 6,6.

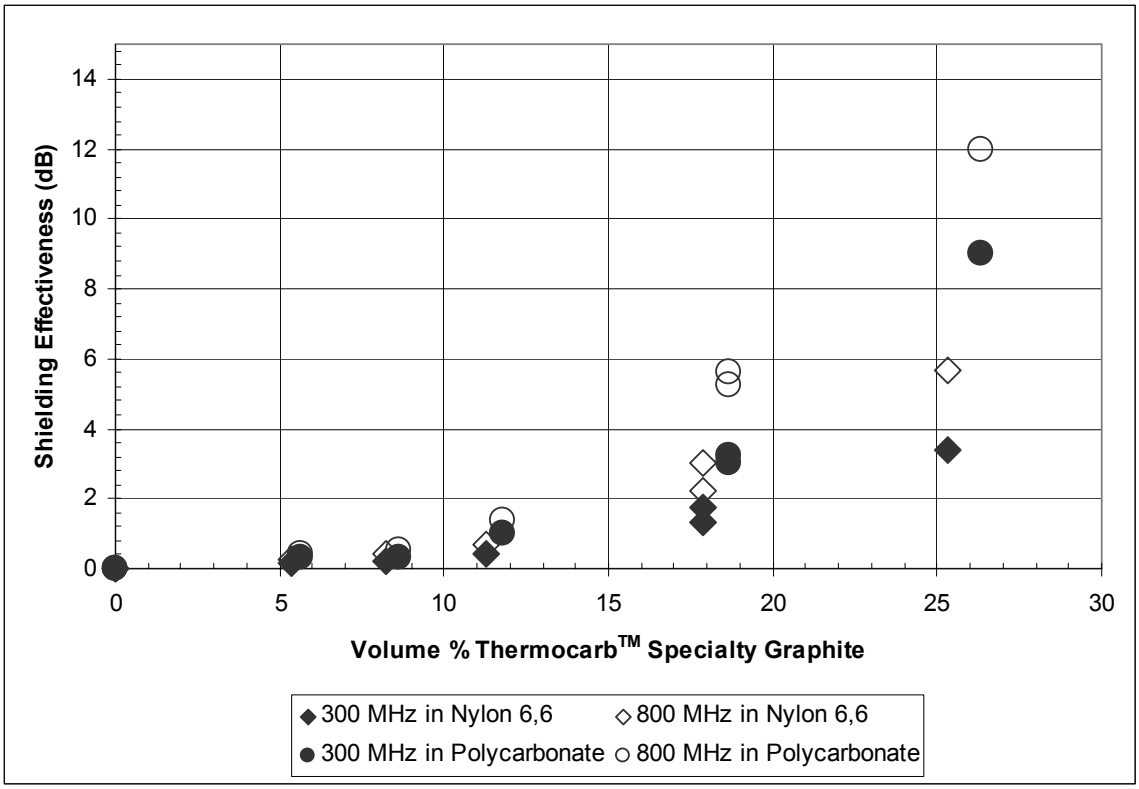

Figure 9.2-2: Shielding Effectiveness of Thermocarb™ Specialty Graphite

For carbon fiber it can be shown that shielding effectiveness increases with volume percent as well. Carbon fiber has a moderate electrical conductivity that is higher than Thermocarb™ Specialty Graphite, but lower than carbon black. It is expected to give us a moderate shielding effectiveness as shown in Figure 9.2-3 below. This can also be confirmed by factoral design analysis as performed in Chapter 8. Notice that frequency did matter on how effective carbon fiber was in either nylon 6,6 or polycarbonate matrix. Shielding was slightly higher at 800 MHz compared to 300 MHz. Again the shielding effectiveness was higher in polycarbonate than in nylon 6,6.

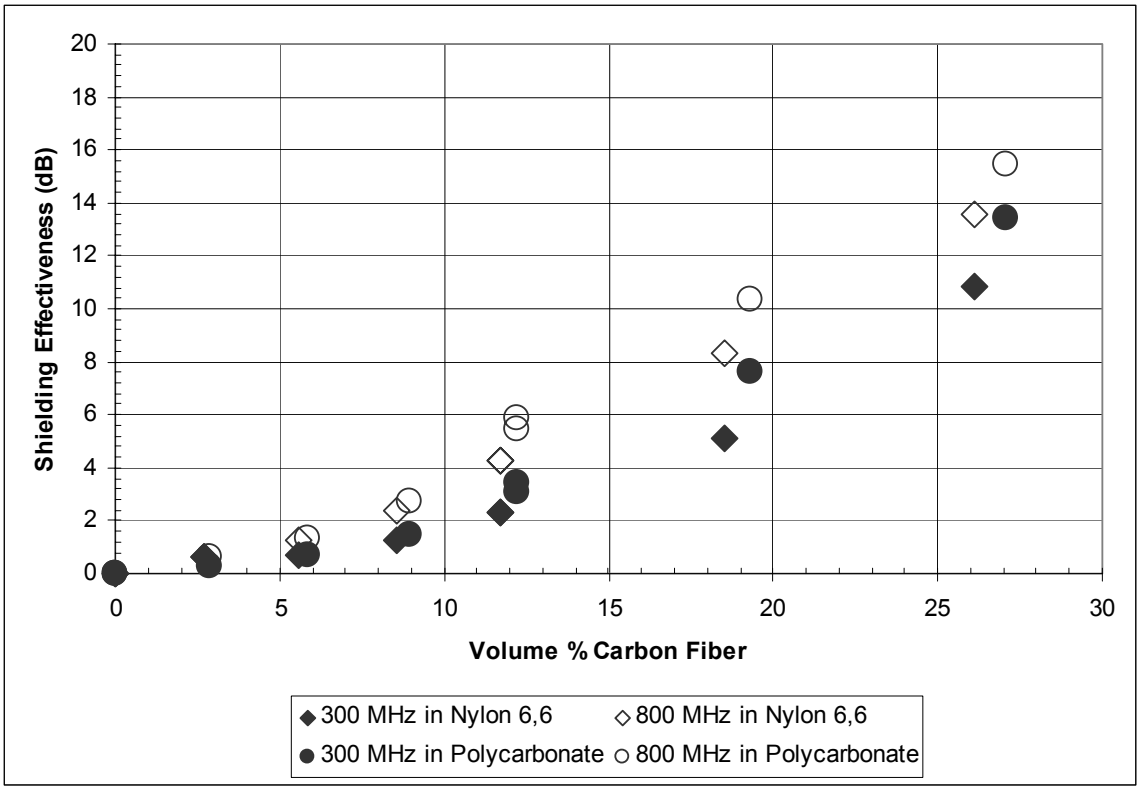

Figure 9.2-3: Shielding Effectiveness of Carbon Fiber

9.3 Multiple Filler Analysis

Figure 9.3-1 shows carbon black and Thermocarb™ Specialty Graphite's shielding effectiveness for the combination of the two fillers. It can be shown that shielding effectiveness remains unchanged for all frequencies measured. Carbon black and Thermocarb™ Specialty Graphite have a high combined electrical conductivity and is expected to give us a high shielding effectiveness as shown in Figure 9.3-1 below. This can also be confirmed by factoral design analysis as performed in Chapter 8. As discussed in the previously, the polycarbonate matrix gave higher shielding values when compared to nylon 6,6.

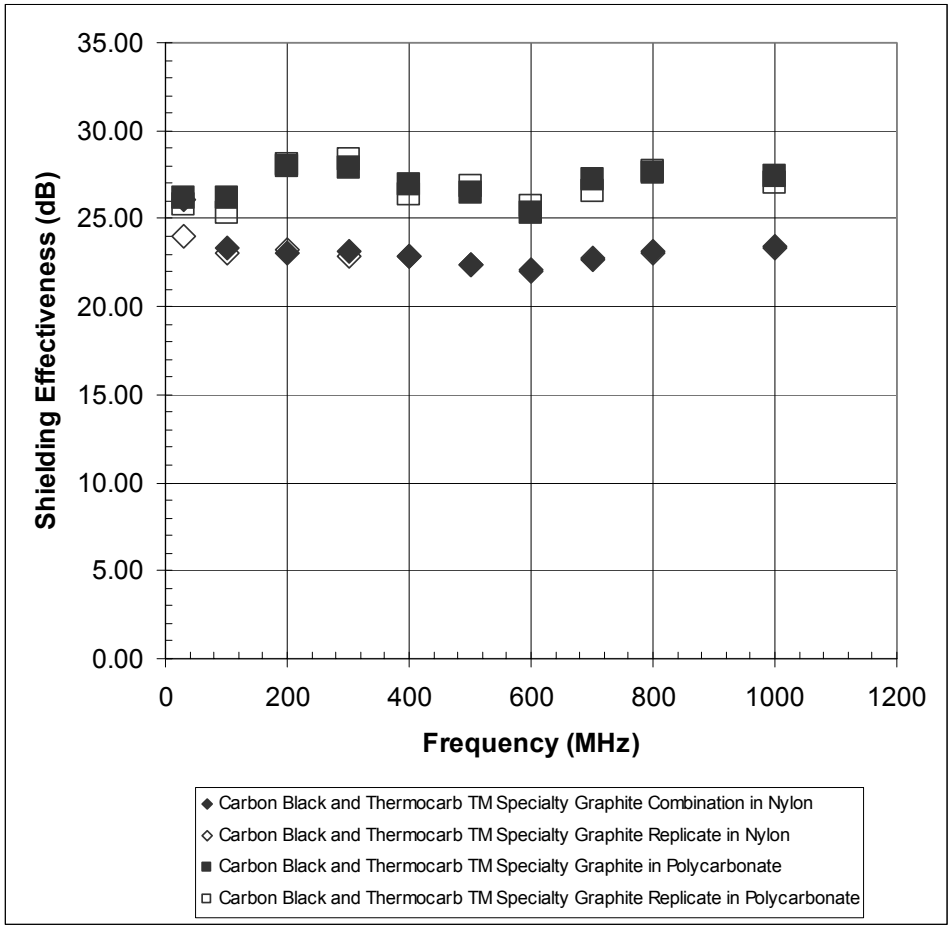

Figure 9.3-1: Shielding Effectiveness of Carbon Black and Thermocarb™ Specialty Graphite

Figure 9.3-2 shows carbon black and carbon fiber's shielding effectiveness for the combination of the two fillers. It can be shown that shielding effectiveness remains unchanged for all frequencies measured. Carbon black and carbon fiber have a high combined electrical conductivity and are expected to give us a high shielding effectiveness as shown in Figure 9.3-2. This can also be confirmed by factoral design analysis as performed in Chapter 8. As discussed in the previous section, the polycarbonate matrix gave higher shielding values when compared to nylon 6,6 at each frequency.

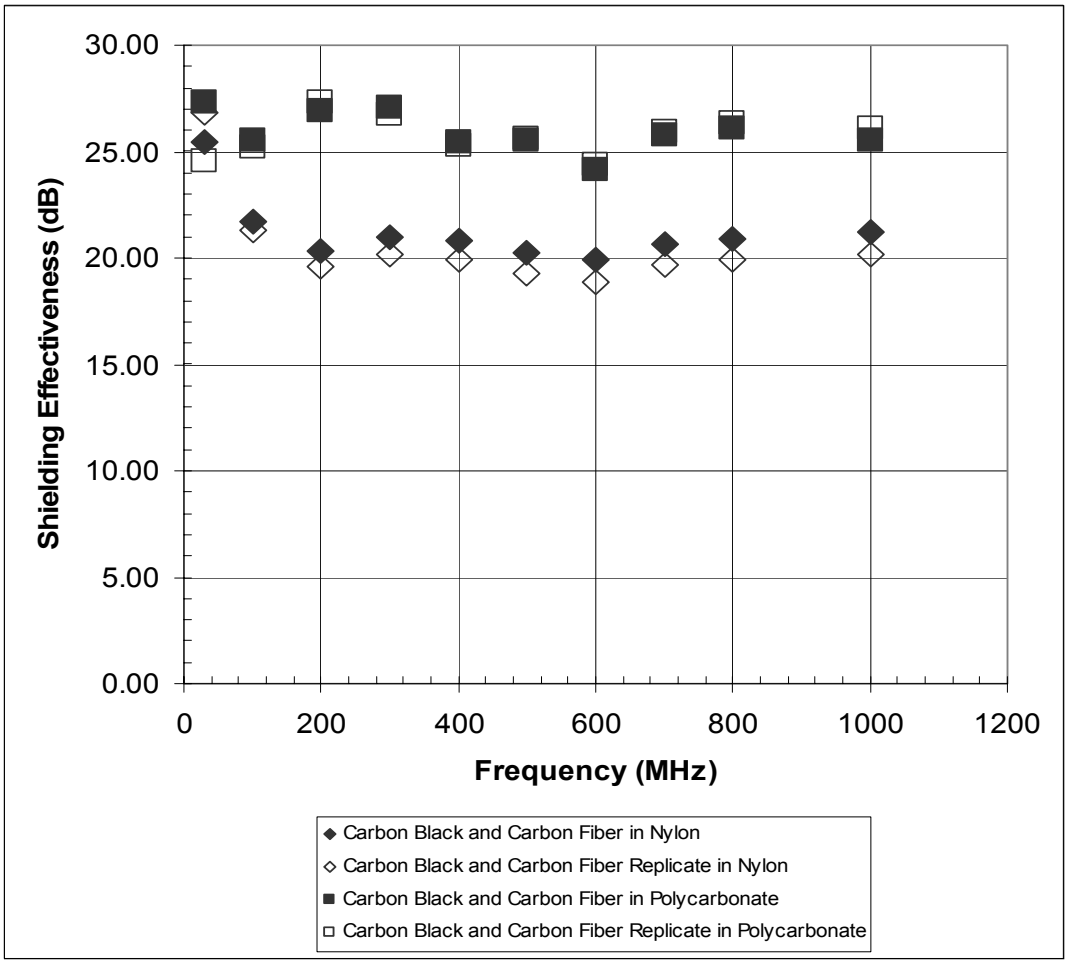

Figure 9.3-2: Shielding Effectiveness of Carbon Black and Carbon Fiber

Figure 9.3-3 shows the Thermocarb™ Specialty Graphite and carbon fiber combination's shielding effectiveness. Since carbon black is not used in this formulation, the SE is lower than other combinations of fillers that do not contain carbon black. As discussed previously the polycarbonate matrix gave higher shielding values when compared to nylon 6,6 at each frequency.

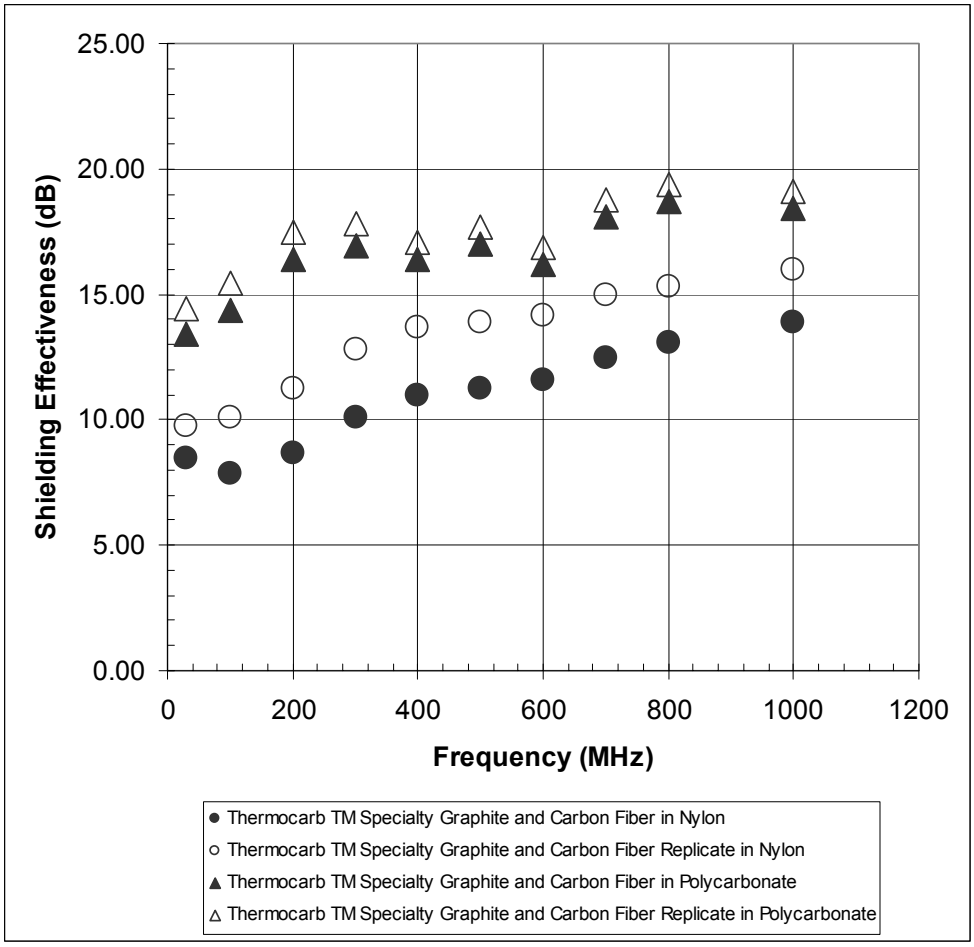

Figure 9.3-3: Shielding Effectiveness of Thermocarb™ Specialty Graphite and Carbon Fiber

Figure 9.3-4 shows the carbon black, Thermocarb™ Specialty Graphite and carbon fiber combination's shielding effectiveness. Since all 3 fillers were used, a high SE is expected. This formulation had the highest shielding effectiveness. The 3 fillers in polycarbonate combination were too viscous to injection mold into shielding specimens.

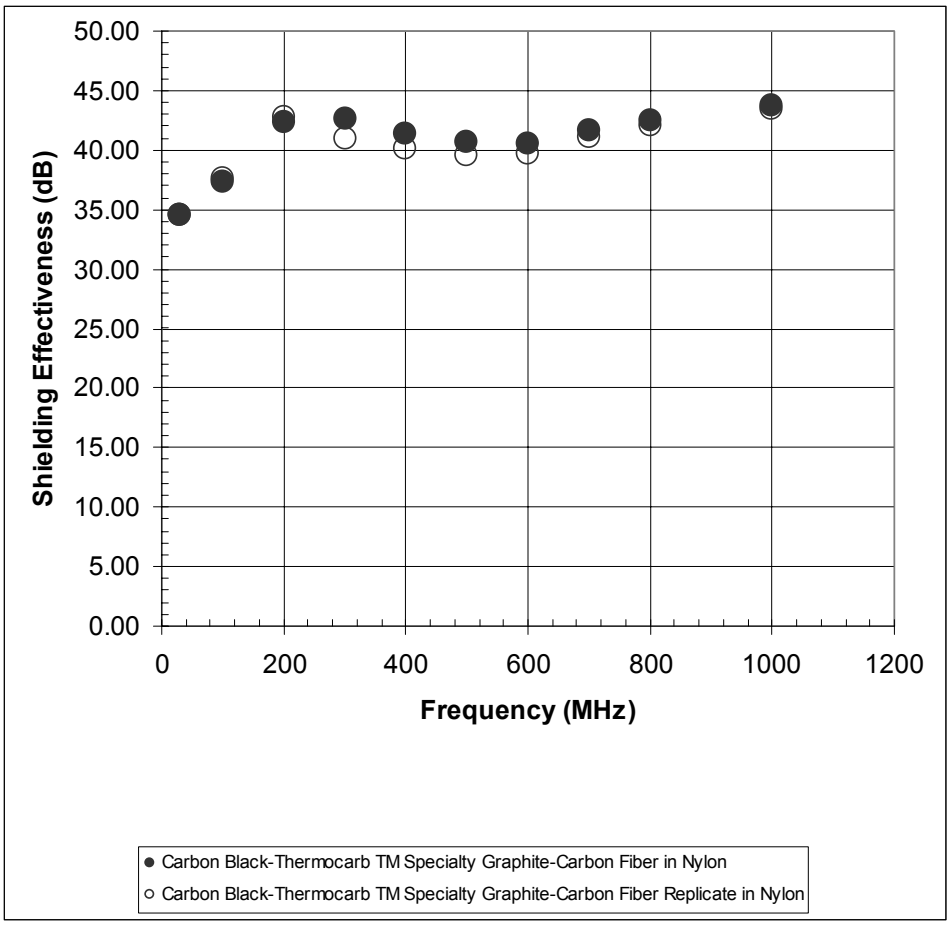

Figure 9.3-4: Shielding Effectiveness of Carbon Black and Thermocarb™ Specialty Graphite and Carbon Fiber

9.4 Shielding Results Analysis

The single fillers in polycarbonate had higher shielding effectiveness values than the nylon 6,6 counterparts. The filler lengths, as discussed in Chapter 7.4, were longer in nylon than they were in polycarbonate (90 μm to 80μm respectively). This goes against the theory of electrical conduction. It has been assumed and shown that fillers with longer lengths have an easier time forming a conductive network.

9.5 Surface Energy Analysis

Table 9.5-1 gives the results for all materials, including the polar and dispersive components of the surface energy (53). The total surface energy for the pure nylon 6,6 was measured at 45.92 mJ/m^2 in the melt phase. The pure polycarbonate has a total surface energy of 38.05 mJ/m^2 in the melt phase.

Table 9.5-1: Surface Energy Results (53)

Material	Phase	Polar Component mJ/m^2	Dispersive Component mJ/m^2	Total Surface Energy mJ/m^2	Surface Polarity %
Zytel 101 NC010		--	--	--	--
(Nylon 6,6)	melt	17.24	28.68	45.92	37.5
Lexan HF1110-111N		--	--	--	--
(Polycarbonate)	melt	8.55	29.5	38.05	22.5
Carbon Black	powder	2.18	19.59	21.77	10.0
Synthetic Graphite	powder	3.99	20.01	24.00	16.6
Pitch-based Carbon Fiber	powder	5.47	16.76	22.23	24.6

These results can be used to determine which polymers would provide for more complete dispersion with each of the carbons. Comparing the two polymer melts, the Lexan (polycarbonate) has a surface polarity, which is more comparable with the surface polarities of the carbon fillers. It should provide for more complete dispersion of each carbon filler when compared to Zytel (nylon 6,6). If surface energy is the deciding factor than that would explain why the shielding effectiveness values are higher in polycarbonate than in nylon 6,6. All three fillers have surface polarities closer to polycarbonate than to nylon 6,6 and this could lead to increasing shielding effectiveness.

9.6 Theoretical Comparison

As discussed in Chapter 3.6, work has been done by White (49) and Bushko (73) to derive shielding effectiveness theory. The theory first developed by White was used and validated for a solid, planar, homogenous metals. By applying the theory to a heterogonous system, one can see how well it predicts compared to actual data obtained using the direct shielding method as explained in Chapter 6.6. All theoretical and actual shielding effectiveness results can be found in Appendix F.

9.6.1 Results

Shown below is the Equation 9.6-1 that was derived by Bushko from White's original work (73).

$$S_{eff} = 3.34t\sqrt{f\mu_r\sigma_r} + 168 - 10 * Log_{10}\left(\frac{f\mu_r}{\sigma_r}\right) \qquad \text{Equation 9.6-1}$$

$t =$ Thickness of material in inches
$f =$ Frequency in Hz
$\sigma_r =$ Electrical conductivity relative to copper
$\mu_r =$ Magnetic permeability relative to copper = 1

The thickness and magnetic permeability are constants. Magnetic permeability is assumed to be one. Magnetic permeability is a property of materials that consists of the ratio of the magnetic induction in the substance to the magnetizing field to which it is subjected. The resins used give us one because they do not attract any materials, because they are not magnetic in nature. The frequency of the system changes

incrementally. The only variable for prediction is the electrical conductivity. This equation was originally developed for solid homogeneous metals.

$$Term\,1 = 3.34t\sqrt{f\mu_r\sigma_r} \qquad \text{Equation 9.6-2}$$

$$Term\,2 = 168 - 10 * Log_{10}\left(\frac{f\mu_r}{\sigma_r}\right) \qquad \text{Equation 9.6-3}$$

$t =$ Thickness of material in inches
$f =$ Frequency in Hz
$\sigma_r =$ Electrical conductivity relative to copper = $5.8*10^{-5}$ (S/cm) for Cu
$\mu_r =$ Magnetic permeability relative to copper = 1

Equation 9.6-1 can be broken up into separate mechanisms. The first term of the theory equation is a square root function and the last term of the equation is a logarithmic function as shown in Equations 9.6-2 and 9.6-3, respectively. Equation 9.6-2 represents the adsorption of the wave on the material and Equation 9.6-3 represents the reflection of the wave on the material. The internal reflection term is negligible and is not shown in the simplified form of White's equation as demonstrated by Bushko. Chapter 3.6 contains the derivation of White's original calculations.

The composite's electrical conductivity is what governs Equation 9.6-1. If the electrical conductivity increases, then the square root term of Equation 9.6-2 will get larger and grow as frequency increases. The logarithmic term in Equation 9.6-3 will also increase as electrical conductivity does, but it gets smaller as frequency grows. At 100 GHz the logarithmic term will produce a negative contribution to the shielding

effectiveness. The logarithmic portion of the equation dominates the shielding effectiveness at frequencies below 1 GHz. Above 1 GHz Equation 9.6-2 dominates the determination of shielding effectiveness. Equation 9.6-1 is only valid for certain conditions. Refer to Appendix K for detailed information and results for 30 MHz to 1 GHz.

From Figure 9.6-1 one sees that 10 wt % carbon black in nylon 6,6 has a high electrical conductivity of 0.108 ohm-cm; therefore, the theory equation will closely match the direct method approach. Compare this to Figure 9.6-2 for the 2.5 wt % of carbon black in nylon 6,6. The electrical conductivity of 2.5 wt % carbon black is $1.80*10^{-16}$ ohm-cm. The theoretical equation predicts a negative shielding effectiveness value, which is not observed experimentally.

For shielding values above 10 dB the theory approximates actual shielding effectiveness quite well. As you can see in Figure 9.6-1, the theory slightly underestimates the actual shielding effectiveness. Bushko found that at higher weight percents of filler that the theory will more closely match the actual shielding effectiveness (73). Notice in Figure 9.6-2 that at low weight percents of filler for carbon black that the shielding theory vastly under estimates the actual shielding effectiveness. This was found to be the case in this experiment where the shielding effectiveness was less than 10 db. At that point, the theory would predict negative values for shielding effectiveness.

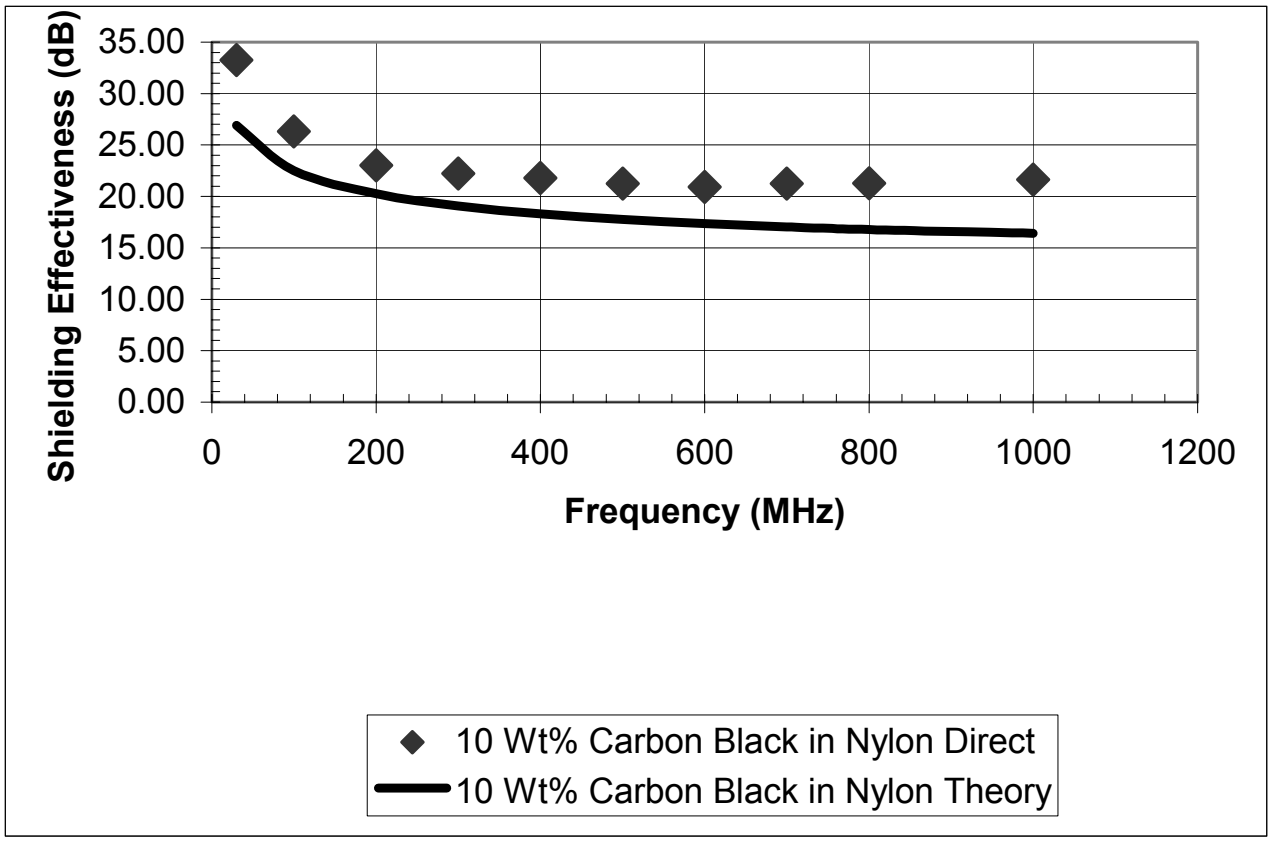

Figure 9.6-1: 10 Wt% Carbon Black Shielding Effectiveness Theory in Nylon 6,6

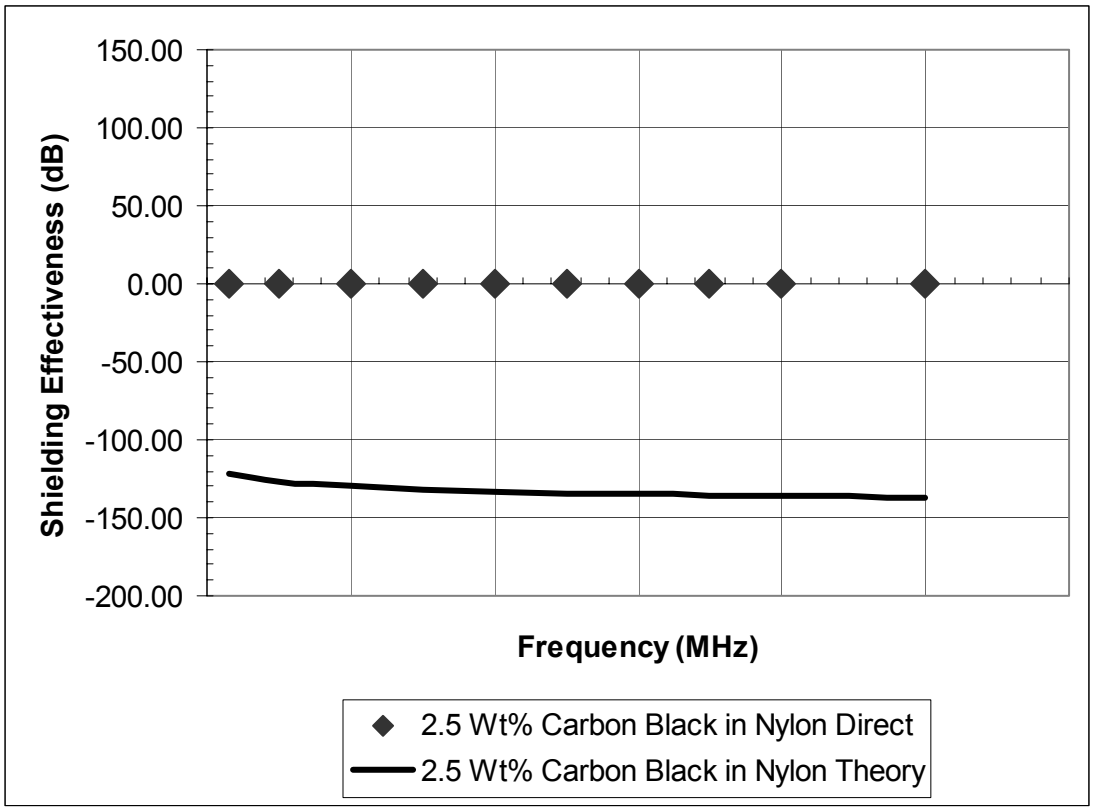

Figure 9.6-2: 2.5 Wt% Carbon Black Shielding Effectiveness Theory in Nylon 6,6

From Figure 9.6-1 you can see that the shielding effectiveness for formulations with a high weight percent of filler will always compare well with theory. This happens because as filler weight increases so does conductivity. If a formulation has little filler it will have a low electrical conductivity. Hence, this will be related to how close its actual shielding effectiveness compares with the theoretical prediction. This was observed in all cases where shielding effectiveness was above 10 dB. To confirm that a low electrical conductivity will always predict a negative shielding effectiveness, the nylon 6,6 and polycarbonate matrix without any fillers were tested. Nylon 6,6 and polycarbonate both had a shielding effectiveness of 0 dB. Shown in

Figure 9.6-3 are the results for nylon 6,6 and in Figure 9.6-4 are the results for polycarbonate. For both pure polymers, Equation 9.1-1 predicts a negative SE.

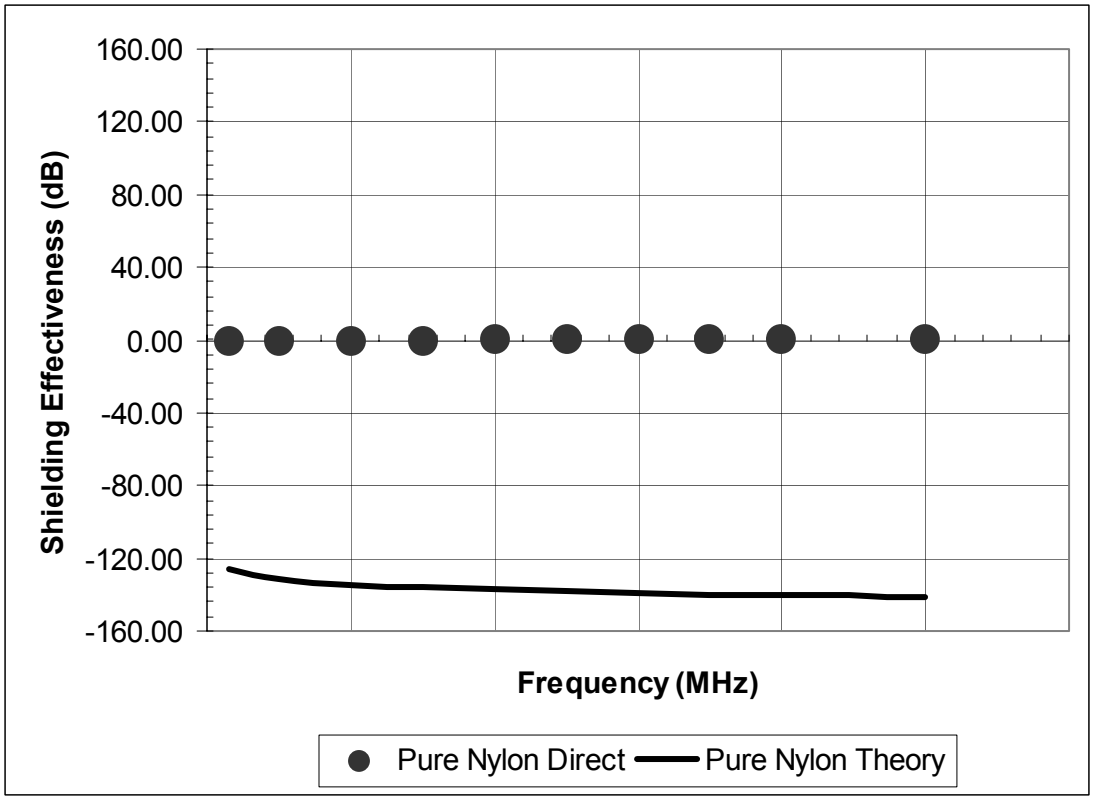

Figure 9.6-3: Pure Nylon 6,6 Shielding Effectiveness Theory

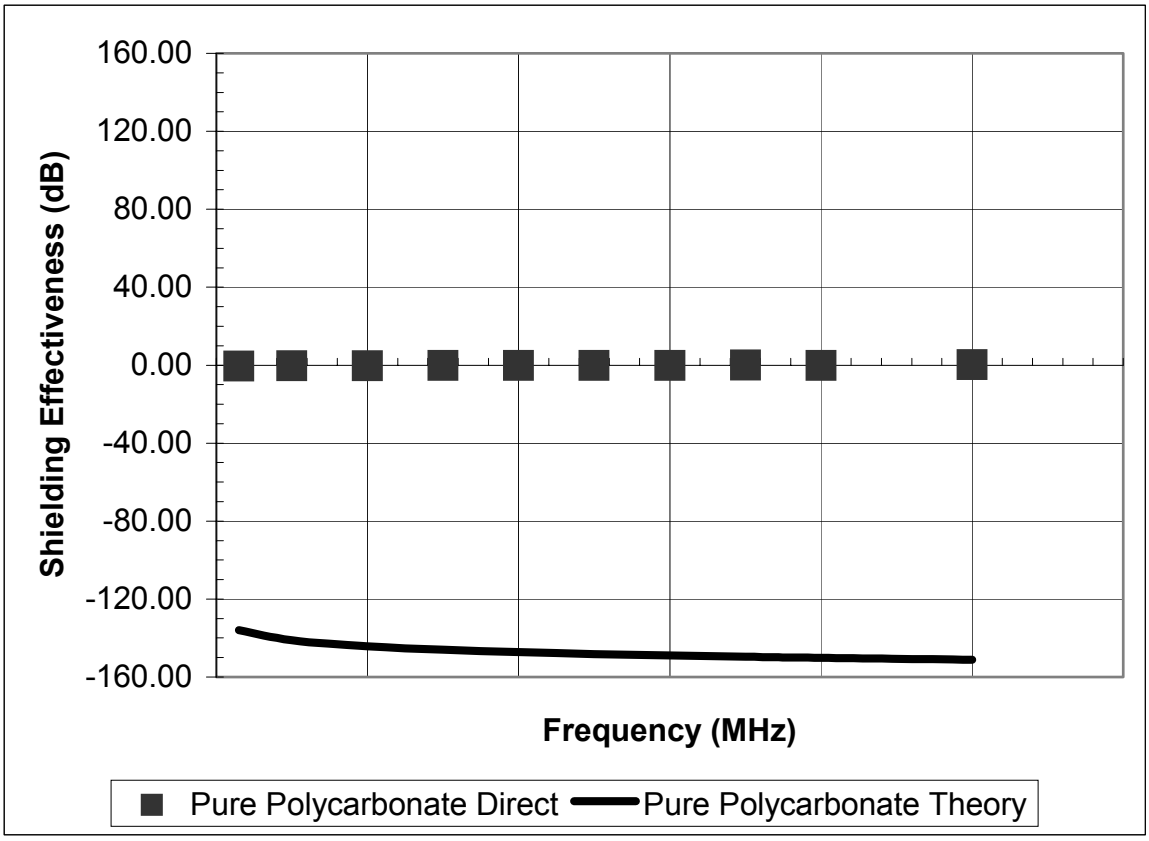

Figure 9.6-4: Pure Polycarbonate 6,6 Shielding Effectiveness Theory

Figure 9.6-5 shows a two-filler interaction formulation, carbon black and Thermocarb™ Synthetic Graphite in polycarbonate. Notice that the direct experimental method is higher than the shielding theory. Both plots do not deviate very much as frequency increases.

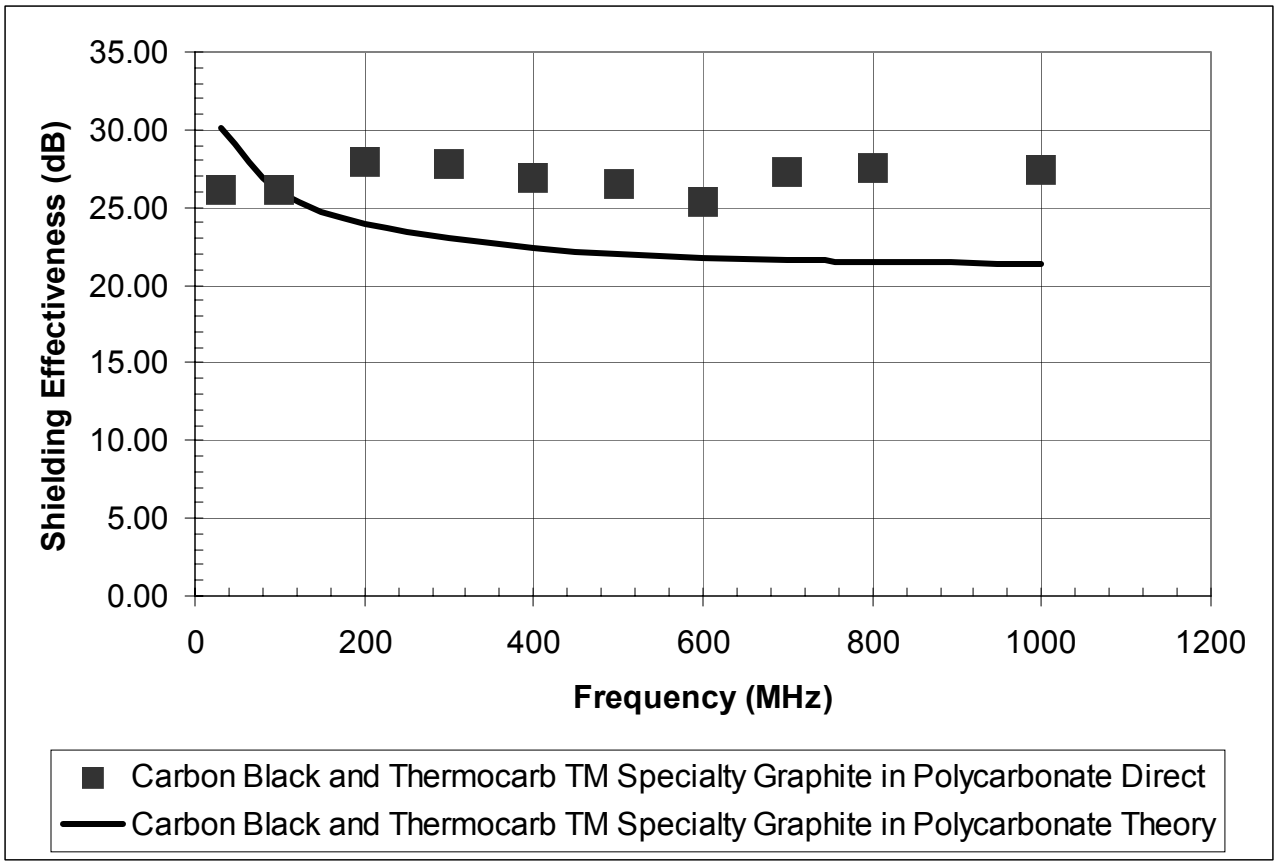

Figure 9.6-5: Carbon black, Thermocarb™ Shielding Effectiveness Theory in Polycarbonate

The above results were consistent for carbon black added with any other filler. For multiple fillers, where carbon black was not present, a noteworthy trend was seen in nylon 6,6 and polycarbonate as shown in Figure 9.6-6. For Thermocarb™ Specialty Graphite and carbon fiber, the theory would over estimate and then under estimate within the same plot, as frequency increased as shown in Figure 9.6-6.

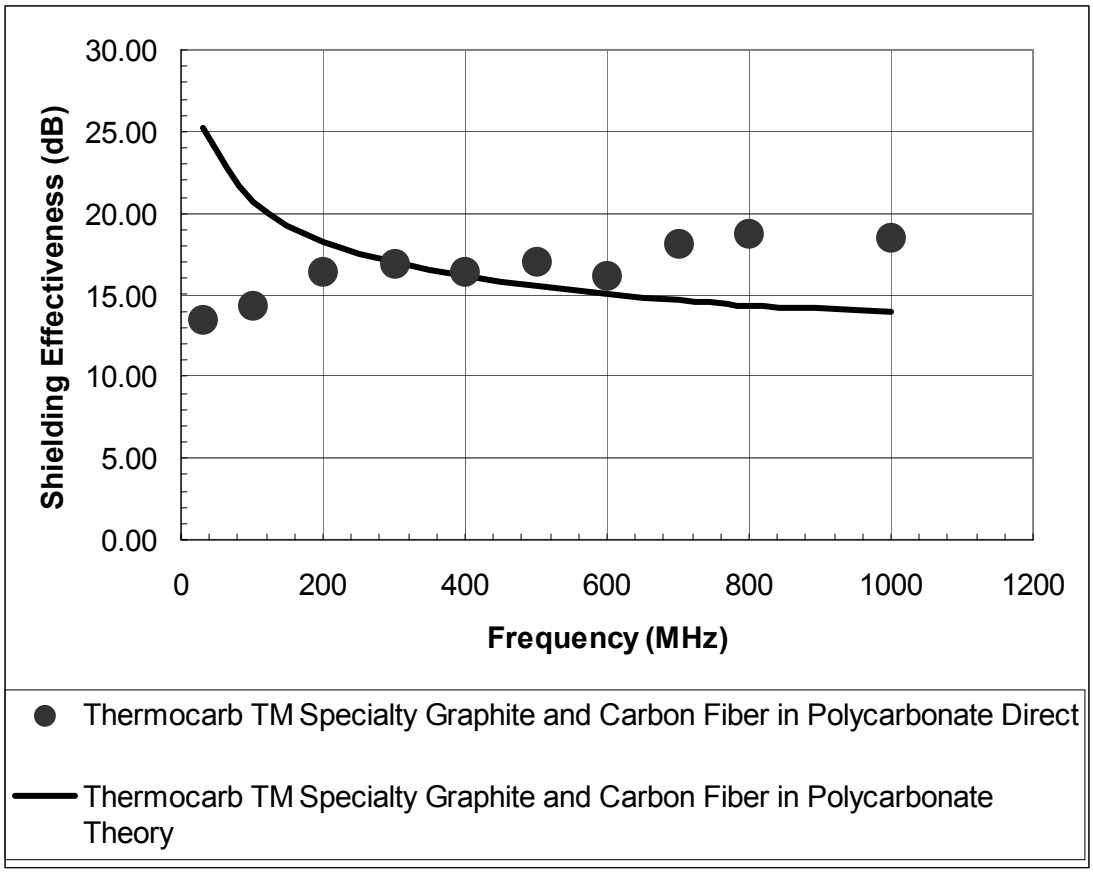

Figure 9.6-6: Thermocarb™ Specialty Graphite and Carbon Fiber Shielding Effectiveness Theory in Polycarbonate

This same trend was also observed in nylon 6,6 as shown in Figure 9.6-7. Notice how the two plots cross in both figures. However, from 200 MHz to 1000 MHz, the predicted and actual shielding effectiveness values were typically within 4 dB. SE measurement error is within ± 1.0 dB.

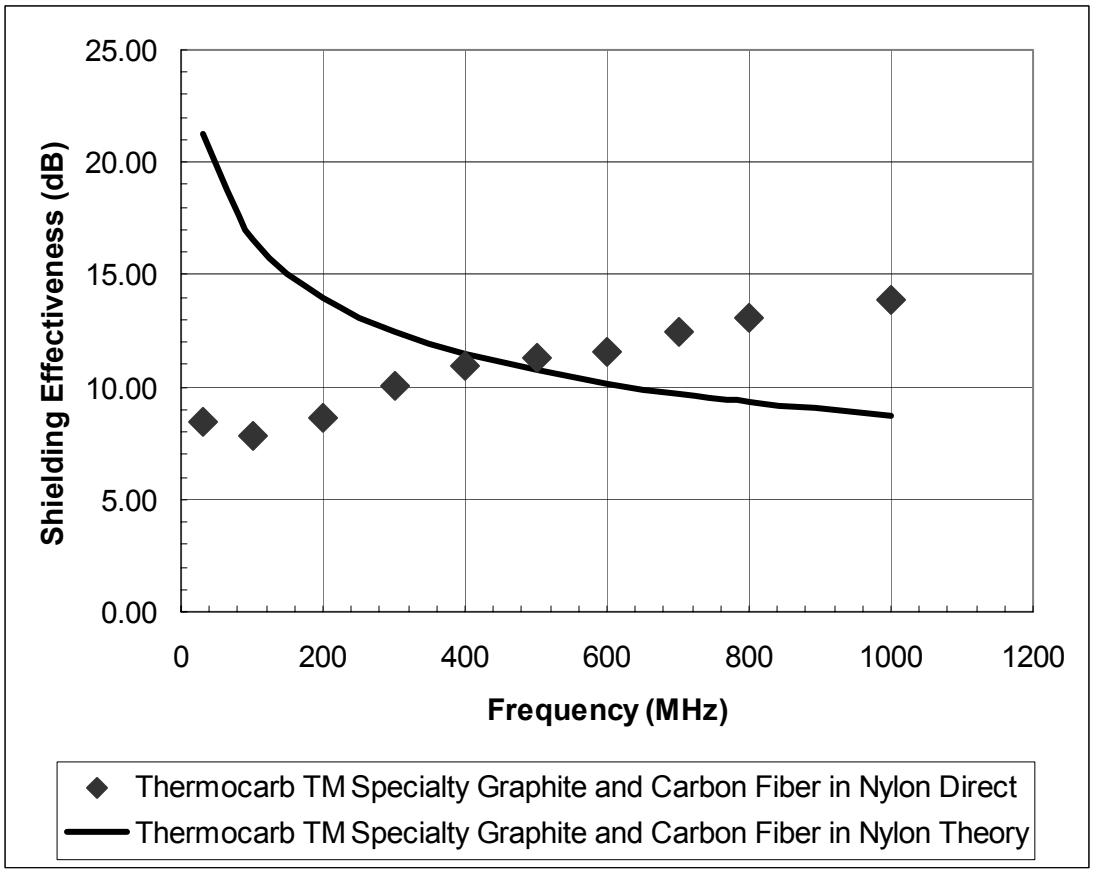

Figure 9.6-7: Thermocarb™ Specialty Graphite and Carbon Fiber Shielding Effectiveness Theory in Nylon

For the three-interaction formulation of carbon black, Thermocarb™ Specialty Graphite and carbon fiber only, a nylon 6,6 matrix was used because the polycarbonate formulation was too viscous to injection mold into test specimens. In Figure 9.6-8 one sees the SE results for the carbon black, Thermocarb™ Specialty Graphite and carbon fiber formulation in nylon. This formulation had the highest shielding effectiveness of all the formulations. Notice how the theory over estimates the direct measurement where the shielding effectiveness is greater than 30 dB. However, the difference between the experimental and predicted shielding effectiveness for 200 MHz to 800 MHz is 1 dB to 10 dB.

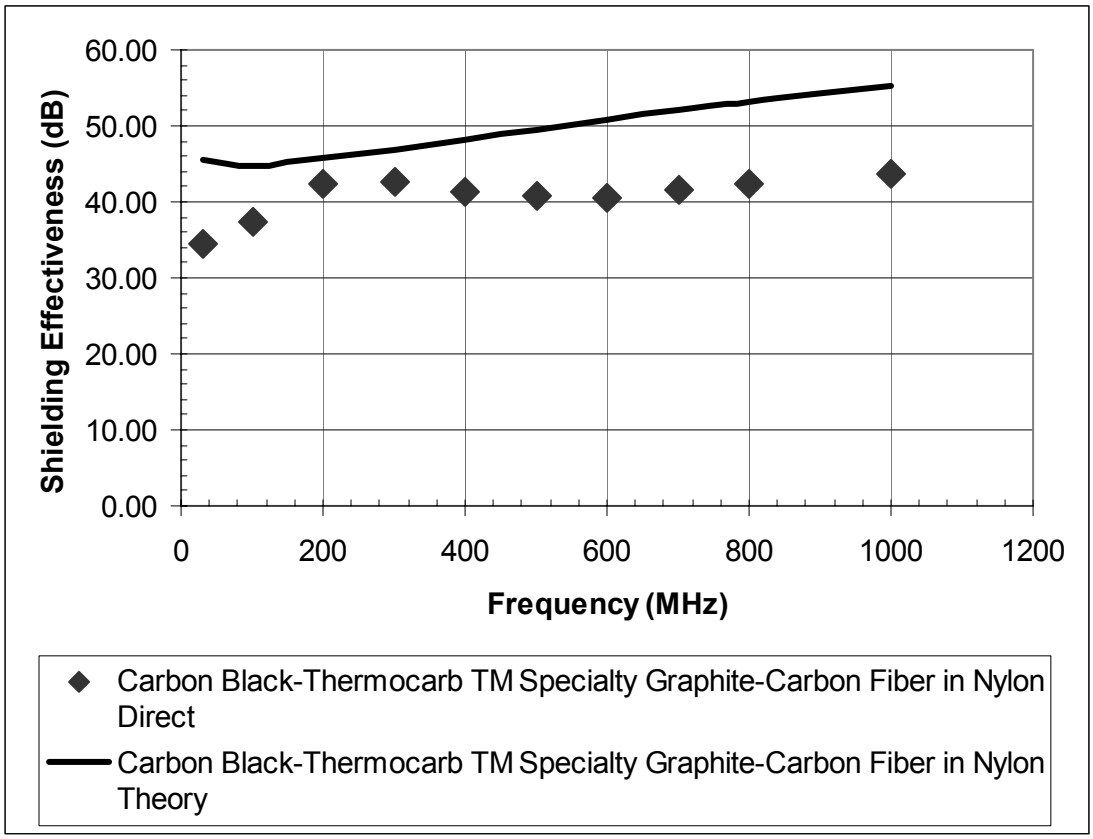

Figure 9.6-8: Carbon black, Thermocarb™ and Carbon Fiber Shielding Effectiveness Theory

Bushko argues that the electrical conductivity or resistivity tests themselves do not provide enough information alone to predict SE (73). Figure 9.6-9 is a diagram showing the errors in a typical electrical resistivity test. From this diagram, Bushko states that the electrical resistivity test does not take account for all of the filler present that is not in the conductive network as shown in Figure 9.6-9 (A). Also shown in Figure 9.6-9 (A), many fibers embedded in the plastic matrix are not detected during the conductivity measurement. These unconnected fibers are contributing to the shielding by absorbing and reflecting electromagnetic waves

passing through the material. The discrepancy grows with frequency as the significance of wave scattering, (absorbing or reflecting), becomes important.

The scattering phenomenon becomes more relevant when the wavelength is comparable in size with the scattering filler. The length of an electromagnetic wave in air varies from 10 m at 30 MHz to 19 cm at 1500 MHz (73). This is considerably larger than any of the filler lengths, typically 80 –100 μm, that were determined. When an electromagnetic wave enters the composite from the test fixture it slows down and its wavelength decreases to about 32 mm at 1500 MHz for a composite of low electrical conductivity (73). The wavelength shrinks considerably becomes it is being absorbed and dielectric constants of the material change. Due to the excess fillers that were not accounted for in the electrical resistivity test as shown in Figure 9.6-9 (A), the scattering becomes more pronounced.

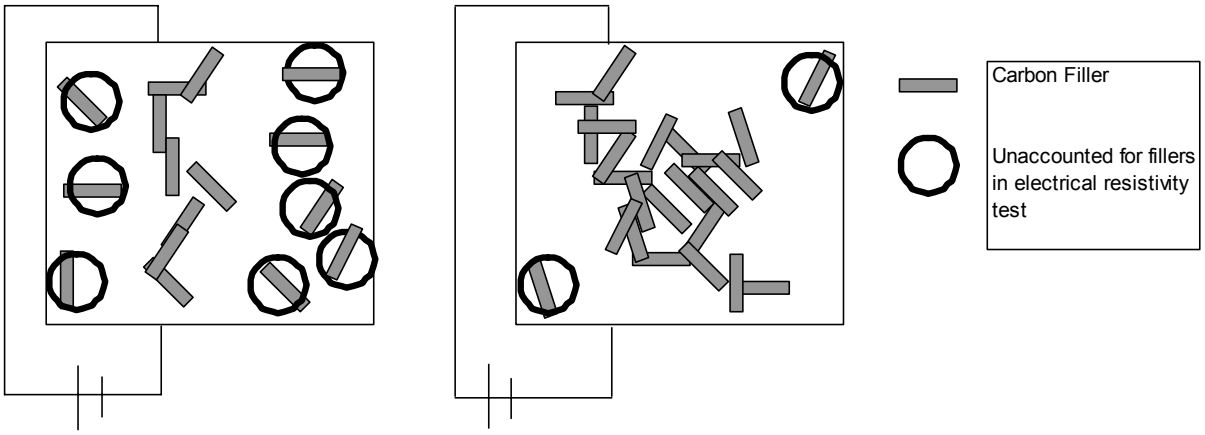

(A) Low Weight Percent Filler **(B)** High Weight Percent Filler

Figure 9.6-9: Electrical Resistivity Test Comparison

At high concentrations of fillers as shown in Figure 9.6-9 (B) the fillers provide a direct path for the current to follow. The resistivity is low and the effective shielding based on the homogeneous material model is high. This occurs because some waves can pass through resin rich areas in the material. This results in giving lower than expected shielding effectiveness values as seen in Figure 9.6-8. The wavelength becomes closer to some of the resin rich areas at higher frequencies. Therefore, more leakage of the current is occurring as frequency increases. The wavelength shrinkage is also why shielding effectiveness increases as frequency does. At higher frequencies the wavelengths become shorter and cannot penetrate the material as easily, which gives a higher shielding effectiveness for direct measurements. This same phenomenon also cause Equation 9.6-1 to over predict SE at high electrical conductivities.

By looking at Figure 9.5-9 (B), one can see that in a high weight percent filler has almost all fibers in contact with each other. When an electrical resistivity reading is taken, fewer of the fibers are left out of the reading because most are forming a conductive network. Conversely, in Figure 9.6-9 (A), one can see that for a low weight percent of filler, there are alot of fibers that are not involved in the conductive network. So the electrical resistivity reading is giving a false reading for predicting shielding effectiveness for heterogeneous materials. This relates to shielding because the theory, according to White and Bushko, is dependent on electrical conductivity (resistivity = 1/conductivity). This author agrees that Bushko is correct on his assumption regarding electrical resistivity testing. This theory was originally

designed for homogeneous metals. Hence, the electrical conductivity parameter is not the only term needed to determine shielding effectiveness

A new shielding effectiveness theory needs to be developed that would incorporate filler length, orientation, thickness, permeability, frequency, and conductivity into a unified model that works over all ranges of interest for heterogeneous materials. This model would be increasingly complex for adding multiple fibers. A good starting point for this model would be for materials that insulate to produce a predictive shielding effectiveness of zero dB. The current theory does not. The existing theory based on metals does give a good estimate of shielding effectiveness in nylon 6,6 and polycarbonate for those formulations that have a high conductivity, which is directly related to the volume or weight percent of filler in each formulation. By examining the theory equation, one can determine how much electrical conductivity is needed to achieve various shielding effectiveness. For a sample being held at 300 MHz, one can determine how much conductivity is required to achieve 10 dB, 20 dB, 30 dB and 40 dB of shielding effectiveness using Equation 9.6-1. This is shown in Table 9.6-1. In order to get 10 db, 20 dB, 30 dB and 40 dB an electrical conductivity of 0.02 S/cm, 0.13 S/cm, 0.55 S/cm and 1.66 S/cm, respectively is required.

Table 9.6-1: Theory Equation Comparison to Experimental Data at 300 MHz

Formulation at 300 MHz	Electrical Conductivity (S/cm)	Theoretical Target (dB)
1	0.02	10
2	0.13	20
3	0.55	30
4	1.66	40

Table 9.6-2 shows the actual SE data with groupings of formulations of approximately 10 dB, 20 dB, 30 dB and 40 dB. The corresponding EC of each resin is also shown along with the predicted SE from Equation 9.6-1. Several observations can be made from this table. First, when the EC is less than 0.001 S/cm, the modeled SE from Equation 9.6-1 does not predict actual shielding effectiveness well. Second, several formulations, (NCN40, NAN10 and NACN), have an electrical resistivity (ER) of 10 ohm-cm, but the SE ranges from approximately 10 to 20 dB. Third, several formulations, (NAP10, NABP and NABPR), have an ER of 5 ohm-cm, but the shielding effectiveness ranges from approximately 21.8 dB to 28.4 dB. Other factors in addition to the EC (1/ER) of the composite influence the shielding effectiveness (SE). Therefore, a new model needs to be developed for heterogeneous materials.

Table 9.6-2: Experimental Shielding Effectiveness Comparison to Predicted Theory

Formulation	Electrical Resitivity (S/cm)	Electrical Conductivity (S/cm)	Actual Experimentally Measured SE at 300 MHz (dB)	Theoretically Determined SE at 300 MHz (dB)
(10 dB Set)				
NANR05	9.86E+06	1.01E-07	7.35	-43.34
NANRR05	1.61E+06	6.21E-07	7.42	-36.46
NAN06	1.34E+02	0.01	10.16	5.13
NCN40	10.08	0.10	10.81	18.55
NBCN	30.43	0.03	10.08	12.48
NBCNR	24.41	0.04	12.81	13.64
NAP05	2.39E+06	4.18E-07	10.19	-38.19
NAPR05	1.08E+06	9.26E-07	10.43	-36.95
(20 dB Set)				
NAN10	9.25	0.11	22.21	19.06
NABN	10.62	0.09	23.11	18.26
NABNR	6.94	0.14	22.90	20.79
NACN	13.47	0.07	21.00	16.89
NACNR	25.15	0.04	20.19	13.48
NAP10	4.89	0.20	21.84	23.00
(30 dB Set)				
NABP	4.88	0.20	27.84	23.01
NABPR	5.61	0.18	28.37	22.10
NACP	2.89	0.35	27.07	26.57
NACPR	2.77	0.36	26.77	26.87
(40 dB Set)				
NABCN	0.33	3.03	42.63	46.94
NABCNR	0.32	3.13	40.88	48.18

CHAPTER 10: CONCLUSIONS AND FUTURE WORK

10.1 Conclusions

The goal of this thesis was to establish the effect of single and multiple fillers on shielding effectiveness. Comparison of experimental data with a known model was investigated in order to determine the necessary properties that control shielding effectiveness for a heterogeneous composite. By analyzing the fillers, matrix and the composite formulations, one can reach several conclusions.

Factorial design analysis from Chapter 8 showed that carbon black had the largest effect on increasing the shielding effectiveness of a conductive resin. Any formulation that contained carbon black would have higher shielding effectiveness. Also single filler and two filler interactions were statistically significant at the 95% confidence level. The fact that all two-way interaction terms were significant indicates that the composite SE is higher than what would be expected from the additive effect of each single filler. To the author's knowledge, this is the first time in the literature that a synergistic effect of combining different carbon fillers on the composite SE has been observed. It is likely that the conductive pathways are formed that 'link' the high surface area carbon black, synthetic graphite particles and carbon fibers. The different shapes of these fillers also contribute to this 'linking effect'.

Finding an optimum combination of fillers for a given application is highly desirable. One could have low electrically conductive filler that has great strength properties paired with a filler with high electrical conductivity. Maybe the result is a formulation with superior strength and shielding. Also combination of rods may work better or worse than a rod and sphere pairing. There are limitless possibilities

for exploring applications of these materials in EMI/RFRI. More research into these effects needs to be done. The three filler combination consisting of carbon black, Thermocarb™ Specialty Graphite and carbon fiber gave the highest shielding effectiveness result, but was not statistically significant at the 95 % confidence level.

Shielding effectiveness was also observed to be higher in polycarbonate compared to nylon 6, 6. Surface energy and surface polarity of the matrix material has an influence on how well the fillers will adhere. Better wetting of the filler can improve its dispersion within the matrix material. This will likely increase the overall conductivity of the composite. A smaller difference between the surface energy of the filler and polymer is desirable to obtain good filler-matrix adhesion. If surface polarity of the fillers is similar to that of the matrix, then the fillers will be better dispersed. The surface polarity of the fillers is closer to that of the polycarbonate matrix (versus nylon). Hence, this could cause increased SE in polycarbonate as compared to nylon.

Shielding effectiveness increased as frequency increased. This is attributed to planar wave physics. Wavelengths become smaller at higher frequencies and therefore, the wave cannot penetrate the composite as easy. Wave physics is dependent upon the dielectric constant of the composite material and surrounding environment. The dielectric constant of air is much smaller than that of a metal or conductive composite. This directly relates to how much energy is absorbed and makes shielding effectiveness increase with frequency.

The predictive theory equation developed by White for homogeneous planar metal materials works well for composites that have an electrical resistivity (ER) of 100

ohm-cm or lower. The equation does not work well for heterogeneous materials that have a shielding effectiveness below 10 dB. This author agrees with Bushko that the electrical conductivity test does not account for all of the filler interactions. A new model needs to be developed for a heterogeneous material that includes composite electrical conductivity, filler length, filler orientation, filler aspect ratio and filler-matrix adhesion.

10.2 FUTURE WORK

The following recommendations are suggested for the future work in this area.

10.2.1 Processing Conditions

Conductive fillers are currently being evaluated for their ability to produce conductive plastic parts, which shield electromagnetic interference (EMI). These fillers all have a geometrical characteristic to them, which makes them susceptible to damage during compounding and processing. Further research is recommended in this area to make several batches of sample disks at extremely different processing conditions. Tracking extrusion and injection molding conditions and varying them should also be done. By being able to make disks under different conditions and then actually characterize which processing conditions have the most effect, on SE for certain filler matrix systems would be a worthwhile endeavor.

10.2.2 Development of a Heterogeneous Shielding Effectiveness Model

A new model for shielding effectiveness needs to be developed that takes account for filler length, aspect ratio, orientation, adhesion and constituent properties. Filler lengths need to be varied to measure their effect on shielding effectiveness. Using varying filler lengths of the same filler material would allow one to determine the effect of filler length and aspect ratio on SE.

The orientation could also be varied in the resin. By having a 0 degrees orientated filler in a composite aligned with the flow direction could be compared to a perfectly transverse composite of 90 degrees to the flow direction. By having the extremes one could begin to determine the effect of the filer orientation on shielding effectiveness.

Adhesion also needs to be investigated to determine its effect on SE. Different filler-matrix systems could be chosen to represent poor and good adhesion. Then this effect could be quantified.

In order to develop a new model, one should use different fillers made from other materials to understand what properties have the most influence on shielding effectiveness. Metal flakes, powders and coated fillers could also be used. By collecting data from different types of fillers, one could begin to develop a more accurate model of SE in heterogeneous materials. Various filler shapes, (spherical, flake, rods, etc), should also be studied to determine their effect on SE.

By evaluating the effect of each individual property, (filler length, orientation, etc), one could begin to summarize which factors have an influence on shielding effectiveness. A new factorial design could be conduced that involves varying filler length and orientation at constant filler loadings. In this manner, a new model can be

developed that can account for all of the filler properties and their interactions with the matrix materials.

CHAPTER 11: REFERENCES

1. Agari, Y. and Uno, T., *J.Appl.Polym.Sci.,* **30,** p.2225 (1985).

2. Nielsen, L., *Ind.Eng.Chem.Fundam.,* **13,** 1, p.17 (1974).

3. Nysten, B. and Issi, J-P., *Composites,* **21,** 4, p.339 (1990).

4. Simon, R. M., *Polymer News,* **11,** p.102 (1985).

5. Mapleston, P., *Modern Plastics,* **69,** p.80 (1992).

6. Bigg, D. M., *Polym.Comp.,* **7,** 2, p.69 (1986).

7. Bigg, D. M., *Polym.Eng.Sci.,* 17, 12, p.842 (1977).

8. Murthy, M., *EMI/RFI Shielding of Electronics with Conductive Resins 4th Electronics* SAMPE Conference, 1990 (June 2-14)

9. Wright, W. M. and Woodham, G. W.; in *Conductive Polymers and Plastics;* Chapman and Hall; New York; p.119; (1989).

10. Murthy, M., *Society of Plastics Engineering Regional Technical Conference*, (1988).

11. The Freedonia Group, Inc.; *Conductive Polymers*; Industry Study, (2000).

12. Murthy, M., *Society of Plastics Engineering Regional Technical Conference*, (1988).

13. King, J. A., Tucker, K. W., Meyers, J. D., Weber, E. H., Clingerman, M. L., and Ambrosius, K. R., *Polym.Comp.,* **22,** 1, (2001).

14. Demain, A., Thermal Conductivity of Polymer/Chopped Carbon Fibre Composites, Ph.D. Dissertation, Universite Catholique de Louvain, 1994.

15. Issi, J-P., Nysten, B., Jonas, A., Demain, A., Piraux, L., and Poulaert, B., *Thermal Conductivity,* **21,** p.629 (1990).

16. Bigg, D. M., *Adv.Polym.Tech.* , **4,** p.255 (1984).

17. King, J. A., Tucker, K. W., Vogt, B. D, Weber, E. H., and Quan, C., *Polym.Comp.,* **20,** 5, p.643 (1999).

18. King, J. A., Tucker, K. W., Vogt, B. D, Weber, E. H., and Quan, C., *J.Comp.Mat.,* **34,** 24, p.1038 (2000).

19. King, J. A., Weber, E. H., and Vogt, B. D, Proceedings of the American Institute of Chemical Engineers Annual Meeting, Miami, FL, (1998).

20. King, J. A., Clingerman, M. L., Weber, E. H., and Vogt, B. D, Proceedings of the Society of Plastics Engineers Annual Technical Conference, New York, NY, (1999).

21. Gerteisen, S.R., *Plastics That Sheild Againist EMI/RFI*

22. Simon, R.M. Plastics as Current and Heat Conductors *Polymer Science and Technology* **15**, (1981).

23. Trost, T. Electrostatic Discharge (ESD) – Facts and Faults – A Review. *Packing Technology and Science*, **8** 231247 (1995).

24. Bigg, D.M, The Effect of Compounding on the Conductive Properties of EMI Shielding Compounds Advances in Polymer Technology, May 24 (1984).

25. Conductive-Shielding Resin Claimed Highly Cost-Effective, *Modern Plastics* **64,** May (1987).

26. Broadbent, S. R. and Hammersley, J. M., *Proc.Camb.Phil.Soc.,* 53*,* **3**, p.629 (1957).

27. Stauffer, D., *Introduction of Percolation Theory,* Taylor and Francis, London, 1985 Morphology and properties of conductive Carbon/Polyolefins Composite

28. Vahid Haddadi-Asl School of Chemical Engineering and Industrial Chemistry University of New South Wales, Sydney, NSW 2052, *Australia-Iranian Polymer Jouranal* **5** November, (1996).

29. Bigg, D.M. The Effect of Chemical Exposure on the EMI Shielding of Conductive Plastics, *Polymer Composites* **8**, 1 (1987).

30. Carmona, F. Barreeau, P. Delhaes and R. Canet J, An Experimental Model for Studying the Effect of Anisotropy on Percolative Conduction F. *Physique – Lettres* **41**, L-531-L534, (1980).

31. Jing, X., Zhao, W., and Lan, L, *J.Mat.Sci.Lett.,* **19,** 5, p.377 (2000).

32. Gokturk, H. S., Fiske, T., and Kalyon, D. M., *J.Appl.Polym.Sci.,* **50,** p.1891 (1993).

33. Fiske, T., Gokturk, H. S., and Kalyon, D. M., *J.Mat.Sci.,* **32,** p.5551 (1997).

34. Jae Yeon Yi and Gyeong Man Choi, *Journal of Electroceramics,* **3,** 4, p.361 (1999).

35. Advani, S. G. and Tucker III, C. L., *J.Rheology,* **31,** 8, p.751 (1987).

36. Nagata, K., Iwabuki, H., and Nigo, H, *Composite Interfaces,* **6,** 5, p.483 (1999).

37. Fiske, T., Gokturk, H. S., Yazici, R, and Kalyon, D. M., *Polym.Eng.Sci.,* **37,** 5, p.826 (1997).

38. Yaguchi, H., Hojo, H., Lee, D. G, and Kim, E. G., *International Polymer Processing X,* 3, p.262 (1995).

39. Yin, Y., Mays, T. J., and McEnaney, B, *Carbon,* 27, 1, p.113 (1989).

40. Weber, M. E. and Kamal, M. R., *Polym.Comp.,* 18, 6, p.711 (1997).

41. Mamunya, E. P., Davidenko, V. V., and Lebedev, E. V, *Composite Interfaces,* 4, 4, p.169 (1997).

42. http://www.fibrils.com/ApplicationsPage.htm Hyperion Catalysis International (Graphite Fibrils) ™ Nanotubes (2002).

43. Becker, R., Conductive Containers Protect Sophisticated Electronic Components. *Packaging Technology* 1, p.3 (1987).

44. Beck, D., Cost analysis of an ESD Controlled Systems Based on Latent Damage, *Packaging Technology*, **2**(1), (1988).

45. Frank, D. E. Soft failures-the invisible mode. Annual Reliability and Maintainability Symposium. Los Angles, CA, 26 January 1982. Douglas Paper 7088 (1982).

46. B.P. Grady, W. Berlin Genetti, University of Oklahoma Electrical Static Dissipative Composites Made from Coated Fillers, *ANTEC 2000*

47. S. Fowler, "Tribioelectricity and Surface Resistivity do not correlate", proc. EOS/ESD Symposium, 1988.

48. Huntsman, J.R. and Yenni, D.M., Test Methods for Static Control Products. Reliability Analysis Center EOS/ESD Symposium, Orlando, FL, USA (1982).

49. White, D.R. J., EMI/EMC Handbook Series, Germantown, MD: Don White Consultants, Inc., **4** (1971).

50. John W. Adams Eric J. Vanzura, Sheilding Effectiveness Measurements of Plastics, (NBSIR 85-3035) National Bureau of Standards U.S. Department of Commerece Boulder, CO, (1986).

51. Annual Book of ASTM Standards, D4935-89. Standard Test Method for Measuring the Electormagnetic Sheilding Effectiveness of Planar Materials. D4935-89. Copyright ASTM, (1989).

52. Clinerman, Matt PhD Dissertation, Development and Modeling of electrically Conductive Composite Materials, (2001).

53. Weber, Erik PhD Dissertation, Development and Modeling of Thermally Conductive Polymer/Carbon Composites, (2001).

54. Clingerman, M. L., King, J. A., Schulz, K. H., and Weber, E. H., Proceedings of the American Institute of Chemical Engineers Annual Meeting, Miami, FL, 1998.

55. DuPont Zytel Nylon Resin Product and Properties, Version 95.9, Printed in USA. (2001).

56. Demain, A. and Issi, J-P., *J.Comp.Mat.,* **27,** 7, p.668 (1993).

57. Bigg, D. M., *Polym.Comp.,* **6,** 1, p.20 (1985).

58. Kuhner, G. and Voll, M.; in *Carbon Black, Science and Technology;* Donnet, J. B., Bansal, R. C., and Wang, M. J., Marcel Dekker, Inc; New York; p.1; (1993).

59. Narkis, M., Lidor, G., Vaxman, A., and Zuri, L., *Journal of Electrostatics,* **47 ,** p.201 (1999).

60. Akzo Nobel Electrically Conductive Ketjenblack Product Literature, Akzo Nobel Chemicals Inc., 300 S. Riverside Plaza, Chicago, IL, 60606.

61. Blackman, L. C. F., *Modern Aspects of Graphite Technology,* Academic Press, London, 1970.

62. Conoco Carbon Products Data Sheets, Conoco, Inc., Conoco Center, P. O. Box 2197, Houston, TX 77252-2197.

63. Peebles, L. H., *Carbon Fibers: Formation, Structure and Properties,* CRC Press, Boca Raton, 1995.

64. Bahl, O. P., Shen, Z., Lavin, J. G, and Ross, R. A.; in *Carbon Fibers;* Marcel Dekker, Inc.; New York; p.1; (1998).

65. Amoco Performance Products: High Thermal Conductivity Pitch Based Graphite Fibers, Amoco Polymers; Alpharetta, GA 30005. (2001).

66. "Density of Plastics by Water Displacement", ASTM D792-66 (Re-approved 1975); American Society for Testing and Materials, Philadelphia, Pennsylvania; (1966).

67. Status Report on Shielding Effectiveness Measurements: Release of ASTM Standard D4935-89 John W. Adams 4th International SAMPE Electronics Conference June 12-14, 1990

68. Behzad D. Mottahed, Souran, Manoochehri, Investigation of Composite Materials Selection and Joint design to Enhance EMI Shielding of Electronic Equipment Polymer Engineering and Science, **37**, No. 3 (1997).

69. "Standard Practice for Dissolving Polymer Materials", ASTM Standard D5226-98, American Society for Testing and Materials, Philadelphia, Pennsylvania, (1998).

70. J. C. Russ, The Image Processing Handbook, 3rd ed. CRC and IEEE Press, Boca Raton, (1999).

71. Steven D.,Gerbig, Dealing With EMI/RFI Evaluation Engineering Issues, Wilson-Fiberfil International Proper Molding Technique Key to Optional Shielding Performance, (1985).

72. Mal Murthy, Nickel Coated Graphite Fiber Shielding Society of Plastics Engineers Regional Technical Conference Chicago, IL June (1988)

73. W.C. Bushko, V.K. Stokes, J. Wilson, EMI Shielding effectiveness of fiber-Filled Plastics – Material Testing Issues. GE Corporate research and Development Schenectady, New York, 12301. (2000).

74. Shielding Effectiveness Test Fixture Electro-Metrics Model EM-2107-A Manual, Jan, (1999).

75. Douglas, C., Introduction to Statistical Quality Control. Third edition Montgomery, (1996).

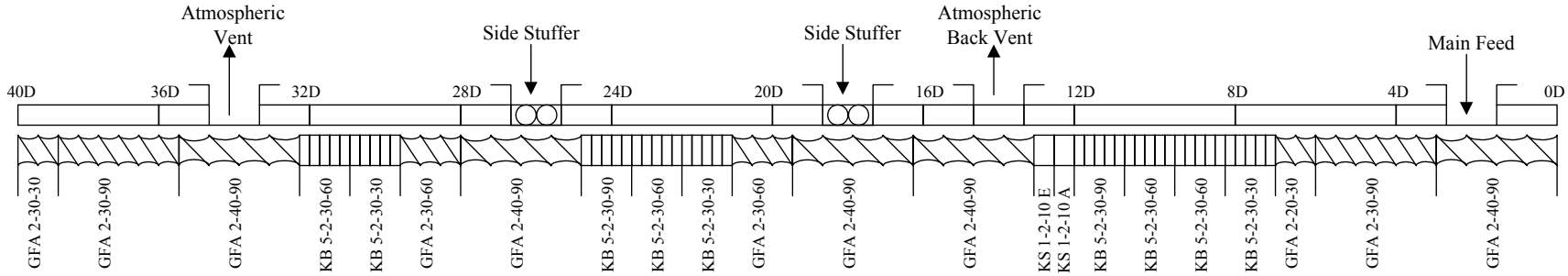

For Screw Type Elements
GFA-d-ee-ff
G = co-rotating
F = conveying
A = Free-Meshing
d = number of threads
ee = pitch (length in millimeters for one complete rotation)
ff = length of screw elements in millimeters

Kneading disks
KBj-d-kk-ll
KB = kneading block
j = number of kneading segments
d = number of threads
k = length of kneading block in millimeters
l = twisting angle of the individual kneading segments

Kneading disks
KS1-d-hh-i
KS1 = Kneading disc
d = number of threads
h = length of kneading disc in millimeters
i = A for initial disc and E for end disc

Zones
0D to 4D is Zone 1 (water cooled, not heated)
4D to 8D is Zone 2 and Heating Zone 1
8D to 12D is Zone 3 and Heating Zone 2
12D to 16D is Zone 4 and Heating Zone 3
16D to 20D is Zone 5 and Heating Zone 4
20D to 24D is Zone 6 and Heating Zone 5
24D to 28D is Zone 7 and Heating Zone 6
28D to 32D is Zone 8 and Heating Zone 7
32D to 36D is Zone 9 and Heating Zone 8
36D to 40D is Zone 10 and Heating Zone 9
Nozzle is Heating Zone 10

Appendix A: Extruder Screw Design

Appendix B: Formulation Summary

Table B-1: Overall Summary

Composite Formulation Name	Description	Wt%	Vol%		Volumetric Transverse Electrical Resistivity (ohm-cm)	Volumetric Longitudinal Electrical Resistivity (ohm-cm)	Shielding Effectiveness (dB) @ 300 MHz	Shielding Effectiveness (dB) @ 800 MHz
NN	Zytel 101 NC010	100	100	Avg s n	1.45E+16 7.70E+15 11	Out of Range	-0.03 0.05 3	0.1 0.04 3
NNR	Zytel 101 NC010	100	100	Avg s n	6.88E+15 3.10E+15 10	Out of Range	-0.07 0.19 3	0.07 0.05 3
NAN02.5	Zytel 101 NC010 KetjenBlack EC-600 JD	97.5 2.5	98.40 1.60	Avg s n	5.55E+15 3.20E+15 9	Out of Range	0.31 0.15 3	0.32 0.04 3
NAN04	Zytel 101 NC010 KetjenBlack EC-600 JD	96 4	97.43 2.57	Avg s n	4.57E+08 6.44E+08 10	Out of Range	3.41 0.24 3	4.06 0.09 3
NANR05	Zytel 101 NC010 KetjenBlack EC-600 JD	95 5	96.77 3.23	Avg s n	9.86E+06 6.72E+06 7	Out of Range	7.35 0.23 3	7.17 0.2 3
NANRR05	Zytel 101 NC010 KetjenBlack EC-600 JD	95 5	96.77 3.23	Avg s n	1.61E+06 3.28E+06 12	Out of Range	7.42 0.03 8.6	7.18 0.01 3

Table B-1: Overall Summary (continued)

Composite Formulation Name	Description	Wt%	Vol%		Volumetric Transverse Electrical Resistivity (ohm-cm)	Volumetric Longitudinal Electrical Resistivity (ohm-cm)	Shielding Effectiveness (dB) @ 300 MHz	Shielding Effectiveness (dB) @ 800 MHz
NAN06	Zytel 101 NC010 KetjenBlack EC-600 JD	94 6	96.11 3.89	Avg s n	Out of Range	134.3 24.99 18	10.16 0.6 3	10.02 0.59 3
NAN7.5	Zytel 101 NC010 KetjenBlack EC-600 JD	92.5 7.5	95.12 4.88	Avg s n	Out of Range	30.77 3.01 14	16.34 0.35 3	15.39 0.15 3
NAN10	Zytel 101 NC010 KetjenBlack EC-600 JD	90 10	93.43 6.57	Avg s n	Out of Range	9.25 0.85 22	22.21 0.5 3	21.26 0.15 3
NBN10	Zytel 101 NC010 Thermocarb ™ CF-300 Specialty Graphite	90 10	94.65 5.35	Avg s n	5.86E+15 7.52E+14 6	Out of Range	0.16 0.11 3	0.27 0.03 3
NBN15	Zytel 101 NC010 Thermocarb ™ CF-300 Specialty Graphite	85 15	91.76 8.24	Avg s n	4.80E+15 5.89E+14 6	Out of Range	0.19 0.18 3	0.43 0.05 3
NBN20	Zytel 101 NC010 Thermocarb ™ CF-300 Specialty Graphite	80 20	88.71 11.29	Avg s n	1.18E+15 4.11E+14 9	Out of Range	0.44 0.1 3	0.69 0.05 3

Table B-1: Overall Summary (continued)

Composite Formulation Name	Description	Wt%	Vol%		Volumetric Transverse Electrical Resistivity (ohm-cm)	Volumetric Longitudinal Electrical Resistivity (ohm-cm)	Shielding Effectiveness (dB) @ 300 MHz	Shielding Effectiveness (dB) @ 800 MHz
NBN30	Zytel 101 NC010	70	82.10	Avg	9.47E+06	Out of Range	1.3	0.04
	Thermocarb ™ CF-300 Specialty Graphite	30	17.90	s	7.05E+06		0.06	2.22
				n	8		3	3
NBNR30	Zytel 101 NC010	70	82.10	Avg	8.92E+06	Out of Range	1.74	3.04
	Thermocarb ™ CF-300 Specialty Graphite	30	17.90	s	8.74E+06		0.08	0.17
				n	9		3	3
NBN40	Zytel 101 NC010	60	74.66	Avg	Out of Range	430.04	3.4	5.65
	Thermocarb ™ CF-300 Specialty Graphite	40	25.34	s		152.96	0.25	0.27
				n		24	3	3
NCN05	Zytel 101 NC010	95	97.29	Avg	1.06E+16	Out of Range	0.61	0.6
	ThermalGraph DKD X	5	2.71	s	4.00E+15		0.12	0.03
				n	12		3	3
NCN10	Zytel 101 NC010	90	94.44	Avg	7.65E+15	Out of Range	0.73	1.28
	ThermalGraph DKD X	10	5.56	s	2.90E+15		0.05	0.09
				n	12		3	3
NCN15	Zytel 101 NC010	85	91.45	Avg	5.24E+15	Out of Range	1.23	2.38
	ThermalGraph DKD X	15	8.55	s	1.23E+15		0.14	0.02
				n	12		3	3

Table B-1: Overall Summary (continued)

Composite Formulation Name	Description	Wt%	Vol%		Volumetric Transverse Electrical Resistivity (ohm-cm)	Volumetric Longitudinal Electrical Resistivity (ohm-cm)	Shielding Effectiveness (dB) @ 300 MHz	Shielding Effectiveness (dB) @ 800 MHz
NCN20	Zytel 101 NC010	80	88.30	Avg	5.04E+08	Out of Range	2.32	4.24
	ThermalGraph DKD X	20	11.70	s	2.27E+08		0.16	5.5
				n	11		3	3
NCNR20	Zytel 101 NC010	80	88.30	Avg	2.35E+09	Out of Range	2.34	4.25
	ThermalGraph DKD X	20	11.70	s	2.84E+09		0.17	0.13
				n	9		3	3
NCN30	Zytel 101 NC010	70	81.48	Avg	Out of Range	120.74	5.08	8.31
	ThermalGraph DKD X	30	18.52	s		53.15	0.31	0.16
				n		19	3	3
NCN40	Zytel 101 NC010	60	73.88	Avg	Out of Range	10.08	10.81	13.56
	ThermalGraph DKD X	40	26.12	s		3.63	0.67	0.25
				n		18	3	3
NABN	Zytel 101 NC010	65	77.9	Avg	Out of Range	10.62	23.11	23.11
	KetjenBlack EC-600 JD	5	3.8	s		2.98	0.4	0.1
	Thermocarb ™ CF-300 Specialty Graphite	30	18.3	n		24	3	3
NABNR	Zytel 101 NC010	65	77.9	Avg	Out of Range	6.94	22.9	23.09
	KetjenBlack EC-600 JD	5	3.8	s		1.43	0.26	0.23
	Thermocarb ™ CF-300 Specialty Graphite	30	18.3	n		24	3	3

Table B-1: Overall Summary (continued)

Composite Formulation Name	Description	Wt%	Vol%		Volumetric Transverse Electrical Resistivity (ohm-cm)	Volumetric Longitudinal Electrical Resistivity (ohm-cm)	Shielding Effectiveness (dB) @ 300 MHz	Shielding Effectiveness (dB) @ 800 MHz
NACN	Zytel 101 NC010	75	84.5	Avg	Out of Range	13.47	21	20.88
	KetjenBlack EC-600 JD	5	3.6	s		4.03	0.45	0.4
	ThermalGraph DKD X	20	11.9	n		22	3	3
NACNR	Zytel 101 NC010	75	84.5	Avg	Out of Range	25.15	20.19	19.89
	KetjenBlack EC-600 JD	5	3.6	s		8.2	0.36	0.15
	ThermalGraph DKD X	20	11.9	n		18	3	3
NBCN	Zytel 101 NC010	50	65.9	Avg	Out of Range	30.43	10.08	13.08
	Thermocarb ™ CF-300 Specialty Graphite	30	20.1	s		7.93	0.06	0.17
	ThermalGraph DKD X	20	14.0	n		24	3	3
NBCNR	Zytel 101 NC010	50	65.9	Avg	Out of Range	24.41	12.81	15.34
	Thermocarb ™ CF-300 Specialty Graphite	30	20.1	s		1.64	0.23	0.17
	ThermalGraph DKD X	20	14.0	n		18	3	3
NABCN	Zytel 101 NC010	45	60.8	Avg	Out of Range	0.33	42.63	42.44
	KetjenBlack EC-600 JD	5	4.30	s		0.05	0.32	0.833
	Thermocarb ™ CF-300 Specialty Graphite	30	20.6	n		24	3	3
	ThermalGraph DKD X	20	14.3					

Table B-1: Overall Summary (continued)

Composite Formulation Name	Description	Wt%	Vol%		Volumetric Transverse Electrical Resistivity (ohm-cm)	Volumetric Longitudinal Electrical Resistivity (ohm-cm)	Shielding Effectiveness (dB) @ 300 MHz	Shielding Effectiveness (dB) @ 800 MHz
NABCNR	Zytel 101 NC010	45	60.8	Avg	Out of Range	0.32	40.88	42.01
	KetjenBlack EC-600 JD	5	4.3	s		0.04	0.4	0.32
	Thermocarb ™ CF-300 Specialty Graphite	30	20.6	n		21	3	3
	ThermalGraph DKD X	20	14.3					
NP	Lexan HF 1110-11 N	100	100	Avg	1.43E+17	Out of Range	-0.1	0
				s	5.16E+16		0	0
				n	6		3	3
NPR	Lexan HF 1110-11 N	100	100	Avg	1.47E+01	Out of Range	-0.07	0.03
				s	4.86E+16		0.06	0.06
				n	6		3	3
NAP2.5	Lexan HF 1110-11 N	97.5	98.32	Avg	2.56E+15	Out of Range	1.47	1.97
	KetjenBlack EC-600 JD	2.5	1.68	s	8.54E+14		0.21	0.29
				n	6		3	3
NAP04	Lexan HF 1110-11 N	96	97.3	Avg	4.77E+13	Out of Range	6.8	7.27
	KetjenBlack EC-600 JD	4	2.71	s	6.54E+13		0.3	0.25
				n	9		3	3
NAP05	Lexan HF 1110-11 N	95	96.61	Avg	2.39E+06	Out of Range	10.19	10.73
	KetjenBlack EC-600 JD	5	3.39	s	1.52E+06		0.25	0.21
				n	11		3	3

Table B-1: Overall Summary (continued)

Composite Formulation Name	Description	Wt%	Vol%		Volumetric Transverse Electrical Resistivity (ohm-cm)	Volumetric Longitudinal Electrical Resistivity (ohm-cm)	Shielding Effectiveness (dB) @ 300 MHz	Shielding Effectiveness (dB) @ 800 MHz
NAPR05	Lexan HF 1110-11 N	95	96.6	Avg	1.80E+06	Out of Range	10.43	10.83
	KetjenBlack EC-600 JD	5	3.39	s	2.38E+05		0.15	0.25
				n	6		3	3
NAP06	Lexan HF 1110-11 N	94	95.9	Avg	Out of Range	55	13.38	13.43
	KetjenBlack EC-600 JD	6	4.08	s		18.43	0.25	0.31
				n		10	3	3
NAP7.5	Lexan HF 1110-11 N	92.5	94.9	Avg	Out of Range	14.86	16.71	17.23
	KetjenBlack EC-600 JD	7.5	5.13	s		4.03	0.15	0.21
				n		23	3	3
NAP10	Lexan HF 1110-11 N	90	93.1	Avg	Out of Range	4.89	21.84	21.9
	KetjenBlack EC-600 JD	10	6.89	s		0.69	0.59	0.36
				n		23	3	3
NBP10	Lexan HF 1110-11 N	90	94.4	Avg	4.10E+16	Out of Range	0.3	0.4
	Thermocarb ™ CF-300 Specialty Graphite	10	5.62	s	2.41E+16		0.2	0
				n	9.0		3	3
NBP15	Lexan HF 1110-11 N	85	91.4	Avg	3.14E+16	Out of Range	0.3	0.53
	Thermocarb ™ CF-300 Specialty Graphite	15	8.64	s	1.31E+16		0.17	0.06
				n	9.0		3	3

Table B-1: Overall Summary (continued)

Composite Formulation Name	Description	Wt%	Vol%		Volumetric Transverse Electrical Resistivity (ohm-cm)	Volumetric Longitudinal Electrical Resistivity (ohm-cm)	Shielding Effectiveness (dB) @ 300 MHz	Shielding Effectiveness (dB) @ 800 MHz
NBP20	Lexan HF 1110-11 N	80	88.2	Avg	1.14E+14	Out of Range	1.03	1.4
	Thermocarb ™ CF-300 Specialty Graphite	20	11.8	s	9.77E+13		0.21	0
				n	7		3	3
NBP30	Lexan HF 1110-11 N	70	81.33	Avg	6.17E+05	Out of Range	3.03	5.27
	Thermocarb ™ CF-300 Specialty Graphite	30	18.67	s	2.72E+05		0.21	0.32
				n	9		3	3
NBPR30	Lexan HF 1110-11 N	70	81.33	Avg	7.22E+05	Out of Range	3.23	5.6
	Thermocarb ™ CF-300 Specialty Graphite	30	18.67	s	5.77E+05		0.31	0.44
				n	9		3	3
NBP40	Lexan HF 1110-11 N	60	73.27	Avg	Out of Range	57.53	9	11.97
	Thermocarb ™ CF-300 Specialty Graphite	40	26.32	s		12.59	0.1	0.06
				n		24	3	3
NCP05	Lexan HF 1110-11 N	95	97.15	Avg	8.17E+06	Out of Range	0.3	0.6
	ThermalGraph DKD X	5	2.85	s	3.39E+16		0.26	0.1
				n	7		3	3
NCP10	Lexan HF 1110-11 N	90	94.2	Avg	6.22E+16	Out of Range	0.67	1.3
	ThermalGraph DKD X	10	5.84	s	2.64E+16		0.06	0.1
				n	10		3	3

Table B-1: Overall Summary (continued)

Composite Formulation Name	Description	Wt%	Vol%		Volumetric Transverse Electrical Resistivity (ohm-cm)	Volumetric Longitudinal Electrical Resistivity (ohm-cm)	Shielding Effectiveness (dB) @ 300 MHz	Shielding Effectiveness (dB) @ 800 MHz
NCP15	Lexan HF 1110-11 N	85	91.03	Avg	9.70E+15	Out of Range	1.47	2.7
	ThermalGraph DKD X	15	8.97	s	6.18E+15		0.06	0.3
				n	10		3	3
NCP20	Lexan HF 1110-11 N	80	87.76	Avg	4.99E+06	Out of Range	3.1	5.43
	ThermalGraph DKD X	20	12.24	s	5.77E+06		0.1	0.12
				n	1.10E+01		3	3
NCPR20	Lexan HF 1110-11 N	80	87.76	Avg	1.26E+06	Out of Range	3.43	5.87
	ThermalGraph DKD X	20	12.24	s	6.68E+05		0.06	0.06
				n	1.10E+01		3	3
NCP30	Lexan HF 1110-11 N	70	80.70	Avg	Out of Range	44.04	7.63	10.33
	ThermalGraph DKD X	30	19.30	s		13.75	0.32	0.23
				n		18	3	3
NCP40	Lexan HF 1110-11 N	60	72.87	Avg	Out of Range	10.49	13.4	15.47
	ThermalGraph DKD X	40	27.13	s		1.12	0.35	0.32
				n		18	3	3
NABP	Lexan HF 1110-11 N	65	78.3	Avg	Out of Range	4.88	27.84	27.6
	KetjenBlack EC-600 JD	5	3.9	s		1.23	0.26	0.1
	Thermocarb ™ CF-300 Specialty Graphite	30	19.0	n		24	3	3

Table B-1: Overall Summary (continued)

Composite Formulation Name	Description	Wt%	Vol%		Volumetric Transverse Electrical Resistivity (ohm-cm)	Volumetric Longitudinal Electrical Resistivity (ohm-cm)	Shielding Effectiveness (dB) @ 300 MHz	Shielding Effectiveness (dB) @ 800 MHz
NABPR	Lexan HF 1110-11 N	65	78.3	Avg	Out of Range	5.61	28.37	27.7
	KetjenBlack EC-600 JD	5	3.9	s		1.4	0.89	0.3
	Thermocarb ™ CF-300 Specialty Graphite	30	19.0	n		18	3	3
NACP	Lexan HF 1110-11 N	75	84.7	Avg	Out of Range	2.89	27.07	26.1
	Ketjen Black EC600 JD	5	3.7	s		0.59	0.06	0.1
	ThermalGraph DKD X	20	12.5	n		24	3	3
NACPR	Lexan HF 1110-11 N	75	84.7	Avg	Out of Range	2.77	26.77	26.33
	KetjenBlack EC-600 JD	5	3.7	s		0.67	0.32	0.06
	ThermalGraph DKD X	20	12.5	n		24	3	3
NBCP	Lexan HF 1110-11 N	50	64.7	Avg	Out of Range	13.26	16.95	18.7
	Thermocarb ™ CF-300 Specialty Graphite	30	20.8	s		2.2	0.15	0.1
	ThermalGraph DKD X	20	14.5	n		24	3	3
NBCPR	Lexan HF 1110-11 N	50	64.7	Avg	Out of Range	9.31	17.83	19.4
	Thermocarb ™ CF-300 Specialty Graphite	30	20.8	s		0.94	0.35	0.3
	ThermalGraph DKD X	20	14.5	n		24	3	3
NABCP	Lexan HF 1110-11 N	45	62.1	Avg	Out of Range	0.69	Did Not Mold	Did Not Mold
	KetjenBlack EC-600 JD	5	4.4	s		0.21		
	Thermocarb ™ CF-300 Specialty Graphite	30	21.3	n		22		
	ThermalGraph DKD X	20	14.8					

Table B-1: Overall Summary (continued)

Composite Formulation Name	Description	Wt%	Vol%		Volumetric Transverse Electrical Resistivity (ohm-cm)	Volumetric Longitudinal Electrical Resistivity (ohm-cm)	Shielding Effectiveness (dB) @ 300 MHz	Shielding Effectiveness (dB) @ 800 MHz
NABCPR	Lexan HF 1110-11 N	45	62.1	Avg	Out of Range	0.75	Did Not Mold	Did Not Mold
	KetjenBlack EC-600 JD	5	4.4	s		0.12		
	Thermocarb ™ CF-300 Specialty Graphite	30	21.3	n		22		
	ThermalGraph DKD X	20	14.8					

Appendix C: Injection Molding Conditions

Table C-1: Injection Molding Conditions for 10/04/01

Notation	Injection Molding Conditions	Zytel 101 NC 010 With Carbon Fiber **Mat. No. NCN05**	Zytel 101 NC 010 With Carbon Fiber **Mat. No. NCN10**	Zytel 101 NC 010 With Carbon Fiber **Mat. No. NCN15**	Zytel 101 NC 010 With Carbon Fiber **Mat. No. NCN20**
T_{Mold}	Mold Temp (^{o}F)	190	190	190	190
E1	Zone 1 Temp (^{o}F) (nozzle)	610	610	610	610
E2	Zone 2 Temp (^{o}F)	585	585	585	585
E3	Zone 3 Temp (^{o}F)	570	570	570	570
E4	Zone 4 Temp (^{o}F) (feed zone)	554	554	554	554
P1	Injection Pressure (psi)	21,480	21,480	21,480	21,480
P2	Hold Pressure (psi)	22,384	22,384	22,384	22,384
P7	Back Pressure (psi)	226	226	226	226
S1	Shot Size (mm)	42.6	42.6	43.4	44.4
S2	Shot Before (mm)	2.5	2.5	2.5	2.5
S3	Shot After (mm)	5.0	5.0	5.0	5.0
S8	Screw Position to Switch (mm)	15.0	15.0	15.0	15.0
T1	Injection Time (s)	10.0	10.0	10.0	10.0
T2	Cool Time (s)	20.0	20.0	20.0	20.0
T3	Interval Time (s)	2.0	2.0	2.0	2.0
T6	Retraction Time (s)	1.0	1.0	1.0	1.0
T7	Nozzle Retraction Delay Time (s)	0.0	0.0	0.0	0.0
T8	Injection Delay Time (s)	0.5	0.5	0.5	0.5
T9	Charge Delay Time (s)	2.0	2.0	2.0	2.0
V1	Injection Velocity (rpm)	288.0	288.0	288.0	288.0
V6	Screw Rotation (rpm)	96.0	96.0	96.0	96.0
V10	Advance Velocity (rpm)	160.0	160.0	160.0	160.0
V11	Retraction Velocity (rpm)	160.0	160.0	160.0	160.0
CF	Clamp Force (US tons)	62.0	62.0	62.0	62.0

Table C-1: Injection Molding Conditions for 10/04/01 (continued)

Notation	Injection Molding Conditions	Zytel 101 NC 010 With Carbon Fiber **Mat. No. NCNR20**	Zytel 101 NC 010 With Carbon Fiber **Mat. No. NCN30**	Zytel 101 NC 010 With Carbon Fiber **Mat. No. NCN40**	Zytel 101 NC 010 With Synthetic Graphite **Mat. No. NBN10**
T_{Mold}	Mold Temp (^{o}F)	190	190	190	190
E1	Zone 1 Temp (^{o}F) (nozzle)	610	610	610	610
E2	Zone 2 Temp (^{o}F)	585	585	585	585
E3	Zone 3 Temp (^{o}F)	570	570	570	570
E4	Zone 4 Temp (^{o}F) (feed zone)	554	554	554	554
P1	Injection Pressure (psi)	21,480	21,480	21,480	21,480
P2	Hold Pressure (psi)	22,384	22,384	22,384	22,384
P7	Back Pressure (psi)	226	226	226	226
S1	Shot Size (mm)	43.2	43.4	43.8	46.0
S2	Shot Before (mm)	2.5	2.5	2.5	2.5
S3	Shot After (mm)	5.0	5.0	5.0	5.0
S8	Screw Position to Switch (mm)	15.0	15.0	15.0	15.0
T1	Injection Time (s)	10.0	10.0	10.0	10.0
T2	Cool Time (s)	20.0	20.0	20.0	20.0
T3	Interval Time (s)	2.0	2.0	2.0	2.0
T6	Retraction Time (s)	1.0	1.0	1.0	1.0
T7	Nozzle Retraction Delay Time (s)	0.0	0.0	0.0	0.0
T8	Injection Delay Time (s)	0.5	0.5	0.5	0.5
T9	Charge Delay Time (s)	2.0	2.0	2.0	2.0
V1	Injection Velocity (rpm)	288.0	288.0	288.0	288.0
V6	Screw Rotation (rpm)	96.0	96.0	96.0	96.0
V10	Advance Velocity (rpm)	160.0	160.0	160.0	160.0
V11	Retraction Velocity (rpm)	160.0	160.0	160.0	160.0
CF	Clamp Force (US tons)	62.0	62.0	62.0	62.0

Table C-1: Injection Molding Conditions for 10/04/01 (continued)

Notation	Injection Molding Conditions	Zytel 101 NC 010 With Synthetic Graphite **Mat. No. NBN15**	Zytel 101 NC 010 With Synthetic Graphite **Mat. No. NBN20**	Zytel 101 NC 010 With Synthetic Graphite **Mat. No. NBN30**	Zytel 101 NC 010 With Synthetic Graphite **Mat. No. NBNR30**
T_{Mold}	Mold Temp (^{o}F)	190	190	190	190
E1	Zone 1 Temp (^{o}F) (nozzle)	610	610	610	610
E2	Zone 2 Temp (^{o}F)	585	585	585	585
E3	Zone 3 Temp (^{o}F)	570	570	570	570
E4	Zone 4 Temp (^{o}F) (feed zone)	554	554	554	554
P1	Injection Pressure (psi)	21,480	21,480	21,480	21,480
P2	Hold Pressure (psi)	22,384	22,384	22,384	22,384
P7	Back Pressure (psi)	226	226	226	226
S1	Shot Size (mm)	44.6	46.0	45.2	43.8
S2	Shot Before (mm)	2.5	2.5	2.5	2.5
S3	Shot After (mm)	5.0	5.0	5.0	5.0
S8	Screw Position to Switch (mm)	15.0	15.0	15.0	15.0
T1	Injection Time (s)	10.0	10.0	10.0	10.0
T2	Cool Time (s)	20.0	20.0	20.0	20.0
T3	Interval Time (s)	2.0	2.0	2.0	2.0
T6	Retraction Time (s)	1.0	1.0	1.0	1.0
T7	Nozzle Retraction Delay Time (s)	0.0	0.0	0.0	0.0
T8	Injection Delay Time (s)	0.5	0.5	0.5	0.5
T9	Charge Delay Time (s)	2.0	2.0	2.0	2.0
V1	Injection Velocity (rpm)	288.0	288.0	288.0	288.0
V6	Screw Rotation (rpm)	96.0	96.0	96.0	96.0
V10	Advance Velocity (rpm)	160.0	160.0	160.0	160.0
V11	Retraction Velocity (rpm)	160.0	160.0	160.0	160.0
CF	Clamp Force (US tons)	62.0	62.0	62.0	62.0

Table C-1: Injection Molding Conditions for 10/04/01 (continued)

Notation	Injection Molding Conditions	Zytel 101 NC 010 With Synthetic Graphite **Mat. No. NBN40**	Zytel 101 NC 010 With Synthetic Graphite and Carbon Fiber **Mat. No. NBCN**	Zytel 101 NC 010 With Synthetic Graphite and Carbon Fiber **Mat. No. NBCNR**	Zytel 101 NC 010 With Carbon Black **Mat. No. NAN02.5**
T_{Mold}	Mold Temp (^{o}F)	190	190	190	190
E1	Zone 1 Temp (^{o}F) (nozzle)	610	610	610	610
E2	Zone 2 Temp (^{o}F)	585	585	585	585
E3	Zone 3 Temp (^{o}F)	570	570	570	570
E4	Zone 4 Temp (^{o}F) (feed zone)	554	554	554	554
P1	Injection Pressure (psi)	21,480	21,480	21,480	21,480
P2	Hold Pressure (psi)	22,384	22,384	22,384	22,384
P7	Back Pressure (psi)	2,261	2,261	2,261	2,261
S1	Shot Size (mm)	43.8	43.8	44.8	42.6
S2	Shot Before (mm)	2.5	2.5	2.5	2.5
S3	Shot After (mm)	5.0	5.0	5.0	5.0
S8	Screw Position to Switch (mm)	15.0	15.0	15.0	15.0
T1	Injection Time (s)	10.0	10.0	10.0	10.0
T2	Cool Time (s)	20.0	20.0	20.0	20.0
T3	Interval Time (s)	2.0	2.0	2.0	2.0
T6	Retraction Time (s)	1.0	1.0	1.0	1.0
T7	Nozzle Retraction Delay Time (s)	0.0	0.0	0.0	0.0
T8	Injection Delay Time (s)	0.5	0.5	0.5	0.5
T9	Charge Delay Time (s)	2.0	2.0	2.0	2.0
V1	Injection Velocity (rpm)	288.0	288.0	288.0	288.0
V6	Screw Rotation (rpm)	96.0	96.0	96.0	96.0
V10	Advance Velocity (rpm)	160.0	160.0	160.0	160.0
V11	Retraction Velocity (rpm)	160.0	160.0	160.0	160.0
CF	Clamp Force (US tons)	62.0	62.0	62.0	62.0

Table C-1: Injection Molding Conditions for 10/04/01 (continued)

Notation	Injection Molding Conditions	Zytel 101 NC 010 With Carbon Black **Mat. No. NAN04**	Zytel 101 NC 010 With Carbon Black **Mat. No. NANR05**	Zytel 101 NC 010 With Carbon Black **Mat. No. NANRR05**	Zytel 101 NC 010 With Carbon Black **Mat. No. NAN06**
T_{Mold}	Mold Temp (^{o}F)	190	190	190	190
E1	Zone 1 Temp (^{o}F) (nozzle)	610	610	610	610
E2	Zone 2 Temp (^{o}F)	585	585	585	585
E3	Zone 3 Temp (^{o}F)	570	570	570	570
E4	Zone 4 Temp (^{o}F) (feed zone)	554	554	554	554
P1	Injection Pressure (psi)	21,480	21,480	21,480	21,480
P2	Hold Pressure (psi)	22,384	22,384	22,384	22,384
P7	Back Pressure (psi)	226	226	226	226
S1	Shot Size (mm)	44.0	43.6	43.6	43.2
S2	Shot Before (mm)	2.5	2.5	2.5	2.5
S3	Shot After (mm)	5.0	5.0	5.0	5.0
S8	Screw Position to Switch (mm)	15.0	15.0	15.0	15.0
T1	Injection Time (s)	10.0	10.0	10.0	10.0
T2	Cool Time (s)	20.0	20.0	20.0	20.0
T3	Interval Time (s)	2.0	2.0	2.0	2.0
T6	Retraction Time (s)	1.0	1.0	1.0	1.0
T7	Nozzle Retraction Delay Time (s)	0.0	0.0	0.0	0.0
T8	Injection Delay Time (s)	0.5	0.5	0.5	0.5
T9	Charge Delay Time (s)	2.0	2.0	2.0	2.0
V1	Injection Velocity (rpm)	288.0	288.0	288.0	288.0
V6	Screw Rotation (rpm)	96.0	96.0	96.0	96.0
V10	Advance Velocity (rpm)	160.0	160.0	160.0	160.0
V11	Retraction Velocity (rpm)	160.0	160.0	160.0	160.0
CF	Clamp Force (US tons)	62.0	62.0	62.0	62.0

Table C-1: Injection Molding Conditions for 10/04/01 (continued)

Notation	Injection Molding Conditions	Zytel 101 NC 010 With Carbon Black **Mat. No. NAN07.5**	Zytel 101 NC 010 With Carbon Black **Mat. No. NAN10**	Zytel 101 NC 010 With Carbon Black and Synthetic Graphite **Mat. No. NABN**	Zytel 101 NC 010 With Carbon Black and Synthetic Graphite **Mat. No. NABNR**
T_{Mold}	Mold Temp (^{o}F)	190	190	190	190
E1	Zone 1 Temp (^{o}F) (nozzle)	610	610	610	610
E2	Zone 2 Temp (^{o}F)	585	585	585	585
E3	Zone 3 Temp (^{o}F)	570	570	570	570
E4	Zone 4 Temp (^{o}F) (feed zone)	554	554	554	554
P1	Injection Pressure (psi)	21,480	21,480	21,480	21,480
P2	Hold Pressure (psi)	22,384	22,384	22,384	22,384
P7	Back Pressure (psi)	226	226	226	226
S1	Shot Size (mm)	43.2	43.2	44.0	44.0
S2	Shot Before (mm)	2.5	2.5	2.5	2.5
S3	Shot After (mm)	5.0	5.0	5.0	5.0
S8	Screw Position to Switch (mm)	15.0	15.0	15.0	15.0
T1	Injection Time (s)	10.0	10.0	10.0	10.0
T2	Cool Time (s)	20.0	20.0	20.0	20.0
T3	Interval Time (s)	2.0	2.0	2.0	2.0
T6	Retraction Time (s)	1.0	1.0	1.0	1.0
T7	Nozzle Retraction Delay Time (s)	0.0	0.0	0.0	0.0
T8	Injection Delay Time (s)	0.5	0.5	0.5	0.5
T9	Charge Delay Time (s)	2.0	2.0	2.0	2.0
V1	Injection Velocity (rpm)	288.0	288.0	288.0	288.0
V6	Screw Rotation (rpm)	96.0	96.0	96.0	96.0
V10	Advance Velocity (rpm)	160.0	160.0	160.0	160.0
V11	Retraction Velocity (rpm)	160.0	160.0	160.0	160.0
CF	Clamp Force (US tons)	62.0	62.0	62.0	62.0

Table C-1: Injection Molding Conditions for 10/04/01 (continued)

Notation	Injection Molding Conditions	Zytel 101 NC 010 With Carbon Black and Carbon Fiber **Mat. No. NACN**	Zytel 101 NC 010 With Carbon Black and Carbon Fiber **Mat. No. NACNR**
T_{Mold}	Mold Temp (^{o}F)	190	190
E1	Zone 1 Temp (^{o}F) (nozzle)	610	610
E2	Zone 2 Temp (^{o}F)	585	585
E3	Zone 3 Temp (^{o}F)	570	570
E4	Zone 4 Temp (^{o}F) (feed zone)	554	554
P1	Injection Pressure (psi)	21,480	21,480
P2	Hold Pressure (psi)	22,384	22,384
P7	Back Pressure (psi)	226	226
S1	Shot Size (mm)	44.0	44.0
S2	Shot Before (mm)	2.5	2.5
S3	Shot After (mm)	5.0	5.0
S8	Screw Position to Switch (mm)	15.0	15.0
T1	Injection Time (s)	10.0	10.0
T2	Cool Time (s)	20.0	20.0
T3	Interval Time (s)	2.0	2.0
T6	Retraction Time (s)	1.0	1.0
T7	Nozzle Retraction Delay Time (s)	0.0	0.0
T8	Injection Delay Time (s)	0.5	0.5
T9	Charge Delay Time (s)	2.0	2.0
V1	Injection Velocity (rpm)	288.0	288.0
V6	Screw Rotation (rpm)	96.0	96.0
V10	Advance Velocity (rpm)	160.0	160.0
V11	Retraction Velocity (rpm)	160.0	160.0
CF	Clamp Force (US tons)	62.0	62.0

Table C-1: Injection Molding Conditions for 10/04/01 (continued)

Notation	Injection Molding Conditions	Zytel 101 NC 010 With Carbon Black, Carbon Fiber, and Synthetic Graphite **Mat. No. NABCN**	Zytel 101 NC 010 With Carbon Black, Carbon Fiber, and Synthetic Graphite **Mat. No. NABCNR**
T_{Mold}	Mold Temp (^{o}F)	190	190
E1	Zone 1 Temp (^{o}F) (nozzle)	610	610
E2	Zone 2 Temp (^{o}F)	585	585
E3	Zone 3 Temp (^{o}F)	570	570
E4	Zone 4 Temp (^{o}F) (feed zone)	554	554
P1	Injection Pressure (psi)	21,480	21,480
P2	Hold Pressure (psi)	22,384	22,384
P7	Back Pressure (psi)	226	226
S1	Shot Size (mm)	44.8	44.8
S2	Shot Before (mm)	2.5	2.5
S3	Shot After (mm)	5.0	5.0
S8	Screw Position to Switch (mm)	15.0	15.0
T1	Injection Time (s)	10.0	10.0
T2	Cool Time (s)	20.0	20.0
T3	Interval Time (s)	2.0	2.0
T6	Retraction Time (s)	1.0	1.0
T7	Nozzle Retraction Delay Time (s)	0.0	0.0
T8	Injection Delay Time (s)	0.5	0.5
T9	Charge Delay Time (s)	2.0	2.0
V1	Injection Velocity (rpm)	288.0	288.0
V6	Screw Rotation (rpm)	96.0	96.0
V10	Advance Velocity (rpm)	160.0	160.0
V11	Retraction Velocity (rpm)	160.0	160.0
CF	Clamp Force (US tons)	62.0	62.0

Table C-1: Injection Molding Conditions for 10/04/01 (continued)

Notation	Injection Molding Conditions	Lexan HF110-111N With Carbon Fiber **Mat. No. NCP05**	Lexan HF110-111N With Carbon Fiber **Mat. No. NCP10**	Lexan HF110-111N With Carbon Fiber **Mat. No. NCP15**	Lexan HF110-111N With Carbon Fiber **Mat. No. NCP20**
T_{Mold}	Mold Temp (^{o}F)	190	190	190	190
E1	Zone 1 Temp (^{o}F) (nozzle)	610	610	610	610
E2	Zone 2 Temp (^{o}F)	585	585	585	585
E3	Zone 3 Temp (^{o}F)	570	570	570	570
E4	Zone 4 Temp (^{o}F) (feed zone)	554	554	554	554
P1	Injection Pressure (psi)	22,384	22,384	22,384	22,384
P2	Hold Pressure (psi)	22,384	22,384	22,384	22,384
P7	Back Pressure (psi)	226	226	226	226
S1	Shot Size (mm)	43.0	42.0	42.6	42.4
S2	Shot Before (mm)	2.5	2.5	2.5	2.5
S3	Shot After (mm)	5.0	5.0	5.0	5.0
S8	Screw Position to Switch (mm)	15.0	15.0	15.0	15.0
T1	Injection Time (s)	10.0	10.0	10.0	10.0
T2	Cool Time (s)	20.0	20.0	20.0	20.0
T3	Interval Time (s)	2.0	2.0	2.0	2.0
T6	Retraction Time (s)	1.0	1.0	1.0	1.0
T7	Nozzle Retraction Delay Time (s)	0.0	0.0	0.0	0.0
T8	Injection Delay Time (s)	0.5	0.5	0.5	0.5
T9	Charge Delay Time (s)	2.0	2.0	2.0	2.0
V1	Injection Velocity (rpm)	304.0	192.0	288.0	288.0
V6	Screw Rotation (rpm)	128.0	128.0	128.0	128.0
V10	Advance Velocity (rpm)	160.0	160.0	160.0	160.0
V11	Retraction Velocity (rpm)	160.0	160.0	160.0	160.0
CF	Clamp Force (US tons)	62.0	62.0	62.0	62.0

Table C-1: Injection Molding Conditions for 10/04/01 (continued)

Notation	Injection Molding Conditions	Lexan HF110-111N With Carbon Fiber **Mat. No. NCPR20**	Lexan HF110-111N With Carbon Fiber **Mat. No. NCP30**	Lexan HF110-111N With Carbon Fiber **Mat. No. NCP40**	Lexan HF110-111N With Synthetic Graphite **Mat. No. NBP10**
T_{Mold}	Mold Temp (^{o}F)	190	190	190	190
E1	Zone 1 Temp (^{o}F) (nozzle)	610	610	610	610
E2	Zone 2 Temp (^{o}F)	585	585	585	585
E3	Zone 3 Temp (^{o}F)	570	570	570	570
E4	Zone 4 Temp (^{o}F) (feed zone)	554	554	554	554
P1	Injection Pressure (psi)	22,384	22,384	22,384	22,384
P2	Hold Pressure (psi)	22,384	22,384	22,384	22,384
P7	Back Pressure (psi)	226	226	226	226
S1	Shot Size (mm)	42.0	42.2	42.6	42.8
S2	Shot Before (mm)	2.5	2.5	2.5	2.5
S3	Shot After (mm)	5.0	5.0	5.0	5.0
S8	Screw Position to Switch (mm)	15.0	15.0	15.0	15.0
T1	Injection Time (s)	10.0	10.0	10.0	10.0
T2	Cool Time (s)	20.0	20.0	20.0	20.0
T3	Interval Time (s)	2.0	2.0	2.0	2.0
T6	Retraction Time (s)	1.0	1.0	1.0	1.0
T7	Nozzle Retraction Delay Time (s)	0.0	0.0	0.0	0.0
T8	Injection Delay Time (s)	0.5	0.5	0.5	0.5
T9	Charge Delay Time (s)	2.0	2.0	2.0	2.0
V1	Injection Velocity (rpm)	288.0	288.0	288.0	288.0
V6	Screw Rotation (rpm)	128.0	128.0	128.0	128.0
V10	Advance Velocity (rpm)	160.0	160.0	160.0	160.0
V11	Retraction Velocity (rpm)	160.0	160.0	160.0	160.0
CF	Clamp Force (US tons)	62.0	62.0	62.0	62.0

Table C-1: Injection Molding Conditions for 10/04/01 (continued)

Notation	Injection Molding Conditions	Lexan HF110-111N With Synthetic Graphite **Mat. No. NBP15**	Lexan HF110-111N With Synthetic Graphite **Mat. No. NBP20**	Lexan HF110-111N With Synthetic Graphite **Mat. No. NBP30**	Lexan HF110-111N With Synthetic Graphite **Mat. No. NBPR30**
T_{Mold}	Mold Temp (^{o}F)	190	190	190	190
E1	Zone 1 Temp (^{o}F) (nozzle)	610	610	610	610
E2	Zone 2 Temp (^{o}F)	585	585	585	585
E3	Zone 3 Temp (^{o}F)	570	570	570	570
E4	Zone 4 Temp (^{o}F) (feed zone)	554	554	554	554
P1	Injection Pressure (psi)	22,384	22,384	22,384	22,384
P2	Hold Pressure (psi)	22,384	22,384	22,384	22,384
P7	Back Pressure (psi)	226	226	226	226
S1	Shot Size (mm)	43.0	44.0	44.0	44.0
S2	Shot Before (mm)	2.5	2.5	2.5	2.5
S3	Shot After (mm)	5.0	5.0	5.0	5.0
S8	Screw Position to Switch (mm)	15.0	15.0	15.0	15.0
T1	Injection Time (s)	10.0	10.0	10.0	10.0
T2	Cool Time (s)	10.0	10.0	10.0	10.0
T3	Interval Time (s)	2.0	2.0	2.0	2.0
T6	Retraction Time (s)	1.0	1.0	1.0	1.0
T7	Nozzle Retraction Delay Time (s)	0.0	0.0	0.0	0.0
T8	Injection Delay Time (s)	0.5	0.5	0.5	0.5
T9	Charge Delay Time (s)	2.0	2.0	2.0	2.0
V1	Injection Velocity (rpm)	288.0	288.0	288.0	288.0
V6	Screw Rotation (rpm)	128.0	128.0	128.8	128.0
V10	Advance Velocity (rpm)	160.0	160.0	160.0	160.0
V11	Retraction Velocity (rpm)	160.0	160.0	160.0	160.0
CF	Clamp Force (US tons)	62.0	62.0	62.0	62.0

Table C-1: Injection Molding Conditions for 10/04/01 (continued)

Notation	Injection Molding Conditions	Lexan HF110-111N With Synthetic Graphite **Mat. No. NBP40**	Lexan HF110-111N With Carbon Fiber and Synthetic Graphite **Mat. No. NBCP**	Lexan HF110-111N With Carbon Fiber and Synthetic Graphite **Mat. No. NBCPR**	Lexan HF110-111N With Carbon Black **Mat. No. NAP02.5**
T_{Mold}	Mold Temp (^{o}F)	190	190	190	190
E1	Zone 1 Temp (^{o}F) (nozzle)	610	610	610	610
E2	Zone 2 Temp (^{o}F)	585	585	585	585
E3	Zone 3 Temp (^{o}F)	570	570	570	570
E4	Zone 4 Temp (^{o}F) (feed zone)	554	554	554	554
P1	Injection Pressure (psi)	22,384	22,384	22,384	22,384
P2	Hold Pressure (psi)	22,384	22,384	22,384	22,384
P7	Back Pressure (psi)	226	226	226	226
S1	Shot Size (mm)	44.0	44.4	44.4	42.8
S2	Shot Before (mm)	2.5	2.5	2.5	2.5
S3	Shot After (mm)	5.0	5.0	5.0	5.0
S8	Screw Position to Switch (mm)	15.0	15.0	15.0	15.0
T1	Injection Time (s)	10.0	10.0	10.0	10.0
T2	Cool Time (s)	10.0	10.0	10.0	10.0
T3	Interval Time (s)	2.0	2.0	2.0	2.0
T6	Retraction Time (s)	1.0	1.0	1.0	1.0
T7	Nozzle Retraction Delay Time (s)	0.0	0.0	0.0	0.0
T8	Injection Delay Time (s)	0.5	0.5	0.5	0.5
T9	Charge Delay Time (s)	2.0	2.0	2.0	2.0
V1	Injection Velocity (rpm)	288.0	288.0	288.0	288.0
V6	Screw Rotation (rpm)	128.0	128.0	128.0	128.0
V10	Advance Velocity (rpm)	160.0	160.0	160.0	160.0
V11	Retraction Velocity (rpm)	160.0	160.0	160.0	160.0
CF	Clamp Force (US tons)	62.0	62.0	62.0	62.0

Table C-2: Injection Molding Conditions for 10/05/01

Notation	Injection Molding Conditions	Lexan HF110-111N With Carbon Black **Mat. No. NAP04**	Lexan HF110-111N With Carbon Black **Mat. No. NAP05**	Lexan HF110-111N With Carbon Black **Mat. No. NAPR05**	Lexan HF110-111N With Carbon Black **Mat. No. NAP06**
T_{Mold}	Mold Temp (^{o}F)	190	190	190	190
E1	Zone 1 Temp (^{o}F) (nozzle)	610	610	610	610
E2	Zone 2 Temp (^{o}F)	585	585	585	585
E3	Zone 3 Temp (^{o}F)	570	570	570	570
E4	Zone 4 Temp (^{o}F) (feed zone)	554	554	554	554
P1	Injection Pressure (psi)	22,384	22,384	22,384	22,384
P2	Hold Pressure (psi)	22,384	22,384	22,384	22,384
P7	Back Pressure (psi)	226	226	226	226
S1	Shot Size (mm)	43.2	43.2	43.2	43.0
S2	Shot Before (mm)	2.5	2.5	2.5	2.5
S3	Shot After (mm)	5.0	5.0	5.0	5.0
S8	Screw Position to Switch (mm)	15.0	15.0	15.0	15.0
T1	Injection Time (s)	10.0	10.0	10.0	10.0
T2	Cool Time (s)	15.0	15.0	15.0	15.0
T3	Interval Time (s)	2.0	2.0	2.0	2.0
T6	Retraction Time (s)	1.0	1.0	1.0	1.0
T7	Nozzle Retraction Delay Time (s)	0.0	0.0	0.0	0.0
T8	Injection Delay Time (s)	0.5	0.5	0.5	0.5
T9	Charge Delay Time (s)	2.0	2.0	2.0	2.0
V1	Injection Velocity (rpm)	288.0	288.0	288.0	288.0
V6	Screw Rotation (rpm)	128.0	128.0	128.0	128.0
V10	Advance Velocity (rpm)	160.0	160.0	160.0	160.0
V11	Retraction Velocity (rpm)	160.0	160.0	160.0	160.0
CF	Clamp Force (US tons)	62.0	62.0	62.0	62.0

Table C-2: Injection Molding Conditions for 10/05/01 (continued)

Notation	Injection Molding Conditions	Lexan HF110-111N With Carbon Black **Mat. No. NAP07.5**	Lexan HF110-111N With Carbon Black **Mat. No. NAP10**	Lexan HF110-111N With Carbon Black and Synthetic Graphite **Mat. No. NABP**	Lexan HF110-111N With Carbon Black and Synthetic Graphite **Mat. No. NABPR**
T_{Mold}	Mold Temp (^{o}F)	190	190	190	190
E1	Zone 1 Temp (^{o}F) (nozzle)	610	610	610	610
E2	Zone 2 Temp (^{o}F)	585	585	585	585
E3	Zone 3 Temp (^{o}F)	570	570	570	570
E4	Zone 4 Temp (^{o}F) (feed zone)	554	554	554	554
P1	Injection Pressure (psi)	22,384	22,384	22,384	22,384
P2	Hold Pressure (psi)	22,384	22,384	22,384	22,384
P7	Back Pressure (psi)	226	226	226	226
S1	Shot Size (mm)	43.0	43.4	43.6	43.8
S2	Shot Before (mm)	2.5	2.5	2.5	2.5
S3	Shot After (mm)	5.0	5.0	5.0	5.0
S8	Screw Position to Switch (mm)	15.0	15.0	15.0	15.0
T1	Injection Time (s)	10.0	10.0	10.0	10.0
T2	Cool Time (s)	15.0	15.0	15.0	15.0
T3	Interval Time (s)	2.0	2.0	2.0	2.0
T6	Retraction Time (s)	1.0	1.0	1.0	1.0
T7	Nozzle Retraction Delay Time (s)	0.0	0.0	0.0	0.0
T8	Injection Delay Time (s)	0.5	0.5	0.5	0.5
T9	Charge Delay Time (s)	2.0	2.0	2.0	2.0
V1	Injection Velocity (rpm)	288.0	288.0	288.0	288.0
V6	Screw Rotation (rpm)	128.0	128.0	128.0	128.0
V10	Advance Velocity (rpm)	160.0	160.0	160.0	160.0
V11	Retraction Velocity (rpm)	160.0	160.0	160.0	160.0
CF	Clamp Force (US tons)	62.0	62.0	62.0	62.0

Table C-2: Injection Molding Conditions for 10/05/01 (continued)

Notation	Injection Molding Conditions	Lexan HF110-111N With Carbon Black and Carbon Fiber **Mat. No. NACP**	Lexan HF110-111N With Carbon Black and Carbon Fiber **Mat. No. NACPR**
T_{Mold}	Mold Temp (^{o}F)	190	190
E1	Zone 1 Temp (^{o}F) (nozzle)	610	610
E2	Zone 2 Temp (^{o}F)	585	585
E3	Zone 3 Temp (^{o}F)	570	570
E4	Zone 4 Temp (^{o}F) (feed zone)	554	554
P1	Injection Pressure (psi)	22,384	22,384
P2	Hold Pressure (psi)	22,384	22,384
P7	Back Pressure (psi)	226	226
S1	Shot Size (mm)	43.8	43.8
S2	Shot Before (mm)	2.5	2.5
S3	Shot After (mm)	5.0	5.0
S8	Screw Position to Switch (mm)	15.0	15.0
T1	Injection Time (s)	10.0	10.0
T2	Cool Time (s)	15.0	15.0
T3	Interval Time (s)	2.0	2.0
T6	Retraction Time (s)	1.0	1.0
T7	Nozzle Retraction Delay Time (s)	0.0	0.0
T8	Injection Delay Time (s)	0.5	0.5
T9	Charge Delay Time (s)	2.0	2.0
V1	Injection Velocity (rpm)	288.0	288.0
V6	Screw Rotation (rpm)	128.0	128.0
V10	Advance Velocity (rpm)	160.0	160.0
V11	Retraction Velocity (rpm)	160.0	160.0
CF	Clamp Force (US tons)	62.0	62.0

Table C-3: Injection Molding Conditions for 10/09/01

Notation	Injection Molding Conditions	Zytel 101 NC 010 **Mat. No. NN**	Zytel 101 NC 010 **Mat. No. NNR**	Lexan HF110-111N **Mat. No. NP**	Lexan HF110-111N **Mat. No. NPR**
T_{Mold}	Mold Temp (^{o}F)	190	190	190	190
E1	Zone 1 Temp (^{o}F) (nozzle)	590	590	590	590
E2	Zone 2 Temp (^{o}F)	554	554	554	554
E3	Zone 3 Temp (^{o}F)	554	554	554	554
E4	Zone 4 Temp (^{o}F) (feed zone)	535	535	535	535
P1	Injection Pressure (psi)	15,827	15,827	15,827	15,827
P2	Hold Pressure (psi)	22,384	22,384	22,384	22,384
P7	Back Pressure (psi)	226	226	226	226
S1	Shot Size (mm)	45.0	45.0	42.8	42.8
S2	Shot Before (mm)	2.5	2.5	2.5	2.5
S3	Shot After (mm)	5.0	5.0	5.0	5.0
S8	Screw Position to Switch (mm)	15.0	15.0	15.0	15.0
T1	Injection Time (s)	15.0	15.0	15.0	15.0
T2	Cool Time (s)	30.0	30.0	20.0	20.0
T3	Interval Time (s)	2.0	2.0	2.0	2.0
T6	Retraction Time (s)	2.0	2.0	2.0	2.0
T7	Nozzle Retraction Delay Time (s)	0.0	0.0	0.0	0.0
T8	Injection Delay Time (s)	0.5	0.5	0.5	0.5
T9	Charge Delay Time (s)	2.0	2.0	2.0	2.0
V1	Injection Velocity (rpm)	32.0	32.0	64.0	64.0
V6	Screw Rotation (rpm)	128.0	128.0	128.0	128.0
V10	Advance Velocity (rpm)	160.0	160.0	160.0	160.0
V11	Retraction Velocity (rpm)	160.0	160.0	160.0	160.0
CF	Clamp Force (US tons)	62.0	62.0	62.0	62.0

Appendix D: Density Results (ASTM D792)

Table D-1: Density for NN (molded 10-09-01)

#	Tested	Sample Number	Theoretical Density (g/mL)	Measured Density (g/mL)
1	12/19/01	NN-S-2	1.1400	1.1484
2	12/19/01	NN-S-4	1.1400	1.1501
3	12/19/01	NN-S-6	1.1400	1.1540
			Average	1.1508
			Standard Deviation	0.0012
			Number of Samples	3

Table D-2: Density for NNR (molded 10-09-01)

#	Tested	Sample Number	Theoretical Density (g/mL)	Measured Density (g/mL)
1	12/19/01	NNR-S-2	1.1400	1.1485
2	12/19/01	NNR-S-4	1.1400	1.1482
3	12/19/01	NNR-S-6	1.1400	1.1455
			Average	1.1474
			Standard Deviation	0.0002
			Number of Samples	3

Table D-3: Density for NAN02.5 (molded 10-04-01)

#	Tested	Sample Number	Theoretical Density (g/mL)	Measured Density (g/mL)
1	11/28/01	NAN02.5-S-2	1.1505	1.1504
2	11/28/01	NAN02.5-S-4	1.1505	1.1483
3	11/28/01	NAN02.5-S-6	1.1505	1.1511
			Average	1.1499
			Standard Deviation	0.0015
			Number of Samples	3

Table D-4: Density for NAN04 (molded 10-04-01)

#	Tested	Sample Number	Theoretical Density (g/mL)	Measured Density (g/mL)
1	11/28/01	NAN04-S-2	1.1570	1.1596
2	11/28/01	NAN04-S-3	1.1570	1.1529
3	11/28/01	NAN04-S-7	1.1570	1.1599
			Average	1.1575
			Standard Deviation	0.0048
			Number of Samples	3

Table D-5: Density for NANR05 (molded 10-04-01)

#	Tested	Sample Number	Theoretical Density (g/mL)	Measured Density (g/mL)
1	11/28/01	NANR05-S-3	1.1613	1.1626
2	11/28/01	NANR05-S-4	1.1613	1.1695
3	11/28/01	NANR05-S-6	1.1613	1.1705
			Average	1.1675
			Standard Deviation	0.0049
			Number of Samples	3

Table D-6: Density for NANRR05 (molded 10-04-01)

#	Tested	Sample Number	Theoretical Density (g/mL)	Measured Density (g/mL)
1	11/28/01	NANRR05-S-2	1.1613	1.1593
2	11/28/01	NANRR05-S-4	1.1613	1.1629
3	11/28/01	NANRR05-S-6	1.1613	1.1565
			Average	1.1596
			Standard Deviation	0.0026
			Number of Samples	3

Table D-7: Density for NAN06 (molded 10-04-01)

#	Tested	Sample Number	Theoretical Density (g/mL)	Measured Density (g/mL)
1	11/28/01	NAN06-S-2	1.1656	1.1684
2	11/28/01	NAN06-S-3	1.1656	1.1638
3	11/28/01	NAN06-S-6	1.1656	1.1638
			Average	1.1654
			Standard Deviation	0.0033
			Number of Samples	3

Table D-8: Density for NAN07.5 (molded 10-04-01)

#	Tested	Sample Number	Theoretical Density (g/mL)	Measured Density (g/mL)
1	11/28/01	NAN07.5-S-2	1.1722	1.1746
2	11/28/01	NAN07.5-S-4	1.1722	1.1727
3	11/28/01	NAN07.5-S-6	1.1722	1.1735
			Average	1.1736
			Standard Deviation	0.0013
			Number of Samples	3

Table D-9: Density for NAN10 (molded 10-04-01)

#	Tested	Sample Number	Theoretical Density (g/mL)	Measured Density (g/mL)
1	11/28/01	NAN10-S-3	1.1834	1.1830
2	11/28/01	NAN10-S-4	1.1834	1.1944
3	11/28/01	NAN10-S-7	1.1834	1.1908
			Average	1.1894
			Standard Deviation	0.0081
			Number of Samples	3

Table D-10: Density for NBN10 (molded 10-04-01)

#	Tested	Sample Number	Theoretical Density (g/mL)	Measured Density (g/mL)
1	11/28/01	NBN10-S-2	1.1989	1.1934
2	11/28/01	NBN10-S-3	1.1989	1.1944
3	11/28/01	NBN10-S-6	1.1989	1.1910
			Average	1.1929
			Standard Deviation	0.0007
			Number of Samples	3

Table D-11: Density for NBN15 (molded 10-04-01)

#	Tested	Sample Number	Theoretical Density (g/mL)	Measured Density (g/mL)
1	11/28/01	NBN15-S-2	1.2307	1.2287
2	11/28/01	NBN15-S-4	1.2307	1.2291
3	11/28/01	NBN15-S-6	1.2307	1.2337
			Average	1.2305
			Standard Deviation	0.0002
			Number of Samples	3

Table D-12: Density for NBN20 (molded 10-04-01)

#	Tested	Sample Number	Theoretical Density (g/mL)	Measured Density (g/mL)
1	11/28/01	NBN20-S-2	1.2642	1.2627
2	11/28/01	NBN20-S-3	1.2642	1.2601
3	11/28/01	NBN20-S-6	1.2642	1.2595
			Average	1.2608
			Standard Deviation	0.0018
			Number of Samples	3

Table D-13: Density for NBN30 (molded 10-04-01)

#	Tested	Sample Number	Theoretical Density (g/mL)	Measured Density (g/mL)
1	11/28/01	NBN30-3	1.3370	1.3442
2	11/28/01	NBN30-4	1.3370	1.3346
3	11/28/01	NBN30-8	1.3370	1.3316
			Average	1.3368
			Standard Deviation	0.0068
			Number of Samples	3

Table D-14: Density for NBNR30 (molded 10-04-01)

#	Tested	Sample Number	Theoretical Density (g/mL)	Measured Density (g/mL)
1	11/28/01	NBNR30-S-3	1.3370	1.3338
2	11/28/01	NBNR30-S-4	1.3370	1.3471
3	11/28/01	NBNR30-S-7	1.3370	1.3338
			Average	1.3382
			Standard Deviation	0.0094
			Number of Samples	3

Table D-15: Density for NBN40 (molded 10-04-01)

#	Tested	Sample Number	Theoretical Density (g/mL)	Measured Density (g/mL)
1	11/28/01	NBN40-S-3	1.4187	1.4202
2	11/28/01	NBN40-S-5	1.4187	1.4126
3	11/28/01	NBN40-S-7	1.4187	1.4087
			Average	1.4138
			Standard Deviation	0.0054
			Number of Samples	3

Table D-16: Density for NCN5 (molded 10-04-01)

#	Tested	Sample Number	Theoretical Density (g/mL)	Measured Density (g/mL)
1	11/28/01	NCN5-S-3	1.1674	1.1626
2	11/28/01	NCN5-S-6	1.1674	1.1758
3	11/28/01	NCN5-S-7	1.1674	1.1655
			Average	1.1680
			Standard Deviation	0.0094
			Number of Samples	3

Table D-17: Density for NCN10 (molded 10-04-01)

#	Tested	Sample Number	Theoretical Density (g/mL)	Measured Density (g/mL)
1	11/28/01	NCN10-S-3	1.1962	1.1908
2	11/28/01	NCN10-S-4	1.1962	1.2029
3	11/28/01	NCN10-S-6	1.1962	1.2071
			Average	1.2003
			Standard Deviation	0.0086
			Number of Samples	3

Table D-18: Density for NCN15 (molded 10-04-01)

#	Tested	Sample Number	Theoretical Density (g/mL)	Measured Density (g/mL)
1	11/28/01	NCN15-S-2	1.2264	1.2194
2	11/28/01	NCN15-S-4	1.2264	1.2149
3	11/28/01	NCN15-S-6	1.2264	1.2129
			Average	1.2157
			Standard Deviation	0.0032
			Number of Samples	3

Table D-19: Density for NCN20 (molded 10-04-01)

#	Tested	Sample Number	Theoretical Density (g/mL)	Measured Density (g/mL)
1	11/28/01	NCN20-S-2	1.2582	1.2668
2	11/28/01	NCN20-S-4	1.2582	1.2496
3	11/28/01	NCN20-S-7	1.2582	1.2568
			Average	1.2578
			Standard Deviation	0.0122
			Number of Samples	3

Table D-20: Density for NCNR20 (molded 10-04-01)

#	Tested	Sample Number	Theoretical Density (g/mL)	Measured Density (g/mL)
1	11/28/01	NCNR20-S-2	1.2582	1.2519
2	11/28/01	NCNR20-S-4	1.2582	1.2531
3	11/28/01	NCNR20-S-6	1.2582	1.2467
			Average	1.2505
			Standard Deviation	0.0008
			Number of Samples	3

Table D-21: Density for NCN30 (molded 10-04-01)

#	Tested	Sample Number	Theoretical Density (g/mL)	Measured Density (g/mL)
1	11/28/01	NCN30-S-2	1.3270	1.3187
2	11/28/01	NCN30-S-4	1.3270	1.3251
3	11/28/01	NCN30-S-6	1.3270	1.3233
			Average	1.3224
			Standard Deviation	0.0045
			Number of Samples	3

Table D-22: Density for NCN40 (molded 10-04-01)

#	Tested	Sample Number	Theoretical Density (g/mL)	Measured Density (g/mL)
1	11/28/01	NCN40-2	1.4038	1.3931
2	11/28/01	NCN40-3	1.4038	1.4168
3	11/28/01	NCN40-6	1.4038	1.3923
			Average	1.4007
			Standard Deviation	0.0168
			Number of Samples	3

Table D-23: Density for NABN (molded 10-04-01)

#	Tested	Sample Number	Theoretical Density (g/mL)	Measured Density (g/mL)
1	11/28/01	NABN-S-2	1.3663	1.3813
2	11/28/01	NABN-S-4	1.3663	1.3703
3	11/28/01	NABN-S-6	1.3663	1.3834
			Average	1.3783
			Standard Deviation	0.0078
			Number of Samples	3

Table D-24: Density for NABNR (molded 10-04-01)

#	Tested	Sample Number	Theoretical Density (g/mL)	Measured Density (g/mL)
1	11/28/01	NABNR-S-2	1.3663	1.3588
2	11/28/01	NABNR-S-4	1.3663	1.3640
3	11/28/01	NABNR-S-6	1.3663	1.3592
			Average	1.3607
			Standard Deviation	0.0036
			Number of Samples	3

Table D-25: Density for NACN (molded 10-04-01)

#	Tested	Sample Number	Theoretical Density (g/mL)	Measured Density (g/mL)
1	11/28/01	NACN-S-4	1.2842	1.2827
2	11/28/01	NACN-S-6	1.2842	1.2932
3	12/19/01	NACN-S-5	1.2842	1.2852
			Average	1.2870
			Standard Deviation	0.0074
			Number of Samples	3

Table D-26: Density for NACNR (molded 10-04-01)

#	Tested	Sample Number	Theoretical Density (g/mL)	Measured Density (g/mL)
1	11/28/01	NACNR-S-2	1.2842	1.2838
2	11/28/01	NACNR-S-4	1.2842	1.2970
3	11/28/01	NACNR-S-7	1.2842	1.2822
			Average	1.2877
			Standard Deviation	0.0093
			Number of Samples	3

Table D-27: Density for NBCN (molded 10-04-01)

#	Tested	Sample Number	Theoretical Density (g/mL)	Measured Density (g/mL)
1	11/28/01	NBCN-S-2	1.5025	1.4985
2	11/28/01	NBCN-S-3	1.5025	1.4961
3	11/28/01	NBCN-S-7	1.5025	1.5132
			Average	1.5026
			Standard Deviation	0.0093
			Number of Samples	3

Table D-28: Density for NBCNR (molded 10-04-01)

#	Tested	Sample Number	Theoretical Density (g/mL)	Measured Density (g/mL)
1	11/28/01	NBCNR-S-2	1.5025	1.4877
2	11/28/01	NBCNR-S-4	1.5025	1.4873
3	11/28/01	NBCNR-S-6	1.5025	1.4941
			Average	1.4897
			Standard Deviation	0.0003
			Number of Samples	3

Table D-29: Density for NABCN (molded 10-04-01)

#	Tested	Sample Number	Theoretical Density (g/mL)	Measured Density (g/mL)
1	11/28/01	NABCN-S-3	1.5397	1.5312
2	11/28/01	NABCN-S-4	1.5397	1.5280
3	11/28/01	NABCN-S-6	1.5397	1.5281
			Average	1.5291
			Standard Deviation	0.0022
			Number of Samples	3

Table D-30: Density for NABCNR (molded 10-04-01)

#	Tested	Sample Number	Theoretical Density (g/mL)	Measured Density (g/mL)
1	11/28/01	NABCNR-S-3	1.5397	1.5425
2	11/28/01	NABCNR-S-4	1.5397	1.5410
3	11/28/01	NABCNR-S-6	1.5397	1.5356
			Average	1.5397
			Standard Deviation	0.0010
			Number of Samples	3

Table D-31: Density for NP (molded 10-09-01)

#	Tested	Sample Number	Theoretical Density (g/mL)	Measured Density (g/mL)
1	11/28/01	NP-S-2	1.2000	1.1895
2	11/28/01	NP-S-4	1.2000	1.1840
3	11/28/01	NP-S-6	1.2000	1.1870
			Average	1.1868
			Standard Deviation	0.0038
			Number of Samples	3

Table D-32: Density for NPR (molded 10-09-01)

#	Tested	Sample Number	Theoretical Density (g/mL)	Measured Density (g/mL)
1	11/28/01	NPR-S-2	1.2000	1.1853
2	11/28/01	NPR-S-4	1.2000	1.1903
3	11/28/01	NPR-S-6	1.2000	1.1846
			Average	1.1868
			Standard Deviation	0.0035
			Number of Samples	3

Table D-33: Density for NAP02.5 (molded 10-04-01)

#	Tested	Sample Number	Theoretical Density (g/mL)	Measured Density (g/mL)
1	11/27/01	NAP02.5-S-2	1.2101	1.1949
2	11/27/01	NAP02.5-S-3	1.2101	1.2170
3	11/27/01	NAP02.5-S-6	1.2101	1.2049
			Average	1.2056
			Standard Deviation	0.0156
			Number of Samples	3

Table D-34: Density for NAP04 (molded 10-05-01)

#	Tested	Sample Number	Theoretical Density (g/mL)	Measured Density (g/mL)
1	11/28/01	NAP04-S-2	1.2162	1.2077
2	11/28/01	NAP04-S-3	1.2162	1.2139
3	11/28/01	NAP04-S-7	1.2162	1.2103
			Average	1.2106
			Standard Deviation	0.0044
			Number of Samples	3

Table D-35: Density for NAP05 (molded 10-05-01)

#	Tested	Sample Number	Theoretical Density (g/mL)	Measured Density (g/mL)
1	11/27/01	NAP05-S-2	1.2203	1.2171
2	11/27/01	NAP05-S-4	1.2203	1.2197
3	11/27/01	NAP05-S-6	1.2203	1.2202
			Average	1.2190
			Standard Deviation	0.0018
			Number of Samples	3

Table D-36: Density for NAPR05 (molded 10-05-01)

#	Tested	Sample Number	Theoretical Density (g/mL)	Measured Density (g/mL)
1	11/28/01	NAPR05-S-3	1.2203	1.2342
2	11/28/01	NAPR05-S-5	1.2203	1.2171
3	11/28/01	NAPR05-S-7	1.2203	1.2226
			Average	1.2247
			Standard Deviation	0.0121
			Number of Samples	3

Table D-37: Density for NAP06 (molded 10-05-01)

#	Tested	Sample Number	Theoretical Density (g/mL)	Measured Density (g/mL)
1	11/28/01	NAP06-S-3	1.2245	1.2371
2	11/28/01	NAP06-S-5	1.2245	1.2267
3	11/28/01	NAP06-S-6	1.2245	1.2178
			Average	1.2272
			Standard Deviation	0.0073
			Number of Samples	3

Table D-38: Density for NAP07.5 (molded 10-05-01)

#	Tested	Sample Number	Theoretical Density (g/mL)	Measured Density (g/mL)
1	11/27/01	NAP07.5-S-2	1.2308	1.2263
2	11/27/01	NAP07.5-S-4	1.2308	1.2295
3	11/27/01	NAP07.5-S-6	1.2308	1.2215
			Average	1.2258
			Standard Deviation	0.0022
			Number of Samples	3

Table D-39: Density for NAP10 (molded 10-05-01)

#	Tested	Sample Number	Theoretical Density (g/mL)	Measured Density (g/mL)
1	11/28/01	NAP10-S-3	1.2414	1.2490
2	11/28/01	NAP10-S-8	1.2414	1.2432
3	11/28/01	NAP10-S-6	1.2414	1.2312
			Average	1.2411
			Standard Deviation	0.0041
			Number of Samples	3

Table D-40: Density for NBP10 (molded 10-04-01)

#	Tested	Sample Number	Theoretical Density (g/mL)	Measured Density (g/mL)
1	11/27/01	NBP10-S-2	1.2584	1.2609
2	11/27/01	NBP10-S-4	1.2584	1.2579
3	11/27/01	NBP10-S-7	1.2584	1.2512
			Average	1.2567
			Standard Deviation	0.0021
			Number of Samples	3

Table D-41: Density for NBP15 (molded 10-04-01)

#	Tested	Sample Number	Theoretical Density (g/mL)	Measured Density (g/mL)
1	11/28/01	NBP15-S-2	1.2898	1.2756
2	11/28/01	NBP15-S-3	1.2898	1.2810
3	11/28/01	NBP15-S-7	1.2898	1.2902
			Average	1.2823
			Standard Deviation	0.0039
			Number of Samples	3

Table D-42: Density for NBP20 (molded 10-04-01)

#	Tested	Sample Number	Theoretical Density (g/mL)	Measured Density (g/mL)
1	11/27/01	NBP20-S-2	1.3228	1.3190
2	11/27/01	NBP20-S-3	1.3228	1.3223
3	12/19/01	NBP20-S-7	1.3228	1.3253
			Average	1.3222
			Standard Deviation	0.0023
			Number of Samples	3

Table D-43: Density for NBP30 (molded 10-04-01)

#	Tested	Sample Number	Theoretical Density (g/mL)	Measured Density (g/mL)
1	11/28/01	NBP30-S-3	1.3942	1.3820
2	11/28/01	NBP30-S-6	1.3942	1.3989
3	11/28/01	NBP30-S-7	1.3942	1.3924
			Average	1.3911
			Standard Deviation	0.0120
			Number of Samples	3

Table D-44: Density for NBPR30 (molded 10-04-01)

#	Tested	Sample Number	Theoretical Density (g/mL)	Measured Density (g/mL)
1	11/28/01	NBPR30-S-2	1.3942	1.3768
2	11/28/01	NBPR30-S-4	1.3942	1.3788
3	11/28/01	NBPR30-S-6	1.3942	1.3717
			Average	1.3758
			Standard Deviation	0.0014
			Number of Samples	3

Table D-45: Density for NBP40 (molded 10-04-01)

#	Tested	Sample Number	Theoretical Density (g/mL)	Measured Density (g/mL)
1	11/28/01	NBP40-S-3	1.4737	1.4716
2	11/28/01	NBP40-S-4	1.4737	1.4786
3	11/28/01	NBP40-S-7	1.4737	1.4681
			Average	1.4727
			Standard Deviation	0.0049
			Number of Samples	3

Table D-46: Density for NCP05 (molded 10-04-01)

#	Tested	Sample Number	Theoretical Density (g/mL)	Measured Density (g/mL)
1	11/28/01	NCP05-S-2	1.2271	1.2233
2	11/28/01	NCP05-S-4	1.2271	1.2191
3	11/28/01	NCP05-S-6	1.2271	1.2192
			Average	1.2205
			Standard Deviation	0.0030
			Number of Samples	3

Table D-47: Density for NCP10 (molded 10-04-01)

#	Tested	Sample Number	Theoretical Density (g/mL)	Measured Density (g/mL)
1	11/28/01	NCP10-S-2	1.2555	1.2604
2	11/28/01	NCP10-S-4	1.2555	1.2564
3	11/28/01	NCP10-S-6	1.2555	1.2596
			Average	1.2588
			Standard Deviation	0.0029
			Number of Samples	3

Table D-48: Density for NCP15 (molded 10-04-01)

#	Tested	Sample Number	Theoretical Density (g/mL)	Measured Density (g/mL)
1	11/27/01	NCP15-S-2	1.2852	1.2848
2	11/27/01	NCP15-S-4	1.2852	1.2775
3	11/27/01	NCP15-S-6	1.2852	1.2772
			Average	1.2798
			Standard Deviation	0.0052
			Number of Samples	3

Table D-49: Density for NCP20 (molded 10-04-01)

#	Tested	Sample Number	Theoretical Density (g/mL)	Measured Density (g/mL)
1	11/27/01	NCP20-S-2	1.3163	1.3106
2	11/27/01	NCP20-S-4	1.3163	1.3121
3	11/27/01	NCP20-S-6	1.3163	1.3137
			Average	1.3121
			Standard Deviation	0.0011
			Number of Samples	3

Table D-50: Density for NCPR20 (molded 10-04-01)

#	Tested	Sample Number	Theoretical Density (g/mL)	Measured Density (g/mL)
1	11/28/01	NCPR20-S-2	1.3163	1.3059
2	11/28/01	NCPR20-S-3	1.3163	1.3264
3	11/28/01	NCPR20-S-7	1.3163	1.3246
			Average	1.3190
			Standard Deviation	0.0145
			Number of Samples	3

Table D-51: Density for NCP30 (molded 10-04-01)

#	Tested	Sample Number	Theoretical Density (g/mL)	Measured Density (g/mL)
1	11/27/01	NCP30-S-2	1.3834	1.3733
2	11/27/01	NCP30-S-3	1.3834	1.3813
3	11/27/01	NCP30-S-6	1.3834	1.3774
			Average	1.3773
			Standard Deviation	0.0056
			Number of Samples	3

Table D-52: Density for NCP40 (molded 10-04-01)

#	Tested	Sample Number	Theoretical Density (g/mL)	Measured Density (g/mL)
1	11/27/01	NCP40-S-2	1.4576	1.4537
2	11/27/01	NCP40-S-3	1.4576	1.4578
3	11/27/01	NCP40-S-6	1.4576	1.4557
			Average	1.4558
			Standard Deviation	0.0028
			Number of Samples	3

Table D-53: Density for NABP (molded 10-05-01)

#	Tested	Sample Number	Theoretical Density (g/mL)	Measured Density (g/mL)
1	11/27/01	NABP-S-3	1.4217	1.4101
2	11/27/01	NABP-S-4	1.4217	1.4099
3	11/27/01	NABP-S-6	1.4217	1.4138
			Average	1.4113
			Standard Deviation	0.0001
			Number of Samples	3

Table D-54: Density for NABPR (molded 10-05-01)

#	Tested	Sample Number	Theoretical Density (g/mL)	Measured Density (g/mL)
1	11/27/01	NABPR-S-2	1.4217	1.4180
2	11/27/01	NABPR-S-3	1.4217	1.4184
3	11/27/01	NABPR-S-6	1.4217	1.4079
			Average	1.4148
			Standard Deviation	0.0002
			Number of Samples	3

Table D-55: Density for NACP (molded 10-05-01)

#	Tested	Sample Number	Theoretical Density (g/mL)	Measured Density (g/mL)
1	11/28/01	NACP-S-3	1.3408	1.3570
2	11/28/01	NACP-S-5	1.3408	1.3358
3	11/28/01	NACP-S-7	1.3408	1.3454
			Average	1.3461
			Standard Deviation	0.0150
			Number of Samples	3

Table D-56: Density for NACPR (molded 10-05-01)

#	Tested	Sample Number	Theoretical Density (g/mL)	Measured Density (g/mL)
1	11/27/01	NACPR-S-2	1.3408	1.3301
2	11/27/01	NACPR-S-4	1.3408	1.3388
3	11/27/01	NACPR-S-8	1.3408	1.3496
			Average	1.3395
			Standard Deviation	0.0097
			Number of Samples	3

Table D-57: Density for NBCP (molded 10-04-01)

#	Tested	Sample Number	Theoretical Density (g/mL)	Measured Density (g/mL)
1	11/27/01	NBCP-S-3	1.5537	1.5563
2	11/27/01	NBCP-S-6	1.5537	1.5474
3	11/27/01	NBCP-S-7	1.5537	1.5581
			Average	1.5506
			Standard Deviation	0.0063
			Number of Samples	3

Table D-58: Density for NBCPR (molded 10-04-01)

#	Tested	Sample Number	Theoretical Density (g/mL)	Measured Density (g/mL)
1	11/27/01	NBCPR-S-2	1.5537	1.5417
2	11/27/01	NBCPR-S-4	1.5537	1.5529
3	11/27/01	NBCPR-S-7	1.5537	1.5703
			Average	1.5550
			Standard Deviation	0.0079
			Number of Samples	3

Appendix E: Thickness Results

Table E-1: Reference Sample Thickness Measurements Dry as Molded for Outer Ring Tested on 1/18/02

		Outer Ring Measurements (mm)					Outer Ring Statistics	
#	Sample Name	Point 1	Point 2	Point 3	Point 4	Point 5	Average (mm)	STD (mm)
1	NABCN-5	3.19	3.09	3.24	3.30	3.33	3.23	0.10
2	NABCNR-5	3.31	3.33	3.31	3.29	3.27	3.30	0.02
3	NABN-5	3.19	3.24	3.27	3.18	3.13	3.20	0.05
4	NABNR-5	3.28	3.31	3.19	3.15	3.23	3.23	0.06
5	NABP-5	3.20	3.26	3.16	3.13	3.16	3.18	0.05
6	NABPR-5	3.21	3.27	3.18	3.19	3.25	3.22	0.04
7	NACN-5(3)	3.20	3.03	3.19	3.26	3.29	3.19	0.10
8	NACNB-5	3.32	3.34	3.10	3.17	3.25	3.24	0.10
9	NACP-5	3.25	3.26	3.16	3.17	3.21	3.21	0.05
10	NACPR-5	3.30	3.21	3.17	3.16	3.26	3.22	0.06
11	NAN02.5-5	3.38	3.24	3.17	3.25	3.24	3.26	0.08
12	NAN04-5(3)	3.22	3.05	3.28	3.33	3.23	3.22	0.11
13	NANR05-5	3.26	3.21	3.16	3.16	3.21	3.20	0.04
14	NANRR05-5	3.00	3.14	3.19	3.29	3.27	3.18	0.12
15	NAN06-5	3.20	3.13	3.18	3.29	3.24	3.21	0.06
16	NAN07.5-5	3.21	3.13	3.19	3.28	3.22	3.21	0.05
17	NAN10-5	3.16	3.04	3.18	3.24	3.18	3.16	0.07
18	NAP02.5-5	3.23	3.16	3.25	3.28	3.33	3.25	0.06
19	NAP04-5	3.26	3.14	3.19	3.27	3.30	3.23	0.07
20	NAP05-5	3.30	3.41	3.26	3.28	3.33	3.32	0.06

Table E-1: Reference Sample Thickness Measurements Dry as Molded for Outer Ring Tested on 1/18/02 (continued)

		Outer Ring Measurements (mm)					Outer Ring Statistics	
#	Sample Name	Point 1	Point 2	Point 3	Point 4	Point 5	Average (mm)	STD (mm)
21	NAPR05-5	3.26	3.15	3.19	3.30	3.29	3.24	0.07
22	NAP06-5	3.27	3.23	3.15	3.15	3.25	3.21	0.06
23	NAP07.5-5	3.14	3.17	3.24	3.14	3.24	3.19	0.05
24	NAP10-5	3.14	3.17	3.24	3.14	3.24	3.19	0.05
25	NBCN-5	3.17	3.21	3.23	3.15	3.16	3.18	0.03
26	NBCNR-5	3.47	3.39	3.47	3.60	3.52	3.49	0.08
27	NBCP-5	3.33	3.35	3.24	3.29	3.41	3.32	0.06
28	NBCPR-5	3.26	3.16	3.29	3.32	3.29	3.26	0.06
29	NBN10-5	3.31	3.21	3.36	3.40	3.35	3.33	0.07
30	NBN15-5	3.39	3.11	3.41	3.47	3.43	3.36	0.14
31	NBN20-5	3.36	3.24	3.31	3.40	3.40	3.34	0.07
32	NBN30-5	3.37	3.18	3.34	3.49	3.45	3.37	0.12
33	NBNR30-5	3.31	3.21	3.27	3.41	3.36	3.31	0.08
34	NBN40-5	3.31	3.29	3.11	3.22	3.25	3.24	0.08
35	NBP10-5	3.20	3.14	3.27	3.36	3.31	3.26	0.09
36	NBP15-5	3.16	3.22	3.28	3.31	3.27	3.25	0.06
37	NBP20-5	3.13	3.16	3.28	3.13	3.15	3.17	0.06
38	NBP30-5	3.22	3.26	3.22	3.23	3.17	3.22	0.03
39	NBPR30-5	3.26	3.19	3.25	3.29	3.30	3.26	0.04
40	NBP40-5	3.26	3.36	3.17	3.18	3.22	3.24	0.08

Table E-1: Reference Sample Thickness Measurements Dry as Molded for Outer Ring Tested on 1/18/02 (continued)

		Outer Ring Measurements (mm)					Outer Ring Statistics	
#	Sample Name	Point 1	Point 2	Point 3	Point 4	Point 5	Average (mm)	STD (mm)
41	NCN05-5	3.37	3.23	3.37	3.47	3.40	3.37	0.09
42	NCN10-5	3.22	3.14	3.23	3.34	3.26	3.24	0.07
43	NCN15-5	3.17	3.17	3.09	3.11	3.11	3.13	0.04
44	NCN20-5	3.10	3.27	3.07	3.12	3.08	3.13	0.08
45	NCNR20-5	3.26	3.46	3.34	3.28	3.28	3.32	0.08
46	NCN30-5	3.46	3.26	3.24	3.25	3.40	3.32	0.10
47	NCN40-5(3)	3.19	3.15	3.25	3.31	3.38	3.26	0.09
48	NCP05-5	3.67	3.51	3.45	3.56	3.48	3.53	0.09
49	NCP10-5	3.35	3.26	3.31	3.46	3.40	3.36	0.08
50	NCP15-5	3.36	3.39	3.47	3.38	3.29	3.38	0.06
51	NCP20-5	3.26	3.33	3.15	3.17	3.22	3.23	0.07
52	NCPR20-5	3.26	3.32	3.20	3.15	3.22	3.23	0.06
53	NCP30-5	3.29	3.27	3.21	3.36	3.37	3.30	0.07
54	NCP40-5	3.27	3.24	3.18	3.15	3.33	3.23	0.07
55	NN-5	3.40	3.66	3.32	3.36	3.39	3.43	0.13
56	NNR-5	3.19	3.25	3.19	3.09	3.18	3.18	0.06
57	NP-5	3.26	3.17	3.16	3.24	3.28	3.22	0.05
58	NPR-5	3.19	3.23	3.19	3.24	3.27	3.22	0.03

Table E-2: Reference Sample Thickness Measurements Dry as Molded for Inner Ring Tested on 1/18/02

		Inner Circle (mm)			Inner Circle Statistics	
#	Sample Name	Point 1	Point 2	Point 3	Average (mm)	STD (mm)
1	NABCN-5	3.13	3.15	3.17	3.15	0.02
2	NABCNR-5	3.15	3.24	3.24	3.21	0.05
3	NABN-5	3.08	3.08	3.11	3.09	0.02
4	NABNR-5	3.14	3.14	3.11	3.13	0.02
5	NABP-5	3.15	3.10	3.11	3.12	0.03
6	NABPR-5	3.13	3.13	3.15	3.14	0.01
7	NACN-5(3)	3.10	3.11	3.10	3.10	0.01
8	NACNB-5	3.12	3.15	3.09	3.12	0.03
9	NACP-5	3.13	3.12	3.17	3.14	0.03
10	NACPR-5	3.18	3.11	3.12	3.14	0.04
11	NAN02.5-5	3.18	3.17	3.18	3.18	0.01
12	NAN04-5(3)	3.11	3.12	3.12	3.12	0.01
13	NANR05-5	3.14	3.11	3.11	3.12	0.02
14	NANRR05-5	3.10	3.07	3.11	3.09	0.02
15	NAN06-5	3.10	3.14	3.12	3.12	0.02
16	NAN07.5-5	3.08	3.12	3.10	3.10	0.02
17	NAN10-5	3.07	3.09	3.10	3.09	0.02
18	NAP02.5-5	3.18	3.15	3.11	3.15	0.04
19	NAP04-5	3.15	3.10	3.10	3.12	0.03
20	NAP05-5	3.12	3.13	3.16	3.14	0.02

Table E-2: Reference Sample Thickness Measurements Dry as Molded for Inner Ring Tested on 1/18/02 (continued)

		Inner Circle (mm)			Inner Circle Statistics	
#	Sample Name	Point 1	Point 2	Point 3	Average (mm)	STD (mm)
21	NAPR05-5	3.11	3.15	3.13	3.13	0.02
22	NAP06-5	3.10	3.13	3.08	3.10	0.03
23	NAP07.5-5	3.07	3.08	3.11	3.09	0.02
24	NAP10-5	3.05	3.08	3.06	3.06	0.02
25	NBCN-5	3.09	3.10	3.09	3.09	0.01
26	NBCNR-5	3.39	3.34	3.38	3.37	0.03
27	NBCP-5	3.30	3.29	3.32	3.30	0.02
28	NBCPR-5	3.22	3.21	3.25	3.23	0.02
29	NBN10-5	3.21	3.20	3.23	3.21	0.02
30	NBN15-5	3.26	3.26	3.27	3.26	0.01
31	NBN20-5	3.26	3.26	3.24	3.25	0.01
32	NBN30-5	3.25	3.30	3.24	3.26	0.03
33	NBNR30-5	3.20	3.24	3.23	3.22	0.02
34	NBN40-5	3.11	3.17	3.11	3.13	0.03
35	NBP10-5	3.13	3.18	3.12	3.14	0.03
36	NBP15-5	3.14	3.14	3.19	3.16	0.03
37	NBP20-5	3.17	3.10	3.11	3.13	0.04
38	NBP30-5	3.11	3.18	3.12	3.14	0.04
39	NBPR30-5	3.18	3.13	3.19	3.17	0.03
40	NBP40-5	3.18	3.15	3.18	3.17	0.02

Table E-2: Reference Sample Thickness Measurements Dry as Molded for Inner Ring Tested on 1/18/02 (continued)

		Inner Circle (mm)			Inner Circle Statistics	
#	Sample Name	Point 1	Point 2	Point 3	Average (mm)	STD (mm)
41	NCN05-5	3.24	3.28	3.21	3.24	0.04
42	NCN10-5	3.03	3.00	3.06	3.03	0.03
43	NCN15-5	2.96	3.01	2.99	2.99	0.03
44	NCN20-5	3.03	3.00	3.03	3.02	0.02
45	NCNR20-5	3.18	3.22	3.18	3.19	0.02
46	NCN30-5	3.28	3.18	3.24	3.23	0.05
47	NCN40-5(3)	3.15	3.15	3.15	3.15	0.00
48	NCP05-5	3.29	3.28	3.24	3.27	0.03
49	NCP10-5	3.17	3.21	3.16	3.18	0.03
50	NCP15-5	3.27	3.19	3.16	3.21	0.06
51	NCP20-5	3.13	3.14	3.14	3.14	0.01
52	NCPR20-5	3.13	3.15	3.12	3.13	0.02
53	NCP30-5	3.21	3.22	3.22	3.22	0.01
54	NCP40-5	3.12	3.19	3.12	3.14	0.04
55	NN-5	3.28	3.29	3.27	3.28	0.01
56	NNR-5	3.07	3.11	3.14	3.11	0.04
57	NP-5	3.23	3.16	3.22	3.20	0.04
58	NPR-5	3.19	3.18	3.17	3.18	0.01

Table E-3: Reference Sample Thickness Measurements Comparison

		Comparison of Outer Ring vs. Inner Circle (mm)			Error Difference (%)	
#	Sample Name	Average Outer (mm)	Average Inner (mm)	Outer - Inner (mm)	% Error (Outer)	% Error (Inner)
1	NABCN-5	3.23	3.15	0.08	2.48	2.54
2	NABCNR-5	3.30	3.21	0.09	2.79	2.87
3	NABN-5	3.20	3.09	0.11	3.50	3.62
4	NABNR-5	3.23	3.13	0.10	3.16	3.26
5	NABP-5	3.18	3.12	0.06	1.95	1.99
6	NABPR-5	3.22	3.14	0.08	2.59	2.66
7	NACN-5(3)	3.19	3.10	0.09	2.84	2.92
8	NACNB-5	3.24	3.12	0.12	3.58	3.72
9	NACP-5	3.21	3.14	0.07	2.18	2.23
10	NACPR-5	3.22	3.14	0.08	2.59	2.66
11	NAN02.5-5	3.26	3.18	0.08	2.44	2.50
12	NAN04-5(3)	3.22	3.12	0.11	3.27	3.38
13	NANR05-5	3.20	3.12	0.08	2.50	2.56
14	NANRR05-5	3.18	3.09	0.08	2.66	2.74
15	NAN06-5	3.21	3.12	0.09	2.74	2.82
16	NAN07.5-5	3.21	3.10	0.11	3.31	3.42
17	NAN10-5	3.16	3.09	0.07	2.32	2.38
18	NAP02.5-5	3.25	3.15	0.10	3.18	3.28
19	NAP04-5	3.23	3.12	0.12	3.57	3.70
20	NAP05-5	3.32	3.14	0.18	5.41	5.72

Table E-3: Reference Sample Thickness Measurements Comparison (continued)

		Comparison of Outer Ring vs. Inner Circle (mm)			Error Difference (%)	
#	Sample Name	Average Outer (mm)	Average Inner (mm)	Outer - Inner (mm)	% Error (Outer)	% Error (Inner)
21	NAPR05-5	3.24	3.13	0.11	3.34	3.45
22	NAP06-5	3.21	3.10	0.11	3.32	3.44
23	NAP07.5-5	3.19	3.09	0.10	3.12	3.22
24	NAP10-5	3.19	3.06	0.12	3.85	4.00
25	NBCN-5	3.18	3.09	0.09	2.85	2.93
26	NBCNR-5	3.49	3.37	0.12	3.44	3.56
27	NBCP-5	3.32	3.30	0.02	0.62	0.63
28	NBCPR-5	3.26	3.23	0.04	1.14	1.16
29	NBN10-5	3.33	3.21	0.11	3.39	3.51
30	NBN15-5	3.36	3.26	0.10	2.93	3.02
31	NBN20-5	3.34	3.25	0.09	2.65	2.73
32	NBN30-5	3.37	3.26	0.10	3.05	3.15
33	NBNR30-5	3.31	3.22	0.09	2.68	2.75
34	NBN40-5	3.24	3.13	0.11	3.28	3.39
35	NBP10-5	3.26	3.14	0.11	3.46	3.58
36	NBP15-5	3.25	3.16	0.09	2.81	2.89
37	NBP20-5	3.17	3.13	0.04	1.37	1.39
38	NBP30-5	3.22	3.14	0.08	2.59	2.66
39	NBPR30-5	3.26	3.17	0.09	2.80	2.88
40	NBP40-5	3.24	3.17	0.07	2.10	2.15

Table E-3: Reference Sample Thickness Measurements Comparison (continued)

		Comparison of Outer Ring vs. Inner Circle (mm)			Error Difference (%)	
#	Sample Name	Average Outer (mm)	Average Inner (mm)	Outer - Inner (mm)	% Error (Outer)	% Error (Inner)
41	NCN05-5	3.37	3.24	0.12	3.70	3.84
42	NCN10-5	3.24	3.03	0.21	6.42	6.86
43	NCN15-5	3.13	2.99	0.14	4.58	4.80
44	NCN20-5	3.13	3.02	0.11	3.45	3.58
45	NCNR20-5	3.32	3.19	0.13	3.93	4.09
46	NCN30-5	3.32	3.23	0.09	2.67	2.74
47	NCN40-5(3)	3.26	3.15	0.11	3.26	3.37
48	NCP05-5	3.53	3.27	0.26	7.47	8.07
49	NCP10-5	3.36	3.18	0.18	5.24	5.53
50	NCP15-5	3.38	3.21	0.17	5.07	5.34
51	NCP20-5	3.23	3.14	0.09	2.77	2.85
52	NCPR20-5	3.23	3.13	0.10	2.99	3.09
53	NCP30-5	3.30	3.22	0.08	2.53	2.59
54	NCP40-5	3.23	3.14	0.09	2.80	2.88
55	NN-5	3.43	3.28	0.15	4.26	4.45
56	NNR-5	3.18	3.11	0.07	2.31	2.36
57	NP-5	3.22	3.20	0.02	0.58	0.58
58	NPR-5	3.22	3.18	0.04	1.36	1.38

Table E-4: Load Sample Thickness Measurements Dry as Molded for Outer Ring Tested on 1/18/02

		Outer Ring Measurements (mm)					Outer Ring Statistics	
#	Sample Name	Point 1	Point 2	Point 3	Point 4	Point 5	Average (mm)	STD (mm)
1	NABP-3	3.09	3.12	3.18	3.17	3.10	3.13	0.04
2	NABP-7	3.11	3.13	3.22	3.20	3.10	3.15	0.05
3	NABP-8	3.11	3.18	3.24	3.20	3.11	3.17	0.06
4	NABPR-3	3.12	3.17	3.21	3.19	3.12	3.16	0.04
5	NABPR-7	3.11	3.15	3.29	3.27	3.16	3.20	0.08
6	NABPR-8	3.16	3.17	3.25	3.20	3.15	3.19	0.04
7	NACP-3	3.12	3.26	3.25	3.25	3.12	3.20	0.07
8	NACP-7	3.13	3.15	3.24	3.18	3.13	3.17	0.05
9	NACP-8	3.12	3.18	3.28	3.25	3.13	3.19	0.07
10	NACPR-3	3.14	3.21	3.30	3.27	3.14	3.21	0.07
11	NACPR-7	3.15	3.19	3.30	3.35	3.28	3.25	0.08
12	NACPR-8	3.15	3.26	3.30	3.30	3.26	3.25	0.06
13	NAP02.5-3	3.15	3.20	3.26	3.28	3.14	3.21	0.06
14	NAP02.5-7	3.13	3.21	3.27	3.29	3.15	3.21	0.07
15	NAP02.5-8	3.20	3.30	3.33	3.36	3.24	3.29	0.07
16	NAP04-3	3.14	3.12	3.25	3.29	3.15	3.19	0.08
17	NAP04-7	3.14	3.20	3.31	3.29	3.15	3.22	0.08
18	NAP04-8	3.15	3.22	3.24	3.25	3.14	3.20	0.05
19	NAP05-3	3.13	3.21	3.25	3.24	3.12	3.19	0.06
20	NAP05-7	3.13	3.21	3.29	3.24	3.13	3.20	0.07

Table E-4: Load Sample Thickness Measurements Dry as Molded for Outer Ring Tested on 1/18/02 (continued)

		Outer Ring Measurements (mm)					Outer Ring Statistics	
#	Sample Name	Point 1	Point 2	Point 3	Point 4	Point 5	Average (mm)	STD (mm)
21	NAP05-8	3.16	3.19	3.27	3.21	3.12	3.19	0.06
22	NAPR05-3	3.12	3.16	3.22	3.25	3.13	3.18	0.06
23	NAPR05-7	3.12	3.18	3.26	3.28	3.19	3.21	0.06
24	NAPR05-8	3.13	3.20	3.29	3.26	3.17	3.21	0.07
25	NAP06-3	3.11	3.15	3.20	3.23	3.13	3.16	0.05
26	NAP06-7	3.11	3.15	3.22	3.23	3.12	3.17	0.06
27	NAP06-8	3.12	3.15	3.29	3.19	3.13	3.18	0.07
28	NAP07.5-3	3.11	3.21	3.29	3.39	3.26	3.25	0.10
29	NAP07.5-7	3.18	3.21	3.24	3.29	3.13	3.21	0.06
30	NAP07.5-8	3.14	3.15	3.23	3.20	3.17	3.18	0.04
31	NAP10-3	3.12	3.16	3.15	3.27	3.90	3.32	0.33
32	NAP10-7	3.16	3.15	3.18	3.22	3.18	3.18	0.03
33	NAP10-8	3.12	3.21	3.18	3.20	3.27	3.20	0.05
34	NBCP-3	3.27	3.34	3.43	3.39	3.33	3.35	0.06
35	NBCP-7	3.28	3.32	3.39	3.41	3.27	3.33	0.06
36	NBCP-8	3.26	3.27	3.41	3.36	3.24	3.31	0.07
37	NBCPR-3	3.17	3.21	3.26	3.25	3.17	3.21	0.04
38	NBCPR-7	3.22	3.24	3.31	3.31	3.22	3.26	0.05
39	NBCPR-8	3.23	3.27	3.37	3.34	3.25	3.29	0.06
40	NBP10-3	3.11	3.16	3.27	3.23	3.12	3.18	0.07

Table E-4: Load Sample Thickness Measurements Dry as Molded for Outer Ring Tested on 1/18/02 (continued)

		Outer Ring Measurements (mm)					Outer Ring Statistics	
#	Sample Name	Point 1	Point 2	Point 3	Point 4	Point 5	Average (mm)	STD (mm)
41	NBP10-7	3.11	3.16	3.26	3.24	3.12	3.18	0.07
42	NBP10-8	3.11	3.18	3.24	3.23	3.13	3.18	0.06
43	NBP15-3	3.11	3.17	3.26	3.23	3.13	3.18	0.06
44	NBP15-7	3.12	3.18	3.23	3.24	3.17	3.19	0.05
45	NBP15-8	3.17	3.19	3.25	3.29	3.15	3.21	0.06
46	NBP20-3	3.10	3.11	3.19	3.17	3.10	3.13	0.04
47	NBP20-7	3.17	3.17	3.23	3.24	3.14	3.19	0.04
48	NBP20-8	3.09	3.12	3.13	3.18	3.11	3.13	0.03
49	NBP30-3	3.15	3.21	3.32	3.20	3.21	3.22	0.06
50	NBP30-7	3.17	3.28	3.33	3.30	3.18	3.25	0.07
51	NBP30-8	3.13	3.20	3.27	3.27	3.13	3.20	0.07
52	NBPR30-3	3.15	3.23	3.32	3.29	3.17	3.23	0.07
53	NBPR30-7	3.13	3.19	3.27	3.27	3.15	3.20	0.07
54	NBPR30-8	3.18	3.25	3.35	3.30	3.20	3.26	0.07
55	NBP40-3	3.15	3.21	3.27	3.31	3.27	3.24	0.06
56	NBP40-7	3.21	3.22	3.28	3.29	3.19	3.24	0.04
57	NBP40-8	3.15	3.21	3.28	3.26	3.14	3.21	0.06
58	NCP05-3	3.29	3.25	3.41	3.42	3.51	3.38	0.11
59	NCP05-7	3.31	3.23	3.25	3.33	3.36	3.30	0.05
60	NCP05-8	3.24	3.10	3.18	3.31	3.17	3.20	0.08

Table E -4: Load Sample Thickness Measurements Dry as Molded for Outer Ring Tested on 1/18/02 (continued)

		Outer Ring Measurements (mm)					Outer Ring Statistics	
#	Sample Name	Point 1	Point 2	Point 3	Point 4	Point 5	Average (mm)	STD (mm)
61	NCP10-3	3.16	3.08	3.15	3.19	3.18	3.15	0.04
62	NCP10-7	3.31	3.30	3.19	3.31	3.25	3.27	0.05
63	NCP10-8	3.20	3.36	3.31	3.29	3.19	3.27	0.07
64	NCP15-3	3.19	3.26	3.37	3.33	3.20	3.27	0.08
65	NCP15-7	3.22	3.32	3.41	3.34	3.25	3.31	0.08
66	NCP15-8	3.23	3.33	3.42	3.37	3.30	3.33	0.07
67	NCP20-3	3.15	3.16	3.25	3.25	3.15	3.19	0.05
68	NCP20-7	3.11	3.17	3.27	3.23	3.11	3.18	0.07
69	NCP20-8	3.03	3.19	3.21	3.21	3.09	3.15	0.08
70	NCPR20-3	3.22	3.25	3.31	3.23	3.15	3.23	0.06
71	NCPR20-7	3.19	3.13	3.23	3.13	3.29	3.19	0.07
72	NCPR20-8	3.15	3.16	3.15	3.20	3.25	3.18	0.04
73	NCP30-3	3.11	3.14	3.23	3.21	3.10	3.16	0.06
74	NCP30-7	3.09	3.14	3.25	3.22	3.12	3.16	0.07
75	NCP30-8	3.09	3.13	3.24	3.21	3.11	3.16	0.07
76	NCP40-3	3.09	3.04	3.18	3.19	3.15	3.13	0.06
77	NCP40-7	3.15	3.21	3.29	3.24	3.15	3.21	0.06
78	NCP40-8	3.13	3.18	3.26	3.27	3.14	3.20	0.07
79	NP-3	3.13	3.25	3.20	3.27	3.17	3.20	0.06
80	NP-7	3.12	3.24	3.27	3.21	3.14	3.20	0.06

Table E-4: Load Sample Thickness Measurements Dry as Molded for Outer Ring Tested on 1/18/02 (continued)

		Outer Ring Measurements (mm)					Outer Ring Statistics	
#	Sample Name	Point 1	Point 2	Point 3	Point 4	Point 5	Average (mm)	STD (mm)
81	NP-8	3.13	3.21	3.32	3.18	3.14	3.20	0.08
82	NPR-3	3.12	3.21	3.25	3.23	3.13	3.19	0.06
83	NPR-7	3.10	3.27	3.22	3.24	3.17	3.20	0.07
84	NPR-8	3.15	3.30	3.25	3.21	3.13	3.21	0.07

Table E-5: Load Sample Thickness Measurements Dry as Molded for Inner Ring Tested on 1/18/02

		Inner Circle (mm)			Inner Circle Statistics	
#	Sample Name	Point 1	Point 2	Point 3	Average (mm)	STD (mm)
1	NABP-3	3.02	3.08	3.11	3.07	0.05
2	NABP-7	3.05	3.12	3.12	3.10	0.04
3	NABP-8	3.03	3.09	3.09	3.07	0.03
4	NABPR-3	3.15	3.04	3.08	3.09	0.06
5	NABPR-7	3.06	3.16	3.10	3.11	0.05
6	NABPR-8	3.08	3.19	3.13	3.13	0.06
7	NACP-3	3.05	3.12	3.13	3.10	0.04
8	NACP-7	3.04	3.09	3.06	3.06	0.03
9	NACP-8	3.07	3.15	3.15	3.12	0.05
10	NACPR-3	3.18	3.08	3.24	3.17	0.08
11	NACPR-7	3.09	3.16	3.21	3.15	0.06
12	NACPR-8	3.13	3.11	3.21	3.15	0.05
13	NAP02.5-3	3.05	3.14	3.12	3.10	0.05
14	NAP02.5-7	3.07	3.15	3.20	3.14	0.07
15	NAP02.5-8	3.13	3.26	3.22	3.20	0.07
16	NAP04-3	3.05	3.18	3.15	3.13	0.07
17	NAP04-7	3.07	3.13	3.17	3.12	0.05
18	NAP04-8	3.04	3.12	3.15	3.10	0.06
19	NAP05-3	3.04	3.17	3.10	3.10	0.07
20	NAP05-7	3.06	3.18	3.15	3.13	0.06

Table E-5: Load Sample Thickness Measurements Dry as Molded for Inner Ring Tested on 1/18/02 (continued)

		Inner Circle (mm)			Inner Circle Statistics	
#	Sample Name	Point 1	Point 2	Point 3	Average (mm)	STD (mm)
21	NAP05-8	3.05	3.16	3.13	3.11	0.06
22	NAPR05-3	3.05	3.13	3.14	3.11	0.05
23	NAPR05-7	3.05	3.14	3.15	3.11	0.06
24	NAPR05-8	3.06	3.15	3.13	3.11	0.05
25	NAP06-3	3.03	3.09	3.11	3.08	0.04
26	NAP06-7	3.03	3.09	3.10	3.07	0.04
27	NAP06-8	3.04	3.11	3.11	3.09	0.04
28	NAP07.5-3	3.05	3.08	3.10	3.08	0.03
29	NAP07.5-7	3.12	3.08	3.09	3.10	0.02
30	NAP07.5-8	3.07	3.05	3.11	3.08	0.03
31	NAP10-3	3.05	3.12	3.07	3.08	0.04
32	NAP10-7	3.10	3.08	3.05	3.08	0.03
33	NAP10-8	3.15	3.04	3.09	3.09	0.06
34	NBCP-3	3.25	3.31	3.36	3.31	0.06
35	NBCP-7	3.23	3.30	3.31	3.28	0.04
36	NBCP-8	3.18	3.24	3.27	3.23	0.05
37	NBCPR-3	3.23	3.18	3.25	3.22	0.04
38	NBCPR-7	3.18	3.28	3.24	3.23	0.05
39	NBCPR-8	3.31	3.30	3.31	3.31	0.01
40	NBP10-3	3.06	3.16	3.12	3.11	0.05

Table E-5: Load Sample Thickness Measurements Dry as Molded for Inner Ring Tested on 1/18/02 (continued)

		Inner Circle (mm)			Inner Circle Statistics	
#	Sample Name	Point 1	Point 2	Point 3	Average (mm)	STD (mm)
41	NBP10-7	3.08	3.18	3.15	3.14	0.05
42	NBP10-8	3.06	3.14	3.15	3.12	0.05
43	NBP15-3	3.08	3.11	3.14	3.11	0.03
44	NBP15-7	3.09	3.11	3.17	3.12	0.04
45	NBP15-8	3.07	3.15	3.18	3.13	0.06
46	NBP20-3	3.07	3.12	3.09	3.09	0.03
47	NBP20-7	3.11	3.16	3.20	3.16	0.05
48	NBP20-8	3.26	3.09	3.11	3.15	0.09
49	NBP30-3	3.13	3.21	3.20	3.18	0.04
50	NBP30-7	3.14	3.26	3.22	3.21	0.06
51	NBP30-8	3.12	3.19	3.15	3.15	0.04
52	NBPR30-3	3.12	3.27	3.20	3.20	0.08
53	NBPR30-7	3.12	3.26	3.22	3.20	0.07
54	NBPR30-8	3.14	3.26	3.24	3.21	0.06
55	NBP40-3	3.11	3.18	3.20	3.16	0.05
56	NBP40-7	3.14	3.19	3.22	3.18	0.04
57	NBP40-8	3.10	3.18	3.23	3.17	0.07
58	NCP05-3	3.17	3.25	3.29	3.24	0.06
59	NCP05-7	3.27	3.17	3.21	3.22	0.05
60	NCP05-8	3.21	3.09	3.15	3.15	0.06

Table E-5: Load Sample Thickness Measurements Dry as Molded for Inner Ring Tested on 1/18/02 (continued)

		Inner Circle (mm)			Inner Circle Statistics	
#	Sample Name	Point 1	Point 2	Point 3	Average (mm)	STD (mm)
61	NCP10-3	3.14	3.14	3.17	3.15	0.02
62	NCP10-7	3.14	3.27	3.17	3.19	0.07
63	NCP10-8	3.17	3.21	3.19	3.19	0.02
64	NCP15-3	3.11	3.22	3.16	3.16	0.06
65	NCP15-7	3.18	3.29	3.17	3.21	0.07
66	NCP15-8	3.17	3.27	3.16	3.20	0.06
67	NCP20-3	3.04	3.18	3.14	3.12	0.07
68	NCP20-7	3.05	3.18	3.12	3.12	0.07
69	NCP20-8	3.05	3.08	3.07	3.07	0.02
70	NCPR20-3	3.10	3.09	3.16	3.12	0.04
71	NCPR20-7	3.19	3.17	3.07	3.14	0.06
72	NCPR20-8	3.09	3.10	3.11	3.10	0.01
73	NCP30-3	3.04	3.13	3.13	3.10	0.05
74	NCP30-7	3.04	3.13	3.12	3.10	0.05
75	NCP30-8	3.02	3.10	3.12	3.08	0.05
76	NCP40-3	3.09	3.04	3.08	3.07	0.03
77	NCP40-7	3.09	3.17	3.17	3.14	0.05
78	NCP40-8	3.08	3.19	3.14	3.14	0.06
79	NP-3	3.12	3.19	3.14	3.15	0.04
80	NP-7	3.11	3.16	3.16	3.14	0.03

Table E-5: Load Sample Thickness Measurements Dry as Molded for Inner Ring Tested on 1/18/02 (continued)

		Inner Circle (mm)			Inner Circle Statistics	
#	Sample Name	Point 1	Point 2	Point 3	Average (mm)	STD (mm)
81	NP-8	3.10	3.19	3.10	3.13	0.05
82	NPR-3	3.09	3.16	3.15	3.13	0.04
83	NPR-7	3.10	3.15	3.17	3.14	0.04
84	NPR-8	3.14	3.16	3.19	3.16	0.03

Table E-6: Load Sample Thickness Measurements Comparison

		Comparison of Outer Ring vs. Inner Circle (mm)			Error Difference (%)	
#	Sample Name	Average Outer (mm)	Average Inner (mm)	Outer - Inner (mm)	% Error (Outer)	% Error (Inner)
1	NABP-3	3.13	3.07	0.06	1.98	2.02
2	NABP-7	3.15	3.10	0.06	1.76	1.79
3	NABP-8	3.17	3.07	0.10	3.09	3.19
4	NABPR-3	3.16	3.09	0.07	2.28	2.33
5	NABPR-7	3.20	3.11	0.09	2.80	2.88
6	NABPR-8	3.19	3.13	0.05	1.65	1.68
7	NACP-3	3.20	3.10	0.10	3.13	3.23
8	NACP-7	3.17	3.06	0.10	3.24	3.35
9	NACP-8	3.19	3.12	0.07	2.15	2.20
10	NACPR-3	3.21	3.17	0.05	1.41	1.43
11	NACPR-7	3.25	3.15	0.10	3.09	3.19
12	NACPR-8	3.25	3.15	0.10	3.20	3.30
13	NAP02.5-3	3.21	3.10	0.10	3.20	3.31
14	NAP02.5-7	3.21	3.14	0.07	2.18	2.23
15	NAP02.5-8	3.29	3.20	0.08	2.52	2.58
16	NAP04-3	3.19	3.13	0.06	1.99	2.03
17	NAP04-7	3.22	3.12	0.09	2.94	3.03
18	NAP04-8	3.20	3.10	0.10	3.02	3.11
19	NAP05-3	3.19	3.10	0.09	2.72	2.79
20	NAP05-7	3.20	3.13	0.07	2.19	2.24

Table E-6: Load Sample Thickness Measurements Comparison (continued)

		Comparison of Outer Ring vs. Inner Circle (mm)			Error Difference (%)	
#	Sample Name	Average Outer (mm)	Average Inner (mm)	Outer - Inner (mm)	% Error (Outer)	% Error (Inner)
21	NAP05-8	3.19	3.11	0.08	2.40	2.46
22	NAPR05-3	3.18	3.11	0.07	2.18	2.23
23	NAPR05-7	3.21	3.11	0.09	2.89	2.98
24	NAPR05-8	3.21	3.11	0.10	3.01	3.10
25	NAP06-3	3.16	3.08	0.09	2.76	2.84
26	NAP06-7	3.17	3.07	0.09	2.93	3.02
27	NAP06-8	3.18	3.09	0.09	2.81	2.89
28	NAP07.5-3	3.25	3.08	0.18	5.39	5.70
29	NAP07.5-7	3.21	3.10	0.11	3.53	3.66
30	NAP07.5-8	3.18	3.08	0.10	3.19	3.29
31	NAP10-3	3.32	3.08	0.24	7.23	7.79
32	NAP10-7	3.18	3.08	0.10	3.19	3.29
33	NAP10-8	3.20	3.09	0.10	3.21	3.32
34	NBCP-3	3.35	3.31	0.05	1.35	1.37
35	NBCP-7	3.33	3.28	0.05	1.62	1.65
36	NBCP-8	3.31	3.23	0.08	2.36	2.41
37	NBCPR-3	3.21	3.22	-0.01	-0.25	-0.25
38	NBCPR-7	3.26	3.23	0.03	0.82	0.82
39	NBCPR-8	3.29	3.31	-0.01	-0.45	-0.44
40	NBP10-3	3.18	3.11	0.06	2.03	2.08

Table E-6: Load Sample Thickness Measurements Comparison (continued)

		Comparison of Outer Ring vs. Inner Circle (mm)			Error Difference (%)	
#	Sample Name	Average Outer (mm)	Average Inner (mm)	Outer - Inner (mm)	% Error (Outer)	% Error (Inner)
41	NBP10-7	3.18	3.14	0.04	1.30	1.32
42	NBP10-8	3.18	3.12	0.06	1.93	1.97
43	NBP15-3	3.18	3.11	0.07	2.20	2.25
44	NBP15-7	3.19	3.12	0.06	2.03	2.07
45	NBP15-8	3.21	3.13	0.08	2.39	2.45
46	NBP20-3	3.13	3.09	0.04	1.30	1.31
47	NBP20-7	3.19	3.16	0.03	1.04	1.06
48	NBP20-8	3.13	3.15	-0.03	-0.87	-0.87
49	NBP30-3	3.22	3.18	0.04	1.18	1.19
50	NBP30-7	3.25	3.21	0.05	1.39	1.41
51	NBP30-8	3.20	3.15	0.05	1.46	1.48
52	NBPR30-3	3.23	3.20	0.04	1.09	1.11
53	NBPR30-7	3.20	3.20	0.00	0.06	0.06
54	NBPR30-8	3.26	3.21	0.04	1.31	1.33
55	NBP40-3	3.24	3.16	0.08	2.43	2.49
56	NBP40-7	3.24	3.18	0.05	1.69	1.72
57	NBP40-8	3.21	3.17	0.04	1.18	1.20
58	NCP05-3	3.38	3.24	0.14	4.13	4.30
59	NCP05-7	3.30	3.22	0.08	2.41	2.47
60	NCP05-8	3.20	3.15	0.05	1.56	1.59

Table E -6: Load Sample Thickness Measurements Comparison (continued)

		Comparison of Outer Ring vs. Inner Circle (mm)			Error Difference (%)	
#	Sample Name	Average Outer (mm)	Average Inner (mm)	Outer - Inner (mm)	% Error (Outer)	% Error (Inner)
61	NCP10-3	3.15	3.15	0.00	0.06	0.06
62	NCP10-7	3.27	3.19	0.08	2.40	2.46
63	NCP10-8	3.27	3.19	0.08	2.45	2.51
64	NCP15-3	3.27	3.16	0.11	3.26	3.37
65	NCP15-7	3.31	3.21	0.09	2.86	2.95
66	NCP15-8	3.33	3.20	0.13	3.90	4.06
67	NCP20-3	3.19	3.12	0.07	2.26	2.31
68	NCP20-7	3.18	3.12	0.06	1.93	1.97
69	NCP20-8	3.15	3.07	0.08	2.52	2.59
70	NCPR20-3	3.23	3.12	0.12	3.57	3.70
71	NCPR20-7	3.19	3.14	0.05	1.59	1.61
72	NCPR20-8	3.18	3.10	0.08	2.58	2.65
73	NCP30-3	3.16	3.10	0.06	1.84	1.87
74	NCP30-7	3.16	3.10	0.07	2.13	2.17
75	NCP30-8	3.16	3.08	0.08	2.41	2.47
76	NCP40-3	3.13	3.07	0.06	1.92	1.95
77	NCP40-7	3.21	3.14	0.06	2.02	2.06
78	NCP40-8	3.20	3.14	0.06	1.86	1.89
79	NP-3	3.20	3.15	0.05	1.69	1.71
80	NP-7	3.20	3.14	0.05	1.65	1.68

Table E-6: Load Sample Thickness Measurements Comparison (continued)

		Comparison of Outer Ring vs. Inner Circle (mm)			Error Difference (%)	
#	Sample Name	Average Outer (mm)	Average Inner (mm)	Outer - Inner (mm)	% Error (Outer)	% Error (Inner)
81	NP-8	3.20	3.13	0.07	2.07	2.11
82	NPR-3	3.19	3.13	0.05	1.71	1.74
83	NPR-7	3.20	3.14	0.06	1.88	1.91
84	NPR-8	3.21	3.16	0.04	1.39	1.41

Table E-7: Load Sample Thickness Measurements Dry as Molded for Outer Ring Tested on 1/21/02

		Outer Ring Measurements (mm)					Outer Ring Statistics	
#	Sample Name	Point 1	Point 2	Point 3	Point 4	Point 5	Average (mm)	STD (mm)
1	NABCN-3	3.16	3.16	3.18	3.10	3.08	3.14	0.04
2	NABCN-7	3.08	3.08	3.10	3.05	3.07	3.08	0.02
3	NABCN-8	3.20	3.20	3.12	3.07	3.08	3.13	0.06
4	NABCNR-3	3.26	3.35	3.22	3.17	3.20	3.24	0.07
5	NABCNR-7	3.27	3.07	3.21	3.18	3.32	3.21	0.10
6	NABCNR-8	3.20	3.13	3.23	3.35	3.30	3.24	0.09
7	NABN-3	3.19	3.12	3.11	3.04	3.08	3.11	0.06
8	NABN-7	3.05	3.05	3.07	3.14	3.17	3.10	0.06
9	NABN-8	3.10	3.05	3.08	3.11	3.17	3.10	0.04
10	NABNR-3	3.12	3.12	3.09	3.12	3.08	3.11	0.02
11	NABNR-7	3.00	3.00	3.17	3.14	3.04	3.07	0.08
12	NABNR-8	3.13	3.13	3.03	3.03	3.00	3.06	0.06
13	NACN-5	3.07	3.11	3.26	3.19	3.06	3.14	0.09
14	NACN-7	3.10	3.16	3.23	3.19	3.09	3.15	0.06
15	NACN-8	3.23	3.11	3.11	3.07	3.21	3.15	0.07
16	NACNR-3	3.00	3.07	3.12	3.02	3.01	3.04	0.05
17	NACNR-7	3.03	3.10	3.14	3.14	3.03	3.09	0.06
18	NACNR-8	3.17	3.12	3.08	3.15	3.14	3.13	0.03
19	NAN02.5-3	3.14	3.17	3.19	3.05	3.03	3.12	0.07
20	NAN02.5-7	3.04	3.04	3.07	3.27	3.21	3.13	0.11

Table E-7: Load Sample Thickness Measurements Dry as Molded for Outer Ring Tested on 1/21/02 (continued)

		Outer Ring Measurements (mm)					Outer Ring Statistics	
#	Sample Name	Point 1	Point 2	Point 3	Point 4	Point 5	Average (mm)	STD (mm)
21	NAN02.5-8	3.04	3.00	3.04	3.09	3.14	3.06	0.05
22	NAN04-5	3.21	3.12	3.05	3.15	3.27	3.16	0.08
23	NAN04-7	3.09	3.00	2.98	3.13	3.21	3.08	0.09
24	NAN04-8	3.11	3.09	3.01	3.17	3.24	3.12	0.09
25	NANR05-3	3.20	3.19	3.09	3.14	3.22	3.17	0.05
26	NANR05-7	3.08	3.03	3.00	3.13	3.13	3.07	0.06
27	NANR05-8	3.20	3.15	3.11	3.06	3.12	3.13	0.05
28	NANRR05-3	3.28	3.23	3.21	3.14	3.11	3.19	0.07
29	NANRR05-7	3.14	3.21	3.22	3.28	3.15	3.20	0.06
30	NANRR05-8	3.26	3.24	3.18	3.03	3.19	3.18	0.09
31	NAN06-3	3.10	3.17	3.19	3.24	3.15	3.17	0.05
32	NAN06-7	3.12	3.23	3.26	3.25	3.04	3.18	0.10
33	NAN06-8	3.19	3.11	3.10	3.10	3.19	3.14	0.05
34	NAN07.5-3	3.20	3.16	3.17	3.12	3.11	3.15	0.04
35	NAN07.5-7	3.08	3.11	3.19	3.20	3.16	3.15	0.05
36	NAN07.5-8	3.17	3.11	3.07	3.03	3.05	3.09	0.06
37	NAN10-3	3.09	3.03	3.03	3.05	3.11	3.06	0.04
38	NAN10-7	3.00	3.04	3.04	3.14	3.04	3.05	0.05
39	NAN10-8	3.08	3.04	3.04	2.99	3.12	3.05	0.05
40	NBCN-3	3.22	3.23	3.37	3.30	3.21	3.27	0.07

Table E-7: Load Sample Thickness Measurements Dry as Molded for Outer Ring Tested on 1/21/02 (continued)

		Outer Ring Measurements (mm)					Outer Ring Statistics	
#	Sample Name	Point 1	Point 2	Point 3	Point 4	Point 5	Average (mm)	STD (mm)
41	NBCN-7	3.04	3.12	3.23	3.26	3.09	3.15	0.09
42	NBCN-8	3.13	3.15	3.19	3.21	3.17	3.17	0.03
43	NBCNR-3	3.40	3.27	3.28	3.38	3.43	3.35	0.07
44	NBCNR-7	3.30	3.29	3.35	3.45	3.55	3.39	0.11
45	NBCNR-8	3.31	3.41	3.35	3.25	3.31	3.33	0.06
46	NBN10-3	3.29	3.15	3.12	3.24	3.36	3.23	0.10
47	NBN10-7	3.20	3.29	3.32	3.32	3.12	3.25	0.09
48	NBN10-8	3.41	3.26	3.24	3.34	3.45	3.34	0.09
49	NBN15-3	3.23	3.15	3.13	3.28	3.33	3.22	0.08
50	NBN15-7	3.21	3.15	3.14	3.34	3.29	3.23	0.09
51	NBN15-8	3.36	3.25	3.19	3.34	3.42	3.31	0.09
52	NBN20-3	3.03	2.98	2.99	3.02	3.08	3.02	0.04
53	NBN20-7	3.07	3.05	3.24	3.13	3.21	3.14	0.08
54	NBN20-8	3.29	3.23	3.19	3.10	3.12	3.19	0.08
55	NBN30-3	3.04	3.22	3.27	3.21	3.23	3.19	0.09
56	NBN30-7	3.23	3.33	3.40	3.45	3.30	3.34	0.09
57	NBN30-8	3.30	3.22	3.17	3.37	3.44	3.30	0.11
58	NBNR30-3	3.23	3.35	3.48	3.45	3.30	3.36	0.10
59	NBNR30-7	3.23	3.39	3.44	3.35	3.21	3.32	0.10
60	NBNR30-8	3.16	3.10	3.13	3.19	3.17	3.15	0.04

Table E-7: Load Sample Thickness Measurements Dry as Molded for Outer Ring Tested on 1/21/02 (continued)

		Outer Ring Measurements (mm)					Outer Ring Statistics	
#	Sample Name	Point 1	Point 2	Point 3	Point 4	Point 5	Average (mm)	STD (mm)
61	NBN40-3	2.87	2.96	3.04	3.05	3.07	3.00	0.08
62	NBN40-7	3.05	3.00	3.06	3.04	3.07	3.04	0.03
63	NBN40-8	3.11	3.08	2.99	3.11	3.09	3.08	0.05
64	NCN05-3	3.21	3.21	3.15	3.20	3.32	3.22	0.06
65	NCN05-7	3.20	3.20	3.10	3.23	3.33	3.21	0.08
66	NCN05-8	3.15	3.15	3.20	3.29	3.23	3.20	0.06
67	NCN10-3	3.18	3.20	3.21	3.03	2.98	3.12	0.11
68	NCN10-7	3.00	3.22	3.27	3.15	3.16	3.16	0.10
69	NCN10-8	3.23	3.29	3.06	3.26	3.12	3.19	0.10
70	NCN15-3	2.97	3.06	3.11	3.02	3.10	3.05	0.06
71	NCN15-7	3.03	3.04	3.16	3.11	3.11	3.09	0.05
72	NCN15-8	3.04	3.07	3.14	3.09	3.08	3.08	0.04
73	NCN20-3	3.15	3.18	3.14	3.10	3.01	3.12	0.07
74	NCN20-7	2.94	2.94	2.93	3.01	3.02	2.97	0.04
75	NCN20-8	2.93	2.92	3.04	3.01	3.00	2.98	0.05
76	NCN30-3	3.24	3.13	3.11	3.29	3.31	3.22	0.09
77	NCN30-7	3.31	3.35	3.26	3.14	3.16	3.24	0.09
78	NCN30-8	3.20	3.07	3.06	3.24	3.25	3.16	0.09
79	NCN40-5	3.23	3.23	2.99	3.13	3.25	3.17	0.11
80	NCN40-7	3.24	3.12	3.09	3.12	3.15	3.14	0.06

Table E-7: Load Sample Thickness Measurements Dry as Molded for Outer Ring Tested on 1/21/02 (continued)

		Outer Ring Measurements (mm)					Outer Ring Statistics	
#	Sample Name	Point 1	Point 2	Point 3	Point 4	Point 5	Average (mm)	STD (mm)
81	NCN40-8	3.28	3.15	3.16	3.28	3.35	3.24	0.09
82	NCNR20-3	3.07	3.13	3.19	3.05	3.06	3.10	0.06
83	NCNR20-7	3.11	3.08	3.12	3.18	3.17	3.13	0.04
84	NCNR20-8	3.17	3.13	3.08	3.21	3.22	3.16	0.06
85	NN-3	3.18	3.21	3.18	3.16	3.19	3.18	0.02
86	NN-7	3.31	3.05	3.15	3.15	3.23	3.18	0.10
87	NN-8	3.26	3.04	3.14	3.17	3.23	3.17	0.09
88	NNR-3	3.07	2.91	3.05	3.11	3.20	3.07	0.11
89	NNR-7	3.23	3.02	3.14	3.29	3.41	3.22	0.15
90	NNR-8	3.06	3.12	3.07	3.24	3.13	3.12	0.07

Table E-8: Load Sample Thickness Measurements Dry as Molded for Inner Ring Tested on 1/21/02

		Inner Circle (mm)			Inner Circle Statistics	
#	Sample Name	Point 1	Point 2	Point 3	Average (mm)	STD (mm)
1	NABCN-3	3.08	3.17	3.18	3.14	0.06
2	NABCN-7	3.09	3.13	3.08	3.10	0.03
3	NABCN-8	3.11	3.14	3.04	3.10	0.05
4	NABCNR-3	3.20	3.14	3.20	3.18	0.03
5	NABCNR-7	3.28	3.17	3.20	3.22	0.06
6	NABCNR-8	3.18	3.17	3.29	3.21	0.07
7	NABN-3	3.12	3.29	3.19	3.20	0.09
8	NABN-7	3.18	3.15	3.14	3.16	0.02
9	NABN-8	3.17	3.10	3.11	3.13	0.04
10	NABNR-3	3.10	3.16	3.09	3.12	0.04
11	NABNR-7	3.03	3.13	3.21	3.12	0.09
12	NABNR-8	3.13	3.12	3.06	3.10	0.04
13	NACN-5	3.04	3.08	3.34	3.15	0.16
14	NACN-7	3.11	3.07	3.14	3.11	0.04
15	NACN-8	3.15	3.06	3.09	3.10	0.05
16	NACNR-3	3.06	3.08	3.21	3.12	0.08
17	NACNR-7	3.16	3.20	3.05	3.14	0.08
18	NACNR-8	3.14	3.09	3.16	3.13	0.04
19	NAN02.5-3	3.08	3.05	3.04	3.06	0.02
20	NAN02.5-7	3.14	3.05	3.33	3.17	0.14

Table E-8: Load Sample Thickness Measurements Dry as Molded for Inner Ring Tested on 1/21/02

		Inner Circle (mm)			Inner Circle Statistics	
#	Sample Name	Point 1	Point 2	Point 3	Average (mm)	STD (mm)
21	NAN02.5-8	3.10	3.06	3.18	3.11	0.06
22	NAN04-5	3.20	3.18	3.06	3.15	0.08
23	NAN04-7	3.20	3.17	3.24	3.20	0.04
24	NAN04-8	3.14	3.21	3.14	3.16	0.04
25	NANR05-3	3.23	3.15	3.22	3.20	0.04
26	NANR05-7	3.07	3.09	3.15	3.10	0.04
27	NANR05-8	3.17	3.10	3.15	3.14	0.04
28	NANRR05-3	3.22	3.14	3.17	3.18	0.04
29	NANRR05-7	3.24	3.14	3.17	3.18	0.05
30	NANRR05-8	3.18	3.16	3.33	3.22	0.09
31	NAN06-3	3.27	3.21	3.19	3.22	0.04
32	NAN06-7	3.21	3.17	3.19	3.19	0.02
33	NAN06-8	3.21	3.12	3.20	3.18	0.05
34	NAN07.5-3	3.15	3.32	3.16	3.21	0.10
35	NAN07.5-7	3.20	3.16	3.19	3.18	0.02
36	NAN07.5-8	3.16	3.13	3.16	3.15	0.02
37	NAN10-3	3.12	3.13	3.12	3.12	0.01
38	NAN10-7	3.12	3.09	3.11	3.11	0.02
39	NAN10-8	3.14	3.09	3.15	3.13	0.03
40	NBCN-3	3.20	3.23	3.32	3.25	0.06

Table E-8: Load Sample Thickness Measurements Dry as Molded for Inner Ring Tested on 1/21/02 (continued)

		Inner Circle (mm)			Inner Circle Statistics	
#	Sample Name	Point 1	Point 2	Point 3	Average (mm)	STD (mm)
41	NBCN-7	3.25	3.32	3.25	3.27	0.04
42	NBCN-8	3.15	3.20	3.26	3.20	0.06
43	NBCNR-3	3.30	3.30	3.35	3.32	0.03
44	NBCNR-7	3.45	3.31	3.33	3.36	0.08
45	NBCNR-8	3.24	3.36	3.26	3.29	0.06
46	NBN10-3	3.29	3.08	3.11	3.16	0.11
47	NBN10-7	3.12	3.16	3.39	3.22	0.15
48	NBN10-8	3.50	3.28	3.17	3.32	0.17
49	NBN15-3	3.19	3.08	3.20	3.16	0.07
50	NBN15-7	3.20	3.07	3.22	3.16	0.08
51	NBN15-8	3.30	3.14	3.25	3.23	0.08
52	NBN20-3	3.06	2.97	2.99	3.01	0.05
53	NBN20-7	3.17	2.99	3.16	3.11	0.10
54	NBN20-8	3.14	3.20	3.16	3.17	0.03
55	NBN30-3	3.14	3.16	3.29	3.20	0.08
56	NBN30-7	3.30	3.30	3.40	3.33	0.06
57	NBN30-8	3.34	3.30	3.22	3.29	0.06
58	NBNR30-3	3.38	3.20	3.25	3.28	0.09
59	NBNR30-7	3.28	3.25	3.22	3.25	0.03
60	NBNR30-8	3.08	3.08	3.16	3.11	0.05

Table E-8: Load Sample Thickness Measurements Dry as Molded for Inner Ring Tested on 1/21/02 (continued)

		Inner Circle (mm)			Inner Circle Statistics	
#	Sample Name	Point 1	Point 2	Point 3	Average (mm)	STD (mm)
61	NBN40-3	3.10	3.04	3.10	3.08	0.03
62	NBN40-7	3.10	3.07	3.08	3.08	0.02
63	NBN40-8	3.15	3.17	3.10	3.14	0.04
64	NCN05-3	3.18	3.16	3.24	3.19	0.04
65	NCN05-7	3.26	3.08	3.26	3.20	0.10
66	NCN05-8	3.24	3.10	3.26	3.20	0.09
67	NCN10-3	3.01	2.95	3.09	3.02	0.07
68	NCN10-7	3.02	3.12	3.07	3.07	0.05
69	NCN10-8	3.09	3.02	3.11	3.07	0.05
70	NCN15-3	3.01	2.97	3.01	3.00	0.02
71	NCN15-7	3.07	3.11	3.04	3.07	0.04
72	NCN15-8	3.07	2.97	3.05	3.03	0.05
73	NCN20-3	2.95	3.08	2.87	2.97	0.11
74	NCN20-7	3.01	2.94	2.96	2.97	0.04
75	NCN20-8	2.96	2.92	2.76	2.88	0.11
76	NCN30-3	3.18	3.07	3.17	3.14	0.06
77	NCN30-7	3.12	3.29	3.20	3.20	0.09
78	NCN30-8	3.14	3.14	3.00	3.09	0.08
79	NCN40-5	3.17	3.18	3.02	3.12	0.09
80	NCN40-7	3.14	3.03	3.21	3.13	0.09

Table E-8: Load Sample Thickness Measurements Dry as Molded for Inner Ring Tested on 1/21/02 (continued)

		Inner Circle (mm)			Inner Circle Statistics	
#	Sample Name	Point 1	Point 2	Point 3	Average (mm)	STD (mm)
81	NCN40-8	3.28	3.13	3.23	3.21	0.08
82	NCNR20-3	3.09	3.10	3.16	3.12	0.04
83	NCNR20-7	3.14	3.07	3.24	3.15	0.09
84	NCNR20-8	3.08	3.11	3.08	3.09	0.02
85	NN-3	3.19	3.16	3.23	3.19	0.04
86	NN-7	3.26	3.20	3.24	3.23	0.03
87	NN-8	3.26	3.18	3.24	3.23	0.04
88	NNR-3	3.27	3.15	3.17	3.20	0.06
89	NNR-7	3.24	3.21	3.22	3.22	0.02
90	NNR-8	3.17	3.16	3.19	3.17	0.02

Table E-9: Load Sample Thickness Comparison

		Comparison of Outer Ring vs. Inner Circle (mm)			Error Difference (%)	
#	Sample Name	Average Outer (mm)	Average Inner (mm)	Outer - Inner (mm)	% Error (Outer)	% Error (Inner)
1	NABCN-3	3.14	3.14	-0.01	-0.23	-0.23
2	NABCN-7	3.08	3.10	-0.02	-0.78	-0.77
3	NABCN-8	3.13	3.10	0.04	1.19	1.21
4	NABCNR-3	3.24	3.18	0.06	1.85	1.89
5	NABCNR-7	3.21	3.22	-0.01	-0.21	-0.21
6	NABCNR-8	3.24	3.21	0.03	0.88	0.89
7	NABN-3	3.11	3.20	-0.09	-2.96	-2.87
8	NABN-7	3.10	3.16	-0.06	-1.96	-1.92
9	NABN-8	3.10	3.13	-0.02	-0.80	-0.79
10	NABNR-3	3.11	3.12	-0.01	-0.34	-0.34
11	NABNR-7	3.07	3.12	-0.05	-1.74	-1.71
12	NABNR-8	3.06	3.10	-0.04	-1.28	-1.27
13	NACN-5	3.14	3.15	-0.02	-0.49	-0.49
14	NACN-7	3.15	3.11	0.05	1.50	1.52
15	NACN-8	3.15	3.10	0.05	1.46	1.48
16	NACNR-3	3.04	3.12	-0.07	-2.39	-2.33
17	NACNR-7	3.09	3.14	-0.05	-1.58	-1.55
18	NACNR-8	3.13	3.13	0.00	0.06	0.06
19	NAN02.5-3	3.12	3.06	0.06	1.90	1.94
20	NAN02.5-7	3.13	3.17	-0.05	-1.51	-1.49

Table E-9: Load Sample Thickness Measurements Dry as Molded Comparison (continued)

		Comparison of Outer Ring vs. Inner Circle (mm)			Error Difference (%)	
#	Sample Name	Average Outer (mm)	Average Inner (mm)	Outer - Inner (mm)	% Error (Outer)	% Error (Inner)
21	NAN02.5-8	3.06	3.11	-0.05	-1.68	-1.65
22	NAN04-5	3.16	3.15	0.01	0.42	0.42
23	NAN04-7	3.08	3.20	-0.12	-3.94	-3.79
24	NAN04-8	3.12	3.16	-0.04	-1.26	-1.24
25	NANR05-3	3.17	3.20	-0.03	-1.01	-1.00
26	NANR05-7	3.07	3.10	-0.03	-0.95	-0.95
27	NANR05-8	3.13	3.14	-0.01	-0.38	-0.38
28	NANRR05-3	3.19	3.18	0.02	0.54	0.55
29	NANRR05-7	3.20	3.18	0.02	0.52	0.52
30	NANRR05-8	3.18	3.22	-0.04	-1.36	-1.34
31	NAN06-3	3.17	3.22	-0.05	-1.68	-1.65
32	NAN06-7	3.18	3.19	-0.01	-0.31	-0.31
33	NAN06-8	3.14	3.18	-0.04	-1.23	-1.22
34	NAN07.5-3	3.15	3.21	-0.06	-1.84	-1.81
35	NAN07.5-7	3.15	3.18	-0.04	-1.12	-1.11
36	NAN07.5-8	3.09	3.15	-0.06	-2.07	-2.03
37	NAN10-3	3.06	3.12	-0.06	-2.00	-1.96
38	NAN10-7	3.05	3.11	-0.05	-1.79	-1.76
39	NAN10-8	3.05	3.13	-0.07	-2.38	-2.32
40	NBCN-3	3.27	3.25	0.02	0.49	0.49

Table E-9: Load Sample Thickness Measurements Dry as Molded Comparison

		Comparison of Outer Ring vs. Inner Circle (mm)			Error Difference (%)	
#	Sample Name	Average Outer (mm)	Average Inner (mm)	Outer - Inner (mm)	% Error (Outer)	% Error (Inner)
41	NBCN-7	3.15	3.27	-0.13	-3.98	-3.83
42	NBCN-8	3.17	3.20	-0.03	-1.05	-1.04
43	NBCNR-3	3.35	3.32	0.04	1.05	1.07
44	NBCNR-7	3.39	3.36	0.02	0.73	0.73
45	NBCNR-8	3.33	3.29	0.04	1.18	1.20
46	NBN10-3	3.23	3.16	0.07	2.23	2.28
47	NBN10-7	3.25	3.22	0.03	0.82	0.83
48	NBN10-8	3.34	3.32	0.02	0.70	0.70
49	NBN15-3	3.22	3.16	0.07	2.09	2.13
50	NBN15-7	3.23	3.16	0.06	1.94	1.98
51	NBN15-8	3.31	3.23	0.08	2.48	2.54
52	NBN20-3	3.02	3.01	0.01	0.44	0.44
53	NBN20-7	3.14	3.11	0.03	1.06	1.07
54	NBN20-8	3.19	3.17	0.02	0.61	0.61
55	NBN30-3	3.19	3.20	0.00	-0.08	-0.08
56	NBN30-7	3.34	3.33	0.01	0.26	0.26
57	NBN30-8	3.30	3.29	0.01	0.40	0.41
58	NBNR30-3	3.36	3.28	0.09	2.54	2.60
59	NBNR30-7	3.32	3.25	0.07	2.23	2.28
60	NBNR30-8	3.15	3.11	0.04	1.38	1.39

Table E-9: Load Sample Thickness Measurements Dry as Molded Comparison

		Comparison of Outer Ring vs. Inner Circle (mm)			Error Difference (%)	
#	Sample Name	Average Outer (mm)	Average Inner (mm)	Outer - Inner (mm)	% Error (Outer)	% Error (Inner)
61	NBN40-3	3.00	3.08	-0.08	-2.74	-2.66
62	NBN40-7	3.04	3.08	-0.04	-1.29	-1.28
63	NBN40-8	3.08	3.14	-0.06	-2.08	-2.04
64	NCN05-3	3.18	3.16	3.24	101.89	102.53
65	NCN05-7	3.26	3.08	3.26	100.00	105.84
66	NCN05-8	3.24	3.10	3.26	100.62	105.16
67	NCN10-3	3.12	3.02	0.10	3.31	3.43
68	NCN10-7	3.16	3.07	0.09	2.85	2.93
69	NCN10-8	3.19	3.07	0.12	3.72	3.86
70	NCN15-3	3.05	3.00	0.06	1.81	1.85
71	NCN15-7	3.09	3.07	0.02	0.54	0.54
72	NCN15-8	3.08	3.03	0.05	1.75	1.78
73	NCN20-3	3.12	2.97	0.15	4.79	5.03
74	NCN20-7	2.97	2.97	0.00	-0.07	-0.07
75	NCN20-8	2.98	2.88	0.10	3.36	3.47
76	NCN30-3	3.22	3.14	0.08	2.36	2.42
77	NCN30-7	3.24	3.20	0.04	1.25	1.27
78	NCN30-8	3.16	3.09	0.07	2.23	2.28
79	NCN40-5	3.17	3.12	0.04	1.35	1.37
80	NCN40-7	3.14	3.13	0.02	0.55	0.55

Table E-9: Load Sample Thickness Measurements Dry as Molded Comparison

		Comparison of Outer Ring vs. Inner Circle (mm)			Error Difference (%)	
#	Sample Name	Average Outer (mm)	Average Inner (mm)	Outer - Inner (mm)	% Error (Outer)	% Error (Inner)
81	NCN40-8	3.24	3.21	0.03	0.95	0.95
82	NCNR20-3	3.10	3.12	-0.02	-0.54	-0.53
83	NCNR20-7	3.13	3.15	-0.02	-0.57	-0.57
84	NCNR20-8	3.16	3.09	0.07	2.28	2.33
85	NN-3	3.18	3.19	-0.01	-0.29	-0.29
86	NN-7	3.18	3.23	-0.06	-1.74	-1.71
87	NN-8	3.17	3.23	-0.06	-1.85	-1.82
88	NNR-3	3.07	3.20	-0.13	-4.19	-4.03
89	NNR-7	3.22	3.22	-0.01	-0.17	-0.17
90	NNR-8	3.12	3.17	-0.05	-1.58	-1.55

Table E-10: Overall Thickness Summary and Comparison

		Reference Samples (mm)		Load Samples (mm)		Summary
#	Sample Name	Average Outer (mm)	Average Inner	Average Outer (mm)	Average Inner	Average Difference (mm)
1	NN-5	3.43	3.28	3.18	3.22	0.15
2	NNR-5	3.18	3.11	3.14	3.20	-0.03
3	NAN02.5-5	3.26	3.18	3.10	3.11	0.11
4	NAN04-5(3)	3.22	3.12	3.12	3.17	0.02
5	NANR05-5	3.20	3.12	3.12	3.15	0.03
6	NANRR05-5	3.18	3.09	3.19	3.19	-0.05
7	NAN06-5	3.21	3.12	3.16	3.20	-0.02
8	NAN07.5-5	3.21	3.10	3.13	3.18	0.00
9	NAN10-5	3.16	3.09	3.06	3.12	0.03
10	NBN10-5	3.33	3.21	3.27	3.23	0.02
11	NBN15-5	3.36	3.26	3.25	3.18	0.10
12	NBN20-5	3.34	3.25	3.12	3.09	0.19
13	NBN30-5	3.37	3.26	3.28	3.27	0.04
14	NBNR30-5	3.31	3.22	3.28	3.21	0.02
15	NBN40-5	3.24	3.13	3.04	3.10	0.11
16	NCN05-5	3.37	3.24	3.21	3.20	0.10
17	NCN10-5	3.24	3.03	3.16	3.05	0.03
18	NCN15-5	3.13	2.99	3.08	3.03	0.00
19	NCN20-5	3.13	3.02	3.02	2.94	0.09
20	NCNR20-5	3.32	3.19	3.13	3.12	0.13

Table E-10: Overall Thickness Summary and Comparison (continued)

		Reference Samples (mm)		Load Samples (mm)		Summary
#	Sample Name	Average Outer (mm)	Average Inner	Average Outer (mm)	Average Inner	Average Difference (mm)
21	NCN30-5	3.32	3.23	3.21	3.15	0.10
22	NCN40-5(3)	3.26	3.15	3.18	3.15	0.04
23	NABN-5	3.20	3.09	3.10	3.16	0.02
24	NABNR-5	3.23	3.13	3.08	3.11	0.09
25	NACN-5(3)	3.19	3.10	3.15	3.12	0.01
26	NACNR-5	3.24	3.12	3.09	3.13	0.07
27	NBCN-5	3.18	3.09	3.19	3.24	-0.08
28	NBCNR-5	3.49	3.37	3.36	3.32	0.09
29	NABCN-5	3.23	3.15	3.12	3.11	0.07
30	NABCNR-5	3.30	3.21	3.23	3.20	0.04
31	NP-5	3.22	3.20	3.20	3.14	0.04
32	NPR-5	3.22	3.18	3.20	3.15	0.03
33	NAP02.5-5	3.25	3.15	3.23	3.15	0.01
34	NAP04-5	3.23	3.12	3.20	3.12	0.01
35	NAP05-5	3.32	3.14	3.19	3.12	0.07
36	NAPR05-5	3.24	3.13	3.20	3.11	0.03
37	NAP06-5	3.21	3.10	3.17	3.08	0.03
38	NAP07.5-5	3.19	3.09	3.21	3.08	-0.01
39	NAP10-5	3.19	3.06	3.23	3.08	-0.03
40	NBP10-5	3.26	3.14	3.18	3.12	0.05

Table E-10: Overall Thickness Summary and Comparison (continued)

		Reference Samples (mm)		Load Samples (mm)		Summary
#	Sample Name	Average Outer (mm)	Average Inner	Average Outer (mm)	Average Inner	Average Difference (mm)
41	NBP15-5	3.25	3.16	3.19	3.12	0.04
42	NBP20-5	3.17	3.13	3.15	3.13	0.01
43	NBP30-5	3.22	3.14	3.22	3.18	-0.02
44	NBPR30-5	3.26	3.17	3.23	3.20	0.00
45	NBP40-5	3.24	3.17	3.23	3.17	0.00
46	NCP05-5	3.53	3.27	3.29	3.20	0.16
47	NCP10-5	3.36	3.18	3.23	3.18	0.06
48	NCP15-5	3.38	3.21	3.30	3.19	0.04
49	NCP20-5	3.23	3.14	3.17	3.10	0.04
50	NCPR20-5	3.23	3.13	3.20	3.12	0.02
51	NCP30-5	3.30	3.22	3.16	3.09	0.13
52	NCP40-5	3.23	3.14	3.18	3.12	0.04
53	NABP-5	3.18	3.12	3.15	3.08	0.04
54	NABPR-5	3.22	3.14	3.18	3.11	0.03
55	NACP-5	3.21	3.14	3.19	3.10	0.03
56	NACPR-5	3.22	3.14	3.24	3.16	-0.02
57	NBCP-5	3.32	3.30	3.33	3.27	0.01
58	NBCPR-5	3.26	3.23	3.25	3.25	-0.01

Appendix F: Shielding Effectiveness

Table F-1: Shielding Results for Gold Standard at Start of Test (Tested on 2/14/02)

Date: 2/14/01	**Frequency MHz**									
Sample Name	**30**	**100**	**200**	**300**	**400**	**500**	**600**	**700**	**800**	**1000**
GOLD REFERENCE			4.30				1.80			1.70
GOLD LOAD			39.30				33.40			34.80
Sample n=1										
Sheilding Effectiveness Exp. (dB)			35.00				31.60			33.10
Actual (dB) from Manual			35.00				33.00			31.00
Difference (dB)			0.00				1.40			-2.10

Table F-2: Shielding Results for Gold Standard at End of Test (Tested on 2/14/02)

Date: 2/14/01	**Frequency MHz**									
Sample Name	**30**	**100**	**200**	**300**	**400**	**500**	**600**	**700**	**800**	**1000**
GOLD REFERENCE			4.60				1.90			1.90
GOLD LOAD			39.80				34.40			35.40
Sample n=1										
Sheilding Effectiveness Exp. (dB)			35.20				32.50			33.50
Actual (dB) from Manual			35.00				33.00			31.00
Difference (dB)			-0.20				0.50			-2.50

Table F-3: Shielding Results for Gold Standard at Start of Test (Tested on 2/21/02)

Date: 2/21/01	**Frequency MHz**									
Sample Name	**30**	**100**	**200**	**300**	**400**	**500**	**600**	**700**	**800**	**1000**
GOLD REFERENCE			4.51				1.85			1.90
GOLD LOAD			39.54				34.60			35.10
Sample n=1										
Sheilding Effectiveness Exp. (dB)			35.03				32.75			33.20
Actual (dB) from Manual			35.00				33.00			31.00
Difference (dB)			-0.03				0.25			-2.20

Table F-4: Shielding Results for Gold Standard at End of Test (Tested on 2/21/02)

Date: 2/21/01	**Frequency MHz**									
Sample Name	**30**	**100**	**200**	**300**	**400**	**500**	**600**	**700**	**800**	**1000**
GOLD REFERENCE			4.56				1.95			1.89
GOLD LOAD			39.68				34.80			35.50
Sample n=1										
Sheilding Effectiveness Exp. (dB)			35.12				32.85			33.61
Actual (dB) from Manual			35.00				33.00			31.00
Difference (dB)			-0.12				0.15			-2.61

Table F-5: Shielding Results for NN (Tested on 2/21/02)

Shielding Effectiveness (dB)	**Frequency MHz**									
Sample Name	**30**	**100**	**200**	**300**	**400**	**500**	**600**	**700**	**800**	**1000**
NN-5 REF	17.90	8.28	4.21	3.07	2.20	1.87	1.82	1.52	1.50	1.81
NN-3-S	17.60	8.06	4.12	3.08	2.25	1.94	1.91	1.64	1.65	2.08
NN-7-S	17.30	7.98	3.99	2.98	2.19	1.88	1.87	1.58	1.57	1.95
NN-8-S	17.50	8.15	4.09	3.05	2.23	1.92	1.90	1.61	1.58	1.96
Sample Average n=3	17.47	8.06	4.07	3.04	2.22	1.91	1.89	1.61	1.60	2.00
Standard Deviation	0.15	0.09	0.07	0.05	0.03	0.03	0.02	0.03	0.04	0.07
Average Shielding (dB)	-0.43	-0.22	-0.14	-0.03	0.02	0.04	0.07	0.09	0.10	0.19
Theoretical Shielding (dB)	-126.03	-131.26	-134.27	-136.03	-137.28	-138.25	-139.04	-139.71	-140.29	-141.26

Table F-6: Shielding Results for NNR (Tested on 2/21/02)

Shielding Effectiveness (dB)	**Frequency MHz**									
Sample Name	**30**	**100**	**200**	**300**	**400**	**500**	**600**	**700**	**800**	**1000**
NNR-5 REF	18.00	8.41	4.31	3.13	2.24	1.89	1.84	1.55	1.53	1.84
NNR-3-S	18.10	8.60	4.48	3.27	2.33	2.00	2.00	1.71	1.65	1.90
NNR-7-S	17.60	8.09	4.11	3.02	2.17	1.94	1.89	1.60	1.58	1.97
NNR-8-S	17.10	7.70	3.87	2.90	2.14	1.85	1.85	1.57	1.56	1.94
Sample Average n=3	17.60	8.13	4.15	3.06	2.21	1.93	1.91	1.63	1.60	1.94
Standard Deviation	0.50	0.45	0.31	0.19	0.10	0.08	0.08	0.07	0.05	0.04
Average Shielding (dB)	-0.40	-0.28	-0.16	-0.07	-0.03	0.04	0.07	0.08	0.07	0.10
Theoretical Shielding (dB)	-122.78	-128.01	-131.02	-132.78	-134.03	-135.00	-135.79	-136.46	-137.04	-138.01

Table F-7: Shielding Results for NAN2.5 (Tested on 2/21/02)

Shielding Effectiveness (dB)	**Frequency MHz**									
Sample Name	**30**	**100**	**200**	**300**	**400**	**500**	**600**	**700**	**800**	**1000**
NAN02.5-5 REF	15.40	6.30	2.99	2.25	1.70	1.51	1.57	1.43	1.44	1.65
NAN02.5-3-S	15.50	6.45	3.20	2.53	1.99	1.87	1.98	1.80	1.80	2.21
NAN02.5-7-S	16.10	6.89	3.45	2.72	2.12	1.91	1.95	1.74	1.77	2.33
NAN02.5-8-S	15.30	6.26	3.07	2.43	1.91	1.75	1.87	1.71	1.72	2.10
Sample Average n=3	15.63	6.53	3.24	2.56	2.01	1.84	1.93	1.75	1.76	2.21
Standard Deviation	0.42	0.32	0.19	0.15	0.11	0.08	0.06	0.05	0.04	0.12
Average Shielding (dB)	0.23	0.23	0.25	0.31	0.31	0.33	0.36	0.32	0.32	0.56
Theoretical Shielding (dB)	-121.85	-127.07	-130.08	-131.85	-133.09	-134.06	-134.86	-135.53	-136.10	-137.07

Table F-8: Shielding Results for NAN04 (Tested on 2/21/02)

Shielding Effectiveness (dB)	**Frequency MHz**									
Sample Name	**30**	**100**	**200**	**300**	**400**	**500**	**600**	**700**	**800**	**1000**
NAN04-5(3) REF	6.63	1.99	1.31	1.37	1.38	1.34	1.44	1.44	1.54	1.73
NAN04-3-S	13.00	6.33	4.88	5.05	5.16	5.01	5.15	5.45	5.69	6.45
NAN04-7-S	9.15	4.89	4.36	4.69	4.88	4.90	5.09	5.40	5.61	6.27
NAN04-8-S	8.91	4.78	4.27	4.59	4.80	4.83	5.01	5.30	5.51	6.19
Sample Average n=3	10.35	5.33	4.50	4.78	4.95	4.91	5.08	5.38	5.60	6.30
Standard Deviation	2.30	0.86	0.33	0.24	0.19	0.09	0.07	0.08	0.09	0.13
Average Shielding (dB)	3.72	3.34	3.19	3.41	3.57	3.57	3.64	3.94	4.06	4.57
Theoretical Shielding (dB)	-51.00	-56.23	-59.24	-61.00	-62.25	-63.22	-64.01	-64.68	-65.26	-66.23

Table F-9: Shielding Results for NANR05 (Tested on 2/21/02)

Shielding Effectiveness (dB)	Frequency MHz									
Sample Name	**30**	**100**	**200**	**300**	**400**	**500**	**600**	**700**	**800**	**1000**
NANR05-5 REF	4.83	1.41	1.04	1.18	1.19	1.21	1.33	1.37	1.47	1.65
NANR05-3-S	20.80	11.80	9.10	8.51	8.61	8.31	8.19	8.37	8.65	9.20
NANR05-7-S	19.80	11.10	8.45	8.31	8.20	8.00	8.03	8.34	8.43	9.09
NANR05-8-S	20.10	11.60	8.90	8.76	8.76	8.44	8.45	8.76	8.83	9.48
Sample Average n=3	20.23	11.50	8.82	8.53	8.52	8.25	8.22	8.49	8.64	9.26
Standard Deviation	0.51	0.36	0.33	0.23	0.29	0.23	0.21	0.23	0.20	0.20
Average Shielding (dB)	15.40	10.09	7.78	7.35	7.33	7.04	6.89	7.12	7.17	7.61
Theoretical Shielding (dB)	-34.34	-39.57	-42.58	-44.34	-45.59	-46.56	-47.35	-48.02	-48.60	-49.57

Table F-10: Shielding Results for NANRR05 (Tested on 2/21/02)

Shielding Effectiveness (dB)	Frequency MHz									
Sample Name	**30**	**100**	**200**	**300**	**400**	**500**	**600**	**700**	**800**	**1000**
NANRR05-5 REF	5.41	1.52	1.05	1.18	1.18	1.20	1.32	1.36	1.47	1.63
NANRR05-3-S	20.60	11.60	8.81	8.62	8.48	8.26	8.28	8.58	8.65	9.30
NANRR05-7-S	20.17	11.30	8.71	8.57	8.61	8.29	8.29	8.59	8.65	9.31
NANRR05-8-S	20.40	11.50	8.76	8.60	8.47	8.26	8.29	8.59	8.66	9.31
Sample Average n=3	20.39	11.47	8.76	8.60	8.52	8.27	8.29	8.59	8.65	9.31
Standard Deviation	0.22	0.15	0.05	0.03	0.08	0.02	0.01	0.01	0.01	0.01
Average Shielding (dB)	14.98	9.95	7.71	7.42	7.34	7.07	6.97	7.23	7.18	7.68
Theoretical Shielding (dB)	-26.47	-31.69	-34.70	-36.46	-37.71	-38.68	-39.47	-40.14	-40.72	-41.68

Table F-11: Shielding Results for NAN06 (Tested on 2/21/02)

Shielding Effectiveness (dB)	Frequency MHz									
Sample Name	**30**	**100**	**200**	**300**	**400**	**500**	**600**	**700**	**800**	**1000**
NAN06-5 REF	5.41	1.53	1.06	1.21	1.17	1.19	1.31	1.35	1.45	1.63
NAN06-3-S	24.20	15.30	12.20	12.00	11.90	11.60	11.50	11.90	11.90	12.60
NAN06-7-S	19.90	12.80	11.10	11.30	11.40	11.20	11.10	11.60	11.70	12.30
NAN06-8-S	20.10	12.70	10.90	10.80	10.90	10.50	10.40	10.70	10.80	11.30
Sample Average n=3	21.40	13.60	11.40	11.37	11.40	11.10	11.00	11.40	11.47	12.07
Standard Deviation	2.43	1.47	0.70	0.60	0.50	0.56	0.56	0.62	0.59	0.68
Average Shielding (dB)	15.99	12.07	10.34	10.16	10.23	9.91	9.69	10.05	10.02	10.44
Theoretical Shielding (dB)	14.57	9.56	6.74	5.13	4.01	3.15	2.46	1.89	1.39	0.58

Table F-12: Shielding Results for NAN7.5 (Tested on 2/21/02)

Shielding Effectiveness (dB)	Frequency MHz									
Sample Name	**30**	**100**	**200**	**300**	**400**	**500**	**600**	**700**	**800**	**1000**
NAN07.5-5 REF	3.88	1.13	0.93	1.09	1.10	1.14	1.26	1.32	1.44	1.62
NAN07.5-3-S	29.90	21.00	17.50	17.10	16.80	16.40	16.20	16.70	16.70	17.30
NAN07.5-7-S	30.60	21.50	17.80	17.40	17.00	16.60	16.40	16.80	16.80	17.40
NAN07.5-8-S	32.50	22.70	18.60	17.80	17.30	16.90	16.70	17.00	17.00	17.50
Sample Average n=3	31.00	21.73	17.97	17.43	17.03	16.63	16.43	16.83	16.83	17.40
Standard Deviation	1.35	0.87	0.57	0.35	0.25	0.25	0.25	0.15	0.15	0.10
Average Shielding (dB)	27.12	20.60	17.04	16.34	15.93	15.49	15.17	15.51	15.39	15.78
Theoretical Shielding (dB)	21.25	16.47	13.87	12.42	11.44	10.70	10.12	9.65	9.25	8.61

Table F-13: Shielding Results for NAN10 (Tested on 2/21/02)

Shielding Effectiveness (dB)	Frequency MHz									
Sample Name	**30**	**100**	**200**	**300**	**400**	**500**	**600**	**700**	**800**	**1000**
NAN10-5 REF	2.80	0.87	0.89	1.02	1.10	1.15	1.27	1.34	1.47	1.67
NAN10-3-S	36.60	27.50	24.00	23.70	22.90	22.40	22.20	22.60	22.70	23.30
NAN10-7-S	36.40	27.20	23.90	22.70	23.10	22.60	22.20	22.60	22.90	23.40
NAN10-8-S	35.20	26.90	23.80	23.30	22.70	22.20	22.10	22.50	22.60	23.20
Sample Average n=3	36.07	27.20	23.90	23.23	22.90	22.40	22.17	22.57	22.73	23.30
Standard Deviation	0.76	0.30	0.10	0.50	0.20	0.20	0.06	0.06	0.15	0.10
Average Shielding (dB)	33.27	26.33	23.01	22.21	21.80	21.25	20.90	21.23	21.26	21.63
Theoretical Shielding (dB)	26.92	22.51	20.24	19.06	18.29	17.75	17.34	17.02	16.77	16.40

Table F-14: Shielding Results for NBN10 (Tested on 2/21/02)

Shielding Effectiveness (dB)	Frequency MHz									
Sample Name	**30**	**100**	**200**	**300**	**400**	**500**	**600**	**700**	**800**	**1000**
NBN10-5 REF	16.40	7.04	3.40	2.50	1.80	1.59	1.64	1.45	1.44	1.66
NBN10-3-S	15.70	6.56	3.23	2.54	1.95	1.76	1.89	1.70	1.67	2.07
NBN10-7-S	16.20	7.02	3.49	2.70	2.05	1.84	1.95	1.73	1.72	2.09
NBN10-8-S	16.40	7.12	3.56	2.75	2.09	1.87	1.97	1.76	1.73	2.12
Sample Average n=3	16.10	6.90	3.43	2.66	2.03	1.82	1.94	1.73	1.71	2.09
Standard Deviation	0.36	0.30	0.17	0.11	0.07	0.06	0.04	0.03	0.03	0.03
Average Shielding (dB)	-0.30	-0.14	0.03	0.16	0.23	0.23	0.30	0.28	0.27	0.43
Theoretical Shielding (dB)	-122.09	-127.32	-130.33	-132.09	-133.34	-134.31	-135.10	-135.77	-136.35	-137.32

Table F-15: Shielding Results for NBN15 (Tested on 2/21/02)

Shielding Effectiveness (dB)	**Frequency MHz**									
Sample Name	**30**	**100**	**200**	**300**	**400**	**500**	**600**	**700**	**800**	**1000**
NBN15-5 REF	15.80	6.61	2.15	2.35	1.73	1.53	1.60	1.43	1.44	1.65
NBN15-3-S	14.90	6.06	3.01	2.47	1.98	1.84	1.97	1.84	1.85	2.33
NBN15-7-S	14.70	5.93	2.93	2.41	1.95	1.81	1.95	1.82	1.83	2.31
NBN15-8-S	15.80	6.76	3.42	2.74	2.16	1.97	2.11	1.93	1.92	2.41
Sample Average n=3	15.13	6.25	3.12	2.54	2.03	1.87	2.01	1.86	1.87	2.35
Standard Deviation	0.59	0.45	0.26	0.18	0.11	0.09	0.09	0.06	0.05	0.05
Average Shielding (dB)	-0.67	-0.36	0.97	0.19	0.30	0.34	0.41	0.43	0.43	0.70
Theoretical Shielding (dB)	-121.23	-126.45	-129.46	-131.23	-132.47	-133.44	-134.24	-134.90	-135.48	-136.45

Table F-16: Shielding Results for NBN20 (Tested on 2/21/02)

Shielding Effectiveness (dB)	**Frequency MHz**									
Sample Name	**30**	**100**	**200**	**300**	**400**	**500**	**600**	**700**	**800**	**1000**
NBN20-5 REF	13.70	5.20	2.39	1.89	1.48	1.41	1.46	1.36	1.40	1.61
NBN20-3-S	13.10	4.94	2.51	2.24	1.95	1.88	2.05	1.98	2.04	2.65
NBN20-7-S	13.80	5.43	2.78	2.43	2.06	1.97	2.15	2.07	2.12	2.74
NBN20-8-S	13.30	5.13	2.62	2.33	2.01	1.97	2.12	2.06	2.12	2.75
Sample Average n=3	13.40	5.17	2.64	2.33	2.01	1.94	2.11	2.04	2.09	2.71
Standard Deviation	0.36	0.25	0.14	0.10	0.06	0.05	0.05	0.05	0.05	0.06
Average Shielding (dB)	-0.30	-0.03	0.25	0.44	0.53	0.53	0.65	0.68	0.69	1.10
Theoretical Shielding (dB)	-115.12	-120.35	-123.36	-125.12	-126.37	-127.34	-128.13	-128.80	-129.38	-130.35

Table F-17: Shielding Results for NBN30 (Tested on 2/21/02)

Shielding Effectiveness (dB)	Frequency MHz									
Sample Name	**30**	**100**	**200**	**300**	**400**	**500**	**600**	**700**	**800**	**1000**
NBN30-5 REF	11.50	3.98	1.88	1.60	1.47	1.30	1.39	1.34	1.40	1.61
NBN30-3-S	11.40	4.30	2.74	2.83	2.81	2.88	3.20	3.37	3.58	4.70
NBN30-7-S	12.00	4.76	2.90	2.94	2.87	2.94	3.25	3.42	3.63	4.76
NBN30-8-S	11.90	4.70	2.87	2.93	2.87	2.95	3.27	3.44	3.65	4.77
Sample Average n=3	11.77	4.59	2.84	2.90	2.85	2.92	3.24	3.41	3.62	4.74
Standard Deviation	0.32	0.25	0.09	0.06	0.03	0.04	0.04	0.04	0.04	0.04
Average Shielding (dB)	0.27	0.61	0.96	1.30	1.38	1.62	1.85	2.07	2.22	3.13
Theoretical Shielding (dB)	-34.18	-39.41	-42.41	-44.18	-45.42	-46.39	-47.18	-47.85	-48.43	-49.40

Table F-18: Shielding Results for NBNR30 (Tested on 2/21/02)

Shielding Effectiveness (dB)	Frequency MHz									
Sample Name	**30**	**100**	**200**	**300**	**400**	**500**	**600**	**700**	**800**	**1000**
NBNR30-5 REF	8.33	2.66	1.41	1.33	1.26	1.21	1.32	1.32	1.41	1.59
NBNR30-3-S	9.42	3.79	2.76	3.14	3.44	3.44	3.78	4.16	4.60	6.10
NBNR30-7-S	9.58	3.85	2.74	3.08	3.36	3.41	3.83	4.16	4.49	5.80
NBNR30-8-S	9.57	3.76	2.65	2.98	3.17	3.21	3.53	3.85	4.26	5.69
Sample Average n=3	9.52	3.80	2.72	3.07	3.32	3.35	3.71	4.06	4.45	5.86
Standard Deviation	0.09	0.05	0.06	0.08	0.14	0.13	0.16	0.18	0.17	0.21
Average Shielding (dB)	1.19	1.14	1.31	1.74	2.06	2.14	2.39	2.74	3.04	4.27
Theoretical Shielding (dB)	-33.91	-39.13	-42.14	-43.90	-45.15	-46.12	-46.91	-47.58	-48.16	-49.13

Table F-19: Shielding Results for NBN40 (Tested on 2/21/02)

Shielding Effectiveness (dB)	Frequency MHz									
Sample Name	**30**	**100**	**200**	**300**	**400**	**500**	**600**	**700**	**800**	**1000**
NBN40-5 REF	6.03	2.02	1.25	1.26	1.21	1.20	1.30	1.34	1.43	1.61
NBN40-3-S	9.09	4.65	4.13	4.84	5.42	5.65	6.16	6.78	7.29	8.59
NBN40-7-S	8.70	4.20	3.68	4.38	4.93	5.08	5.52	6.16	6.78	8.28
NBN40-8-S	9.70	4.80	4.11	4.77	5.35	5.53	6.05	6.66	7.16	8.40
Sample Average n=3	9.16	4.55	3.97	4.66	5.23	5.42	5.91	6.53	7.08	8.42
Standard Deviation	0.50	0.31	0.25	0.25	0.27	0.30	0.34	0.33	0.27	0.16
Average Shielding (dB)	3.13	2.53	2.72	3.40	4.02	4.22	4.61	5.19	5.65	6.81
Theoretical Shielding (dB)	9.40	4.29	1.39	-0.28	-1.46	-2.37	-3.10	-3.72	-4.25	-5.13

Table F-20: Shielding Results for NCN05 (Tested on 2/21/02)

Shielding Effectiveness (dB)	Frequency MHz									
Sample Name	**30**	**100**	**200**	**300**	**400**	**500**	**600**	**700**	**800**	**1000**
NCN05-5 REF	17.30	7.86	3.89	2.86	2.06	1.76	1.77	1.47	1.46	1.77
NCN05-3-S	18.10	8.57	4.55	3.51	2.67	2.36	2.41	2.13	2.07	2.57
NCN05-7-S	18.30	8.75	4.64	3.57	2.71	2.40	2.44	2.15	2.08	2.58
NCN05-8-S	17.70	8.26	4.31	3.34	2.56	2.26	2.35	2.08	2.03	2.52
Sample Average n=3	18.03	8.53	4.50	3.47	2.65	2.34	2.40	2.12	2.06	2.56
Standard Deviation	0.31	0.25	0.17	0.12	0.08	0.07	0.05	0.04	0.03	0.03
Average Shielding (dB)	0.73	0.67	0.61	0.61	0.59	0.58	0.63	0.65	0.60	0.79
Theoretical Shielding (dB)	-124.66	-129.89	-132.90	-134.66	-135.91	-136.88	-137.67	-138.34	-138.92	-139.89

Table F-21: Shielding Results for NCN10 (Tested on 2/21/02)

Shielding Effectiveness (dB)	**Frequency MHz**									
Sample Name	**30**	**100**	**200**	**300**	**400**	**500**	**600**	**700**	**800**	**1000**
NCN10-5 REF	17.40	7.89	3.91	2.84	2.86	1.76	1.75	1.47	1.46	1.77
NCN10-3-S	17.30	7.99	4.33	3.53	2.86	2.66	2.86	2.67	2.68	3.52
NCN10-7-S	17.40	8.13	4.41	3.63	2.98	2.72	2.82	2.61	2.70	3.78
NCN10-8-S	17.20	7.98	4.27	3.55	2.92	2.69	2.85	2.72	2.84	3.75
Sample Average n=3	17.30	8.03	4.34	3.57	2.92	2.69	2.84	2.67	2.74	3.68
Standard Deviation	0.10	0.08	0.07	0.05	0.06	0.03	0.02	0.06	0.09	0.14
Average Shielding (dB)	-0.10	0.14	0.43	0.73	0.06	0.93	1.09	1.20	1.28	1.91
Theoretical Shielding (dB)	-123.24	-128.47	-131.48	-133.24	-134.49	-135.46	-136.25	-136.92	-137.50	-138.47

Table F-22: Shielding Results for NCN15 (Tested on 2/21/02)

Shielding Effectiveness (dB)	**Frequency MHz**									
Sample Name	**30**	**100**	**200**	**300**	**400**	**500**	**600**	**700**	**800**	**1000**
NCN15-5 REF	16.20	6.98	3.37	2.48	1.81	1.58	1.64	1.44	1.45	1.66
NCN15-3-S	16.40	7.50	4.23	3.78	3.37	3.30	3.62	3.66	3.82	5.04
NCN15-7-S	15.50	6.77	3.85	3.55	3.24	3.20	3.57	3.65	3.85	5.15
NCN15-8-S	16.40	7.50	4.26	3.80	3.39	3.30	3.63	3.65	3.82	5.06
Sample Average n=3	16.10	7.26	4.11	3.71	3.33	3.27	3.61	3.65	3.83	5.08
Standard Deviation	0.52	0.42	0.23	0.14	0.08	0.06	0.03	0.01	0.02	0.06
Average Shielding (dB)	-0.10	0.28	0.74	1.23	1.52	1.69	1.97	2.21	2.38	3.42
Theoretical Shielding (dB)	-121.60	-126.82	-129.83	-131.60	-132.84	-133.81	-134.61	-135.28	-135.86	-136.82

Table F-23: Shielding Results for NCN20 (Tested on 2/21/02)

Shielding Effectiveness (dB)	**Frequency MHz**									
Sample Name	**30**	**100**	**200**	**300**	**400**	**500**	**600**	**700**	**800**	**1000**
NCN20-5 REF	14.30	5.54	2.56	2.02	1.58	1.54	1.48	1.36	1.42	1.69
NCN20-3-S	14.70	6.60	4.20	4.27	4.24	4.46	4.88	5.22	5.62	7.18
NCN20-7-S	14.90	6.90	4.44	4.52	4.59	4.80	5.19	5.50	5.95	7.49
NCN20-8-S	15.20	6.84	4.25	4.23	4.19	4.36	4.73	5.00	5.40	6.91
Sample Average n=3	14.93	6.78	4.30	4.34	4.34	4.54	4.93	5.24	5.66	7.19
Standard Deviation	0.25	0.16	0.13	0.16	0.22	0.23	0.23	0.25	0.28	0.29
Average Shielding (dB)	0.63	1.24	1.74	2.32	2.76	3.00	3.45	3.88	4.24	5.50
Theoretical Shielding (dB)	-51.43	-56.66	-59.67	-61.43	-62.68	-63.65	-64.44	-65.11	-65.69	-66.66

Table F-24: Shielding Results for NCNR20 (Tested on 2/21/02)

Shielding Effectiveness (dB)	**Frequency MHz**									
Sample Name	**30**	**100**	**200**	**300**	**400**	**500**	**600**	**700**	**800**	**1000**
NCNR20-5 REF	14.80	6.06	2.84	2.18	1.65	1.54	1.55	1.41	1.43	1.65
NCNR20-3-S	15.10	6.83	4.33	4.33	4.25	4.47	4.85	5.17	5.54	7.08
NCNR20-7-S	16.10	7.56	4.78	4.67	4.52	4.65	5.08	5.37	5.72	7.24
NCNR20-8-S	15.50	7.13	4.55	4.57	4.50	4.65	4.93	5.28	5.79	7.53
Sample Average n=3	15.57	7.17	4.55	4.52	4.42	4.59	4.95	5.27	5.68	7.28
Standard Deviation	0.50	0.37	0.23	0.17	0.15	0.10	0.12	0.10	0.13	0.23
Average Shielding (dB)	0.77	1.11	1.71	2.34	2.77	3.05	3.40	3.86	4.25	5.63
Theoretical Shielding (dB)	-58.11	-63.34	-66.35	-68.11	-69.36	-70.33	-71.12	-71.79	-72.37	-73.34

Table F-25: Shielding Results for NCN30 (Tested on 2/21/02)

Shielding Effectiveness (dB)	Frequency MHz									
Sample Name	**30**	**100**	**200**	**300**	**400**	**500**	**600**	**700**	**800**	**1000**
NCN30-5 REF	9.16	3.31	1.80	1.63	1.54	1.38	1.44	1.40	1.48	1.70
NCN30-3-S	10.90	6.04	5.50	6.45	7.38	7.70	8.35	9.17	9.77	11.50
NCN30-7-S	14.50	7.80	6.42	7.06	7.62	8.09	8.63	9.31	9.96	11.50
NCN30-8-S	12.90	6.88	5.84	6.63	7.28	7.68	8.31	9.09	9.64	11.30
Sample Average n=3	12.77	6.91	5.92	6.71	7.43	7.82	8.43	9.19	9.79	11.43
Standard Deviation	1.80	0.88	0.47	0.31	0.17	0.23	0.17	0.11	0.16	0.12
Average Shielding (dB)	3.61	3.60	4.12	5.08	5.89	6.44	6.99	7.79	8.31	9.73
Theoretical Shielding (dB)	15.05	10.05	7.24	5.64	4.52	3.67	2.99	2.42	1.93	1.12

Table F-26: Shielding Results for NCN40 (Tested on 2/21/02)

Shielding Effectiveness (dB)	Frequency MHz									
Sample Name	**30**	**100**	**200**	**300**	**400**	**500**	**600**	**700**	**800**	**1000**
NCN40-5(3) REF	6.00	2.00	1.34	1.42	1.32	1.30	1.40	1.41	1.51	1.71
NCN40-3-S	21.00	13.80	12.10	12.80	13.60	13.60	14.00	14.80	15.10	16.40
NCN40-7-S	16.80	11.70	11.30	12.40	13.20	13.40	13.90	14.70	15.30	16.50
NCN40-8-S	15.60	10.60	10.40	11.50	12.50	12.80	13.30	14.10	14.80	15.70
Sample Average n=3	17.80	12.03	11.27	12.23	13.10	13.27	13.73	14.53	15.07	16.20
Standard Deviation	2.84	1.63	0.85	0.67	0.56	0.42	0.38	0.38	0.25	0.44
Average Shielding (dB)	11.80	10.03	9.93	10.81	11.78	11.97	12.33	13.12	13.56	14.49
Theoretical Shielding (dB)	26.51	22.06	19.76	18.55	17.76	17.20	16.78	16.45	16.18	15.79

Table F-27: Shielding Results for NABN (Tested on 2/21/02)

Shielding Effectiveness (dB)	Frequency MHz									
Sample Name	**30**	**100**	**200**	**300**	**400**	**500**	**600**	**700**	**800**	**1000**
NABN-5 REF	2.56	0.79	0.80	0.96	1.03	1.09	1.21	1.29	1.44	1.65
NABN-3-S	28.80	24.50	23.90	24.00	23.90	23.50	23.30	24.00	24.40	24.90
NABN-7-S	29.00	24.10	24.00	24.50	24.00	23.40	23.00	23.80	24.30	24.80
NABN-8-S	28.10	23.90	23.60	23.70	23.90	23.40	23.20	23.90	24.50	25.00
Sample Average n=3	28.63	24.17	23.83	24.07	23.93	23.43	23.17	23.90	24.40	24.90
Standard Deviation	0.47	0.31	0.21	0.40	0.06	0.06	0.15	0.10	0.10	0.10
Average Shielding (dB)	26.07	23.38	23.03	23.11	22.90	22.34	22.08	22.69	23.11	23.46
Theoretical Shielding (dB)	26.26	21.80	19.48	18.26	17.46	16.89	16.46	16.12	15.84	15.44

Table F-28: Shielding Results for NABNR (Tested on 2/21/02)

Shielding Effectiveness (dB)	Frequency MHz									
Sample Name	**30**	**100**	**200**	**300**	**400**	**500**	**600**	**700**	**800**	**1000**
NABNR-5 REF	3.40	0.93	0.86	1.00	1.05	1.09	1.22	1.30	1.44	1.66
NABNR-3-S	26.80	23.80	23.90	23.70	23.70	23.30	23.10	23.90	24.40	24.90
NABNR-7-S	27.40	24.00	24.20	24.20	24.20	23.70	23.50	24.30	24.80	25.30
NABNR-8-S	28.00	24.00	24.30	23.80	23.90	23.40	23.20	23.90	24.40	24.80
Sample Average n=3	27.40	23.93	24.13	23.90	23.93	23.47	23.27	24.03	24.53	25.00
Standard Deviation	0.60	0.12	0.21	0.26	0.25	0.21	0.21	0.23	0.23	0.26
Average Shielding (dB)	24.00	23.00	23.27	22.90	22.88	22.38	22.05	22.73	23.09	23.34
Theoretical Shielding (dB)	28.32	24.03	21.88	20.79	20.09	19.62	19.27	19.01	18.81	18.53

Table F-29: Shielding Results for NACN (Tested on 2/21/02)

Shielding Effectiveness (dB)	Frequency MHz									
Sample Name	**30**	**100**	**200**	**300**	**400**	**500**	**600**	**700**	**800**	**1000**
NACN-5(3) REF	3.48	1.02	0.87	1.07	1.11	1.15	1.26	1.33	1.45	1.65
NACN-3-S	28.30	22.10	20.70	21.60	21.50	21.00	20.80	21.60	21.90	22.50
NACN-7-S	28.80	23.00	21.60	22.50	22.20	21.70	21.50	22.30	22.70	23.20
NACN-8-S	29.60	23.00	21.40	22.10	22.00	21.50	21.20	22.00	22.40	22.90
Sample Average n=3	28.90	22.70	21.23	22.07	21.90	21.40	21.17	21.97	22.33	22.87
Standard Deviation	0.66	0.52	0.47	0.45	0.36	0.36	0.35	0.35	0.40	0.35
Average Shielding (dB)	25.42	21.68	20.36	21.00	20.79	20.25	19.91	20.64	20.88	21.22
Theoretical Shielding (dB)	25.12	20.57	18.17	16.89	16.04	15.42	14.95	14.57	14.27	13.80

Table F-30: Shielding Results for NACNR (Tested on 2/21/02)

Shielding Effectiveness (dB)	Frequency MHz									
Sample Name	**30**	**100**	**200**	**300**	**400**	**500**	**600**	**700**	**800**	**1000**
NACNR-5 REF	2.10	0.86	0.87	1.01	1.10	1.16	1.27	1.35	1.48	1.68
NACNR-3-S	30.70	23.00	20.80	21.30	21.20	20.50	20.10	21.00	21.40	21.90
NACNR-7-S	28.60	22.10	20.60	21.50	21.10	20.50	20.30	21.10	21.50	22.00
NACNR-8-S	27.40	21.30	20.00	20.80	20.70	20.20	19.90	20.90	21.20	21.70
Sample Average n=3	28.90	22.13	20.47	21.20	21.00	20.40	20.10	21.00	21.37	21.87
Standard Deviation	1.67	0.85	0.42	0.36	0.26	0.17	0.20	0.10	0.15	0.15
Average Shielding (dB)	26.80	21.27	19.60	20.19	19.90	19.24	18.83	19.65	19.89	20.19
Theoretical Shielding (dB)	22.19	17.45	14.90	13.48	12.53	11.81	11.26	10.80	10.42	9.82

Table F-31: Shielding Results for NBCN (Tested on 2/21/02)

Shielding Effectiveness (dB)	Frequency MHz									
Sample Name	**30**	**100**	**200**	**300**	**400**	**500**	**600**	**700**	**800**	**1000**
NBCN-5 REF	1.76	0.69	0.76	0.89	0.99	1.06	1.19	1.29	1.42	1.60
NBCN-3-S	12.40	9.05	9.57	11.00	12.10	12.40	12.90	13.70	14.40	15.40
NBCN-7-S	9.55	8.36	9.32	11.00	11.80	12.30	12.70	13.80	14.40	15.40
NBCN-8-S	8.77	8.25	9.37	10.90	11.90	12.30	12.70	13.85	14.70	15.70
Sample Average n=3	10.24	8.55	9.42	10.97	11.93	12.33	12.77	13.78	14.50	15.50
Standard Deviation	1.91	0.43	0.13	0.06	0.15	0.06	0.12	0.08	0.17	0.17
Average Shielding (dB)	8.48	7.86	8.66	10.08	10.94	11.27	11.58	12.49	13.08	13.90
Theoretical Shielding (dB)	21.31	16.53	13.93	12.48	11.50	10.77	10.19	9.71	9.31	8.68

Table F-32: Shielding Results for NBCNR (Tested on 2/21/02)

Shielding Effectiveness (dB)	Frequency MHz									
Sample Name	**30**	**100**	**200**	**300**	**400**	**500**	**600**	**700**	**800**	**1000**
NBCNR-5 REF	2.60	1.17	1.03	1.12	1.14	1.18	1.29	1.34	1.46	1.65
NBCNR-3-S	12.30	11.20	12.20	13.80	14.70	15.00	15.30	16.20	16.70	17.60
NBCNR-7-S	10.80	11.00	12.30	13.80	14.90	15.30	15.70	16.60	17.00	17.80
NBCNR-8-S	13.90	11.60	12.30	14.20	14.80	15.00	15.30	16.20	16.70	17.50
Sample Average n=3	12.33	11.27	12.27	13.93	14.80	15.10	15.43	16.33	16.80	17.63
Standard Deviation	1.55	0.31	0.06	0.23	0.10	0.17	0.23	0.23	0.17	0.15
Average Shielding (dB)	9.73	10.10	11.24	12.81	13.66	13.92	14.14	14.99	15.34	15.98
Theoretical Shielding (dB)	22.33	17.60	15.05	13.64	12.69	11.98	11.43	10.97	10.60	10.00

Table F-33: Shielding Results for NABCN (Tested on 2/21/02)

Shielding Effectiveness (dB)	Frequency MHz									
Sample Name	**30**	**100**	**200**	**300**	**400**	**500**	**600**	**700**	**800**	**1000**
NABCN-5 REF	3.28	1.24	1.00	1.14	1.13	1.15	1.26	1.31	1.43	1.62
NABCN-3-S	37.00	38.30	43.90	43.90	42.60	42.50	42.80	44.00	44.80	46.20
NABCN-7-S	38.70	39.30	43.30	44.00	42.30	41.80	41.50	42.70	43.60	45.20
NABCN-8-S	37.80	38.00	43.00	43.40	42.60	41.30	41.00	42.00	43.20	44.70
Sample Average n=3	37.83	38.53	43.40	43.77	42.50	41.87	41.77	42.90	43.87	45.37
Standard Deviation	0.850	0.681	0.458	0.321	0.173	0.603	0.929	1.015	0.833	0.764
Average Shielding (dB)	34.55	37.29	42.40	42.63	41.37	40.72	40.51	41.59	42.44	43.75
Theoretical Shielding (dB)	45.64	44.72	45.67	46.94	48.25	49.53	50.77	51.98	53.14	55.36

Table F-34: Shielding Results for NABCNR (Tested on 2/21/02)

Shielding Effectiveness (dB)	Frequency MHz									
Sample Name	**30**	**100**	**200**	**300**	**400**	**500**	**600**	**700**	**800**	**1000**
NABCNR-5 REF	1.74	0.65	0.78	0.92	1.02	1.10	1.23	1.32	1.46	1.66
NABCNR-3-S	35.30	36.20	42.40	42.20	41.20	40.30	40.50	42.00	43.10	44.50
NABCNR-7-S	36.00	40.10	43.70	41.80	41.20	41.10	41.50	42.80	43.70	45.20
NABCNR-8-S	37.60	38.60	44.50	41.40	40.80	40.60	40.90	42.40	43.60	45.60
Sample Average n=3	36.30	38.30	43.53	41.80	41.07	40.67	40.97	42.40	43.47	45.10
Standard Deviation	1.18	1.97	1.06	0.40	0.23	0.40	0.50	0.40	0.32	0.56
Average Shielding (dB)	34.56	37.65	42.75	40.88	40.05	39.57	39.74	41.08	42.01	43.44
Theoretical Shielding (dB)	46.31	45.60	46.74	48.16	49.59	50.99	52.33	53.62	54.87	57.25

Table F-35: Shielding Results for NP (Tested on 2/14/02)

Shielding Effectiveness (dB)	Frequency MHz									
Sample Name	**30**	**100**	**200**	**300**	**400**	**500**	**600**	**700**	**800**	**1000**
NP-5 REF	18.40	8.60	4.50	3.20	2.30	2.00	1.90	1.50	1.50	1.90
NP-3-S	17.90	8.30	4.20	3.10	2.30	2.00	1.90	1.60	1.50	2.10
NP-7-S	17.90	8.20	4.20	3.10	2.30	2.00	1.90	1.60	1.50	2.10
NP-8-S	17.90	8.30	4.20	3.10	2.30	2.00	1.90	1.60	1.50	2.10
Sample Average n=3	17.90	8.27	4.20	3.10	2.30	2.00	1.90	1.60	1.50	2.10
Standard Deviation	0.00	0.06	0.00	0.00	0.00	0.00	0.00	0.00	0.00	0.00
Average Shielding (dB)	-0.50	-0.33	-0.30	-0.10	0.00	0.00	0.00	0.10	0.00	0.20
Theoretical Shielding (dB)	-135.95	-141.18	-144.19	-145.95	-147.20	-148.17	-148.96	-149.63	-150.21	-151.18

Table F-36: Shielding Results for NPR (Tested on 2/14/02)

Shielding Effectiveness (dB)	Frequency MHz									
Sample Name	**30**	**100**	**200**	**300**	**400**	**500**	**600**	**700**	**800**	**1000**
NPR-5 REF	18.30	8.50	4.40	3.20	2.30	2.00	1.90	1.50	1.50	2.00
NPR-3-S	17.80	8.20	4.20	3.10	2.30	2.00	1.90	1.60	1.50	2.10
NPR-7-S	17.90	8.20	4.20	3.10	2.30	2.00	1.90	1.60	1.50	2.10
NPR-8-S	18.20	8.40	4.40	3.20	2.40	2.10	2.00	1.60	1.60	2.10
Sample Average n=3	17.97	8.27	4.27	3.13	2.33	2.03	1.93	1.60	1.53	2.10
Standard Deviation	0.21	0.12	0.12	0.06	0.06	0.06	0.06	0.00	0.06	0.00
Average Shielding (dB)	-0.33	-0.23	-0.13	-0.07	0.03	0.03	0.03	0.10	0.03	0.10
Theoretical Shielding (dB)	-136.08	-141.30	-144.31	-146.08	-147.33	-148.29	-149.09	-149.76	-150.34	-151.30

Table F-37: Shielding Results for NAP2.5 (Tested on 2/14/02)

Shielding Effectiveness (dB)	Frequency MHz									
Sample Name	**30**	**100**	**200**	**300**	**400**	**500**	**600**	**700**	**800**	**1000**
NAP02.5-5 REF	7.10	2.50	1.50	1.50	1.60	1.40	1.40	1.30	1.40	1.60
NAP02.5-3-S	7.70	3.30	2.50	2.80	2.90	2.90	2.70	2.80	3.20	3.60
NAP02.5-7-S	8.80	3.60	2.70	2.90	3.00	3.00	2.70	2.80	3.20	3.60
NAP02.5-8-S	8.10	3.60	2.90	3.20	3.30	3.30	3.00	3.30	3.70	4.20
Sample Average n=3	8.20	3.50	2.70	2.97	3.07	3.07	2.80	2.97	3.37	3.80
Standard Deviation	0.56	0.17	0.20	0.21	0.21	0.21	0.17	0.29	0.29	0.35
Average Shielding (dB)	1.10	1.00	1.20	1.47	1.47	1.67	1.40	1.67	1.97	2.20
Theoretical Shielding (dB)	-118.49	-123.72	-126.73	-128.49	-129.74	-130.71	-131.50	-132.17	-132.75	-133.72

Table F-38: Shielding Results for NAP04 (Tested on 2/14/02)

Shielding Effectiveness (dB)	Frequency MHz									
Sample Name	**30**	**100**	**200**	**300**	**400**	**500**	**600**	**700**	**800**	**1000**
NAP04-5 REF	3.20	0.95	0.79	1.10	1.20	1.10	1.20	1.30	1.30	1.50
NAP04-3-S	10.10	6.80	7.10	7.60	7.30	7.40	6.90	7.90	8.30	8.40
NAP04-7-S	9.70	6.90	7.40	7.90	7.50	7.70	7.20	8.20	8.60	8.70
NAP04-8-S	9.60	7.10	7.60	8.20	7.70	7.90	7.30	8.30	8.80	8.80
Sample Average n=3	9.80	6.93	7.37	7.90	7.50	7.67	7.13	8.13	8.57	8.63
Standard Deviation	0.26	0.15	0.25	0.30	0.20	0.25	0.21	0.21	0.25	0.21
Average Shielding (dB)	6.60	5.98	6.58	6.80	6.30	6.57	5.93	6.83	7.27	7.13
Theoretical Shielding (dB)	-101.19	-106.42	-109.43	-111.19	-112.44	-113.41	-114.20	-114.87	-115.45	-116.42

Table F-39: Shielding Results for NAP05 (Tested on 2/14/02)

Shielding Effectiveness (dB)	Frequency MHz									
Sample Name	**30**	**100**	**200**	**300**	**400**	**500**	**600**	**700**	**800**	**1000**
NAP05-5 REF	2.30	0.80	0.73	0.98	1.10	1.10	1.20	1.30	1.30	1.50
NAP05-3-S	11.40	10.00	10.80	11.20	10.70	11.00	10.30	11.70	12.20	12.00
NAP05-7-S	11.00	9.60	10.40	10.90	10.40	10.70	9.90	11.30	11.80	11.70
NAP05-8-S	12.30	10.10	10.80	11.40	10.70	11.00	10.30	11.70	12.10	12.00
Sample Average n=3	11.57	9.90	10.67	11.17	10.60	10.90	10.17	11.57	12.03	11.90
Standard Deviation	0.67	0.26	0.23	0.25	0.17	0.17	0.23	0.23	0.21	0.17
Average Shielding (dB)	9.27	9.10	9.94	10.19	9.50	9.80	8.97	10.27	10.73	10.40
Theoretical Shielding (dB)	-28.19	-33.42	-36.43	-38.19	-39.44	-40.40	-41.19	-41.86	-42.44	-43.41

Table F-40: Shielding Results for NAPR05 (Tested on 2/14/02)

Shielding Effectiveness (dB)	Frequency MHz									
Sample Name	**30**	**100**	**200**	**300**	**400**	**500**	**600**	**700**	**800**	**1000**
NAPR05-5 REF	2.80	0.84	0.73	1.00	1.10	1.10	1.10	1.20	1.20	1.50
NAPR05-3-S	11.50	10.10	10.90	11.40	10.90	11.20	10.50	11.90	12.30	12.30
NAPR05-7-S	19.00	11.60	11.30	11.60	11.00	11.20	10.30	11.50	12.00	12.00
NAPR05-8-S	12.80	10.00	10.50	11.30	10.60	10.80	10.10	11.40	11.80	11.70
Sample Average n=3	14.43	10.57	10.90	11.43	10.83	11.07	10.30	11.60	12.03	12.00
Standard Deviation	4.01	0.90	0.40	0.15	0.21	0.23	0.20	0.26	0.25	0.30
Average Shielding (dB)	11.63	9.73	10.17	10.43	9.73	9.97	9.20	10.40	10.83	10.50
Theoretical Shielding (dB)	-26.96	-32.19	-35.19	-36.95	-38.20	-39.17	-39.96	-40.63	-41.21	-42.18

Table F-41: Shielding Results for NAP06 (Tested on 2/14/02)

Shielding Effectiveness (dB)	Frequency MHz									
Sample Name	**30**	**100**	**200**	**300**	**400**	**500**	**600**	**700**	**800**	**1000**
NAP06-5 REF	1.70	0.70	0.69	0.89	1.00	1.00	1.10	1.30	1.20	1.50
NAP06-3-S	21.90	14.20	13.70	14.50	13.40	13.50	12.40	13.80	14.30	14.20
NAP06-7-S	13.70	12.60	13.50	14.00	13.30	13.70	12.90	14.30	14.70	14.70
NAP06-8-S	15.40	12.90	13.50	14.30	13.40	13.70	12.80	14.40	14.90	14.80
Sample Average n=3	17.00	13.23	13.57	14.27	13.37	13.63	12.70	14.17	14.63	14.57
Standard Deviation	4.33	0.85	0.12	0.25	0.06	0.12	0.26	0.32	0.31	0.32
Average Shielding (dB)	15.30	12.53	12.88	13.38	12.37	12.63	11.60	12.87	13.43	13.07
Theoretical Shielding (dB)	18.60	13.70	11.00	9.47	8.42	7.63	6.99	6.47	6.02	5.30

Table F-42: Shielding Results for NAP7.5 (Tested on 2/14/02)

Shielding Effectiveness (dB)	Frequency MHz									
Sample Name	**30**	**100**	**200**	**300**	**400**	**500**	**600**	**700**	**800**	**1000**
NAP07.5-5 REF	1.10	0.62	0.69	0.86	1.00	1.00	1.10	1.20	1.20	1.50
NAP07.5-3-S	16.60	16.00	17.00	17.40	16.70	17.00	16.20	18.00	18.50	18.40
NAP07.5-7-S	18.00	16.50	13.30	17.70	16.80	17.00	16.20	17.80	18.20	18.30
NAP07.5-8-S	16.30	16.10	17.20	17.60	16.90	17.30	16.50	18.20	18.60	18.70
Sample Average n=3	16.97	16.20	15.83	17.57	16.80	17.10	16.30	18.00	18.43	18.47
Standard Deviation	0.91	0.26	2.20	0.15	0.10	0.17	0.17	0.20	0.21	0.21
Average Shielding (dB)	15.87	15.58	15.14	16.71	15.80	16.10	15.20	16.80	17.23	16.97
Theoretical Shielding (dB)	24.65	20.07	17.65	16.34	15.47	14.84	14.35	13.96	13.64	13.14

Table F-43: Shielding Results for NAP10 (Tested on 2/14/02)

Shielding Effectiveness (dB)	Frequency MHz									
Sample Name	**30**	**100**	**200**	**300**	**400**	**500**	**600**	**700**	**800**	**1000**
NAP10-5 REF	1.20	0.58	0.67	0.83	1.00	1.00	1.10	1.30	1.30	1.50
NAP10-3-S	22.70	21.40	22.40	22.00	21.10	21.30	20.40	22.30	22.80	22.70
NAP10-7-S	25.00	22.40	24.10	23.10	21.80	22.10	20.90	22.70	23.30	23.20
NAP10-8-S	21.60	22.20	23.30	22.90	21.80	22.10	21.00	22.90	23.50	23.80
Sample Average n=3	23.10	22.00	23.27	22.67	21.57	21.83	20.77	22.63	23.20	23.23
Standard Deviation	1.73	0.53	0.85	0.59	0.40	0.46	0.32	0.31	0.36	0.55
Average Shielding (dB)	21.90	21.42	22.60	21.84	20.57	20.83	19.67	21.33	21.90	21.73
Theoretical Shielding (dB)	30.06	25.95	23.97	23.00	22.41	22.03	21.76	21.58	21.45	21.31

Table F-44: Shielding Results for NBP10 (Tested on 2/14/02)

Shielding Effectiveness (dB)	Frequency MHz									
Sample Name	**30**	**100**	**200**	**300**	**400**	**500**	**600**	**700**	**800**	**1000**
NBP10-5 REF	15.70	6.50	2.60	2.10	2.00	1.60	1.40	1.10	1.30	1.60
NBP10-3-S	14.70	5.60	2.50	2.20	2.20	1.90	1.60	1.40	1.70	2.30
NBP10-7-S	16.40	7.20	3.10	2.60	2.43	2.10	1.70	1.40	1.70	2.30
NBP10-8-S	15.90	6.70	2.90	2.40	2.30	2.00	1.60	1.30	1.70	2.20
Sample Average n=3	15.67	6.50	2.83	2.40	2.31	2.00	1.63	1.37	1.70	2.27
Standard Deviation	0.87	0.82	0.31	0.20	0.12	0.10	0.06	0.06	0.00	0.06
Average Shielding (dB)	-0.03	0.00	0.23	0.30	0.31	0.40	0.23	0.27	0.40	0.67
Theoretical Shielding (dB)	-130.53	-135.76	-138.77	-140.53	-141.78	-142.75	-143.54	-144.21	-144.79	-145.76

Table F-45: Shielding Results for NBP15 (Tested on 2/14/02)

Shielding Effectiveness (dB)	Frequency MHz									
Sample Name	**30**	**100**	**200**	**300**	**400**	**500**	**600**	**700**	**800**	**1000**
NBP15-5 REF	15.10	6.00	2.40	2.00	1.80	1.60	1.30	1.10	1.30	1.60
NBP15-3-S	15.90	6.60	2.90	2.50	2.40	2.10	1.80	1.40	1.90	2.30
NBP15-7-S	14.70	5.70	2.50	2.20	2.20	1.90	1.70	1.40	1.80	2.10
NBP15-8-S	14.60	5.60	2.40	2.20	2.30	1.90	1.60	1.40	1.80	2.30
Sample Average n=3	15.07	5.97	2.60	2.30	2.30	1.97	1.70	1.40	1.83	2.23
Standard Deviation	0.72	0.55	0.26	0.17	0.10	0.12	0.10	0.00	0.06	0.12
Average Shielding (dB)	-0.03	-0.03	0.20	0.30	0.50	0.37	0.40	0.30	0.53	0.63
Theoretical Shielding (dB)	-129.38	-134.61	-137.62	-139.38	-140.63	-141.60	-142.39	-143.06	-143.64	-144.61

Table F-46: Shielding Results for NBP20 (Tested on 2/14/02)

Shielding Effectiveness (dB)	Frequency MHz									
Sample Name	**30**	**100**	**200**	**300**	**400**	**500**	**600**	**700**	**800**	**1000**
NBP20-5 REF	11.60	3.90	1.60	1.50	1.60	1.40	1.20	1.10	1.20	1.50
NBP20-3-S	11.40	4.10	2.20	2.30	2.40	2.30	2.00	2.00	2.60	3.30
NBP20-7-S	13.00	4.90	2.40	2.60	2.50	2.40	2.00	1.90	2.60	3.00
NBP20-8-S	14.40	5.70	2.80	2.70	2.70	2.50	2.10	2.00	2.60	3.30
Sample Average n=3	12.93	4.90	2.47	2.53	2.53	2.40	2.03	1.97	2.60	3.20
Standard Deviation	1.50	0.80	0.31	0.21	0.15	0.10	0.06	0.06	0.00	0.17
Average Shielding (dB)	1.33	1.00	0.87	1.03	0.93	1.00	0.83	0.87	1.40	1.70
Theoretical Shielding (dB)	-104.97	-110.20	-113.21	-114.97	-116.22	-117.19	-117.98	-118.65	-119.23	-120.20

Table F-47: Shielding Results for NBP30 (Tested on 2/14/02)

Shielding Effectiveness (dB)	Frequency MHz									
Sample Name	**30**	**100**	**200**	**300**	**400**	**500**	**600**	**700**	**800**	**1000**
NBP30-5 REF	5.90	2.10	1.30	1.40	1.40	1.30	1.20	1.20	1.30	1.50
NBP30-3-S	6.30	3.60	3.60	4.60	4.70	5.10	4.70	5.70	6.70	7.50
NBP30-7-S	6.30	3.60	3.70	4.50	4.70	5.10	4.80	5.70	6.80	7.60
NBP30-8-S	8.40	3.90	3.40	4.20	4.40	4.70	4.30	5.10	6.20	7.00
Sample Average n=3	7.00	3.70	3.57	4.43	4.60	4.97	4.60	5.50	6.57	7.37
Standard Deviation	1.21	0.17	0.15	0.21	0.17	0.23	0.26	0.35	0.32	0.32
Average Shielding (dB)	1.10	1.60	2.27	3.03	3.20	3.67	3.40	4.30	5.27	5.87
Theoretical Shielding (dB)	-22.31	-27.53	-30.54	-32.30	-33.55	-34.51	-35.30	-35.97	-36.55	-37.52

Table F-48: Shielding Results for NBPR30 (Tested on 2/14/02)

Shielding Effectiveness (dB)	Frequency MHz									
Sample Name	**30**	**100**	**200**	**300**	**400**	**500**	**600**	**700**	**800**	**1000**
NBPR30-5 REF	5.70	2.10	1.30	1.40	1.40	1.30	1.20	1.30	1.30	1.50
NBPR30-3-S	6.30	3.70	3.90	4.70	4.90	5.40	5.00	6.00	7.10	7.90
NBPR30-7-S	7.30	3.70	3.50	4.30	4.40	4.80	4.50	5.40	6.40	7.20
NBPR30-8-S	6.40	3.80	4.00	4.90	5.00	5.50	5.10	6.20	7.20	8.00
Sample Average n=3	6.67	3.73	3.80	4.63	4.77	5.23	4.87	5.87	6.90	7.70
Standard Deviation	0.55	0.06	0.26	0.31	0.32	0.38	0.32	0.42	0.44	0.44
Average Shielding (dB)	0.97	1.63	2.50	3.23	3.37	3.93	3.67	4.57	5.60	6.20
Theoretical Shielding (dB)	-22.98	-28.21	-31.22	-32.98	-34.22	-35.19	-35.98	-36.65	-37.23	-38.20

Table F-49: Shielding Results for NBP40 (Tested on 2/14/02)

Shielding Effectiveness (dB)	Frequency MHz									
Sample Name	**30**	**100**	**200**	**300**	**400**	**500**	**600**	**700**	**800**	**1000**
NBP40-5 REF	2.30	1.10	1.00	1.40	1.20	1.20	1.20	1.30	1.30	1.50
NBP40-3-S	7.50	7.70	9.30	10.50	10.40	11.10	10.70	10.70	13.30	13.70
NBP40-7-S	7.30	7.50	9.10	10.30	10.30	10.90	10.60	12.30	13.20	13.60
NBP40-8-S	7.30	7.50	9.10	10.40	10.20	11.00	10.60	12.40	13.30	13.60
Sample Average n=3	7.37	7.57	9.17	10.40	10.30	11.00	10.63	11.80	13.27	13.63
Standard Deviation	0.12	0.12	0.12	0.10	0.10	0.10	0.06	0.95	0.06	0.06
Average Shielding (dB)	5.07	6.47	8.17	9.00	9.10	9.80	9.43	10.50	11.97	12.13
Theoretical Shielding (dB)	18.39	13.49	10.78	9.25	8.19	7.39	6.76	6.23	5.78	5.05

Table F-50: Shielding Results for NCP05 (Tested on 2/14/02)

Shielding Effectiveness (dB)	Frequency MHz									
Sample Name	**30**	**100**	**200**	**300**	**400**	**500**	**600**	**700**	**800**	**1000**
NCP05-5 REF	19.40	9.40	4.20	3.20	2.90	2.20	1.70	1.20	1.40	1.70
NCP05-3-S	19.70	9.90	4.70	3.70	3.40	2.80	2.30	1.60	2.10	2.60
NCP05-7-S	18.40	8.70	3.90	3.20	2.90	2.40	2.00	1.50	1.90	2.40
NCP05-8-S	19.30	9.50	4.40	3.60	3.20	2.70	2.10	1.60	2.00	2.50
Sample Average n=3	19.13	9.37	4.33	3.50	3.17	2.63	2.13	1.57	2.00	2.50
Standard Deviation	0.67	0.61	0.40	0.26	0.25	0.21	0.15	0.06	0.10	0.10
Average Shielding (dB)	-0.27	-0.03	0.13	0.30	0.27	0.43	0.43	0.37	0.60	0.80
Theoretical Shielding (dB)	-133.53	-138.76	-141.77	-143.53	-144.78	-145.75	-146.54	-147.21	-147.79	-148.76

Table F-51: Shielding Results for NCP10 (Tested on 2/14/02)

Shielding Effectiveness (dB)	**Frequency MHz**									
Sample Name	**30**	**100**	**200**	**300**	**400**	**500**	**600**	**700**	**800**	**1000**
NCP10-5 REF	17.80	8.10	3.40	2.70	2.40	1.90	1.60	1.10	1.30	1.70
NCP10-3-S	17.50	8.00	3.80	3.30	3.20	2.80	2.40	2.00	2.70	3.40
NCP10-7-S	18.00	8.40	4.00	3.40	3.30	2.90	2.40	2.00	2.60	2.40
NCP10-8-S	18.40	8.50	4.00	3.40	3.20	2.80	2.30	1.90	2.50	3.20
Sample Average n=3	17.97	8.30	3.93	3.37	3.23	2.83	2.37	1.97	2.60	3.00
Standard Deviation	0.45	0.26	0.12	0.06	0.06	0.06	0.06	0.06	0.10	0.53
Average Shielding (dB)	0.17	0.20	0.53	0.67	0.83	0.93	0.77	0.87	1.30	1.30
Theoretical Shielding (dB)	-132.34	-137.57	-140.58	-142.34	-143.59	-144.56	-145.35	-146.02	-146.60	-147.57

Table F-52: Shielding Results for NCP15 (Tested on 2/14/02)

Shielding Effectiveness (dB)	**Frequency MHz**									
Sample Name	**30**	**100**	**200**	**300**	**400**	**500**	**600**	**700**	**800**	**1000**
NCP15-5 REF	15.80	6.70	2.90	2.30	2.10	1.70	1.50	1.20	1.40	1.60
NCP15-3-S	15.60	6.90	3.80	3.80	3.90	3.80	3.30	3.40	4.40	5.30
NCP15-7-S	16.10	7.10	3.80	3.80	3.80	3.80	3.20	3.20	4.10	5.10
NCP15-8-S	16.40	7.40	3.80	3.70	3.60	3.40	3.00	3.80	3.80	4.70
Sample Average n=3	16.03	7.13	3.80	3.77	3.77	3.67	3.17	3.47	4.10	5.03
Standard Deviation	0.40	0.25	0.00	0.06	0.15	0.23	0.15	0.31	0.30	0.31
Average Shielding (dB)	0.23	0.43	0.90	1.47	1.67	1.97	1.67	2.27	2.70	3.43
Theoretical Shielding (dB)	-124.27	-129.50	-132.51	-134.27	-135.52	-136.49	-137.28	-137.95	-138.53	-139.50

Table F-53: Shielding Results for NCP20 (Tested on 2/14/02)

Shielding Effectiveness (dB)	Frequency MHz									
Sample Name	**30**	**100**	**200**	**300**	**400**	**500**	**600**	**700**	**800**	**1000**
NCP20-5 REF	11.50	4.70	2.30	2.00	2.00	1.70	1.50	1.30	1.40	1.70
NCP20-3-S	11.80	5.90	4.50	5.00	5.10	5.40	4.90	5.60	6.70	7.60
NCP20-7-S	12.10	6.10	4.70	5.20	5.30	5.60	5.10	5.70	6.90	7.80
NCP20-8-S	11.20	5.70	4.50	5.10	5.30	5.50	5.10	5.80	6.90	7.80
Sample Average n=3	11.70	5.90	4.57	5.10	5.23	5.50	5.03	5.70	6.83	7.73
Standard Deviation	0.46	0.20	0.12	0.10	0.12	0.10	0.12	0.10	0.12	0.12
Average Shielding (dB)	0.20	1.20	2.27	3.10	3.23	3.80	3.53	4.40	5.43	6.03
Theoretical Shielding (dB)	-31.38	-36.61	-39.62	-41.38	-42.63	-43.60	-44.39	-45.06	-45.64	-46.60

Table F-54: Shielding Results for NCPR20 (Tested on 2/14/02)

Shielding Effectiveness (dB)	Frequency MHz									
Sample Name	**30**	**100**	**200**	**300**	**400**	**500**	**600**	**700**	**800**	**1000**
NCPR20-5 REF	10.40	4.40	2.20	2.00	1.90	1.70	1.50	1.30	1.40	1.70
NCPR20-3-S	11.50	6.10	4.90	5.50	5.60	5.90	5.40	6.10	7.30	8.10
NCPR20-7-S	10.90	5.90	4.80	5.40	5.50	5.90	5.50	6.20	7.20	7.90
NCPR20-8-S	10.70	5.80	4.80	5.40	5.60	5.90	5.40	6.20	7.30	8.20
Sample Average n=3	11.03	5.93	4.83	5.43	5.57	5.90	5.43	6.17	7.27	8.07
Standard Deviation	0.42	0.15	0.06	0.06	0.06	0.00	0.06	0.06	0.06	0.15
Average Shielding (dB)	0.63	1.53	2.63	3.43	3.67	4.20	3.93	4.87	5.87	6.37
Theoretical Shielding (dB)	-25.42	-30.64	-33.65	-35.41	-36.66	-37.63	-38.42	-39.09	-39.67	-40.63

Table F-55: Shielding Results for NCP30 (Tested on 2/14/02)

Shielding Effectiveness (dB)	Frequency MHz									
Sample Name	**30**	**100**	**200**	**300**	**400**	**500**	**600**	**700**	**800**	**1000**
NCP30-5 REF	4.30	2.10	1.50	1.50	1.60	1.40	1.40	1.40	1.40	1.60
NCP30-3-S	8.60	7.30	8.10	9.00	9.10	9.60	9.20	10.60	11.60	12.20
NCP30-7-S	9.00	7.80	8.50	9.50	9.50	10.00	9.60	11.10	12.00	12.50
NCP30-8-S	8.50	7.20	7.90	8.90	9.00	9.60	9.20	10.60	11.60	12.20
Sample Average n=3	8.70	7.43	8.17	9.13	9.20	9.73	9.33	10.77	11.73	12.30
Standard Deviation	0.26	0.32	0.31	0.32	0.26	0.23	0.23	0.29	0.23	0.17
Average Shielding (dB)	4.40	5.33	6.67	7.63	7.60	8.33	7.93	9.37	10.33	10.70
Theoretical Shielding (dB)	19.61	14.75	12.09	10.59	9.56	8.78	8.17	7.66	7.23	6.54

Table F-56: Shielding Results for NCP40 (Tested on 2/14/02)

Shielding Effectiveness (dB)	Frequency MHz									
Sample Name	**30**	**100**	**200**	**300**	**400**	**500**	**600**	**700**	**800**	**1000**
NCP40-5 REF	2.10	1.20	1.10	1.20	1.30	1.40	1.30	1.40	1.40	1.60
NCP40-3-S	14.20	12.80	13.20	14.20	14.80	14.90	15.00	15.80	16.50	17.00
NCP40-7-S	17.00	13.80	14.00	14.80	15.30	15.20	15.20	16.10	17.00	17.60
NCP40-8-S	14.40	13.40	13.90	14.80	15.30	15.20	15.20	16.20	17.10	17.70
Sample Average n=3	15.20	13.33	13.70	14.60	15.13	15.10	15.13	16.03	16.87	17.43
Standard Deviation	1.56	0.50	0.44	0.35	0.29	0.17	0.12	0.21	0.32	0.38
Average Shielding (dB)	13.10	12.13	12.60	13.40	13.83	13.70	13.83	14.63	15.47	15.83
Theoretical Shielding (dB)	26.31	21.85	19.54	18.32	17.52	16.95	16.52	16.19	15.91	15.51

Table F-57: Shielding Results for NABP (Tested on 2/14/02)

Shielding Effectiveness (dB)	Frequency MHz									
Sample Name	**30**	**100**	**200**	**300**	**400**	**500**	**600**	**700**	**800**	**1000**
NABP-5 REF	1.1	0.56	0.64	0.86	0.97	0.97	1.1	1.2	1.2	1.5
NABP-3-S	27.5	26.5	28.1	29	27.4	27.7	26.6	28.6	28.9	29
NABP-7-S	26.8	26.7	28.9	28.6	29.2	27.4	26.3	28.3	28.8	29.3
NABP-8-S	27.5	27	28.8	28.5	27	27.2	26.3	28.4	28.7	28.3
Sample Average n=3	27.27	26.73	28.60	28.70	27.87	27.43	26.40	28.43	28.80	28.87
Standard Deviation	0.40	0.25	0.44	0.26	1.17	0.25	0.17	0.15	0.10	0.51
Average Shielding (dB)	26.17	26.17	27.96	27.84	26.90	26.46	25.30	27.23	27.60	27.37
Theoretical Shielding (dB)	30.07	25.96	23.98	23.01	22.42	22.04	21.78	21.60	21.47	21.33

Table F-58: Shielding Results for NABPR (Tested on 2/14/02)

Shielding Effectiveness (dB)	Frequency MHz									
Sample Name	**30**	**100**	**200**	**300**	**400**	**500**	**600**	**700**	**800**	**1000**
NABPR-5 REF	1.20	0.56	0.68	0.83	1.00	1.10	1.10	1.20	1.20	1.50
NABPR-3-S	27.40	26.30	28.60	30.20	27.60	27.60	26.30	28.30	28.60	28.20
NABPR-7-S	27.70	25.30	27.80	28.90	27.30	28.50	27.50	26.50	28.90	28.50
NABPR-8-S	26.00	26.00	29.80	28.50	27.30	27.60	26.50	28.60	29.20	29.00
Sample Average n=3	27.03	25.87	28.73	29.20	27.40	27.90	26.77	27.80	28.90	28.57
Standard Deviation	0.91	0.51	1.01	0.89	0.17	0.52	0.64	1.14	0.30	0.40
Average Shielding (dB)	25.83	25.31	28.05	28.37	26.40	26.80	25.67	26.60	27.70	27.07
Theoretical Shielding (dB)	29.37	25.19	23.14	22.11	21.48	21.06	20.76	20.55	20.39	20.20

Table F-59: Shielding Results for NACP (Tested on 2/14/02)

Shielding Effectiveness (dB)	Frequency MHz									
Sample Name	**30**	**100**	**200**	**300**	**400**	**500**	**600**	**700**	**800**	**1000**
NACP-5 REF	1.00	0.57	0.68	0.86	1.00	1.00	1.10	1.30	1.30	1.50
NACP-3-S	27.20	26.30	27.90	27.90	26.20	26.10	25.00	27.00	27.50	27.10
NACP-7-S	31.70	26.00	26.50	28.00	26.90	26.90	25.40	27.10	27.30	27.00
NACP-8-S	26.00	26.00	28.30	27.90	26.20	26.50	25.40	27.20	27.40	27.10
Sample Average n=3	28.30	26.10	27.57	27.93	26.43	26.50	25.27	27.10	27.40	27.07
Standard Deviation	3.00	0.17	0.95	0.06	0.40	0.40	0.23	0.10	0.10	0.06
Average Shielding (dB)	27.30	25.53	26.89	27.07	25.43	25.50	24.17	25.80	26.10	25.57
Theoretical Shielding (dB)	32.75	28.98	27.31	26.57	26.19	25.98	25.87	25.84	25.85	25.95

Table F-60: Shielding Results for NACPR (Tested on 2/14/02)

Shielding Effectiveness (dB)	Frequency MHz									
Sample Name	**30**	**100**	**200**	**300**	**400**	**500**	**600**	**700**	**800**	**1000**
NACPR-5 REF	1.20	0.60	0.67	0.86	1.00	1.00	1.10	1.20	1.20	1.53
NACPR-3-S	25.90	25.90	27.70	27.40	26.30	26.60	25.40	27.10	27.50	27.80
NACPR-7-S	25.80	25.90	28.20	27.50	26.20	26.50	25.40	27.10	27.50	27.80
NACPR-8-S	25.50	25.60	28.00	28.00	26.40	26.70	25.60	27.30	27.60	27.40
Sample Average n=3	25.73	25.80	27.97	27.63	26.30	26.60	25.47	27.17	27.53	27.67
Standard Deviation	0.21	0.17	0.25	0.32	0.10	0.10	0.12	0.12	0.06	0.23
Average Shielding (dB)	24.53	25.20	27.30	26.77	25.30	25.60	24.37	25.97	26.33	26.14
Theoretical Shielding (dB)	32.97	29.23	27.59	26.87	26.51	26.32	26.23	26.20	26.23	26.36

Table F-61: Shielding Results for NBCP (Tested on 2/14/02)

Shielding Effectiveness (dB)	Frequency MHz									
Sample Name	**30**	**100**	**200**	**300**	**400**	**500**	**600**	**700**	**800**	**1000**
NBCP-5 REF	1.60	0.76	0.82	0.98	1.10	1.10	1.20	1.30	1.30	1.60
NBCP-3-S	15.00	15.30	17.40	18.10	17.70	18.30	17.60	19.50	20.10	20.10
NBCP-7-S	14.80	15.00	17.00	17.80	17.40	18.00	17.30	19.30	19.90	19.90
NBCP-8-S	15.30	15.10	17.30	17.90	17.40	18.00	17.30	19.30	20.00	20.10
Sample Average n=3	15.03	15.13	17.23	17.93	17.50	18.10	17.40	19.37	20.00	20.03
Standard Deviation	0.25	0.15	0.21	0.15	0.17	0.17	0.17	0.12	0.10	0.12
Average Shielding (dB)	13.43	14.37	16.41	16.95	16.40	17.00	16.20	18.07	18.70	18.43
Theoretical Shielding (dB)	25.19	20.65	18.26	16.98	16.13	15.52	15.05	14.67	14.37	13.90

Table F-62: Shielding Results for NBCPR (Tested on 2/14/02)

Shielding Effectiveness (dB)	Frequency MHz									
Sample Name	**30**	**100**	**200**	**300**	**400**	**500**	**600**	**700**	**800**	**1000**
NBCPR-5 REF	2.10	0.73	0.76	1.00	1.10	1.10	1.20	1.30	1.30	1.60
NBCPR-3-S	15.90	15.80	17.80	18.50	17.90	18.50	17.80	19.70	20.40	20.40
NBCPR-7-S	16.40	16.20	18.40	18.80	18.20	18.80	18.10	20.10	20.70	20.70
NBCPR-8-S	17.20	16.60	18.60	19.20	18.50	19.10	18.30	20.30	21.00	21.00
Sample Average n=3	16.50	16.20	18.27	18.83	18.20	18.80	18.07	20.03	20.70	20.70
Standard Deviation	0.66	0.40	0.42	0.35	0.30	0.30	0.25	0.31	0.30	0.30
Average Shielding (dB)	14.40	15.47	17.51	17.83	17.10	17.70	16.87	18.73	19.40	19.10
Theoretical Shielding (dB)	26.89	22.47	20.21	19.02	18.25	17.70	17.30	16.98	16.73	16.36

Appendix G: Solvent Digestion Results

Table G-1: Solvent Digestion Results (Tested on 3/03/02)

Formulation	Composite Weight (g)	Filter Weight 1 (g)	Filter Weight 2 (g)	Petri Dish Weight (g)	Fiber+Filter+Petri Dish Weight (g)	Actual Weight Fraction	Target Weight Fraction
NCP20-1	0.219	0.127		7.883	8.056	0.208	0.20
NCP20-2	0.204	0.128		7.852	8.023	0.207	0.20
NBP30-1	0.203	0.132	0.129	7.791	8.119	0.325	0.30
NBP30-2	0.217	0.132	0.131	7.918	8.255	0.341	0.30
NCN20-1	0.199	0.129		7.847	8.016	0.203	0.20
NCN20-2	0.214	0.132		7.557	7.731	0.198	0.20
NBN30-1	0.204	0.129	0.128	7.448	7.771	0.321	0.30
NBN30-2	0.194	0.131	0.127	7.848	8.166	0.309	0.30

Appendix H: Fiber Length Results

Forumlation	Krueger 2002			Clingerman 2001		Degrees of Freedom (D)	Alpha (A_1)	t	t Ref.
NBN30-1	x_1	72.65		x_2	72.14	3078	0.025	0.23	1.96
	S_1	84.06		S_2	65.4				
	N_1	2007		N_2	1073				
NBN30-2	x_1	79.55		x_2	77.47	4554	0.025	0.70	1.96
	S_1	104.98		S_2	75.58				
	N_1	3488		N_2	1068				
NBP30-1	x_1	41.26		x_2	42.57	14577	0.025	1.19	1.96
	S_1	101.56		S_2	39.57				
	N_1	9684		N_2	4895				
NBP30-2	x_1	46.23		x_2	45	9980	0.025	1.94	1.96
	S_1	34.50		S_2	33.99				
	N_1	7047		N_2	2935				
NCN20-1	x_1	96.76		x_2	94.6	6109	0.025	1.36	1.96
	S_1	71.23		S_2	58.27				
	N_1	4364		N_2	1747				
NCN20-2	x_1	96.54		x_2	96.81	4483	0.025	0.20	1.96
	S_1	68.25		S_2	67.91				
	N_1	1900		N_2	2585				
NCP20-1	x_1	92.87		x_2	94.6	5619	0.025	0.96	1.96
	S_1	68.41		S_2	58.38				
	N_1	4301		N_2	1320				
NCP20-2	x_1	77.56		x_2	76.75	6315	0.025	0.77	1.96
	S_1	60.24		S_2	52.24				
	N_1	3636		N_2	2681				

Note: A value for t-ref was obtained from a Statistics Handbook. T-Ref was pulled from a chart at the corresponding Degrees of Freedom and Confidance Interval.

t - Test Determinataion

$$t = \frac{\left|\left(\bar{x}_1 - \bar{x}_2\right)\right|}{\sqrt{\left(N_1 - 1\right) * S_1^2 + \left(N_2 - 1\right) * S_2^2}} * \sqrt{\frac{N_1 * N_2 * \left(N_1 + N_2 - 2\right)}{N_1 + N_2}}$$

x_1	Sample Average
S_1	Standard Deviation
N_1	Number of Samples
N_2	Number of Samples

t - Ref

$$t - ref = \frac{A_1}{2}, D$$

A_1	Confindence Interval
D	Degrees of Freedom

$$D = \left(N_1 + N_2 - 2\right)$$

Appendix I: Orientation Data

Forumlation	Krueger 2002			Weber 2001	Degrees of Freedom (D)	Alpha (A_1)	t	t Ref.
NBN30-1	x_1	57.64	x_2	56.85	5736	0.025	1.09	1.96
	S_1	24.65	S_2	25.295				
	N_1	4568	N_2	1170				
NBN30-2	x_1	57.01	x_2	58.021	5741	0.025	1.44	1.96
	S_1	23.5	S_2	24.85				
	N_1	4589	N_2	1154				
NBP30-1	x_1	71	x_2	70.35	4178	0.025	1.31	1.96
	S_1	18.65	S_2	20.622				
	N_1	2561.00	N_2	1619				
NBP30-2	x_1	66.5	x_2	67.611	3629	0.025	1.90	1.96
	S_1	21.90	S_2	22.561				
	N_1	2165.00	N_2	1466				
NCN20-1	x_1	67.54	x_2	68.417	6357	0.025	1.41	1.96
	S_1	23.45	S_2	22.226				
	N_1	4986	N_2	1373				
NCN20-2	x_1	68.50	x_2	69.605	6695	0.025	1.94	1.96
	S_1	21	S_2	21.58				
	N_1	5314	N_2	1383				
NCP20-1	x_1	68.15	x_2	67.486	6815	0.025	1.45	1.96
	S_1	20.48	S_2	23.35				
	N_1	4498	N_2	2319				
NCP20-2	x_1	62.14	x_2	61.444	4764	0.025	1.31	1.96
	S_1	25	S_2	25.426				
	N_1	2486	N_2	2280				

Note: A value for t-ref was obtained from a Statistics Handbook. T- pulled from a chart at the corresponding Degrees of Freedom and C Interval.

t - Test Determinataion

$$t = \frac{|\bar{x}_1 - \bar{x}_2|}{\sqrt{N_1 * S_1^2 + N_2 * S_2^2}} * \sqrt{\frac{N_1 * N_2 * (N_1 + N_2)}{N_1 + N_2}}$$

x_1	Sample Average
S_1	Standard Deviation
N_1	Number of Samples
N_2	Number of Samples

t - Ref

$$t = ref\left(\frac{A_1}{2}, D\right)$$

A_1	Confindence Interval
D	Degrees of Freedom

$$D = N_1 + N_2 - 2$$

Figure J-1: Cube Plot for Nylon at 300 MHz

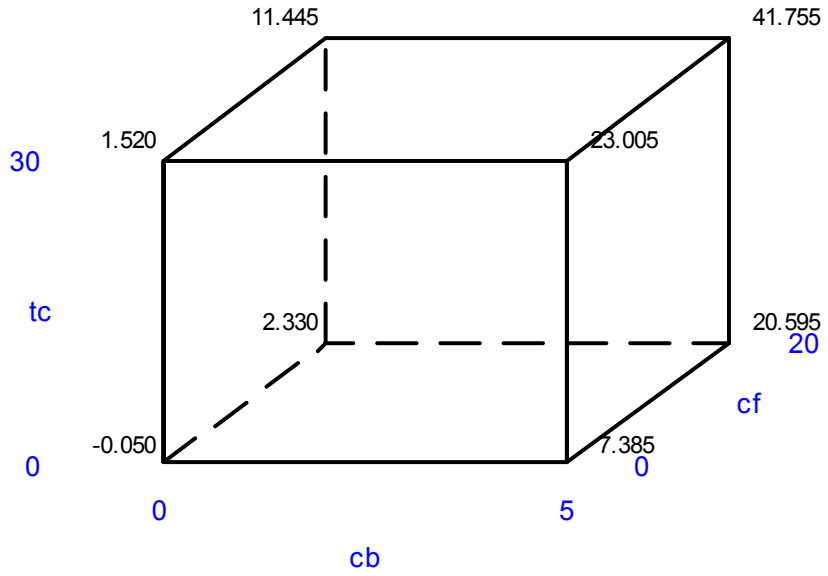

Figure J-2: Main Effects Plot for Nylon at 300 MHz

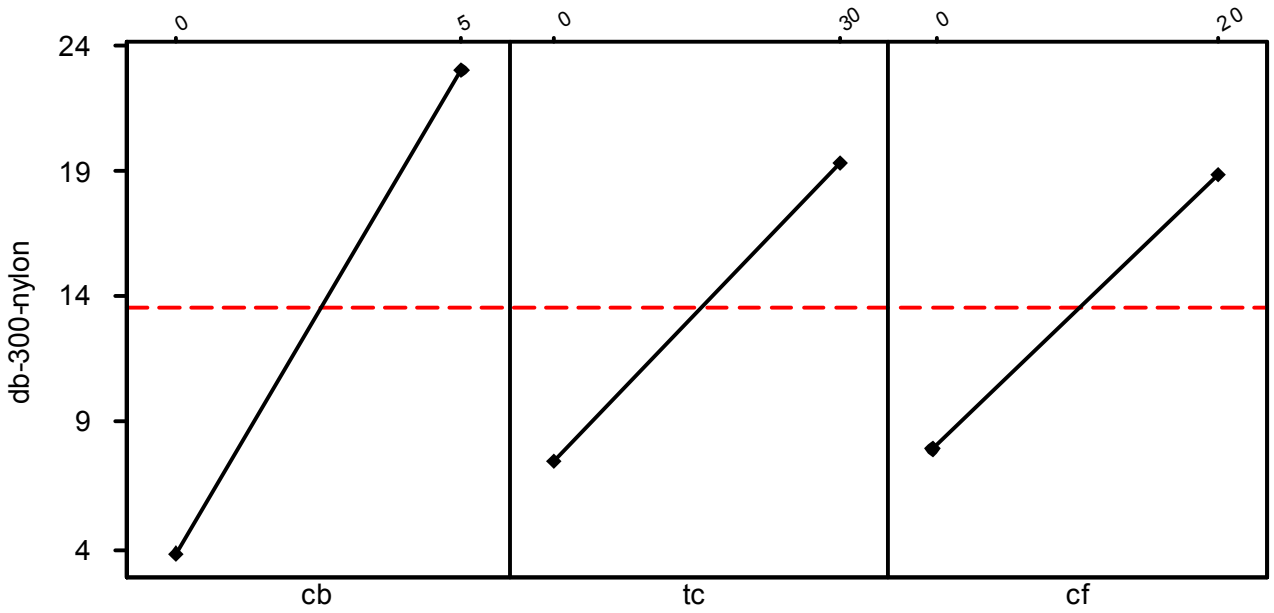

Figure J-3: Interaction Plot for Nylon at 300 MHz

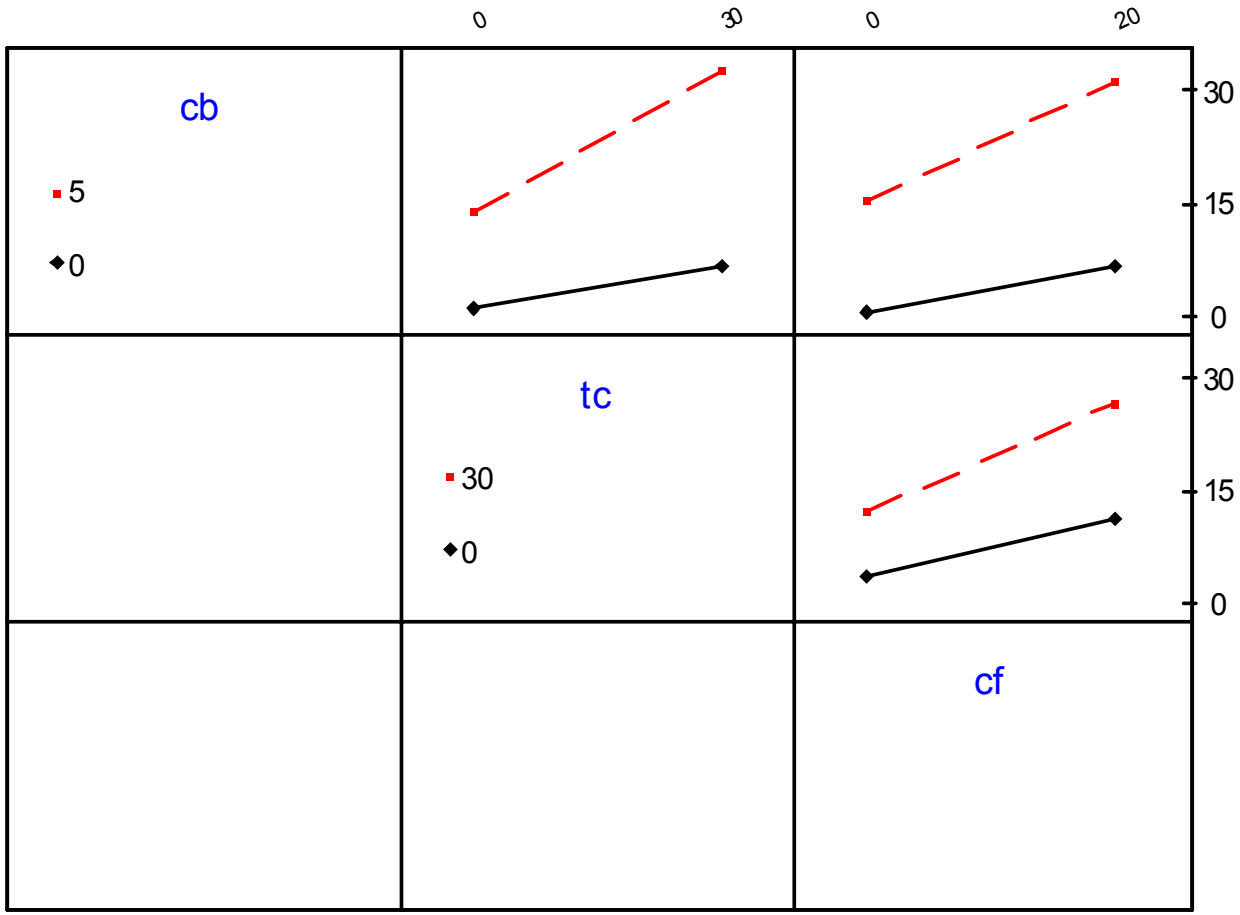

Figure J-4: Cube plot for Nylon at 800 MHz

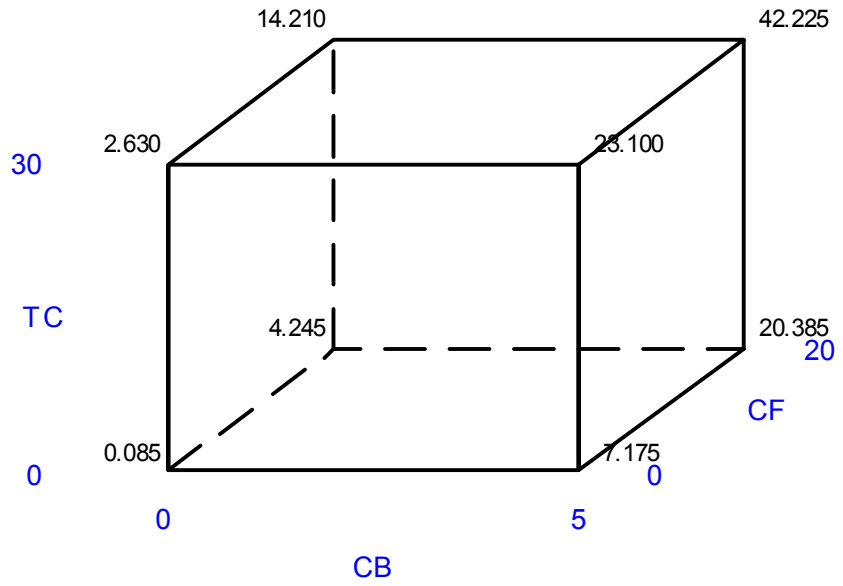

Figure J-5: Main Effects Plot for Nylon at 800 MHz

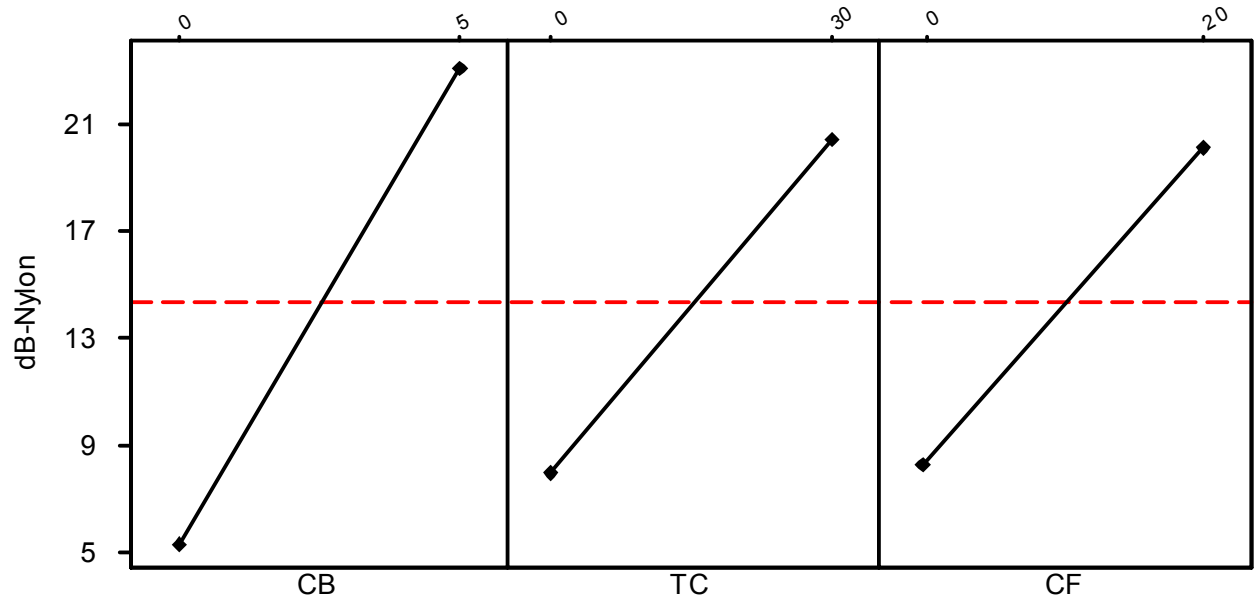

Figure J-6: Interaction Plot for Nylon at 800 MHz

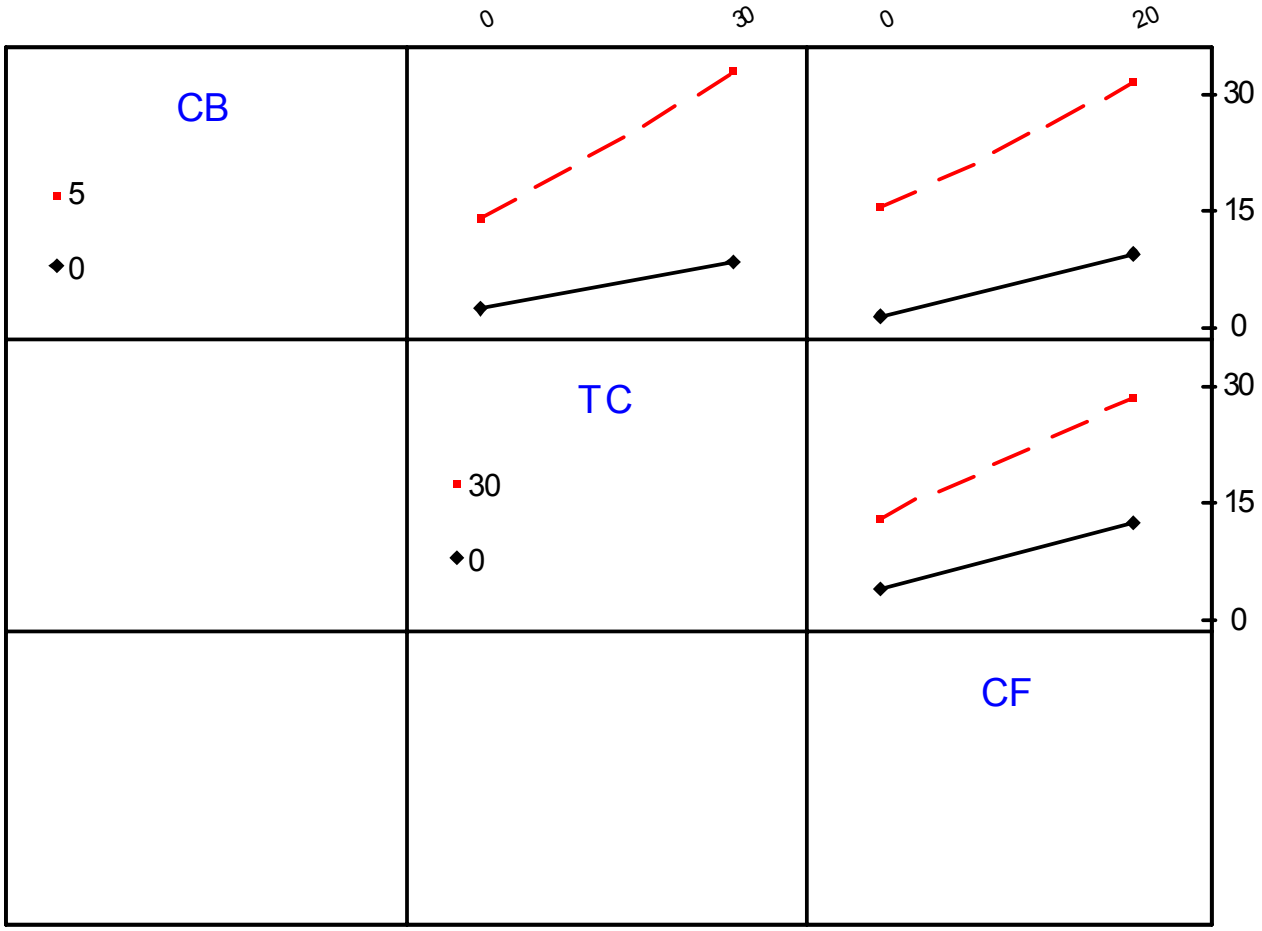

Figure J-7: Cube Plot for Polycarbonate at 300 MHz

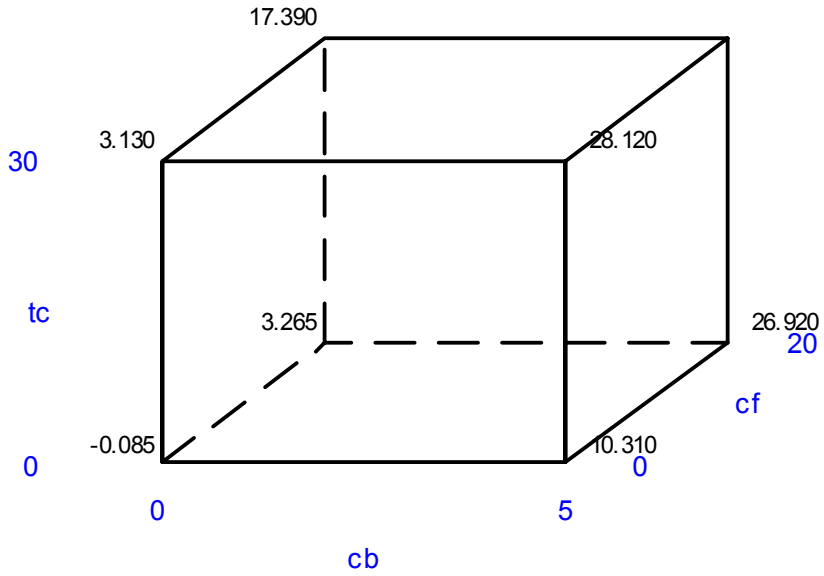

Figure J-8: Main Effects Plot for Polycarbonate at 300 MHz

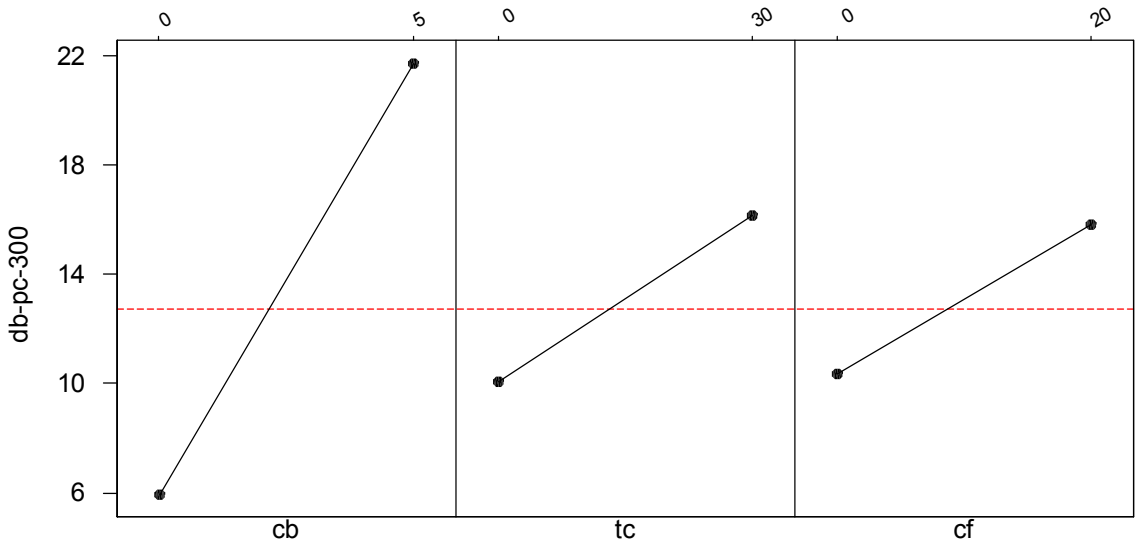

Figure J-9: Interaction Plot for Polycarbonate at 300 MHz

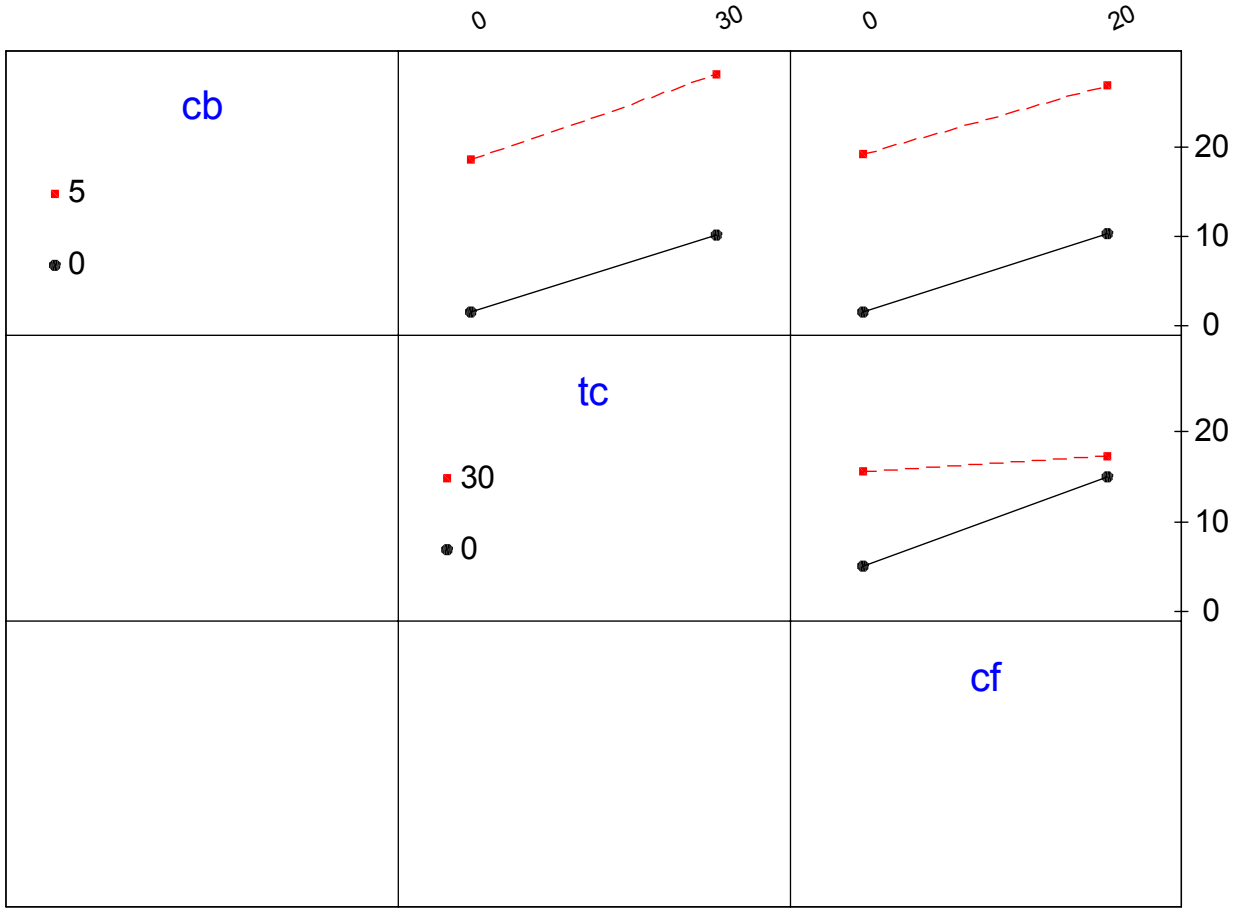

Figure J-10: Cube Plot for Polycarbonate at 800 MHz

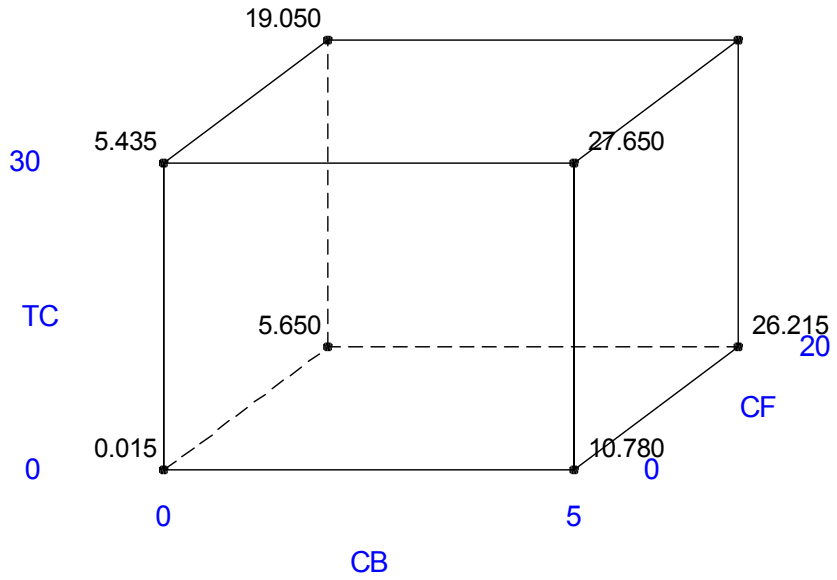

Figure J-11: Main Effects Plot for Polycarbonate at 800 MHz

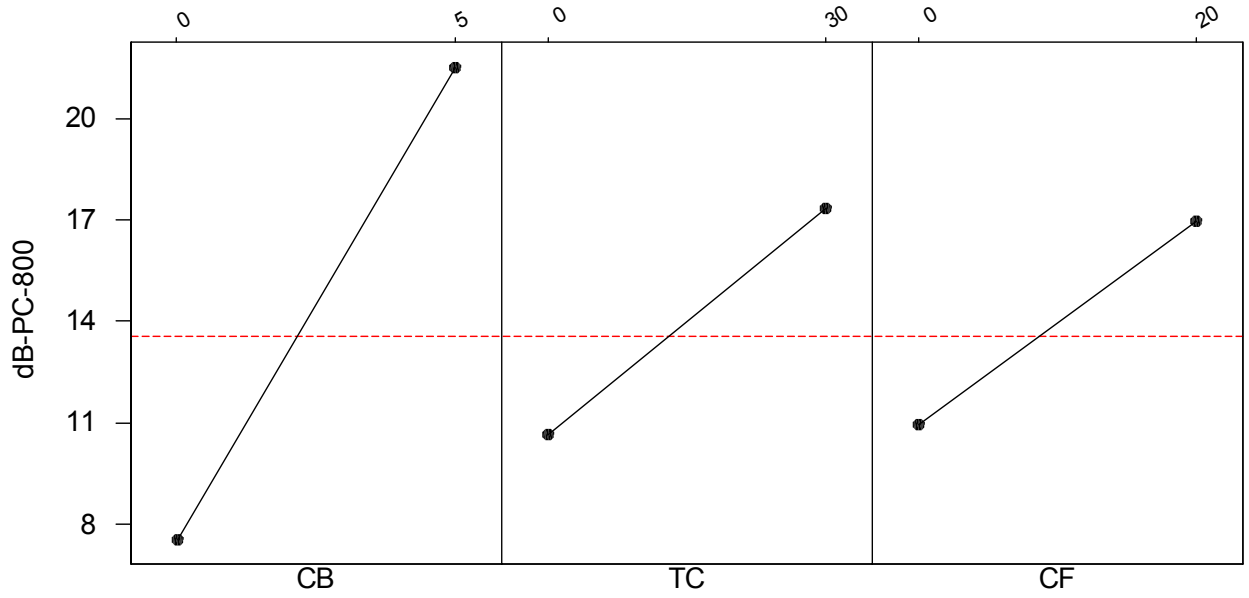

Figure J-12: Interaction Plot for Polycarbonate at 800 MHz

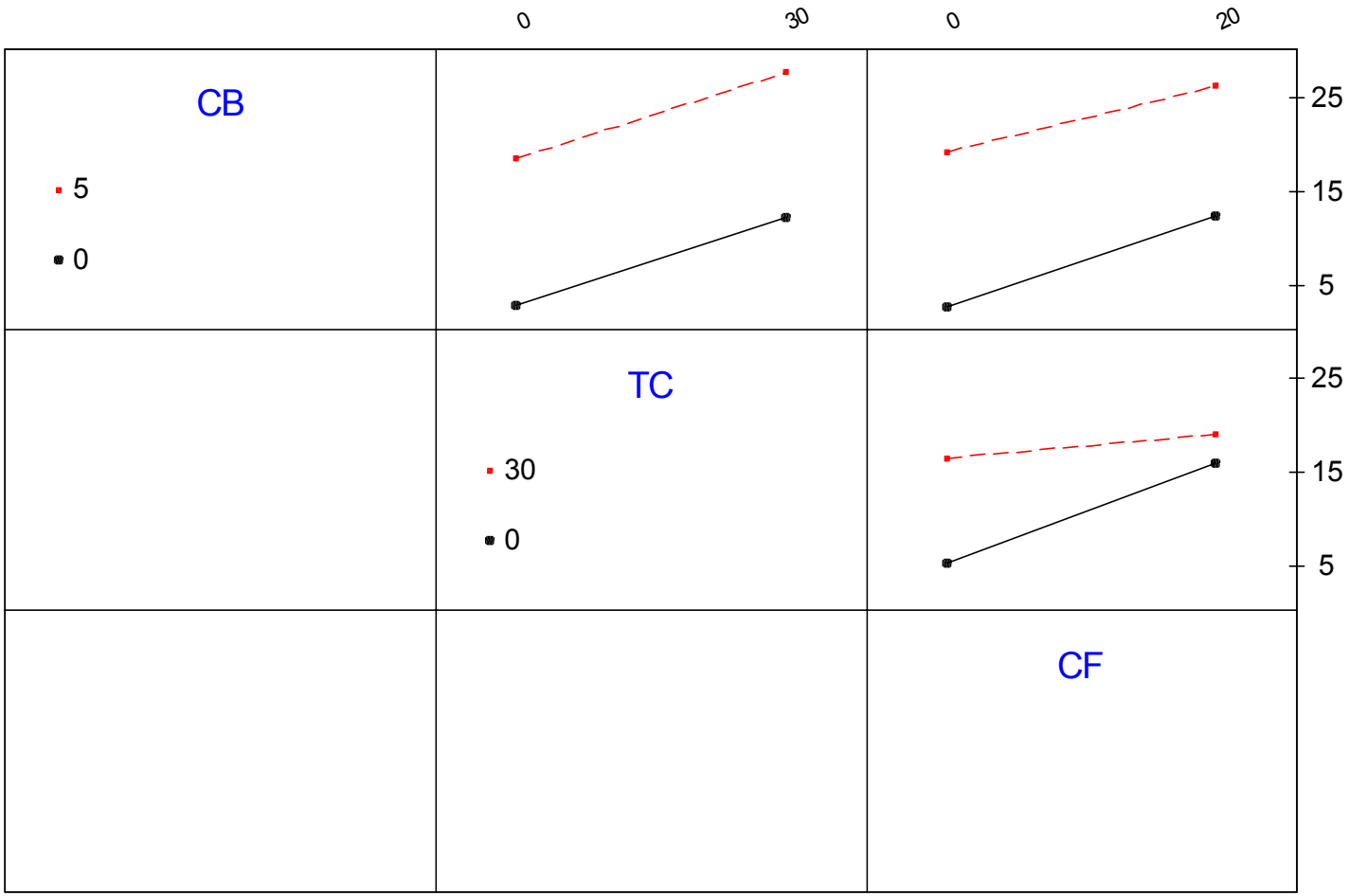

Appendix K: Microsoft Excel Factorial Design Calculations

Table K-1: Nylon 6,6 at 300 MHz Statistical Significance Calculation

Run	Form #	SE #1	SE #2	Total	Avg	Var		$SE1^2$	$SE2^2$
1	**(1)**	-0.03	-0.07	-0.10	-0.05	0.00		0.00	0.00
2	**a**	7.35	7.42	14.77	7.39	0.00		54.02	55.06
3	**b**	1.30	1.74	3.04	1.52	0.10		1.69	3.03
4	**ab**	23.11	22.90	46.01	23.01	0.02		534.07	524.41
5	**c**	2.32	2.34	4.66	2.33	0.00		5.38	5.48
6	**ac**	21.00	20.19	41.19	20.60	0.33		441.00	407.64
7	**bc**	10.08	12.81	22.89	11.45	3.73		101.61	164.10
8	**abc**	42.63	40.88	83.51	41.76	1.53		1817.32	1671.17
				215.97				**2955.09**	**2830.88**

Table K-2: Interaction Chart for Nylon 6,6 at 300 MHz

A	B	C	AB	AC	BC	ABC
-1	-1	-1	1	1	1	-1
1	-1	-1	-1	-1	1	1
-1	1	-1	-1	1	-1	1
1	1	-1	1	-1	-1	-1
-1	-1	1	1	-1	-1	1
1	-1	1	-1	1	-1	-1
-1	1	1	-1	-1	1	-1
1	1	1	1	1	1	1

Table K-3: Summary Results for Nylon 6,6 at 300 MHz

SUM(+)	92.74	77.73	76.13	67.04	63.82	60.54	52.99
SUM(-)	15.25	30.26	31.86	40.95	44.17	47.45	55.00
SUM(+)+SUM(-)	107.99	107.99	107.99	107.99	107.99	107.99	107.99
SUM(+)-SUM(-)	77.50	47.47	44.27	26.10	19.66	13.09	-2.01
EFFECTS	**19.37375**	**11.86625**	**11.06625**	**6.52375**	**4.91375**	**3.27125**	**-0.50125**
sE	0.21	0.21	0.21	0.21	0.21	0.21	0.21
tE	94.06	57.61	53.73	31.67	23.86	15.88	-2.43

Table K-4: Statistical Significance (P) Calculation

Source	SS	Degrees of Freedom	MS	F	P
A	1501.3688	1	1501.3688	2104.2125	0.000
B	563.23156	1	563.23156	789.3856	0.000
C	489.84756	1	489.84756	686.53576	0.000
AB	170.23726	1	170.23726	238.59252	0.000
AC	96.579756	1	96.579756	135.35937	0.000
BC	42.804306	1	42.804306	59.991494	0.000
ABC	1.0050063	1	1.0050063	1.4085458	0.269
Error	5.71	8	0.7135063		
Total	2870.7822	15			

Table K-5: Polycarbonate at 300 MHz Statistical Significance Calculation

Run	Form #	SE 1	SE 2	Total	Avg	Var		$SE1^2$	$SE2^2$
1	**(1)**	-0.10	-0.07	-0.17	-0.09	0.00		0.01	0.00
2	**a**	10.19	10.43	20.62	10.31	0.03		103.84	108.78
3	**b**	3.03	3.23	6.26	3.13	0.02		9.18	10.43
4	**ab**	27.87	28.37	56.24	28.12	0.13		776.74	804.86
5	**c**	3.10	3.43	6.53	3.27	0.05		9.61	11.76
6	**ac**	27.07	26.77	53.84	26.92	0.04		732.78	716.63
7	**bc**	16.95	17.83	34.78	17.39	0.39		287.30	317.91
8	**abc**	0.00	0.00	0.00	0.00	0.00		0.00	0.00
	Totals	**88.11**	**89.99**	**178.10**				**1919.46**	**1970.39**

Table K-6: Interaction Chart for Polycarbonate at 300 MHz

A	B	C	AB	AC	BC	ABC
-1	-1	-1	1	1	1	-1
1	-1	-1	-1	-1	1	1
-1	1	-1	-1	1	-1	1
1	1	-1	1	-1	-1	-1
-1	-1	1	1	-1	-1	1
1	-1	1	-1	1	-1	-1
-1	1	1	-1	-1	1	-1
1	1	1	1	1	1	1

Table K-7: Summary Results for Polycarbonate at 300 MHz

SUM(+)	65.35	48.64	47.58	31.30	29.97	27.62	16.71
SUM(-)	23.70	40.41	41.48	57.75	59.09	61.44	72.35
SUM(+)+SUM(-)	89.05	89.05	89.05	89.05	89.05	89.05	89.05
SUM(+)-SUM(-)	41.65	8.23	6.10	-26.45	-29.12	-33.82	-55.64
EFFECTS	**10.412525**	**2.057525**	**1.525025**	**-6.612475**	**-7.279975**	**-8.454975**	**-13.909975**
sE	0.02	0.02	0.02	0.02	0.02	0.02	0.02
tE	436.55	86.26	63.94	-277.23	-305.22	-354.48	-583.18

Table K-8: Statistical Significance (P) Calculation

Source	SS	Degrees of Freedom	MS	F	P
Blocks	0.2209	1	0.2209	2.3318335	0.0000
A	433.6827075	1	433.68271	4577.9804	0.0000
B	16.9336365	1	16.933637	178.75247	0.0000
C	9.302805003	1	9.302805	98.200961	0.0000
AB	174.8993025	1	174.8993	1846.2474	0.0000
AC	211.992144	1	211.99214	2237.8016	0.0000
BC	285.946409	1	285.94641	3018.4672	0.0000
ABC	773.949618	1	773.94962	8169.858	0.0000
Error	0.66	7	0.0947323		
Total	1907.369749	15			

Appendix L: Shielding Effectiveness Equation Justification

	Frequency MHz										
Sample Name	**30**	**100**	**200**	**300**	**400**	**500**	**600**	**700**	**800**	**1000**	**10000**
NCP40-5 REF	2.1	1.2	1.1	1.2	1.3	1.4	1.3	1.4	1.4	1.6	
NCP40-3-S	14.2	12.8	13.2	14.2	14.8	14.9	15	15.8	16.5	17	
NCP40-7-S	17	13.8	14	14.8	15.3	15.2	15.2	16.1	17	17.6	
NCP40-8-S	14.4	13.4	13.9	14.8	15.3	15.2	15.2	16.2	17.1	17.7	
Sample Average (dB)	15.20	13.33	13.70	14.60	15.13	15.10	15.13	16.03	16.87	17.43	
Standard Deviation (dB)	1.56	0.50	0.44	0.35	0.29	0.17	0.12	0.21	0.32	0.38	
Average Sheilding (dB)	13.10	12.13	12.60	13.40	13.83	13.70	13.83	14.63	15.47	15.83	
Shielding (Theory) (dB)	26.78	22.35	20.08	18.88	18.11	17.56	17.15	16.83	16.57	16.19	
Carbon Fiber 40% in PC											
Electrical Resistivity	1.05E+01	**Ohm-cm**		30	**MHz**						
Electrical Conductivity	9.52E-02	**S/cm**		1000000	**Mega**						
				3.00E+07	**Hz**						
Copper Conductivity	5.80E+05	**(S/cm)**									
Relative Conductivity (σ)	1.64E-07	**(S/cm)**									
u=Relative to copper	**Mu**	**1**									
Frequency (Hz)	**3.00E+07**	**1.00E+08**	**2.00E+08**	**3.00E+08**	**4.00E+08**	**5.00E+08**	**6.00E+08**	**7.00E+08**	**8.00E+08**	**1.00E+09**	**10000000000**
Shielding Theory (dB)	26.31	21.85	19.54	18.31	17.52	16.95	16.52	16.18	15.91	15.50	17.07
Log(10) Factor (dB)	25.3826	20.1538	17.1435	15.3826	14.1332	13.1641	12.3723	11.7028	11.1229	10.1538	0.1538
Square Root Factor (dB)	0.9266	1.6918	2.3926	2.9303	3.3836	3.7830	4.1440	4.4761	4.7851	5.3499	16.9180
SUM (dB)	26.31	21.85	19.54	18.31	17.52	16.95	16.52	16.18	15.91	15.50	17.07

The sum of the two components of the theory equation should equal the shielding theory row. You can see that the log term is dominate at lower frequencies below 1 GHz. The squareroot term dominates at higher frequencies above 1 GHz.